Hyperspectral Remote Sensing of Tropical Grass Quality and Quantity

Onisimo Mutanga
7 April 2004

Promoters
Prof. Dr. A.K. Skidmore
Professor of Vegetation and Agricultural Land Use Survey
International Institute for Geoinformation Science and Earth Observation (ITC),
Enschede and Wageningen University,
The Netherlands

Prof. Dr. H.H.T. Prins
Professor of Tropical Nature Conservation and Vertebrate Ecology,
Wageningen University, The Netherlands

Co-promoter
Dr. H.G.J. Huizing
Associate Professor, Department of Natural Resources,
International Institute for Geoinformation Science and Earth Observation (ITC),
Enschede, The Netherlands

Examination committee:

Prof. Dr. J.P. Bakker
University of Groningen, The Netherlands

Prof. R. De Wulf
University of Gent, Belgium

Prof. Dr. M.E. Schaepman
Wageningen University, The Netherlands

Prof. W. J. Bond
University of Cape Town, South Africa

Hyperspectral Remote Sensing of Tropical Grass Quality and Quantity

Onisimo Mutanga

THESIS

To fulfil the requirements for the degree of doctor on the authority of the Rector Magnificus of Wageningen University, Prof. Dr. Lr. L. Speelman, to be publicly defended on Wednesday 7th of April 2004 at 15:00 hrs in the auditorium of ITC, Enschede.

ISBN: 90-5808-981-9
ITC Dissertation number: 111

Table of contents

Abstract

Resource distribution is a fundamental factor governing the movement and distribution of herbivores. Specifically, the quality (foliar concentration of nitrogen, phosphorous, calcium, magnesium, potassium and sodium) and quantity (biomass) of vegetation are important factors. In this regard, the development of techniques that can model the distribution of vegetation quality and quantity are critical for an improved understanding of wildlife distribution as well as facilitating an optimal management of wildlife resources. The advent of hyperspectral remote sensing has offered unprecedented opportunities to accomplish this task.

This study aimed to investigate the potential of hyperspectral remote sensing in estimating biomass of tropical grass at full canopy cover (a task that could not be achieved using broad band satellite images) and to predict and map the quality of tropical grasses at canopy level. Our approach was to investigate the potential of hyperspectral remote sensing at three levels of investigation – laboratory level, field level and airborne platform level.

Our results showed that, at full canopy cover, tropical grass biomass is more accurately estimated by vegetation indices based on narrow wavelengths located in the red edge than the standard NDVI. At laboratory level, we could discriminate between different foliar nitrogen treatments using high-resolution spectra measured at canopy level. We also showed that there was a shift of the red edge position to longer wavelengths with an increase in nitrogen concentration. The laboratory experiment permitted the extension of the developed techniques to the field level. Using continuum-removed absorption features calculated from field spectra, we could reliably predict the quality (N, K, P, Ca, Mg, Na) of in situ grass measured in the Kruger National Park, South Africa. We also showed a strong interaction between species type and biochemical concentration in effecting spectral reflectance. This provided a basis for the algorithms to use in mapping foliar biochemicals in a mixed species environment using airborne hyperspectral image. Therefore the techniques developed for accomplishing the final stage (airborne platform level) were largely built upon the laboratory and field observations. The new integrated approach, involving the red edge position, continuum-removed absorption features as well as a neural network was applied to map foliar nitrogen concentration in the Kruger National Park, South Africa.

Overall, the study has shown the potential of hyperspectral remote sensing to predict the quality as well as the quantity of tropical grasses. The result is important for wildlife habitat modelling.

Samenvatting

De verspreiding van natuurlijke hulpbronnen (vegetatie in het bijzonder) bepaalt in belangrijke mate de verspreiding van herbivoren. De kwaliteit (concentratie van stikstof fosfor, magnesium, kalium en natrium) en de hoeveelheid (biomassa) van vegetatie zijn belangrijke factoren. Voor het begrijpen van de verspreiding van wild en voor het optimale beheer van de vegetatie waarvan dit wild gebruik maakt is het daarom cruciaal om technieken te ontwikkelen, die de verspreiding van hoeveelheid en kwaliteit van vegetatie kunnen modelleren. Hyperspectrale aardobservatie biedt tot nu toe ongekende mogelijkheden om zo een ontwikkeling mogelijk te maken.

Het doel van deze studie is het onderzoeken van de mogelijkheden van hyperspectrale aardobservatie voor het schatten van de biomassa van tropisch gras bij volledige bodembedekking en het bepalen van de kwaliteit van dit gras (iets wat met conventionele satellietbeelden met brede spectrale banden niet mogelijk is). De studie werd uitgevoerd op drie niveaus: in het laboratorium met potproeven, op veldniveau, en met behulp van digitale opnames vanuit een vliegtuig.

De resultaten van de studie tonen aan dat de biomassa van tropische gras dat de bodem volledig bedekt nauwkeuriger kan worden bepaald met vegetatie indicatoren die gebruik maken van smalle golflengtebanden in het grensgebied van het rode en infrarode deel van het spectrum (“red edge”) dan door de veelal gebruikte NDVI. In het laboratorium was het mogelijk verschillen in stikstofgiften te onderscheiden met behulp van een hyperspectrale scanner. Dit onderzoek toonde aan dat bij een toename van het stikstofgehalte een verschuiving plaats vindt van de “red edge” naar hogere golflengtes. De resultaten van de laboratorium proeven werden verder getest op veldniveau. Met behulp van “continuum-removed absorption features” die uit, met een spectrometer gemeten, veldspectra werden berekend was een betrouwbare schatting van de kwaliteit (N, K, P, Ca, Mg, Na) van grassen in het Kruger Nationaal Park in Zuid Afrika mogelijk. De metingen toonden aan dat grassoort en biochemische samenstelling grote invloed hebben op de spectrale reflectie. Dit vormde de basis voor het ontwikkelen van algoritmes voor het karteren van de bladchemie van graslanden met een gemengde soortensamenstelling met behulp van hyperspectrale opnames vanuit een vliegtuig. De technieken om een kartering met behulp van opnames vanuit de lucht uit te voeren kwamen dus voort uit de laboratoriumproeven en veld observaties. De nieuwe geïntegreerde benadering, die gebruik maakt van “red edge” positie, “continuum-removed absorption features” en neurale netwerken werd toegepast voor het karteren van de stikstof concentratie van grasbestanden in het Kruger Nationaal Park in Zuid Afrika.

De studie heeft het potentieel aangetoond van hyperspectrale aardobservatie voor het bepalen van zowel de kwaliteit als de biomassa van tropische grassen. De resultaten zijn van belang voor het modelleren van het leef- en verspreidingsgebied (habitat) van wild.

To my dear son Shingi

Acknowledgements

A single man cannot surround an anthill! This African saying is confirmed by the support that I received from several individuals and institutions during the last 3 years of my PhD research.

I would like to thank ITC for giving me a scholarship to read for a PhD. My appreciation extends to the commitment of ITC in paying for hyperspectral image acquisition in the Kruger National Park. Undertaking such a commitment by one institution for two PhD students is not easy, considering the high costs involved! Without this image, my story could not have been solid.

My motivation to do a PhD could not have been possible without my first supervisor and promotor, Andrew Skidmore. Soon after completing my MSc thesis, Andrew began to throw ideas for a PhD and together we wrote a proposal, which was accepted by the ITC scientific board. During my PhD, you taught me to be a scientist and from you, I learnt the style of writing that saw our papers sailing through without problems. Your determination is undoubted as confirmed by your solid commitment during the time you had health problems. Cycling to Wilminkweg 9 was a wonderful experience, especially when I knew I would be received with a smiling face. To Eva, I say thank you for the hospitality- you were always running with tea and cake, not forgetting the lamb chops!

To my other promoter Herbert Prins, I say thank you for teaching me how to do science. I don't forget the one week that we spent together in the field in South Africa. From your explanations in the field I could better understand the ecological processes taking place. You were an orator sitting under a mopane tree!

My co-promotor, Herman Huizing was like a father to me. You were always ready to assist both academically and socially. With your assistance, I managed to get funding for my fieldwork from the MEPP/DGIS Project. Your door was always open for me. Thanks for translating my abstract to Dutch.

I would also like to thank other members of staff who helped me with ideas, namely, Lalit Kumar, Sip van Wieren, Jan de Leeuw, Hein van Gils, Freek van der Meer and Alfred Stein. My gratitude goes to Sip who organised logistics for my greenhouse experiments in Wageningen University. To Alfred Stein, I say thank you for your assistance in answering critical scientific questions. Special thanks goes to Henk van Oosten who introduced me into the world of IDL programming. You were always ready to teach me and without you, critical scientific objectives could not have been achieved. To the whole NRS department, I say thank you for your support.

I cannot forget the contribution of special people like Loes Colenbrander, Esther Hondebrink, Petra Weber, Gerard Leppink, Job Duim and Benno Masselink- keep up the smiling faces. From the RSG lab, Wim Bakker, Jelger Kooistra and Wan Bakx were always assisting me with the GER

spectrometer problems. I would also like to thank Marie Chantal Metz, Theresa van den Boogaard, Bettine Geerdink, Carla Gerritsen and Marga Koelen and Roelof Schoppers for their excellent service.

The PhD community at ITC made me feel at home in the Netherlands. Jelle Ferwerda, Chudamani Joshi, Md Istiak Sobhan, Uday Bhaskar Nidumolu, Grace Nangendo, Martin Yemefack, Moses Azong Cho, Marleen Noomen, Peter Minang, Chaichoke Vaiphasa, Mohammed Said, Laurent Sedogo, Dennis Rugege, Jamshid Farifteh, Arta Dilo, to mention a few, you were brothers and sisters to me. In particular, Jelle deserves special thanks. You paid for being physically big by always carrying the 45 Kilos spectrometer in the field, while I pretended to be protecting the laptop from the scorching heat, yet I was enjoying the mopane shade! Don't forget the six-pack when you go back to South Africa.

I extend my gratitude to the Scientific Board of the Kruger National Park in South Africa for providing all the necessary support. Rina Grant, Harry Biggs and Mike Peel from ARC went out of their way to help me with excellent field logistics. Bruce and Theresa from Senalala, thanks for your hospitality. Dr Fatima Ferraz from Anglo America Cooperation (South Africa) thanks for establishing the networks.

The Department of Geography and Environmental Science at the University of Zimbabwe supported me throughout my PhD. I would like to thank Dr Mukora, Prof Mutambirwa, Prof Tevera, my brother, Mr Maruziva, Banda and Nyambodza for their help and support.

The Zimbabwean colleagues in the Netherlands thank you for the support. Sindile Bidla made me feel at home in the Netherlands. Dominic Mazvimavi, thank you for your parental support and advice. I would like to thank Karin Schmidt as a friend and colleague for her steadfast support and critical comments. I was always afraid to give you my papers to review because of your critical comments, but the comments really sharpened my thesis. Amon Murwira, my brother, friend as well as colleague, thanks for the support and encouragement that you have always given me. Again, together we will flourish! Joseph Merka, thank you as a brother who was always there for my family back in Zimbabwe during the last 3 years.

I extend my gratitude to my family, my father and mother, brothers and sisters for your tender love and support.

Finally, to my wife Paula, I say thank you for enduring all the hardships that you faced while alone in Zimbabwe. Thanks for taking care of young Shingi. You have proved to be strong and determined to face the reality of life. Thanks for your steadfast love.

CHAPTER 1:
General introduction

1.1 The quantity and quality of tropical grasses

Research in tropical grasslands has revealed that both quantity and quality of grasses are critical factors influencing the feeding patterns and distribution of wildlife (Drent & Prins, 1987; McNaughton, 1990; McNaughton & Banyikwa, 1995; Prins, 1989; Prins, 1996). Specifically, wildlife exhibits preference for certain sites and certain grass species based on both quality and quantity (Muya & Oguge, 2000; Prins, 1989). In this regard, the measurement of the quality and quantity variables in grasslands is critical for understanding wildlife feeding patterns and distribution. In this thesis, quantity is defined as the biomass of grass (e.g. g cm^{-2}, kg m^{-2}) while quality is defined as the foliar concentration (e.g. mg/g or expressed as % per 100 g of dry weight) of macronutrients such as nitrogen, phosphorous, calcium, magnesium, potassium and sodium.

Several studies in the African grasslands have shown the importance of grass quantity and quality to wildlife feeding behaviour. For example, in a study on the feeding behaviour of the African buffalo in East Africa, Prins (1989) found out that during the dry season the animals select sites with high biomass grass species where the bite size index is large. With regards to quality, studies in East and Southern Africa have shown that nitrogen is commonly the most limiting nutrient for grazers (Grant *et al.*, 2000; Owen-Smith & Novellie, 1982; Prins, 1996). In addition, other mineral nutrients such as potassium, phosphorous, calcium, magnesium and sodium are also limiting factors. For example, Voeten, (1999) found out that phosphorous determines the migratory patterns of wildebeest in the Tarangire ecosystem. Therefore, in order to understand the spatial distribution of wildlife, the need to measure the quantity, as well as the quality of tropical grasslands is critical. In this regard, the advent of remote sensing, particularly hyperspectral remote sensing has offered possibilities to accomplish this task.

1.2 Hyperspectral remote sensing

The prefix hyper, means excessive or above. In this thesis the term hyperspectral is used to refer to spectra consisting of large number of narrow, contiguously spaced spectral bands. In the field of remote sensing, the term hyperspectral is used interchangeably with other terms such as spectroscopy, spectrometry, spectroradiometry and rarely ultraspectral (Clark, 1999). Spectroscopy is a branch of physics concerned with the production, transmission, measurement and interpretation of electromagnetic spectra (Kumar *et al.*, 2001). Spectrometry or spectroradiometry is derived from spectro-photometry, the measure of photons as a function of wavelength. Ultraspectral is beyond hyperspectral, a goal that has not been achieved yet (Clark, 1999). Spectrometers are used in laboratories, field, aircraft or satellites to measure the reflectance spectra of natural surfaces.

When an image is constructed from an imaging spectrometer that records the spectra for contiguous image pixels, the terms shift to become imaging spectroscopy, imaging spectrometry or hyperspectral imaging. Hyperspectral imaging is a new technique for obtaining a spectrum in each position of a large array of spatial positions so that any one spectral wavelength can be used to make a recognisable image (Clark, 1999). By analysing the spectral features in each pixel, and thus specific chemical bonds in materials, we can spatially map materials.

The narrow spectral channels that constitute hyperspectral sensors enable the detection of small spectral features that might otherwise be masked within the broader bands of multi-spectral scanner systems. In this regard, we hypothesise that hyperspectral sensors could help to overcome the traditional problems faced when using the broader bands of multi-spectral scanner systems, such as the saturation problem in estimating quantity (see section 1.3) and the estimation of quality (see section 1.4).

1.3 Vegetation quantity and remote sensing

Based on broadband satellite images, vegetation indices such as Normalised Difference Vegetation Index (NDVI), Simple Ratio (SR), Transformed Vegetation Index (TVI) and Transformed Soil Adjusted Vegetation Index (TSAVI) have been widely used to measure vegetation quantity, leaf area index (LAI) and percent green vegetation cover of vegetation at canopy scale (Blackburn & Steele, 1999; Boegh *et al.*, 2002; Elvidge & Chen, 1995; Gao *et al.*, 2000; Schowengerdt, 1983; Tucker, 1979). Although these indices have been successfully used in areas with open canopy cover or sparsely vegetated regions, they have not been successful in estimating quantity at high canopy density. Specifically, the widely used vegetation indices particularly NDVI derived from broad band satellite images such as NOAA or Landsat TM tend to

saturate after a certain biomass density or LAI (Gao *et al.*, 2000; Sellers, 1985; Thenkabail *et al.*, 2000; Todd *et al.*, 1998; Tucker, 1977). Figure 1.1 shows a hypothetical illustration of this biomass-NDVI relationship.

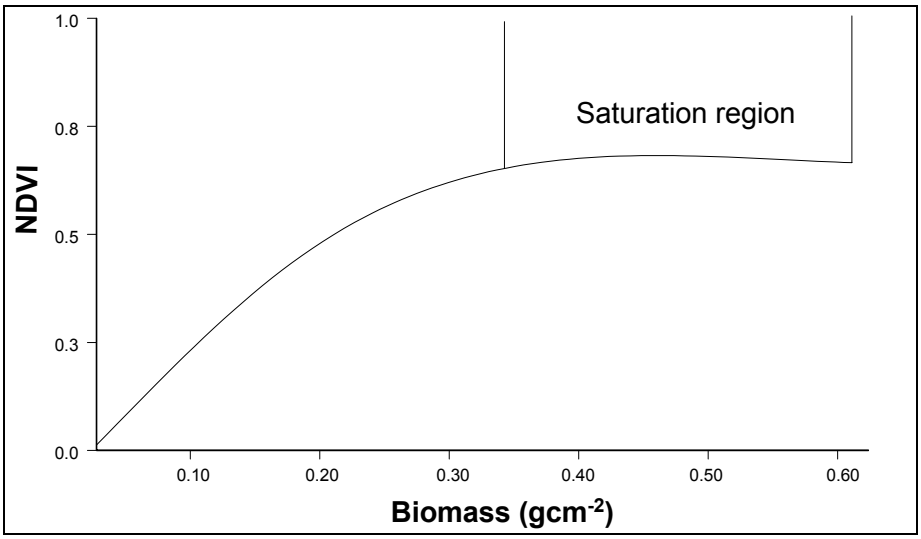

Figure 1.1 Relationship between NDVI and biomass. The saturation level is usually reached at about 0.3 g cm $^{-2}$ (Hurcom & Harrison, 1998)

In view of this limitation, the need to develop or improve techniques that can accurately estimate biomass in more densely vegetated areas is critical. In this thesis, we hypothesise that hyperspectral remote sensing, with its capability to resolve detailed spectral features can solve this problem.

1.4 Vegetation quality and remote sensing

The remote sensing of vegetation quality using available broadband satellite images is more difficult than the remote sensing of biomass or LAI. This is because the biochemicals absorb electromagnetic radiation (Curran, 1989; Johnson *et al.*, 1994; Osborne *et al.*, 1993) in specific wavelength regions, which may be masked by the broadband satellites images. Hyperspectral data acquired in many narrow, contiguous spectral bands can detect local variations in absorption features (Kokaly *et al.*, 2003; Schmidt & Skidmore, 2003). Figure 1.2 shows the mean canopy spectra of grasses measured in the Kruger National Park using a GER 3700 spectrometer. The biochemical absorption feature ($R_{2006\text{-}2196}$) in the shortwave infrared region is shown.

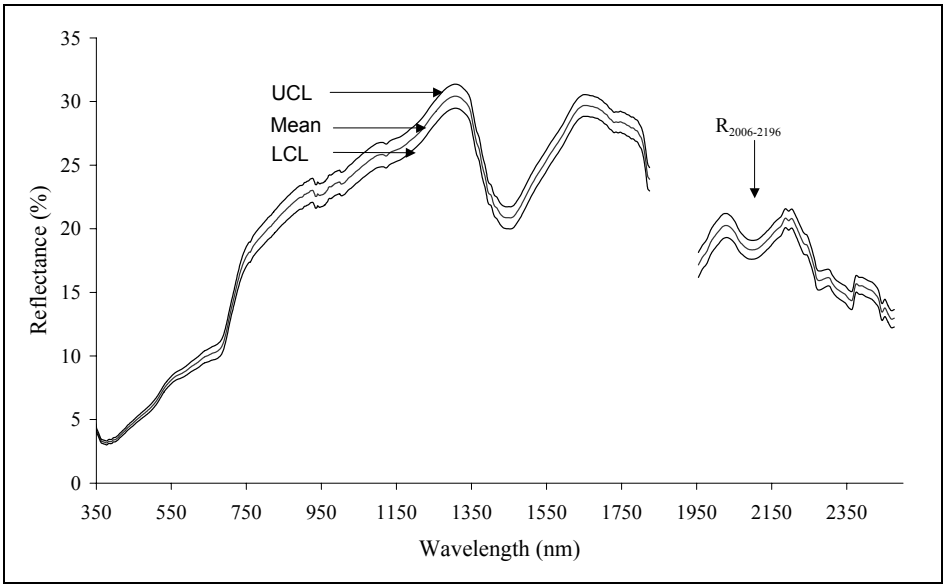

Figure 1.2 Mean reflectance spectrum (flanked by 95 % upper confidence limit (UCL) and 95 % lower confident limit (LCL)) of the data collected at canopy level in the Kruger National Park (n = 96) using a GER 3700 spectrometer. The $R_{2006-2196}$ biochemical absorption feature is shown. The spectral region between 1824 nm and 1954 nm was removed due to excessive noise.

The absorption of electromagnetic radiation in plants originates from the energy transition of the molecular vibration (rotation, bending and stretching) of the C-H, N-H, O-H, C-N and C-C bonds, which are the primary constituents of the organic compounds of plant tissues (Elvidge, 1990). The chemical constituents of the plant tissue determine the nature and number of bonds present. Therefore, the wavelengths and the amount of energy reflected from the plant are partly a function of the chemical composition of that plant material (Foley *et al.*, 1998). Table 1.1 lists the absorption features that have been related to particular foliar biochemical concentrations.

Using this theoretical background, research has focused on using remote sensing techniques such as those developed for laboratory near infrared spectroscopy (NIRS)(Norris *et al.*, 1976) to estimate foliar biochemicals (Foley *et al.*, 1998; Marten *et al.*, 1989). The extension of empirical laboratory NIRS to estimating foliar biochemicals at canopy level has had increasing attention as hyperspectral remote sensor systems of high quality became readily available (Kumar *et al.*, 2001; Gastellu-Etchegorry & Bruniquel-Pinel, 2001; Johnson *et al.*, 1994; Kupiec & Curran, 1995; Wessman *et al.*, 1989; Zagolski *et al.*, 1996).

However, the presence of water in fresh canopies masks the biochemical absorption features, particularly in the shortwave infrared (Clevers, 1999; Kokaly & Clark, 1999) and make the remote sensing of foliar biochemicals more difficult. In addition, leaf orientation and soil background

effects, as well as atmospheric absorption, further complicate the remote sensing of biochemicals at field level (Asner *et al.*, 2000). As a result, the extension of the laboratory-based spectroscopy to canopy level has yielded inconsistent results so far (Grossman *et al.*, 1996). The challenge is, therefore to develop techniques that can predict foliar quality at canopy level. This is the subject of this thesis.

Table 1.1: Absorption features related to particular biochemicals: (Curran, 1989; Elvidge, 1990; Himmelsbach *et al.*, 1988; Kumar *et al.*, 2001)

Wavelength (nm)	Absorbing Compounds	Absorption Mechanism
430	Chlorophyll a	Electron transition
460	Chlorophyll b	Electron transition
640	Chlorophyll b	Electron transition
660	Chlorophyll a	Electron transition
910	Protein	C-H stretch, 3rd overtone
930	Oil	C-H stretch, 3rd overtone
970	Water, starch	O-H bend, 1st overtone
990	Starch	O-H stretch, 2nd overtone
1020	Protein	N-H stretch
1040	Oil	C-H stretch, C-H deformation
1120	Lignin	C-H stretch, 2nd overtone
1200	Water, cellulose, starch, lignin	O-H bend, 1st overtone
1400	Water	O-H bend, 1st overtone
1420	Lignin	C-H stretch, C-H deformation
1450	Starch, sugar, water, lignin	O-H stretch, 1st overtone C-H stretch, C-H deformation
1490	Cellulose, sugar	O-H stretch, 1st overtone
1510	Protein, nitrogen	N-H stretch, 1st overtone
1530	Starch	O-H stretch, 1st overtone
1540	Starch, cellulose	O-H stretch, 1st overtone
1580	Starch, sugar	O-H stretch, 1st overtone
1690	Lignin, starch, protein	C-H stretch, 1st overtone
1730	Protein	C-H stretch
1736	Cellulose	O-H stretch
1780	Cellulose, sugar, starch	C-H stretch, 1st overtone O-H stretch, H-O-H deformation
1820	Cellulose	O-H stretch, C-O stretch
1900	Starch	O-H stretch, C-O stretch
1924	Cellulose	O-H stretch, O-H deformation
1940	Water, protein, lignin, cellulose, Starch, nitrogen	O-H stretch, O-H deformation
1960	Starch, sugar	O-H stretch, O-H rotation
1980	Protein	N-H asymmetry
2000	Starch	O-H deformation, C-O deformation
2060	Protein, nitrogen	N-H stretch, N=H rotation
2080	Starch, sugar	O-H stretch, O-H deformation
2100	Starch, cellulose	O-H rotation, O-H deformation, C-O-C stretch
2130	Protein	N-H stretch
2180	Protein, nitrogen	N-H rotation, C-H stretch, C-O stretch, C=O stretch
2240	Protein	C-H stretch
2250	Starch	O-H stretch, O-H deformation
2270	Cellulose, sugar, starch	C-H stretch, O-H stretch, C-H rotation, CH_2 rotation
2280	Starch, cellulose	C-H stretch, CH_2 deformation
2300	Protein, nitrogen	C-H rotation, C=O stretch, N-H stretch
2310	Oil	C-H bend, 2nd overtone
2320	Starch	C-H stretch, CH_2 deformation
2340	Cellulose	C-H stretch, O-H deformation
2350	Cellulose, nitrogen, protein	CH_2 rotation, C-H deformation

1.5 Objectives of the thesis

The main objectives of this study were: (1) to investigate the potential of hyperspectral remote sensing in estimating biomass of tropical grasses at high canopy density or full canopy cover, and, (2) to develop techniques to predict and map the quality of tropical grasses at canopy level using hyperspectral remote sensing.

1.6 Scope of the study

This thesis investigates the potential of hyperspectral remote sensing to estimate tropical grass quality and quantity. However more emphasis is placed on the estimation and mapping of quality since the quantity of vegetation has been successfully estimated using coarser resolution satellite images, except for the saturation problem, which will be addressed in this thesis.

The potential of hyperspectral remote sensing to predict quality variables at canopy level is investigated, (i) under controlled laboratory conditions, (ii) at field level using a field spectrometer, and (iii) at airborne platform level. Although a number of quality variables (N, P, K, Ca, Mg and Na) were investigated at field level, we placed more emphasis on the prediction and mapping of nitrogen concentration from laboratory level up to airborne platform level. This is mainly because nitrogen is regarded as the most limiting nutrient for grazers (McNaughton, 1988; Prins, 1989; Prins & Olff, 1998). The Kruger National Park (KNP) in South Africa was used as a test site for both field and airborne spectrometry.

1.7 The study area

The study area stretches from west ($22^0 49'$ S and $31^0 01'$ E) to east, ($22^0 44'$ S and $31^0 22'$ E) covering an area of about 25 * 6 km in the far northern region of the Kruger National Park (Figure 1.3). This strip cuts across a basalt and granite landscape mosaic.

The granite areas are characterised by coarse sandy or gravelly soils with high infiltration rate and low clay forming potential. The uplands support broad – leaved savanna and a herbaceous layer dominated by moderate to low quality sandveld species. The midslopes (seepline areas) support few trees and a dense herbaceous layer. The base of the midslope and foot slope that are characterised by clay soils constitute thorny microphyllous shrubs and a productive grass layer (Grant *et al.*, 2000).

The basalt formations in the east are characterised by mafic rocks that are rich in iron, magnesium and rich clay minerals (Grant *et al.*, 2000). This eastern part is mainly characterised by grasslands. The study area was selected

to cover a wide range of terrain gradients and therefore a variation in foliar nutrient concentration.

Following the agreement signed on the 10th of November 2000 to form a Transfrontier National Park (Gaza-Kruger-Gonarezhou Transfrontier) between South Africa, Zimbabwe and Mozambique, traditional migration routes for wildlife were established. This agreement created a total area of around 95700 km^2, allowing the free movement of animals across a large area. Habitat condition, particularly nutrition therefore plays a significant role in determining the movement and distribution of wildlife in this area.

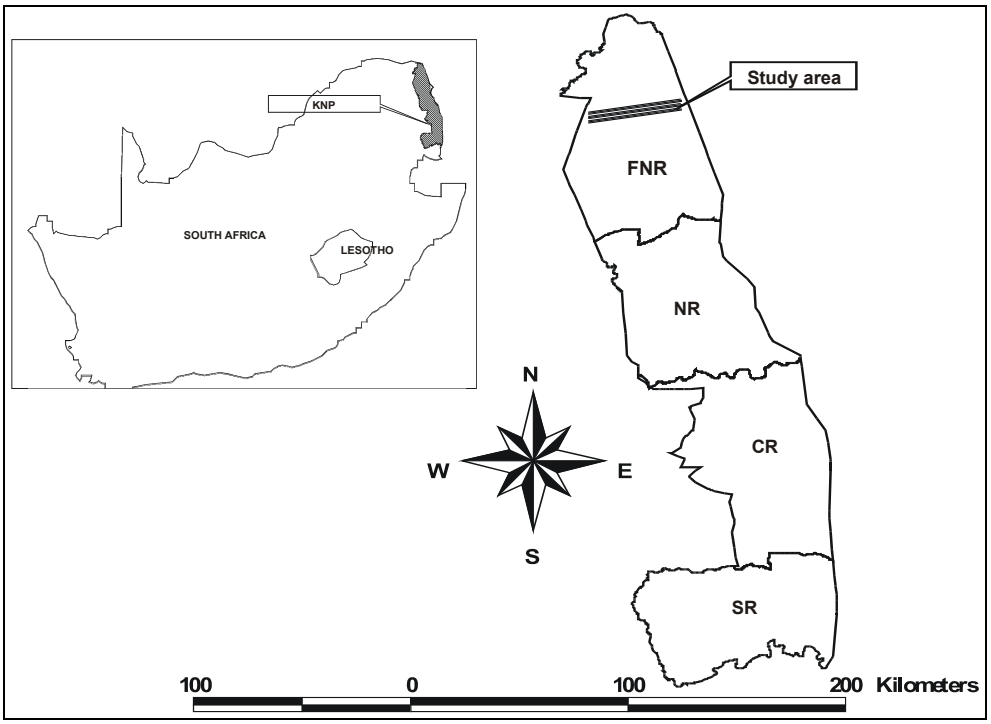

Figure 1.3: Location of the study area in the Kruger National Park (KNP) of South Africa. The study area is located in the far northern region (FNR), close to the Limpopo River and is characterised by grassland plains especially in the eastern part. The other administrative regions in the KNP are the northern region (NR), central region (CR) and the southern region (SR).

1.8 Outline of the thesis

This thesis constitutes a collection of 8 papers that have been submitted to peer reviewed international journals. Out of these 8 papers, 6 papers have been accepted for publication and the remaining 2 papers are still in preparation and preliminary review respectively. Each paper has been presented as a stand-alone chapter, making it a distinct piece of work contributing to the overall research

question. As much as possible, the content of the journal papers have been maintained. In this regard, each chapter is introduced separately with separate conclusions that link with the subsequent chapters. The approach makes some overlaps of method description and illustrations inevitable in the different chapters. This drawback is deemed to be of little significance when we consider the critical peer review process and it makes the different chapters solid papers that can be read individually without losing the context. The chapters are presented under three different levels of investigation:

1.8.1 Laboratory level

Chapter 2 addresses the problem of saturation in biomass estimation using experimental data. Widely used indices (NDVI, TVI, SR) are applied on hyperspectral bands to identify the most important portions of the electromagnetic spectrum that contain biomass information at high canopy density. New indices are proposed.

Chapter 3 investigates whether canopy reflectance can discriminate different levels of foliar nitrogen concentration at canopy level. The concept of continuum removal is introduced and the importance of the visible region in canopy chemistry is demonstrated. Chapter 4 investigates the red edge as an important portion of the electromagnetic spectrum for predicting nitrogen concentration at canopy scale. Chapter 5 extends the observations made in chapter 3 and chapter 4 to HYMAP spectra (resampled resolution). The observations in chapters 3, 4 and 5 permit the up scaling of the approach to field as well as airborne imaging spectrometry.

1.8.2 Field level

Chapter 6 investigates new methods to predict macronutrients in a savanna rangeland using a field spectrometer. Chapter 7 extends the methods to foliar sodium. This nutrient (sodium in plants) was singled out since its importance has been overlooked in ecological studies and to the best of our knowledge, hardly investigated in remote sensing. To put the variations of macronutrients measured in an ecological context, chapter 8 explains the spatial distribution of the nutrients using several biotic and abiotic factors.

1.8.3 Airborne platform level

Chapter 9 uses observations and conclusions from chapter 3 to chapter 8 to develop a new approach for mapping nitrogen concentration using airborne hyperspectral imagery.

Finally, chapter 10 summarises all the findings and discusses the contribution of the thesis in the context of herbivory.

CHAPTER 2:
Estimating quantity at full canopy cover

*This chapter is based on

Mutanga, O and Skidmore, A.K, (2004) Narrow band vegetation indices overcome the saturation problem in biomass estimation, *International Journal of Remote Sensing*, 25, pp. 1-16.

Abstract

Remotely sensed vegetation indices such as NDVI, computed using the red and near infrared bands have been used to estimate grass biomass. These indices are of limited value since they saturate in dense vegetation. In this study, we evaluated the potential of narrow band vegetation indices in characterizing the biomass of *C. ciliaris* grass measured at full canopy cover. Three indices were tested: modified normalised difference vegetation index (NDVI), simple ratio (SR) and transformed vegetation index (TVI) involving all possible two band combinations between 350 nm and 2500 nm. In addition, we evaluated the potential of the red edge position in estimating biomass at full canopy cover. Results indicated that the standard NDVI involving a strong chlorophyll absorption band in the red region and a near infrared band performed poorly in estimating biomass (R^2 = 0.26). The modified NDVIs involving a combination of narrow bands in the shorter wavelengths of the red edge (700 nm – 750 nm) and longer wavelengths of the red edge (750 nm – 780 nm), yielded higher correlations with biomass (mean R^2 = 0.77 for the highest 20 narrow band NDVIs). When the three vegetation indices were compared, SR yielded the highest correlation coefficients with biomass as compared to narrow band NDVI and TVI (average R^2 = 0.80, 0.77 and 0.77 for the first 20 ranked SR, NDVI and TVI respectively). The red edge position yielded an R^2 of 0.66, which is better than the result obtained from the standard NDVI. These results indicate that at high canopy density, grass biomass may be more accurately estimated by vegetation indices based on wavelengths located in the red edge than the standard NDVI.

Key words: Laboratory experiment, red edge, canopy spectra, widely used indices, saturation problem

2.1 Introduction

Remotely sensed vegetation indices have been recommended to remove variability caused by canopy geometry, soil background, sun view angles and atmospheric conditions when measuring biophysical properties (biomass, LAI and percent green vegetation cover) of vegetation at canopy scale (Blackburn & Steele, 1999; Boegh *et al.*, 2002; Elvidge & Chen, 1995; Gao *et al.*, 2000; Schowengerdt, 1983; Tucker, 1979). These indices are critical for assessing rangeland productivity and therefore facilitate effective management of livestock and wildlife.

The most widely used vegetation indices are computed using data from the red and near infrared (NIR) portions of the electromagnetic spectrum (Treitz & Howarth, 1999). These vegetation indices operate by contrasting intense chlorophyll pigment absorptions in the red against the high reflectance due to multiple scattering in the near infrared (Elvidge & Chen, 1995; Hoffer, 1978; Todd *et al.*, 1998). Widely used vegetation indices such as normalised difference vegetation index (NDVI)(Tucker, 1979; Wiegand *et al.*, 1991), transformed vegetation index (TVI)(Richardson & Wiegand, 1977; Rouse *et al.*, 1973), simple ratio (SR)(Jordan, 1969; Maxwell, 1976) and difference vegetation index (DVI) respond to these differences in the near infrared and the visible regions (Lillesand and Kiefer 1994, Schowengerdt 1983). In addition, indices that control for variations in soil background effects as well as atmospheric induced variations have also been developed. These include the perpendicular vegetation index (PVI)(Richardson & Wiegand, 1977), weighted difference vegetation index (WDVI) (Clevers, 1988), soil adjusted vegetation index (SAVI)(Huete, 1988), transformed soil adjusted vegetation index (TSAVI)(Baret & Guyot, 1991) and modified normalised difference vegetation index (MNDVI) (Liu and Huete 1995).

The major limitation of using vegetation indices particularly NDVI based on the red and near infrared portion of the electromagnetic spectrum is that they asymptotically approach a saturation level after a certain biomass density or LAI (Gao *et al.*, 2000; Sellers, 1985; Thenkabail *et al.*, 2000; Todd *et al.*, 1998; Tucker, 1977). NDVI yields poor estimates in areas where there is 100 % vegetation cover and therefore, has limited value in assessing biomass during the peak of seasons (Thenkabail *et al.*, 2000). Given this limitation, there is a need to develop or improve techniques that can accurately estimate biomass in more densely vegetated areas. Hyperspectral remote sensing offer possibilities to investigate vegetation indices based on narrow bands in the whole electromagnetic spectrum (350 nm – 2500 nm), rather than focusing on the red and near infrared bands alone.

Studies have shown that narrow bands located in the red edge (680 nm – 750 nm) are influenced by canopy biomass (LAI), and leaf chlorophyll content (Blackburn & Pitman, 1999; Guyot *et al.*, 1992; Thomas & Gaussman, 1987; Todd *et al.*, 1998). The red edge can be defined as the rise of

reflectance at the boundary between the chlorophyll absorption feature in the red wavelengths and leaf scattering in the near infrared wavelengths (Collins, 1978; Horler *et al.*, 1983). Todd *et al.* (1998) found out that the red edge position (the point of maximum slope on the red infrared curve) appears to be sensitive to biomass variations for green vegetation as compared to senescing vegetation. Lucas *et al.* (2000) found a strong correlation between LAI and the red edge position for a conifer forest in Wales using CASI data. From this background, narrow wavelengths offer potential to estimate biomass at high canopy density as compared to broadband indices computed using the red and near infrared wavelengths.

In this study we evaluated the performance of various hyperspectral vegetation indices as well as the red edge position in characterizing grass biomass in densely vegetated canopies. We selected and calculated band ratios that are widely used and readily adaptable in vegetation studies (Richards, 1993; Schowengerdt, 1983; Thenkabail *et al.*, 2000), *vis*, narrow band normalized vegetation index (NDVI), simple ratio (SR) and transformed vegetation index (TVI) involving all possible two-band combinations of 647 channels between 350 nm and 2500 nm. The band ratios were calculated from reflectance measurements taken on *C. ciliaris* grass at full canopy cover and under controlled laboratory conditions. In this regard, other vegetation indices that control for soil background and atmospheric effects such as SAVI, TSAVI, PVI, WDVI and MNDVI were not considered.

2.2 Methods

2.2.1 Experimental setup

Blue Buffalo grass (*C. ciliaris*) was sown in a greenhouse for this experiment. *C. ciliaris* is a sweet perennial grass that grows naturally in East and Southern Africa and is widely used as a pasture grass (Van Oudtshoorn, 1999). The grass forms swards that range between 10 cm and 150 cm in height. *C. ciliaris* is tufted, erect, branching and rooting at the nodes (Bovey *et al.*, 1984; Mayeux & Hamilton, 1983).

A total of 96 pots (10 liters with a diameter of 24 cm and a height of 22 cm) were used for planting. Five seeds were sown in each pot on 30 July 2001. The seedlings were grown under natural daylength with a night temperature of 21º C and a day temperature of 25º C. The plants were supplied with an initial fertilization of 2.2 g of potassium and 3.6 g of super phosphate per pot and were watered at least once every day.

In order to manipulate a variation in biomass, the pots were randomly divided into three equal groups (32 samples in each group) on 13 August 2001 (14 days after sowing) and were supplied with different levels of nitrogen. The first group was supplied with 3.4 ml (120 kg/ha) of ammonium nitrate per pot.

The second group was supplied with 1.14 ml (40 kg/ha) of ammonium nitrate per pot. The fertilizer was supplied over several days. No nitrogen was added to the third group. To minimize the effect of microclimate on the experiment, the pots were arranged in blocks and were randomized and rotated by about 90 degrees once a week.

2.2.2 Canopy spectral measurements

Measurements were taken after the grass biomass had become dense and completely covered the soil thereby controlling for multiple scattering interactions between the soil and vegetation. In addition, we used the same soil type for all treatments. In order to manipulate a further variation in biomass, measurements were taken at the beginning of every week for four weeks, from September 3rd 2001. The plants were transferred in their pots from the greenhouse to a laboratory on each day of measurement in order to control for atmospheric effects as well as to achieve uniform illumination conditions. A total of eight pots from each treatment were measured every week.

A GER 3700 spectroradiometer was used for spectral measurements. The GER 3700 (Geophysical and Environmental Research Corp.) is a three dispersion grating spectroradiometer using Si and PbS detectors with a single field of view. The wavelength range is 350 nm - 2500 nm with a resolution of 1.5 nm in the 350 nm - 1050 nm, 6.2 nm in the 1050 nm - 1900 nm range and 9.5 nm in the 1900 nm - 2500 nm range. The sensor, with a field of view of 3º was mounted on a tripod in the laboratory and positioned 2 meters above the ground at nadir position. Each pot with standing biomass was placed on a fixed tray, directly under the sensor and a halogen lamp, positioned next to the sensor was used to supply illumination on the target.

The pots were rotated by 45º after every 5th measurement in order to average out differences in canopy orientation on each pot. The radiance was converted to reflectance using scans of a spectralon reference panel. Four target measurements were made after measuring the reference (spectralon) panel.

After spectral measurements, all standing biomass from each pot was clipped and fresh biomass was measured immediately using a digital weighing scale. Biomass was determined by dividing the weight of the harvested grass by the surface area of the pots (expressed as g cm^{-2}) (Hurcom & Harrison, 1998).

2.2.3 Data analysis

Two main approaches were adopted in this study: (i) narrow band vegetation indices and (ii) the red edge position.

The narrow band vegetation indices (NDVI, TVI, SR) were computed from all possible two – band combination indices involving 647 narrow bands between 350 nm and 2500 nm. The discrete 647 narrow bands allowed a computation of N*N = 418,609 narrow band indices. Table 2.1 shows the indices that were

calculated. The narrow bands are shown as λ_1 (350 nm to 2500 nm) and λ_2 (350 nm to 2500 nm) pairs. These indices were selected because they are the most widely used indices in estimating biomass for agricultural and ecological applications (Thenkabail *et al.*, 2000). The indices were calculated covering the whole electromagnetic spectrum in order to recommend on the optimal narrow bands that can be used to estimate biomass.

Table 2.1. Vegetation indices used in this study. The narrow bands are computed as λ_1 (350 nm to 2500 nm) and λ_2 (350 nm to 2500 nm) pairs

Index name	Abbreviation	Computation	Reference
Normalized difference vegetation index	NDVI	$\frac{\lambda_1 - \lambda_2}{\lambda_1 + \lambda_2}$	(Rouse *et al.*, 1973)
Simple ratio	SR	$\frac{\lambda_1}{\lambda_2}$	(Jordan, 1969)
Transformed vegetation index	TVI	$\sqrt{\frac{\lambda_1 - \lambda_2}{\lambda_1 + \lambda_2} + 0.5}$	(Rouse *et al.*, 1973)

To compare the predictive capability of the modified NDVI and the standard NDVI in estimating biomass, bootstrapping was applied on the correlation analyses. Bootstrapping is a technique used to resample the original data in order to generate a distribution for the statistic. This permits the calculation of standard error and confidence intervals, which in turn indicate statistical accuracy (Efron & Tibshirani, 1994; McGarigal *et al.*, 2000). Bootstrapping simulates the sampling distribution of any statistic by treating the observed data as if it were the entire statistical population under study. On each replication, a random sample of size N is selected, with replacement from the available data. The statistic of interest (in this case correlation coefficient) is calculated on this bootstrapped subsample and recorded. The process is repeated in order to obtain the sampling distribution. The main advantage of bootstrapping is that statistical inferences under resampling are based on the distributional properties of a "pseudosample" that is generated by resampling the data itself, and not the distributional properties of a sample drawn from an unknown underlying population (McGarigal *et al.*, 2000). The method therefore facilitates accuracy assessment using the same data set.

The red edge position was derived from the first derivative of the reflectance between 680 nm and 750 nm. A first difference transformation of the reflectance spectrum calculates the slope values from the reflectance and can be derived from the following equation (Dawson & Curran, 1998):

$$FDS_{\lambda(i)} = (R_{\lambda(j+1)} - R_{\lambda(j)}) / \Delta\lambda \quad (1)$$

where FDS is the first derivative reflectance at a wavelength *i* midpoint between wavebands j and j+1. $R_{\lambda(j)}$ is the reflectance at the j waveband, $R_{\lambda(j+1)}$ is the reflectance at the j+1 waveband and $\Delta\lambda$ is the difference in wavelengths between j and j+1. The red edge position was determined as the wavelength inflection point (i.e., point of maximum slope).

2. 3. Results

2. 3.1 Variation in biophysical data and the reflectance spectrum

As expected, the fertilization treatments caused a wide variation in biomass (Table 2.2).

Table 2.2. Description of the data used in this study (total n = 96)

Treatment	No of samples	Minimum g cm $^{-2}$	Mean g cm $^{-2}$	Maximum g cm $^{-2}$	StDev
Low	32	0.21	0.32	0.41	0.05
Medium	32	0.29	0.40	0.53	0.06
High	32	0.33	0.52	0.66	0.08
All combined	96	0.21	0.41	0.66	0.10

Biomass varied between 0.2 g cm $^{-2}$ and 0.66 g cm $^{-2}$ with an average of 0.4 g cm $^{-2}$. Previous studies have revealed that the saturation or curvature in biomass versus the NDVI indices is usually around 2 or 3 LAI (Franklin *et al.*, 1991) and for biomass, around 0.3 g cm $^{-2}$ (Hurcom & Harrison, 1998). The average biomass (0.32 g cm $^{-2}$) recorded in the low nitrogen treatment (Table 2.2) had enough leaf material to cover the soil in the pots and above the saturation threshold level, therefore achieving the main objective of the experiment.

Spectra of the mean reflectance and ± 95 confidence limits of all harvested plants are shown in Figure 2.1. Like any green vegetation spectrum, the average spectrum in Figure 2.1 shows high reflectance in the near infrared and low reflectance in the visible. However, NIR reflectance values are lower than the values for green vegetation, which are generally around 40 %. This can be attributed to the erectophile structure of the grass canopies, which were measured, and their associated shadow effect at nadir position (Sandmeier *et al.*, 1998). Studies have shown that, near infrared reflectance is suppressed in a complex canopy due to increased shadow (Sandmeier & Deering, 1999; Sandmeier *et al.*, 1998; Treitz & Howarth, 1999).

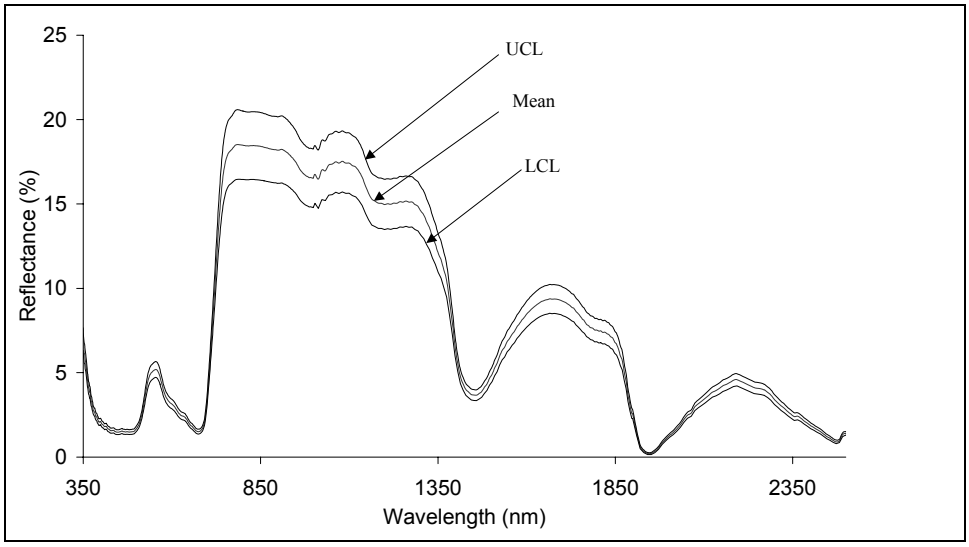

Figure 2.1. Canopy reflectance spectra of *C. ciliaris* grass (n = 96). The mean, upper 95 % confidence limit (UCL) and lower 95 % confidence limit (LCL) of the spectra are shown.

2.3.2 Narrow band NDVI relationship with biomass

The narrow band hyperspectral data contained in 647 discrete channels allowed the computation of 418,609 narrow band NDVIs for biomass estimation. Linear regression coefficients R and R^2 between all two possible narrow band NDVIs and biomass were determined. Results of this analysis are presented in form of R^2 for each λ_1 (350 nm to 2500 nm) and λ_2 (350 nm to 2500 nm) pair in Figure 2.2.

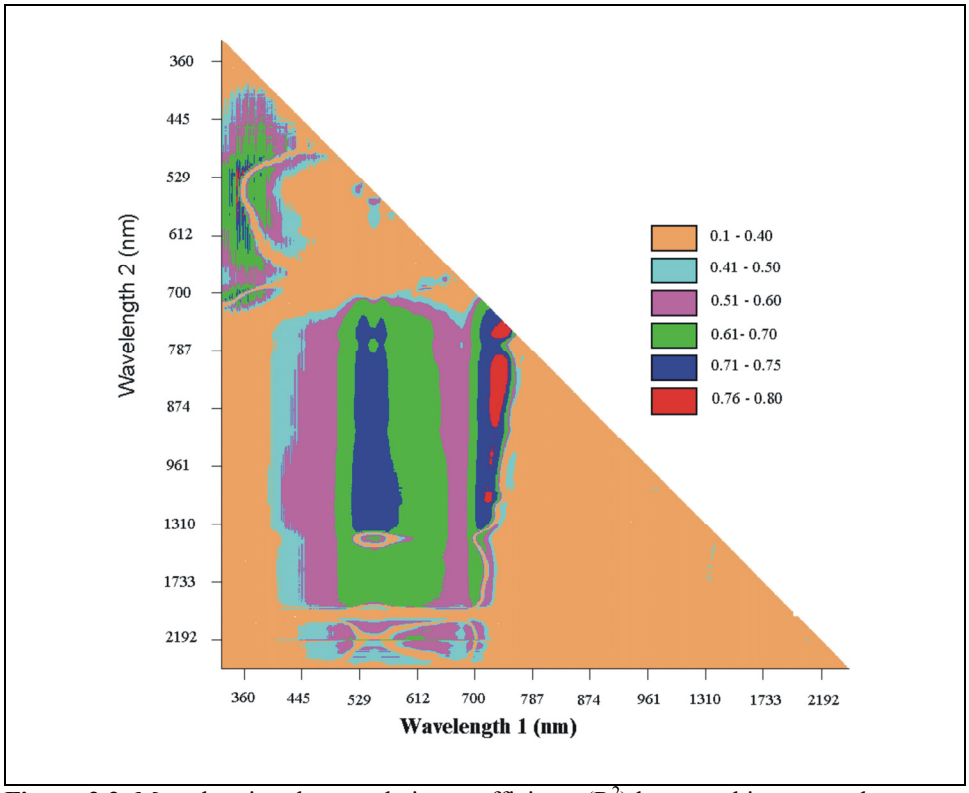

Figure 2.2. Map showing the correlation coefficients (R^2) between biomass and narrow band NDVI values calculated from all possible combinations spread across λ_1 (350 nm to 2500 nm) and λ_2 (350 nm to 2500 nm). The R^2 values, were ranked and the first 20 combinations recorded in Table 2.2.

The R^2 values range between 0.10 and 0.78 reflecting the wide variation in strength of the relationship between NDVIs and biomass. Figure 2.2 shows strong correlations in the portion where shorter wavelengths of the red edge (700 nm – 745 nm) coincided with narrow bands between 750 nm and 900 nm. The second highest R^2 values are centred in the green band, 500 nm – 560 nm, combined with narrow bands in the near infrared portion, 750 nm and 1300 nm. Poor correlation coefficients were obtained beyond 1300 nm.

The correlation coefficients were ranked and two band combinations that yielded the highest 20 R^2 values were recorded as shown in Table 2.3. The narrow wavelength bands that yielded the best 20 R^2 values are located in the red edge portion between 703 nm and 760 nm.

Table 2.3. Two-band combinations (NDVIs) that yielded the highest correlation coefficients (ranked according to R^2) with biomass. A total of 418,609 NDVIs, computed from all possible two-band combinations between 350 nm and 2500 nm were correlated with biomass.

Rank	λ_1	λ_2	R	R^2
1	746	755	0.886	0.784
2	741	753	0.885	0.783
3	735	759	0.885	0.783
4	731	759	0.884	0.782
5	732	757	0.884	0.781
6	721	762	0.883	0.780
7	728	757	0.883	0.779
8	729	755	0.883	0.779
9	716	762	0.882	0.779
10	721	759	0.882	0.779
11	713	762	0.882	0.779
12	716	759	0.882	0.778
13	710	760	0.882	0.778
14	703	763	0.882	0.778
15	715	759	0.882	0.777
16	703	762	0.882	0.777
17	707	760	0.882	0.777
18	727	753	0.881	0.777
19	706	760	0.881	0.777
20	699	762	0.881	0.777

For a detailed investigation, we compared the best-modified narrow band NDVI (746 nm and 755 nm) obtained in this study and an NDVI involving a near infrared narrow band (833 nm) and a red band (680 nm)(Hurcom & Harrison, 1998). Figure 2.3 illustrates the scatter plots obtained from the two indices. The slope of the regression line for the standard NDVI is lower than that of the modified NDVI. To confirm this, we tested the research hypothesis that the slope of the regression model for the modified NDVI was different from the slope of the standard NDVI, *viz*. the null hypothesis Ho: $\beta_1 = \beta_2$ versus the alternate hypothesis Ha: $\beta_1 \neq \beta_2$, where β_1 and β_2 are slopes for the modified NDVI and standard NDVI respectively. The conclusion from this test is that the slopes from the two models are different ($t = 20.35$, $p < 0.001$, $df = 188$).

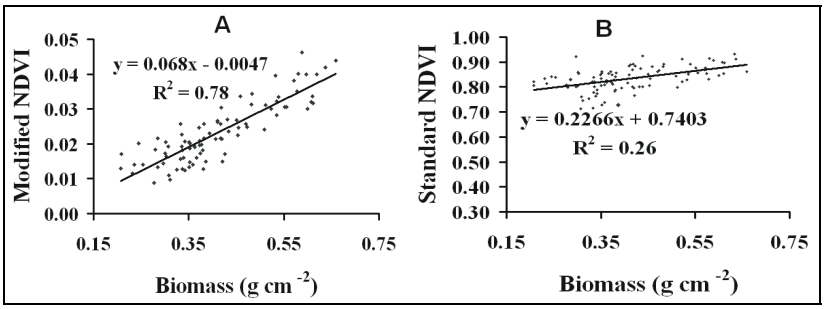

Figure 2.3. Relationship between biomass and the best-modified NDVI (A) calculated from 746 and 755 nm bands as well as the standard NDVI calculated from a near infrared (833 nm) and red band (680 nm) (B). Note the almost flat scatter plot in B (n = 96).

In order to test the performance of the modified NDVI versus the standard NDVI, bootstrapping was applied on the regression models. The bootstrapped correlation coefficients are shown in Table 2.4.

Table 2.4. Bootstrapped coefficients of determination between biomass and the standard NDVI (NIR - red) as well as the best NDVI obtained from an analysis of all possible combinations involving narrow bands between 350 nm – 2500 nm

Index	Mean r^2	95% confidence
Best modified NDVI	0.78	0.001
Standard NDVI	0.25	0.008

Results indicate poor performance of a NIR-red NDVI (standard NDVI) combination as compared to a red edge NDVI combination. The confidence limits for the modified NDVI are lower than those for the standard NDVI. This implies that the bootstrapped mean of the modified NDVI approaches the population estimate with a high precision. Figure 2.4 shows the distribution of R^2 values of the modified NDVI after bootstrapping. Note that the confidence limits are close to the mean.

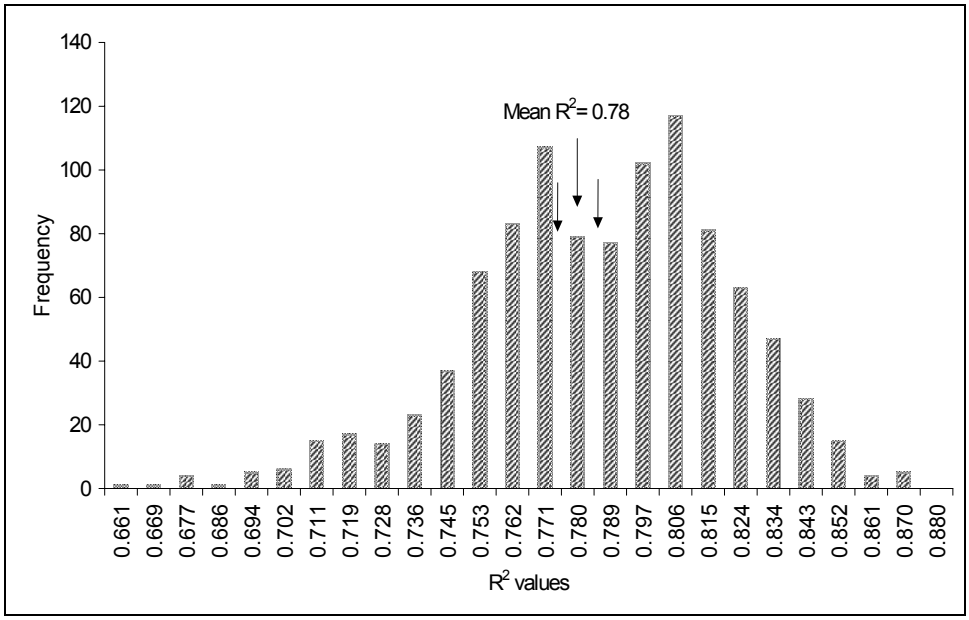

Figure 2.4. Histogram showing the bootstrapped correlation coefficients between the biomass and the modified NDVI (based on 746 nm and 755 nm). A total of 1000 iterations were executed. Two arrows indicating the upper and lower 95 % confidence limits flank the mean.

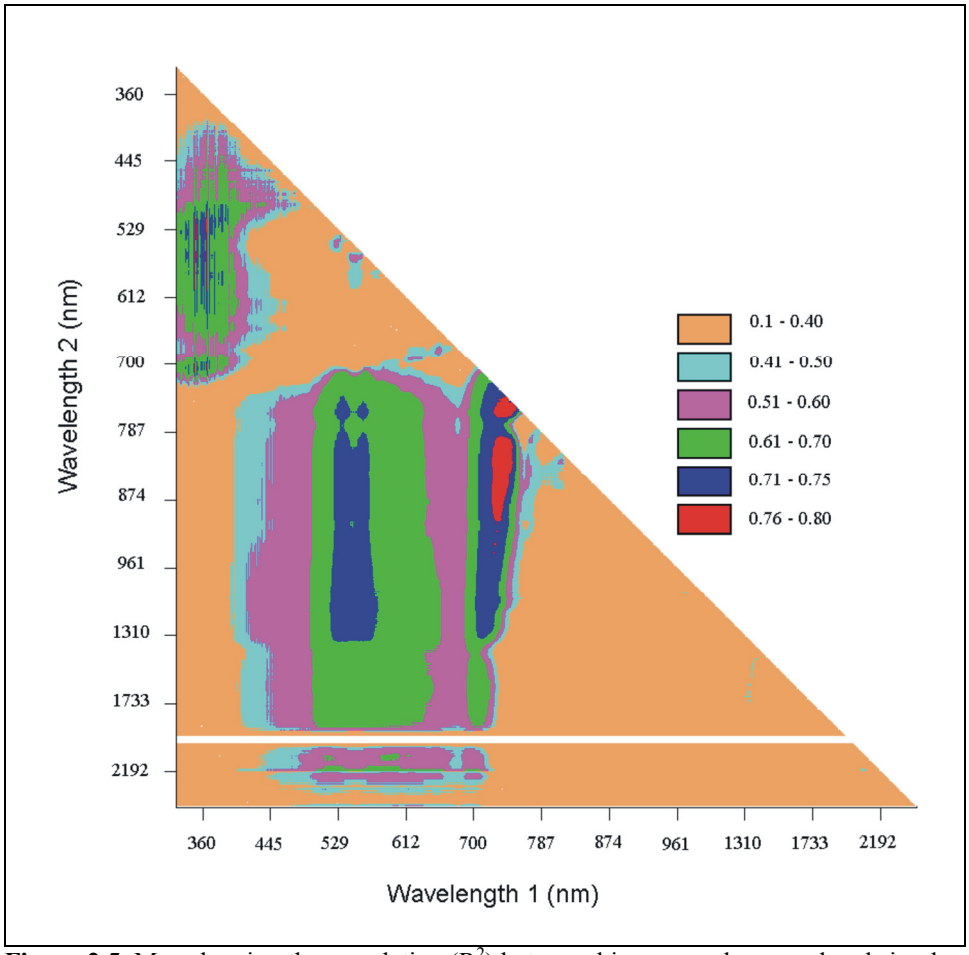

Figure 2.5. Map showing the correlation (R^2) between biomass and narrow band simple ratio (SR) values (n = 96) calculated from all possible combinations spread across λ_1 (350 nm to 2500 nm) and λ_2 (350 nm to 2500 nm).

2.3.3 Narrow band simple ratio (SR) relationship with biomass

The simple ratio index was calculated on all possible two - band combinations involving 647 discrete channels between 350 nm and 2500 nm. The correlation coefficients R^2 obtained between SR and biomass are presented in Figure 2.5. The R^2 values ranged from 0.10 to 0.80 and the pattern of variation in R^2 generally resembles the NDVI pattern in Figure 2.2. The highest R^2 values are also located in the red edge region. The SR combinations were also ranked and the highest 20 combinations recorded (not presented here). The SR combination that yielded the highest R^2 of 0.80 involved 706 nm and 755 nm channels, followed by 702 nm and 753 nm channels. The best 20 SR indices

also involved the green portion (572 nm, 543 nm and 548 nm), combined with the shortwave infrared bands (2464 nm, 2154 nm, 2336 nm).

2.3.4 Narrow band transformed vegetation index (TVI) relationship with biomass

Figure 2.6 depicts R^2 values for the linear relationship between biomass and TVI. The map in Figure 2.6 is slightly different from the NDVI and SR maps. There are lower correlations in the green portion, 500 nm – 560 nm, combined with narrow bands in the longer red edge portion, 750 nm – 1200 nm.

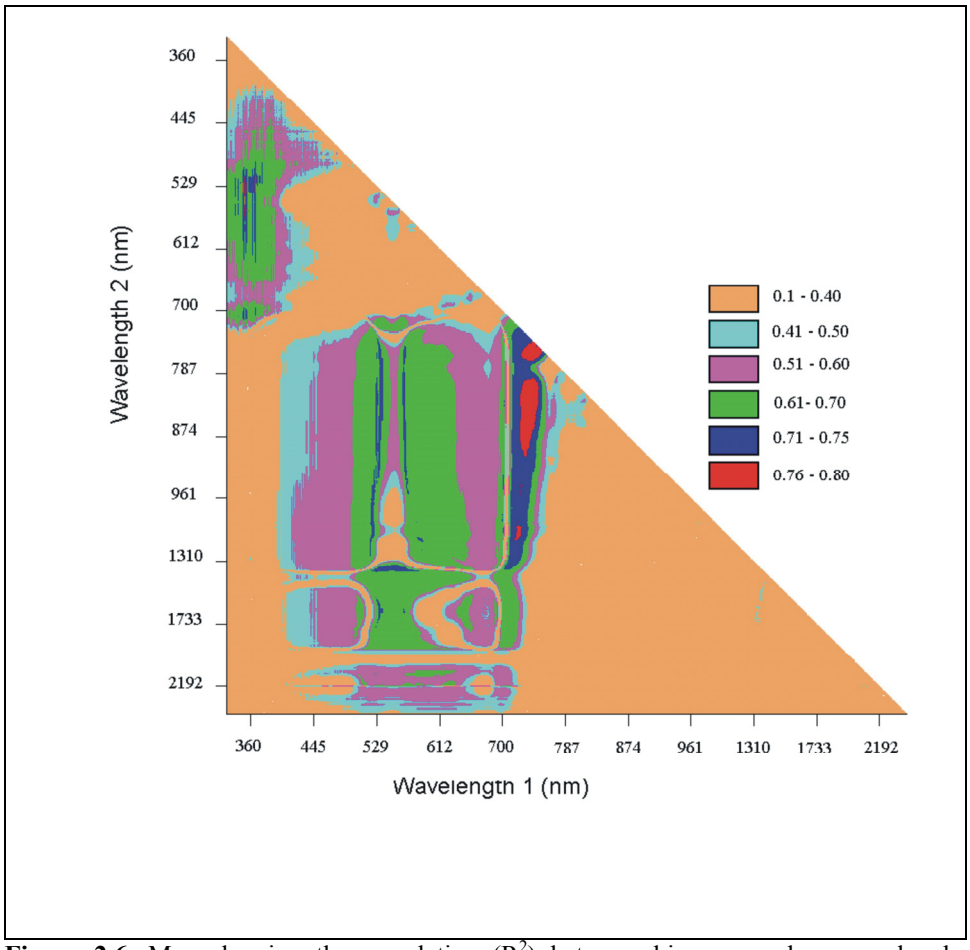

Figure 2.6. Map showing the correlation (R^2) between biomass and narrow band Transformed vegetation index (TVI) values (n = 96) calculated from all possible combinations spread across λ_1 (350 nm to 2500 nm) and λ_2 (350 nm to 2500 nm).

However, the ranked TVI pairs, which yielded the highest 20 correlation coefficients with biomass, are all located in the red edge region, between 722 and 760 nm. Figure 2.7 summarizes the frequently occurring optimum bands using the NDVI, SR and TVI methods.

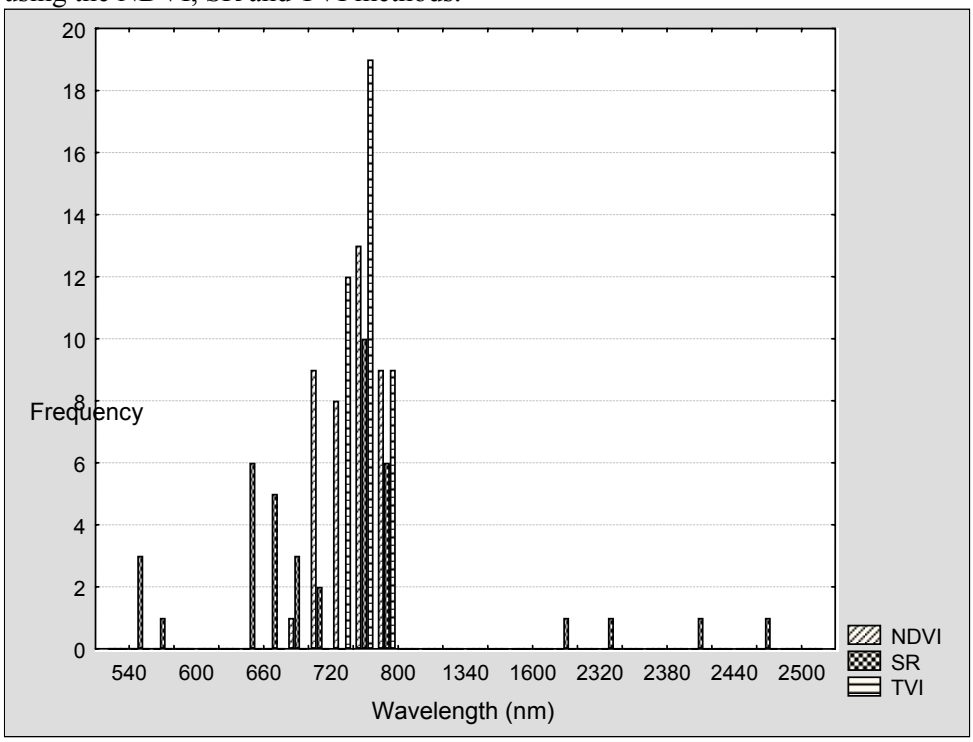

Figure 2.7. Occurrence of the hyperspectral narrow bands in the best 20 models for each index

Figure 2.7 clearly shows that an overwhelming proportion of biomass information is contained in the red edge portion, (680 nm to 780 nm) and the green portion (530 to 560 nm). TVI and NDVI show a larger proportion in the red edge region between 720 nm and 760 nm. Narrow channels selected by the SR are widely spread, covering the green, red and the short wave infrared portion of the electromagnetic spectrum.

2.3.5 Comparing the performance of the indices in estimating biomass

The three methods applied in this study yielded slightly different results. The R^2 values increased from 0.784, 0.785, to 0.80 using NDVI (R_{755}- R_{746} /R_{755}+ R_{746}), TVI ($\sqrt{\frac{R_{755}-R_{752}}{R_{752}+R_{755}}+0.5}$) and SR ($R_{755}$ /R_{706}), respectively.

Box plots in Figure 2.8 show the spread of the ranked correlation coefficients (highest 20 R^2) produced by different ratios involving all possible narrow band combinations stretching from 350 nm to 2500 nm.

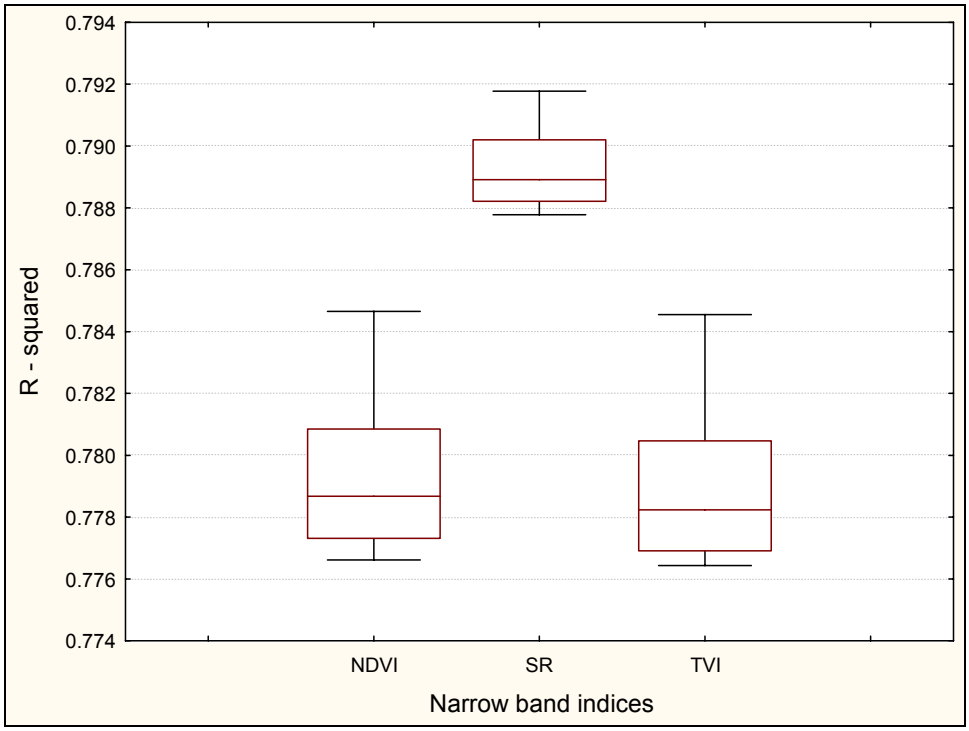

Figure 2.8. Box plots showing the spread of the ranked correlation coefficients (First 20 R^2) produced by different ratios involving all possible narrow band combinations stretching from 350 nm to 2500 nm

The box plots show that SR yielded the highest mean R^2 for the first 20 narrow band combinations as compared to NDVI and TVI. The mean R^2 differences were tested using one – way ANOVA, following normality test of the data using Kolmogrov-Sminov test ($p > 0.05$). We tested the hypothesis that the mean R^2 for NDVI, SR and TVI was different, *viz.* the null hypothesis Ho: $\eta_1 = \eta_2 = \eta_3$ versus the alternate hypothesis Ha: $\eta_1 \neq \eta_2 \neq \eta_3$, where: η_1, η_2 and η_3 are the mean coefficients of determination for NDVI, SR and TVI respectively. The conclusion from this test is that the indices yielded different R^2 ($p < 0.001$). One - way ANOVA only shows that there is a significant difference in the mean coefficients of determination obtained using the three methods, but it does not show which pairs are different. We therefore executed a post hoc Scheffe test in order to establish differences between each pair. Results indicated that the mean R^2 for SR is significantly different from those obtained by NDVI and TVI ($p < 0.05$). However results of NDVI and TVI are not significantly different ($p > 0.05$).

2.3.6 The Red edge position and its relationship with biomass

The correlation between the red edge position and biomass yielded a coefficient of determination (R^2) of 0.66 ($p < 0.001$). The result from the red edge position is lower than the results obtained by the best narrow band NDVI ($R^2 = 0.78$). However, the result from the red edge position is better compared to the result obtained by the standard NDVI, thereby confirming the utility of the information contained in the red edge to estimate biomass at full canopy cover.

2.4. Discussion

The problem of asymptotic saturation of vegetation indices is common on satellite multispectral imagery. This is particularly true for grassland or agricultural imagery (Tucker, 1977). As the growing season progresses and biomass increases, the canopy spectral reflectance in certain parts of the electromagnetic spectrum reaches an asymptotic spectral reflectance making widely used remotely sensed indices less effective. Results of this study indicate that we can overcome this problem by using novel narrow band indices to extract biomass information in areas of dense vegetation with a high degree of accuracy.

2.4.1 Relationship between the narrow band indices and biomass

The wide range in R^2 values indicates that the narrow band combinations respond differently to a variation in biomass. The study has shown that biomass information is not only contained in the red absorption and near infrared wavelengths. Most narrow bands selected by NDVI, SR and TVI, that yielded the highest correlation with biomass are located in the red edge (Figure 2.7). In addition the red edge position yielded high correlation coefficient with biomass. The red edge denotes a region of transition from strong chlorophyll absorption to near infrared reflectance. High correlations in this study were largely obtained by combining narrow bands from the shorter wavelengths of the red edge portion of the electromagnetic spectrum (700 nm - 750 nm) and the longer wavelengths of the red edge (750 nm – 800 nm). The shorter wavelengths of the red edge portion are sensitive to changes in chlorophyll content (Filella & Penuelas, 1994; Lichtenthaler *et al.*, 1996). At longer wavelengths of the red edge portion, multiple scattering from leaf layers results in higher reflectance (Kumar *et al.*, 2001). This confirms strong correlations between the red edge and LAI or biomass (Blackburn & Pitman, 1999; Clevers *et al.*, 2000; Filella & Penuelas, 1994; Todd *et al.*, 1998).

The almost flat scatter plot in Figure 2.3b indicates the asymptotic nature of the standard NDVI computed from a near infrared band and a strong chlorophyll absorption band as compared to high correlations obtained using the red edge bands (Figure 2.3a) for high biomass situations. Filella and Penuelas

(1994) also found strong correlations between LAI and the red edge position. The result in this study demonstrates the validity and significance of the red edge ratios and red edge position as indicators of the biophysical properties of vegetation as compared to the standard NDVI.

The saturation of the relationship between biomass and the standard NDVI is a well-known problem (Gao *et al.*, 2000; Tucker, 1977). However, the physical basis for this asymptotic nature of NDVI is not well documented. The most logical explanation is that, the red band (680 nm) absorbs electromagnetic energy, represented by an exponential function (Tucker, 1977). When canopy cover reaches 100 %, the amount of red light that can be absorbed by leaves reaches a peak (Thenkabail *et al.*, 2000; Tucker, 1977). On the other hand, NIR reflectance will increase because an addition of leaves results in multiple scattering (Kumar *et al.*, 2001). The imbalance between a slight decrease in the red and high NIR reflection results in a slight change in the NDVI ratio, hence yields a poor relationship with biomass. In order to double the ratio, the NIR reflectance should almost double to compensate for the little change in red reflectance, however this is not always the case (Kumar *et al.*, 2001).

2.4.2 Comparison between the methods used in this study in estimating biomass

Although the three indices (NDVI, SR and TVI) yielded high correlation coefficients with biomass, the mean correlation coefficients calculated from the first 20 band combinations are higher for SR as compared to NDVI and TVI (Figure 2.8). Therefore, SR may be a better index for estimating biomass in dense canopies. SR selected narrow bands from a broader part of the spectrum that include the green as well as the mid infrared region apart from the red edge (Figure 2.7). In the green portion, the selected 548 nm band highlights the reflectance peak in the visible portion while the 572 nm band is the greatest negative change in slope per unit change in wavelength (Thenkabail *et al.*, 2000). The selected bands in the mid infrared are water sensitive. Therefore, there could be a strong relationship between biomass and leaf water.

The red edge position yielded lower but significant correlation coefficient with biomass as compared to the narrow band vegetation indices. Nevertheless, the result from the red edge position emphasizes the importance of the slope of the red edge in estimating biomass at full canopy cover.

2.5. Conclusions

We conclude that:

1. Modified normalised difference indices (NDVI) calculated from a combination of narrow channels in the shorter wavelengths of the red edge (700 nm – 750 nm) and longer wavelengths of the red edge (750 – 780 nm) yield higher correlation coefficients with biomass as compared to the standard NDVI.

2. The red edge contains more information on biomass quantity as compared to other parts of the electromagnetic spectrum
3. SR yields the highest correlation coefficients with biomass as compared to narrow band NDVI and TVI. We therefore recommend the use of a simple ratio index based on a waveband located in the shorter red edge portion (706 nm) and a band located in the longer red edge portion (755 nm) for a better estimation of biomass at high canopy density, *vis*. (R_{755} /R_{706}).

Overall, the controlled experiment improved an understanding of the wavelength regions that can be used to estimate biomass at full canopy cover. The study has revealed that, narrow wavelengths located in the red edge slope contain information on biomass estimation at full canopy cover. We therefore recommend that, future research should test the utility of these methods under natural environmental conditions.

Acknowledgements

We thank ITC for funding this project. We also extent our gratitude to UNIFARM experimental station and the Department of Nature Conservation and Vertebrate Ecology in Wageningen University for providing good facilities for the experiment. Many thanks to Sipke van Wieren for his help in setting up the experiment. We would also like to thank Dr. Jan de Leeuw, Dr. Herman Huizing and Dr. Lalit Kumar for reading earlier drafts of the manuscript.

Tropical grass quality at Laboratory Level: Chapter 3-5

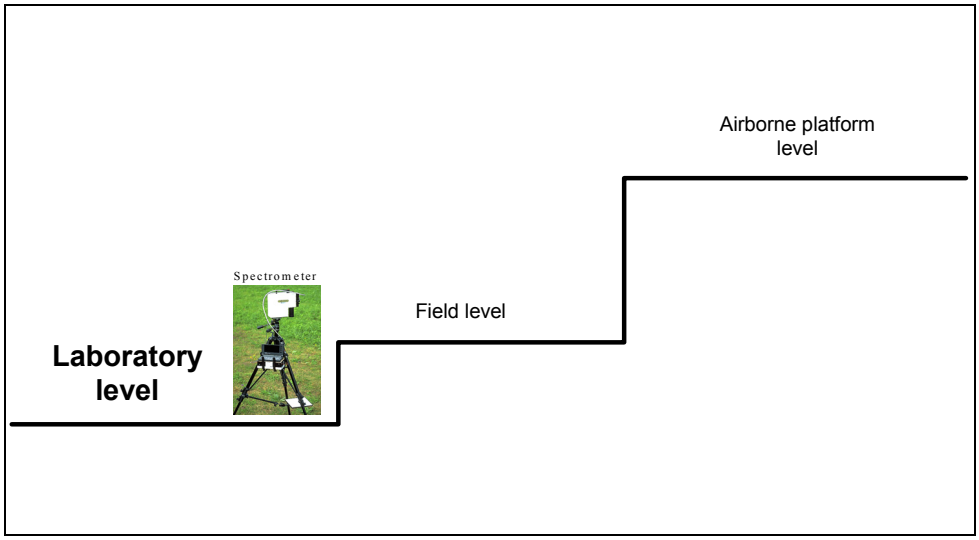

CHAPTER 3:
Discriminating grass grown under different nitrogen treatments using spectrometry

This chapter is based on

Mutanga, O., Skidmore, A.K., and Van Wieren, S. (2003). Discriminating tropical grass canopies (C. ciliaris) grown under different nitrogen treatments using spectroradiometry. *ISPRS Journal of Photogrammetry and Remote Sensing*, **57**, 263 - 272.

Abstract

Techniques for estimating and mapping grass quality are critical for a better understanding of wildlife and livestock grazing patterns. Nitrogen is one of the most important elements that determine quality in plants. We assessed the potential to discriminate differences in nitrogen concentration using high-resolution reflectance by growing *C. ciliaris* grass with different fertilization treatments in a greenhouse. Canopy spectral measurements from each treatment were taken under controlled laboratory conditions within a period of four weeks using a GER 3700 spectroradiometer.
Results show that there were statistically significant differences in spectral reflectance between treatments within certain wavelength regions - an encouraging result for mapping grasslands with different levels of nutrients using hyperspectral remote sensing. We further investigated the effect of varying nitrogen supply to a specific absorption feature in the visible region between 550 nm and 750 nm ($R_{550 - 750}$) using continuum-removed spectra. Results show that the high nitrogen treatment had deeper and wider absorption troughs as compared to the low nitrogen treatment as well as the control (no nitrogen), which is important for the prediction of nitrogen in grass canopies. The potential use of the visible portion of the electromagnetic spectrum is a promising result for the remote sensing of canopy chemistry since foliar water effect is minimal in this region as compared to the shortwave infrared. Overall, the results provide the possibility to map variation in grass quality using hyperspectral remote sensing.

Keywords: Grass quality; absorption features; continuum removal; laboratory experiment

3.1 Introduction

Grass quality is one of the major factors that determine grazing patterns of wildlife and livestock (Bailey *et al.*, 1996). High quality grasses contain a high percentage of total digestible nutrients and have a high percentage of protein. Each of the many foods potentially available to an animal has a different nutritional value and exhibits a different spatial pattern. Between and within (macro and micro) species variation in grass quality can be induced by variations in nutrients such as nitrogen concentration (Cochrane, 2000). Wildlife and livestock exhibit preference for certain sites based on the variation in quality (Muya & Oguge, 2000). This in turn influences the grazing intensity of patches and their relationship to animal movement and distribution (Styles & Skinner, 1997).

The determination of the spatial variation of grasses rich in nutrients helps to explain the distribution of wildlife and livestock. Techniques for estimating grass quality are therefore critical for a better understanding of wildlife feeding patterns, and ultimately to understand and explain animal distribution.

Traditional methods for detecting grass quality require detailed sampling and laboratory analysis. This usually results in the collection and analysis of inadequate data that is not representative of the population (Foley *et al.*, 1998). Hyperspectral remote sensing offers the potential to detect and map both macro and micro-variations in grass quality due to its use of narrow spectral channels of less than 10 nm. These narrow spectral channels allow the detection of detailed features, which could otherwise be masked by broadband satellites such as Landsat TM or Aster (Schmidt & Skidmore, 2001).

In order to map grass quality, the underlying principle is that grasses with varying nutrient levels reflect differently in specific wavelengths. To date, no studies have focused on discriminating tropical grasses with different nutrient levels using their reflectance spectra at canopy scale. Nitrogen is one of the most important elements that induce vigor (plant's physiological condition) in plants (Luther & Carroll, 1999). However, little is known about specific spectral channels that are sensitive to variation in nitrogen concentration in tropical grass canopies. These are important for mapping and therefore monitoring grass condition in space and time using airborne hyperspectral sensors such as HYMAP.

The main research question in this study was whether canopy reflectance could be used to discriminate differences in foliar nitrogen concentration. The objective was to identify high-resolution spectral bands that are most sensitive to variation in nitrogen supply as well as explain any spectral differences between treatments. In order to achieve this we designed an experiment in which we varied the nitrogen concentration available to *C. ciliaris* and measured canopy reflectance spectra over four weeks. A secondary objective was to assess the utility of continuum removal in enhancing the major

absorption feature in the visible (550 nm – 750 nm) for a better separability of different nitrogen classes.

3.2. Materials and methods

3.2.1 Plant preparation

Sweet perennial blue buffalo grass (*C. ciliaris*) was sown in a greenhouse for this experiment. The grass has a height from 10 cm to 150 cm and is tufted, erect, branching and rooting at the nodes (Pooley, 1998).

A total of 96 pots (10 liters with a diameter of 26 cm and a height of 24 cm) were used for planting. Five seeds were sown in each pot in a greenhouse on 30 July 2001. The seedlings were grown under a day temperature of 25º C and a night temperature of 21º C. The plants were supplied with an initial fertilization of 2.2 g of potassium and 3.6 g of super phosphate per pot and were watered at least once every day.

The pots were randomly divided into three equal groups on 13 August 2001. To manipulate foliar concentration of nitrogen, the first group (called high nitrogen) was supplied with 3.4 ml (120 kg/ha) of ammonium nitrate per pot. The second group (called low nitrogen) was supplied with 1.14 ml (40 kg/ha) of ammonium nitrate per pot. This was supplied over several days spreading to the end of harvesting. No nitrogen was added to the control group. The pots were arranged in blocks and rotated once a week to minimize any effect of microclimate on the experiment.

3.2.2 Canopy spectral measurements

To compare the spectral response of the three treatments at different time periods, measurements were taken at the beginning of every week for four weeks, from September 3rd 2001. Measurements were taken from this date onwards because the grass had grown to an extent that it was largely covering the soil, thus minimising the background effects. The plants were transferred in their pots from the greenhouse to a laboratory on each day of measurement. A total of eight pots from each treatment were measured every week. Measurements were done under laboratory conditions in order to control for sources of variation that are not related to chemical absorption such as change in illumination angle and atmospheric effects (Luther & Carroll, 1999).

Reflectance measurements were done using a GER 3700 spectroradiometer. The GER 3700 (Geophysical and Environmental Research corp.) is a three dispersion grating spectroradiometer using Si and PbS detectors with a single field of view. The wavelength range is 350 nm - 2500 nm with a resolution of 1.5 nm in the 350 nm - 1050 nm, 6.2 nm in the 1050 nm - 1900 nm range and 9.5 nm in the 1900 nm - 2500 nm range. The sensor, with a field of

view of 3º, was mounted on a tripod and positioned 2 meters above the ground at nadir position.

A halogen lamp, positioned next to the sensor was used to supply illumination on the target. Each pot was placed on a fixed tray, directly under the sensor for canopy spectral measurements. The pots were rotated by 45º after every 5th measurement in order to average out differences in canopy orientation on each pot. Each spectrum was determined as an average of 20 spectral measurements per pot. The radiance was converted to reflectance using scans of a spectralon reference panel. Four target measurements were made after measuring the reference (spectralon) panel.

3.2.3 Chemical analysis

Samples were oven dried at 70º C for 24 hours and were ground through a 1 mm steel screen with a cyclone sample mill. Digestion of the samples was done before automated determinations. Salicylic acid was added to prevent loss of nitrate. After decomposition of the excess H_2O_2, the digestion was completed by concentrated sulphuric acid at elevated temperature under the influence of selenium powder as a catalyst. Nitrogen was measured with a segmented flow analyzer at 660 nm wavelength and was expressed as milligrams per gram (mg/g).

3.2.4 Data analysis

The research hypothesis was whether the means of the reflectance between the three treatments were significantly different at each wavelength. The research hypothesis was statistically tested using one-way analysis of variance. From this test one can conclude that there are differences between the treatment groups (Siegal & Castellan, 1988). The statistical tests were done at different time periods (first week, second week, third week and fourth week) in order to assess the spectral differences between treatments at different stages of plants' physiological status.

We also tested the utility of the visible absorption feature ($R_{550\ -\ 750\ nm}$) to discriminate different levels of nitrogen concentration after continuum removal. This red absorption feature was selected since it has consistently proved to be an indicator of vegetation condition (Luther & Carroll, 1999) and is not affected by water absorption in fresh plants. This is in contrast to the SWIR bands where chemical absorption is largely masked by water (Elvidge, 1990; Kokaly & Clark, 1999).

Continuum removal normalizes reflectance spectra to allow comparison of individual absorption features from a common baseline (Kokaly, 2001). The continuum is a convex hull fitted over the top of a spectrum utilizing straight-line segments that connect local spectra maxima. The continuum is removed by dividing the reflectance value for each point in the absorption trough by the

reflectance level of the continuum line (convex hull) at the corresponding wavelength. The first and last spectral data values are on the hull and therefore the first and last bands in the output continuum-removed data file are equal to 1. The output curves have values between zero and one, in which the absorption troughs are enhanced and the absolute variance removed (Schmidt & Skidmore, 2001).

This method has been found useful in mapping the distribution of minerals by comparing remotely sensed absorption band shapes to those in a reference library (Clark & Roush, 1984). Kokaly and Clark (1999) applied the method to vegetation science using dried plant material. The extension of this method to fresh canopies for biochemical estimation has not been made to our knowledge.

3.3. Results

3.3.1 Variation in nitrogen concentration

As expected, the experiment resulted in a variation in foliar nitrogen concentration between treatments (Table 3.1).

Table 3.1 Foliar nitrogen concentration

Treatment	Mean	Standard deviation
Control	13.8	4.3
Low	19.3	6.5
High	34.2	6.2

One-way ANOVA was used to test if differences in the mean nitrogen concentration between the treatments were significant. We tested the research hypothesis that the mean nitrogen concentration (mg/g) for the control, low and high nitrogen treatments were different, *viz*. the null hypothesis Ho: $\mu 1 = \mu 2 = \mu 3$ versus the alternate hypothesis Ha: $\mu 1 \neq \mu 2 \neq \mu 3$, where: $\mu 1$, $\mu 2$ and $\mu 3$ are the mean nitrogen concentrations for the control, low and high treatments respectively. The conclusions from these tests are that the mean nitrogen concentrations are significantly different ($p < 0.001$).

There was also a decrease in nitrogen concentration for all treatments from the first week of measurement to the last week of measurement. Figure 3.1 shows the mean decrease (± 95 % confidence limits) in nitrogen concentration from the first week to the fourth week of measurement.

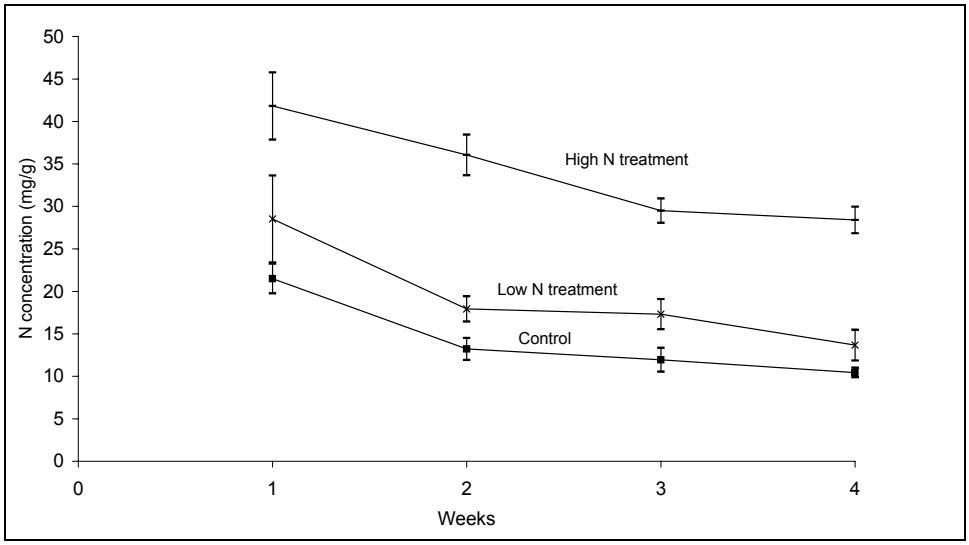

Figure 3.1. Variation of nitrogen concentration (± 95 % CL) from the first week to the fourth week of measurement.

One-way ANOVA was used to test if differences in the mean nitrogen concentration between the four weeks of measurement were significant for each treatment. We also tested the research hypothesis that the mean nitrogen concentration (mg/g) for the first, second, third and fourth weeks were different, *viz*. the null hypothesis Ho: $\mu1 = \mu2 = \mu3 = \mu4$ versus the alternate hypothesis Ha: $\mu1 \neq \mu2 \neq \mu3 \neq \mu4$ where: $\mu1$, $\mu2$, $\mu3$ and $\mu4$ are the mean nitrogen concentrations during the first, second, third and fourth week respectively. The conclusions from these tests are that for all the three treatments, the mean nitrogen concentrations are significantly different between the first, second, third and fourth week of measurement ($p < 0.001$).

3.3.2 Reflectance differences between treatments

Figure 3.2 shows mean reflectance spectra of *C. ciliaris* grass by treatment from the first week to the fourth week of measurement. There is a variation by wavelength in the differences between treatment spectra as highlighted in the results.

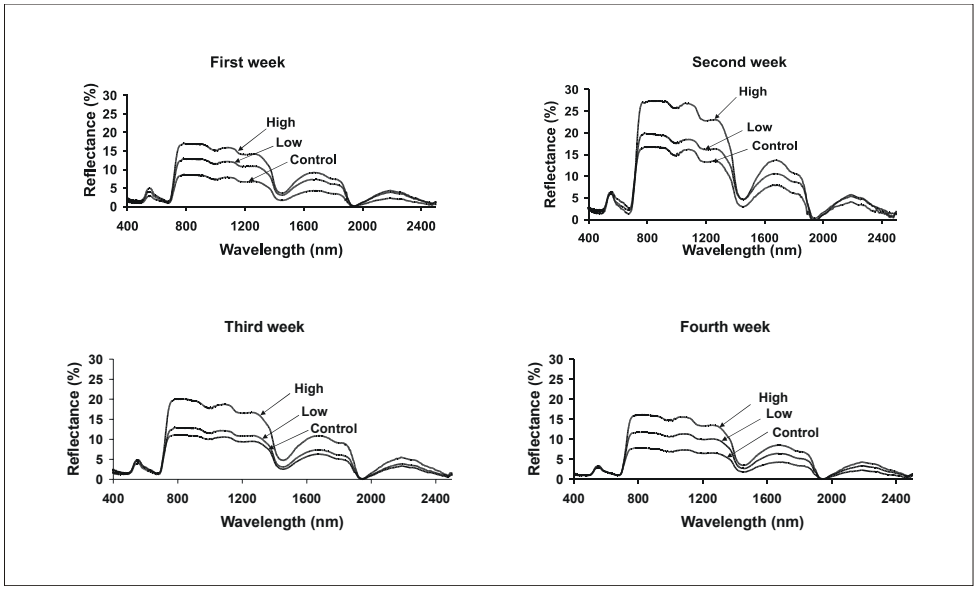

Figure 3.2. Mean canopy reflectance spectra of *C. ciliaris* grass by treatment.

We statistically analysed the difference between treatments in each region of the electromagnetic spectrum at every measurement period as shown in Figure 3.3.

Results of one-way ANOVA (Figure 3.3) show that generally, there is no significant difference between treatments in the visible region during the first, second and third week. There are however a few channels that are significantly different between treatments during the second and third week where canopies from the fertilized pots had a smaller reflectance than the control pots especially in the blue and red bands. Statistically significant bands occurred between 470 nm and 523 nm and also between 584 nm and 725 nm ($p < 0.001$).

Several bands were statistically significant in the fourth week (400 nm to 507 nm, 533 nm to 579 nm), however they were concentrated in the blue and green regions. Channels 480 nm, 553 nm, 560 nm and 569 nm have the lowest p-values ($p < 0.001$).

The near-infrared region experienced statistically significant differences between treatments in all weeks (except for a few bands in the first week). Channels that maximise reflectance are between 1022 nm and 1334 nm. The large differences in the near-infrared can be visually recognized in Figure 3.2.

For the SWIR, Figure 3.3 shows that differences in reflectance were already significant in the first week for several bands, including those of known protein and nitrogen absorption (1509 nm, 1645 nm, 1671 nm – 1820 nm, 1727 nm, 1733 nm, 2084 nm to 2200 nm, 2360 nm to 2307 nm). There were more bands with significantly low p-values in the fourth week (1898 nm, 1909 nm, 1930 nm, 1940 nm, 1961 nm, 1972 nm, 2023 nm, 2183 nm, 2298 nm, 2307 nm, 2345 nm, and 2354 nm). Figure 3.4d shows that reflectance for the high

nitrogen treatment dropped from the first to the fourth week of measurement for selected protein absorption bands.

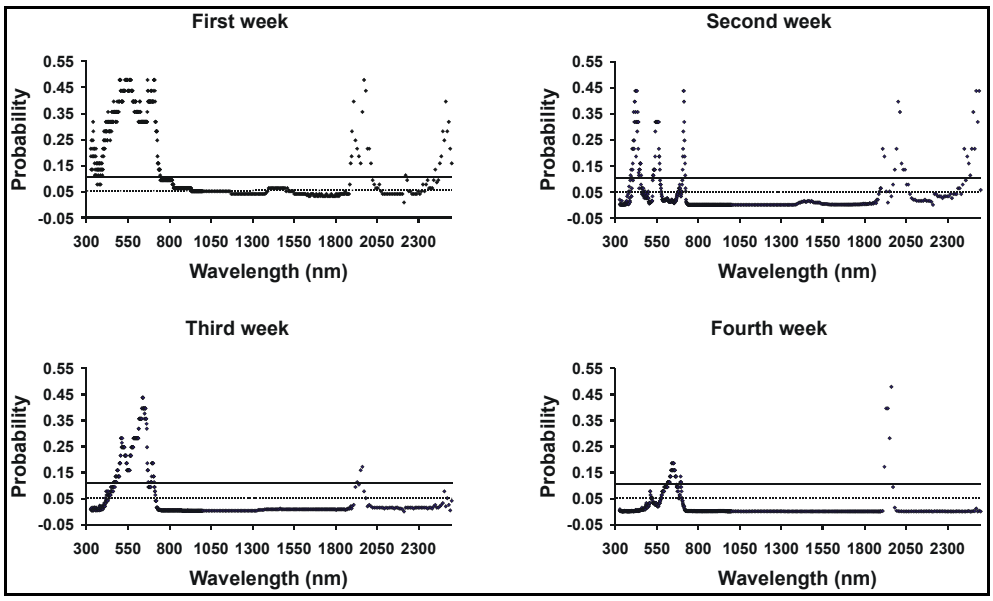

Figure 3.3. Results of One-way ANOVA showing wavelengths where reflectance differences between the three treatments are significant. Horizontal dashed and solid lines show 95% and 90% confidence limits, respectively

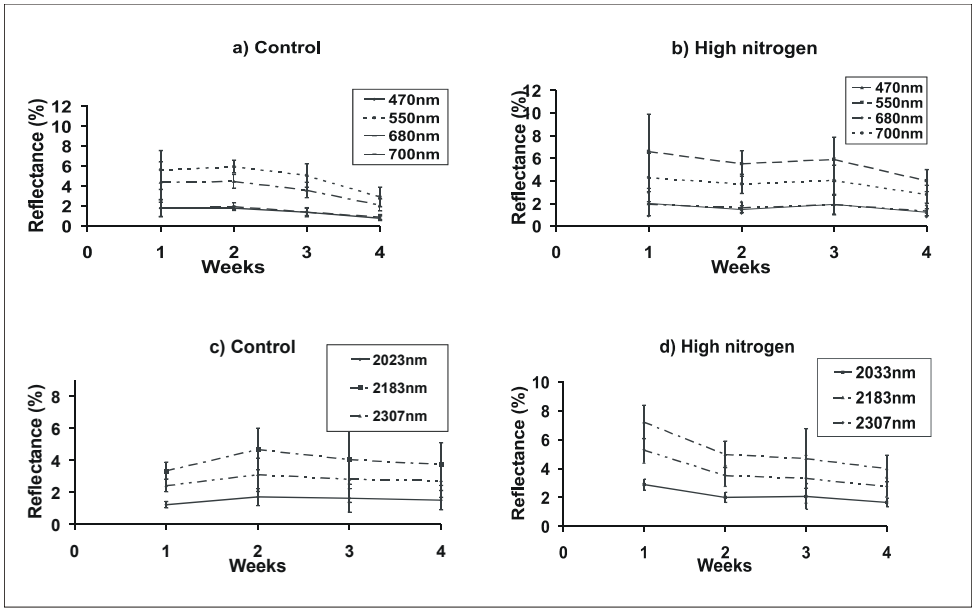

Figure 3.4. Change in mean reflectance (± 95 % CL) from the first week to the fourth week of measurement in the visible (a and b) and the SWIR regions (b and c). Channels that are sensitive to chemical absorption as well as those representing specific portions of the electromagnetic spectrum were selected to illustrate change in reflectance in time series. The low nitrogen treatment was not illustrated since its pattern strongly resembled the control.

3.3.3 Continuum-removed spectra

Figure 3.5 shows the continuum-removed spectra of the red absorption feature ($R_{550 - 750\ nm}$) in the visible region. The absorption feature shows change from a narrow feature in the control to a wider and deeper absorption feature in the high nitrogen treatment. The differences however vary from the first week to the fourth week of measurement. The difference between the three treatments is lowest in the third week and the high nitrogen treatment absorption trough widens rather than increasing in depth during the fourth week.

One-way ANOVA results in Figure 3.6 shows that the treatments are statistically different, especially for the slopes of the absorption features.

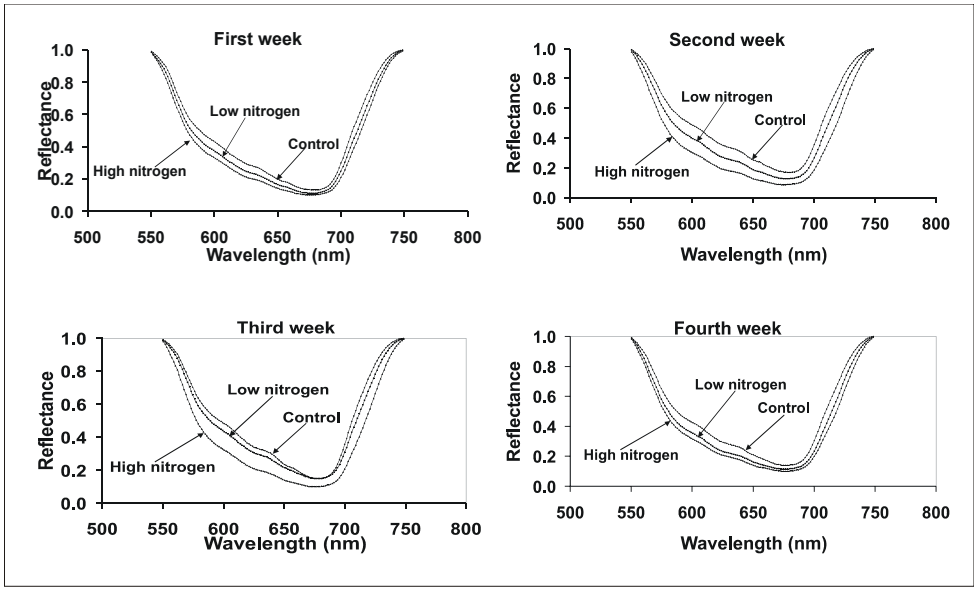

Figure 3.5. Continuum-removed, mean canopy reflectance spectra of *C. ciliaris* grass in the visible region for the three treatments.

3.4. Discussion

3.4.1 Reflectance differences between the treatments

Our results have shown that differences in nitrogen concentration largely influences spectral reflectance. In the visible region, wavelengths between 584 nm and 725 nm, especially during the second week showed statistical differences between treatments, which can largely be explained by a variation in chlorophyll absorption. There is a strong (positive and linear) relationship between nitrogen and chlorophyll (Yoder & Pettigrew-Crosby, 1995). Therefore differences in reflectance between the treatments largely depend on differences in chlorophyll content as induced by nitrogen supply. Our results confirm those of Carter (1993) who reported the region 535 nm to 640 nm and 685 nm to 700 nm as the most sensitive regions of the spectrum.

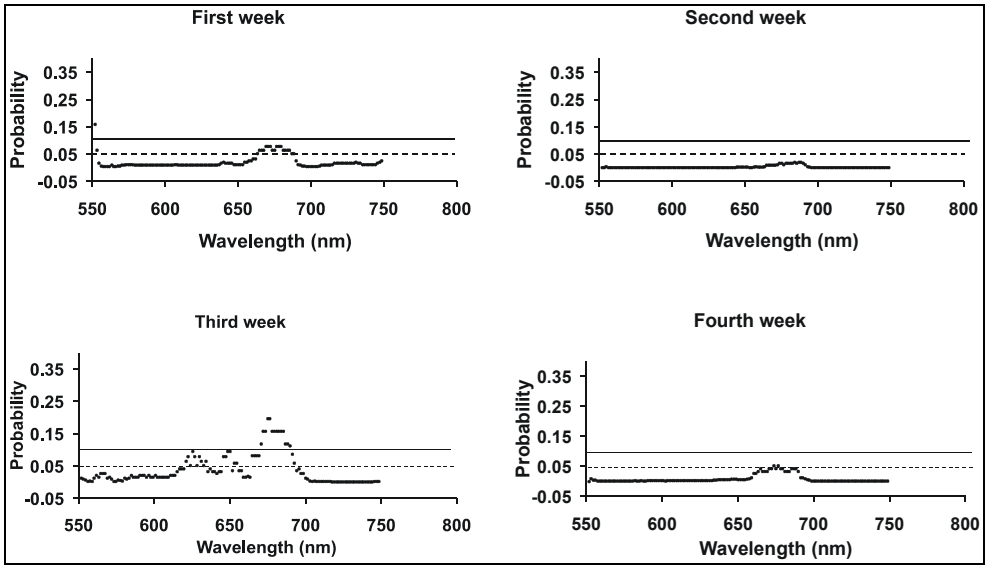

Figure 3.6. Results of One-way ANOVA showing wavelengths where continuum removed reflectance differences between the treatments are significant. Horizontal dashed and solid lines show 95% and 90% confidence limits, respectively.

Differences in the visible reflectance for the fourth week are explained by changes in the physiological status of the control group. Figure 3.4a showed a drop in reflectance of the control in selected bands for the blue and green regions because rapid flowering and senescence resulted in higher absorption by carotenoid pigments and anthocianins. Plants with limited nitrogen supply develop greater concentrations of carotenoids relative to chlorophyll (Salisbury & Ross, 1985). This phenomenon is related to protective effect of carotenoids under conditions of excess radiation (Penuelas *et al.*, 1994). As for the red region, our explanation for the statistical difference is that there was chlorophyll destruction in the control during the fourth week resulting in less absorption as compared to the treatments.

It is perplexing to note that although the 680 nm region is a known centre of chlorophyll *a* absorption (Gitelson *et al.*, 1999; Lichtenthaler *et al.*, 1996; Penuelas *et al.*, 1994; Yoder & Pettigrew-Crosby, 1995), this study has revealed that the slopes of the absorption troughs are more significantly different than the 680 nm centre itself (Figure 3.3). This could be explained by the widening of the absorption trough at the expense of deepening at high chlorophyll levels (Buschmann & Nagel, 1993). Therefore, the development of algorithms that manipulate the slopes of absorption troughs (red edge) in the visible might be useful for the detection of biochemicals in plant canopies.

The near-infrared shows significant differences between the treatments in all weeks. Nitrogen supply apparently effects mesophyll cell structure

resulting in higher reflectance with an increase in nitrogen supply (Kumar *et al.*, 2001). Multiple scattering of radiation due to the larger LAI of fertilized plot canopies may have caused differences between treatments. This is consistent with the theory of light scattering and absorption by tree canopies (Gates *et al.*, 1965).

The SWIR region showed a decrease in reflectance in the nitrogen treatments from the first week to the fourth week (Figure 3.4c and 3.4d), whereas the control remained statistically constant during the same period. This may be explained by increasing leaf mass in the fertilized pots, which contained a greater mass of absorbing water and other biochemicals. Change in the control was not significant over the weeks due to less chemical absorption since the grass had apparently insufficient nitrogen to grow. Statistically significant channels such as, 1972 nm, 2023 nm, 2345 nm and 2354 nm are within ± 10 nm of the protein and nitrogen absorption bands (Dungan *et al.*, 1996; Luther & Carroll, 1999); a promising result for the detection of nitrogen and protein.

3.4.2 Continuum removal in the 550 nm to 750 nm absorption feature

The red absorption feature ($R_{550\text{-}750}$) was further explored. Results revealed widening and deepening of absorption feature with an increase in nitrogen supply. Statistically significant differences were obtained (Figure 3.6) between the treatments. An increase in nitrogen concentration results in an increase in chlorophyll (Penuelas *et al.*, 1994; Yoder & Pettigrew-Crosby, 1995). The porphyrin ring of the chlorophyll molecule contains nitrogen atoms confirming the nitrogen-pigment relationship (Kokaly, 2001).

The role of continuum removal in enhancing differences in depth between the treatment groups (Figure 3.5) as compared to the original spectra (Figure 3.2) has been revealed. This is mainly because the method emphasizes absorption troughs whilst removing the absolute variance caused by albedo effects (Schmidt & Skidmore, 2001). Despite canopy and background effects on reflectance, the continuum removal method has successfully discriminated standing grass canopies. This result is critical for the development of algorithms that analyse the shape, depth and slopes of the major absorption feature in the visible (where water absorption is minimal) to estimate nitrogen and to ultimately map rangeland quality at canopy scale.

3.5. Conclusions

From this study, we conclude that:

1. Canopy reflectance can be used to discriminate differences in foliar nitrogen concentration. This implies that the same species can reflect differently depending on environmental factors such as nutrient levels. This offers the possibility to map variation in grass quality using high-resolution sensors.

2. Band depth analysis has shown that an increase in nitrogen supply widens absorption troughs - an interesting result for estimating nitrogen on grass canopies using hyperspectral remote sensing.
3. The visible ($R_{550 - 750}$) absorption feature distinctively separates the three treatments. This implies that new algorithms in the visible domain can be developed for the direct estimation of nitrogen on standing canopies.
4. Transformation techniques such as continuum removal increase the separability of grass with different levels of nitrogen in specific absorption features, offering possibilities to map rangeland quality.
5. There is variation in spectral response of plants with time. This has potential implications for remote sensing missions in that reflectance at different times could require specific calibration for the time of sampling due to variation in physiology. Timing of field sampling and knowledge of the physiological status of plants is therefore important when acquiring remotely sensed data. To be more precise, seasonal snapshots of hyperspectral imagery might be useful for monitoring rangeland quality.

Overall, results of this study offer possibility to estimate canopy grass quality at the field level. The results trigger the need to investigate band depths and slopes, particularly the red edge to estimate grass quality at canopy level.

Acknowledgements

We would like to thank ITC for providing research funds to collect this data. We extend our gratitude to UNIFARM experimental station at Wageningen University for providing excellent conditions for the success of the experiment. Many thanks to Herman Masselink and Geurt Vesteeg for facilitating this task. We also thank Henk van Oosten for his help in computer programming.

CHAPTER 4:
Red-edge shift and the quality of tropical grass canopies

This chapter is based on
Mutanga, O and. Skidmore, A.K (**In review)** Red edge shift and the quality of tropical grass canopies, *ISPRS Journal of Photogrammetry and Remote Sensing.*

Abstract

Grass quality, as determined by the concentration of nitrogen is one of the major factors that explain the distribution of wildlife and livestock. Therefore the remote sensing of foliar nitrogen is critical to understand wildlife and livestock feeding patterns. This study evaluated the response of the continuum-removed wavelength of the red edge peak to a variation in nitrogen supply to three groups of *C. ciliaris* grass grown in a greenhouse. Canopy spectral measurements from each treatment were taken under controlled laboratory conditions within a period of four weeks using a GER 3700 spectroradiometer. Results indicate that the mean wavelength positions of the three-fertilization treatments were statistically different. An increase in nitrogen supply resulted in the red edge shift to longer wavelengths. The red edge position, amplitude, slope at 713 nm and slope at 725 nm were significantly correlated to nitrogen concentration (bootstrapped r = 0.89, -0.28, 0.63 and 0.75 respectively) at canopy level. From our results, the red edge position is better for estimating quality as compared to the other methods tested. The result is promising for detecting grass quality using remote sensing in rangelands.

Keywords: Nitrogen concentration, red edge position, continuum removal, bootstrapping

4.1. Introduction

Grass quality (expressed as a percentage of total digestible nutrients) is one of the major factors that explain the distribution of wildlife and livestock (Bailey *et al.*, 1996; Grant *et al.*, 2000). The concentration of nitrogen that largely determines quality is important for animal nutrition (van Soest, 1994). Therefore, the remote sensing of grass quality is critical for understanding wildlife and livestock feeding patterns.

Attempts to remotely sense grass quality at canopy level have not been very successful to date (Curran *et al.*, 2001; Kumar *et al.*, 2001). The presence of water in fresh canopies masks the biochemical absorption features especially in the shortwave infrared (Clevers, 1999; Kokaly & Clark, 1999). In addition, leaf orientation, soil background effects, atmospheric absorption as well as BRDF further complicate the remote sensing of grass quality at canopy level (Asner *et al.*, 2000).

Recently, studies have shown that the red edge is less sensitive to soil background and atmospheric effects and can provide information, not covered by the information derived from a combination of near infrared and visible spectral bands (Clevers, 1999; Clevers *et al.*, 2000). The red edge position is the point of maximum slope in vegetation reflectance spectra (Fillella & Penuelas, 1994) that occurs between 680 – 750 nm region. This phenomenon is caused by strong chlorophyll absorption in the red and canopy scattering in the near infrared (Dawson & Curran, 1998). An increase in chlorophyll concentration results in the broadening of the absorption feature centred around 670 nm, causing the movement of the red edge position to longer wavelengths (Dawson & Curran, 1998). As a result, the red edge position has been successfully used in studies to estimate chlorophyll concentration, biomass and LAI (Curran *et al.*, 1991; Danson & Plummer, 1995; Thomas & Gaussman, 1987).

Chlorophyll *a* and chlorophyll *b* concentration in plants have also been shown to correlate strongly with nitrogen (Katz *et al.*, 1966; Penuelas *et al.*, 1994). Nitrogen is related with the protein synthesis, which promote the photosynthetic process. The nitrogen deficiency disturbs the metabolic function of the chlorophyll, which is the photosynthetic element responsible for the absorption of electromagnetic radiation (Ponzoni & Goncalves, 1999). Studies have therefore used the red edge - chlorophyll relationship to infer the nitrogen status of plants in vegetation science (Fillella & Penuelas, 1994).

In this study, we hypothesize that, since chlorophyll largely determines the red edge shift, a strong correlation between the red edge position and nitrogen concentration is also expected. The objective of this study was to evaluate the response of the red edge to a variation in nitrogen supply at canopy level and to establish the relationship between foliar nitrogen concentration and the red edge. The wavelength of the red edge position (λ_{re}), amplitude (reflectance at the maximum slope), slope at 713 nm and 725 nm channels were compared. We designed an experiment in which we varied nitrogen supply to

three groups of *C. ciliaris* grass grown in a greenhouse, and measured canopy reflectance in the laboratory for four weeks.

4.2. Materials and methods

4.2.1. Plant preparation

Blue Buffalo grass (*C. ciliaris*) was sown in a greenhouse for this experiment. *C. ciliaris* is a sweet perennial grass that grows naturally in Southern Africa and is widely used as grass for ruminants. The grass grows from 10 cm to 150 cm and is tufted, erect, branching and rooting at the nodes (Pooley, 1998). The grass grows fast and is currently recommended for planting in dry land areas in order to provide grass to ruminants (Pooley, 1998). Details of the planting, application of nitrogen treatments and monitoring of growth are found in Mutanga *et al.* (2003).

4.2.2. Canopy spectral measurements

To manipulate a variation in chemical concentration, spectral measurements were taken at the beginning of every week for four weeks, from September 3rd 2001. Measurements were taken from this date onwards because the grass had grown to an extent that it was largely covering the soil, thus minimising the background effects. The plants were transferred in their pots from the greenhouse to a laboratory on each day of measurement. A total of eight pots from each treatment were measured every week. A GER 3700 spectroradiometer was used and the measurement protocol is well detailed in Mutanga *et al.* (2003). Figure 4.1 shows the mean and standard deviation of the measured spectra.

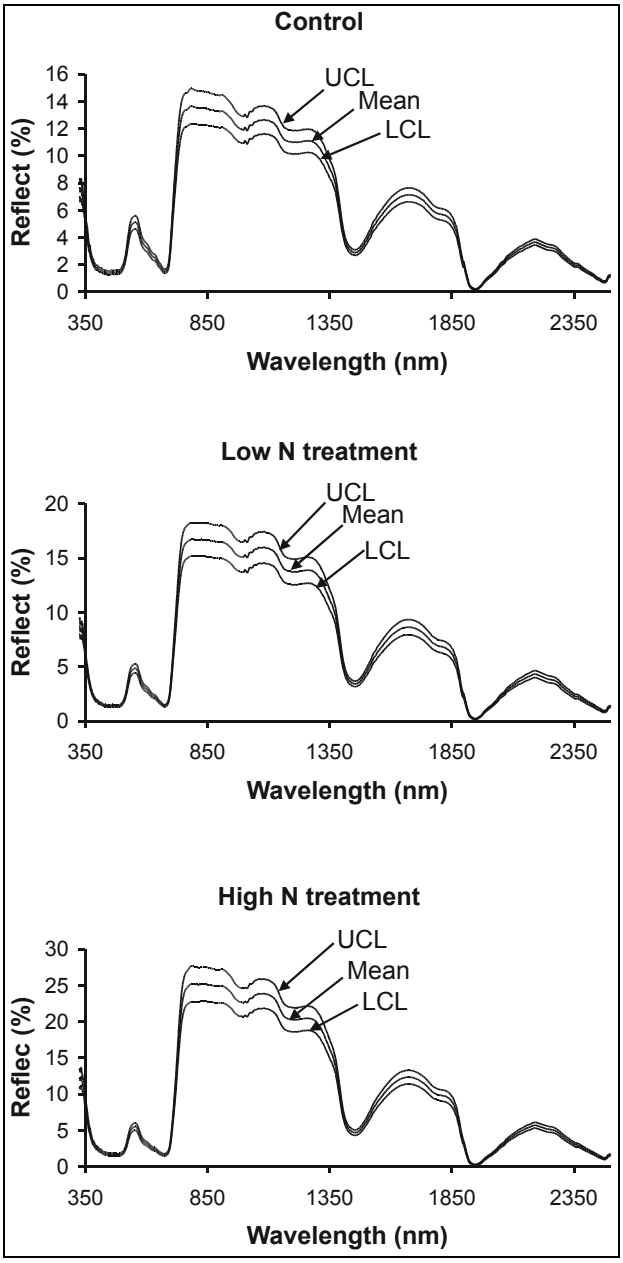

Figure 4.1. Mean canopy reflectance and standard deviations (n = 32 for each treatment) of C. ciliaris grass canopy measured under controlled laboratory conditions

4.2.3. Chemical analysis

All standing grass from each pot was clipped and oven dried at 70º C for 24 hours. The samples were ground through a 1mm steel screen with a cyclone sample mill. Destruction of the samples was done before automated determinations. Organic matter was oxidized by applying hydrogen peroxide at relatively low temperature. Salicylic acid was added to prevent loss of nitrate. After decomposition of the excess H_2O_2, the destruction was completed by concentrated sulphuric acid at elevated temperature under the influence of Selenium powder as a catalyst.

Nitrogen concentration was measured with a segmented flow analyser at 660 nm wavelength. Table 4.1 shows the resulting data set.

Table 4.1: Nitrogen concentration of the plant material collected over the four-week period (n = 96)

Treatment	Mean	Min	max	CL (95%)
Control (mg/g)	13.8	9.27	24.1	1.59
Low (mg/g)	19.3	11.4	42.2	2.52
High (mg/g)	34.2	25.8	44.9	2.37

4.2.4. Calculating the red edge parameters

The red edge parameters were derived from the first derivative of the reflectance. The first derivative is commonly used to enhance absorption features that might be masked by interfering background absorptions and canopy background effects (Dawson & Curran, 1998; Elvidge, 1990). The first derivative spectra were calculated from each reflectance spectrum. A first difference transformation of the reflectance spectrum calculates the slope values from the reflectance and can be derived from the following equation (Dawson & Curran, 1998):

$$FDS_{\lambda(i)} = (R_{\lambda(j+1)} - R_{\lambda(j)}) / \Delta\lambda \qquad (1)$$

where FDS is the first derivative reflectance at a wavelength *i* midpoint between wavebands j and j+1. $R_{\lambda(j)}$ is the Reflectance at the j waveband, $R_{\lambda(j+1)}$ is the reflectance at the j+1 waveband and $\Delta\lambda$ is the difference in wavelengths between j and j+1. Table 4.2 summarizes the parameters derived from the first derivative reflectance.

Table 4.2. The red edge parameters

Red edge parameter	Definition
Position (λ_{re})	Wavelength of the red edge peak (maximum slope position)
Amplitude	First derivative value at the red edge peak (maximum slope)
Slope 1	First derivative reflectance at 713 nm
Slope 2	First derivative reflectance at 725 nm

Slope 1 was obtained from the corresponding mean red edge position. Slope 2 was selected since the 725 nm wavelength has been used as a red edge parameter for estimating chlorophyll and LAI (Fillella & Penuelas, 1994). The first derivative spectra were calculated on the continuum-removed spectra.

Continuum removal was applied on the absorption feature centred on 670 nm. The continuum is a convex hull fit over the top of a spectrum utilizing straight-line segments that connect local spectra maxima. The continuum is removed by dividing the reflectance value for each point in the absorption troughs by the reflectance level of the continuum line (convex hull) at the corresponding wavelength. The first and last spectral data values are on the hull and therefore the first and last bands in the output continuum-removed data file are equal to 1. The output curves have values between zero and one, in which the absorption troughs are enhanced (Mutanga *et al.*, 2003) and the absolute variance removed (Schmidt & Skidmore, 2001).

4.2.5. Statistical analysis

We tested the hypothesis that there is no significant difference in the position of the red edge inflection point among nitrogen supply treatments. This was tested using one-way analysis of variance following a confirmation of normality in the data set using the Kolmogrov-Smirnov test. The null hypothesis was that the mean wavelengths (λ_{re}) of the red edge position are equal for all treatments versus the alternative that they are not equal. A post hoc-Scheffe´ test was used to determine the significant differences between two treatment means in an analysis of variance setting.

In order to ascertain a relationship between the red edge parameters and nitrogen concentration, bootstrapping correlation was executed. Bootstrapping is a technique for estimating standard error, confidence intervals and sampling distributions for any statistic as the most common way of indicating statistical accuracy (Efron, 1982). Bootstrapping simulates the sampling distribution of any statistic by treating the observed data as if it were the entire statistical population under study. On each replication, a random sample of size N is selected, with replacement from the available data. The statistic of interest (in this case correlation coefficient) is calculated on this bootstrapped subsample and recorded. The process is repeated for several times in order to obtain the sampling distribution. The method facilitates accuracy assessment using the same data set.

A total of 200 replications were executed for each correlation between the wavelength position of the red edge and nitrogen concentration. The mean and confidence intervals were calculated for the bootstrapped data. Analysis of variance and hoc-Scheffe´ tests were executed between bootstrapped correlations from the four red edge parameters. This was done to ascertain if the results produced by the four methods are comparable.

4.3. Results

4.3.1. Shift in the red edge

Figure 4.2 shows the continuum-removed mean canopy reflectance in the red edge. The reflectance curves shift to longer wavelength with an increase in the amount of nitrogen to the treatments.

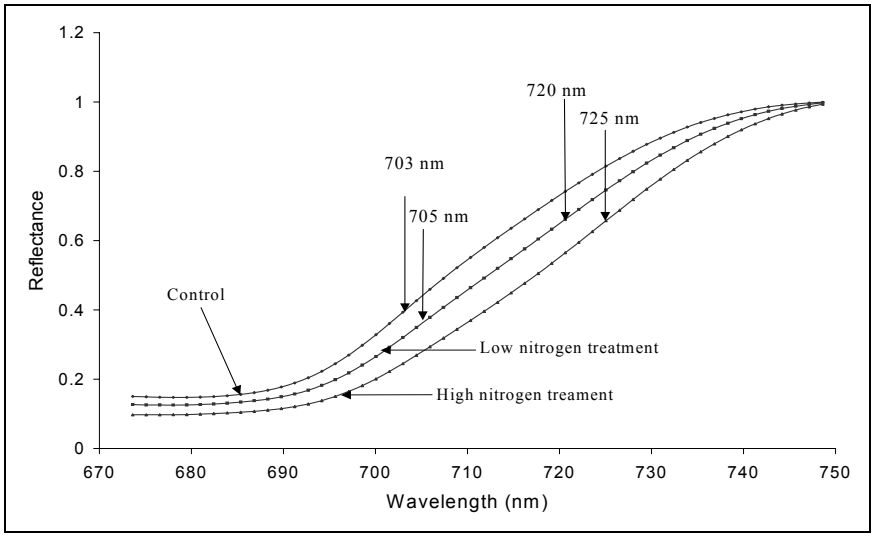

Figure 4.2. Continuum-removed, mean canopy reflectance spectra of *C. ciliaris* grass by treatment. Continuum removal was applied on the absorption feature between 550 nm and 750 nm. The reflectance values were normalised and have output values between 0 and 1. The red edge positions for each treatment are shown. The low N treatment shows two peaks, at 705 nm and at 725 nm.

4.3.2. The red inflection point

Figure 4.3 shows the first derivative reflectance on continuum-removed spectra. The inflection points of the three treatments are located at different positions. The inflection point for the control is at 703 nm, which implies that the curve for the control in Figure 4.2 quickly changes from concave to convex at shorter wavelength as compared to the high nitrogen treatment which remained

concave, and then changes into convex at longer wavelengths, around 725 nm. The inflection point for the high nitrogen treatment therefore shifted to longer wavelength. It is also interesting to note from Figure 4.3 that the low nitrogen treatment has a plateau (with a slight dip in the middle) between 705 nm and 720 nm. This confirms the long straight slope between 705 nm and 720 nm in Figure 4.2.

Although the peak of the low nitrogen treatment is at 705 nm, the height of the peak is not statistically different from the one at 720 nm. This implies that there are two peaks in the low nitrogen treatment as compared to the control and the high nitrogen treatments.

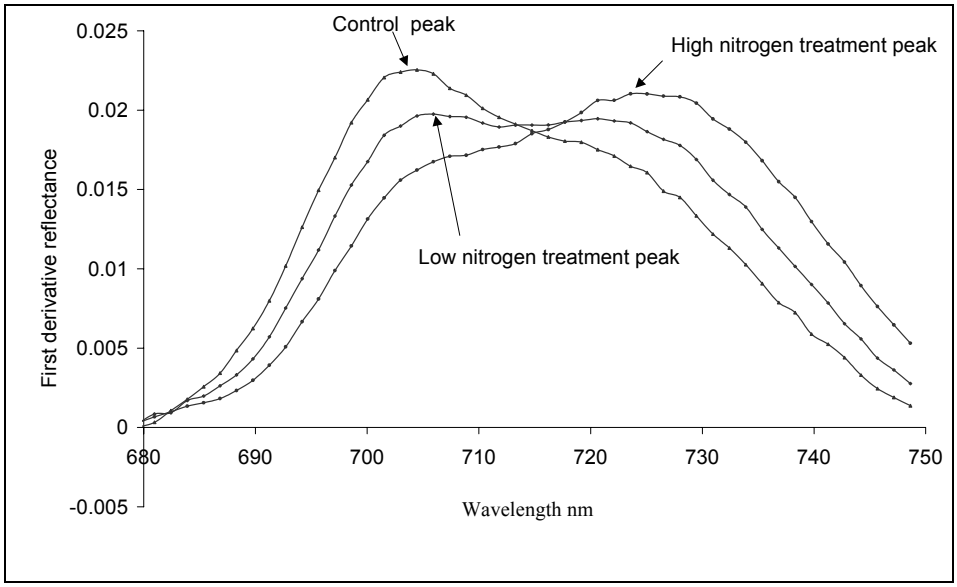

Figure 4.3. First derivative reflectance on continuum-removed spectra of *C. ciliaris* grass measured under controlled laboratory conditions. The highest peaks show the position of the red edge inflection point. Note the plateau on the low nitrogen treatment.

The box plots in Figure 4.4 show the medians and spread of the red edge positions in three different treatments. Results of one - way analysis of variance (ANOVA) indicate that the means of the three treatments (red edge positions) are statistically different ($p < 0.000$).

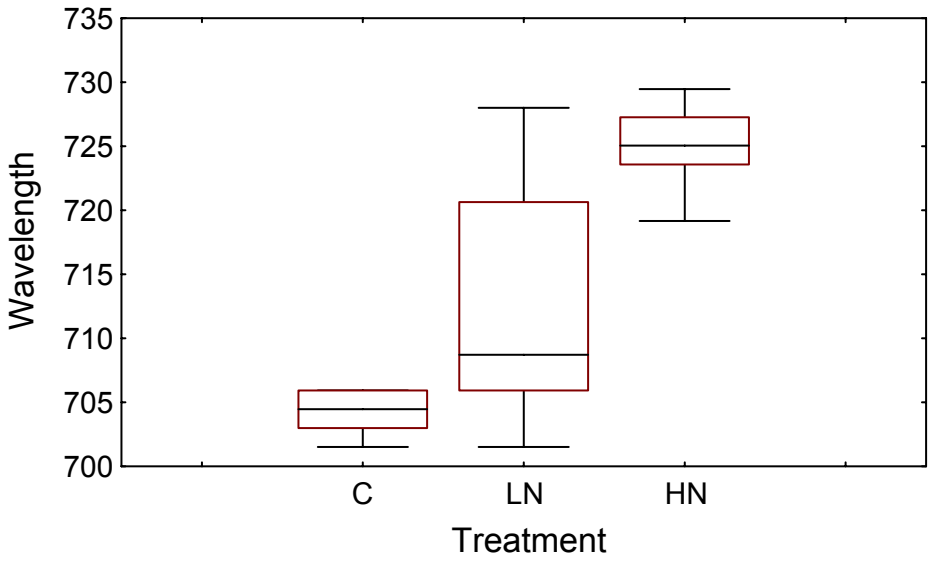

Figure 4.4. The red edge inflection points related to their corresponding levels of nitrogen supply (C = control, LN = Low nitrogen, HN = High nitrogen) in *C. ciliaris* grass. The red edge positions were obtained from maximum peak of the continuum removed, first derivative reflectance spectra.

A hoc-Scheffe´ test was used to test if there was any significant difference between two treatments. Results indicate that there is statistically significant difference between each pair of treatments tested ($p < 0.000$).

4.3.3.Relationship between the red edge parameters and nitrogen concentration

We investigated if the position and slope components (amplitude, slope at 713 nm and 725 nm) of the red edge are related to the concentration of nitrogen in grass. Table 4.3 shows the mean, standard errors and confidence intervals of the bootstrapped correlation coefficient between the red edge parameters and nitrogen.

Table 4.3. Bootstrapped correlation coefficients between nitrogen concentration and the red edge parameters (n = 96). A total of 200 iterations were executed for each pair.

	Mean	SE	95% CL
Red edge position	0.89**	0.0011	0.0022
Amplitude	-0.28*	0.0056	0.011
Slope 1	0.63**	0.0042	0.0083
Slope 2	0.75**	0.003	0.006

**Significant: $p < 0.01$ * Significant: $P < 0.05$

The red edge position yielded the highest correlation with nitrogen concentration. The maximum slope (amplitude) yielded the lowest negative correlation with nitrogen. Note that the 95% confidence limits for all the red edge parameters are lower than 0.05. Figure 4.5 shows the histogram of the bootstrapped correlations between the red edge parameters and nitrogen concentration. The histograms show the normal distribution correlations produced by the bootstrapping methodology. The small 95% confidence limits in Table 4.3 imply that the bootstrapped mean correlation coefficients approach the population estimate with a high precision.

One - way analysis of variance was used to test if there was any difference in the bootstrapped correlations produced by the different red edge parameters. Results show that the mean correlation coefficients from the four red edge parameters were significantly different ($p < 0.000$). A hoc-Scheffe´ test confirmed that the mean correlation coefficients between each pair were significantly different ($p < 0.000$).

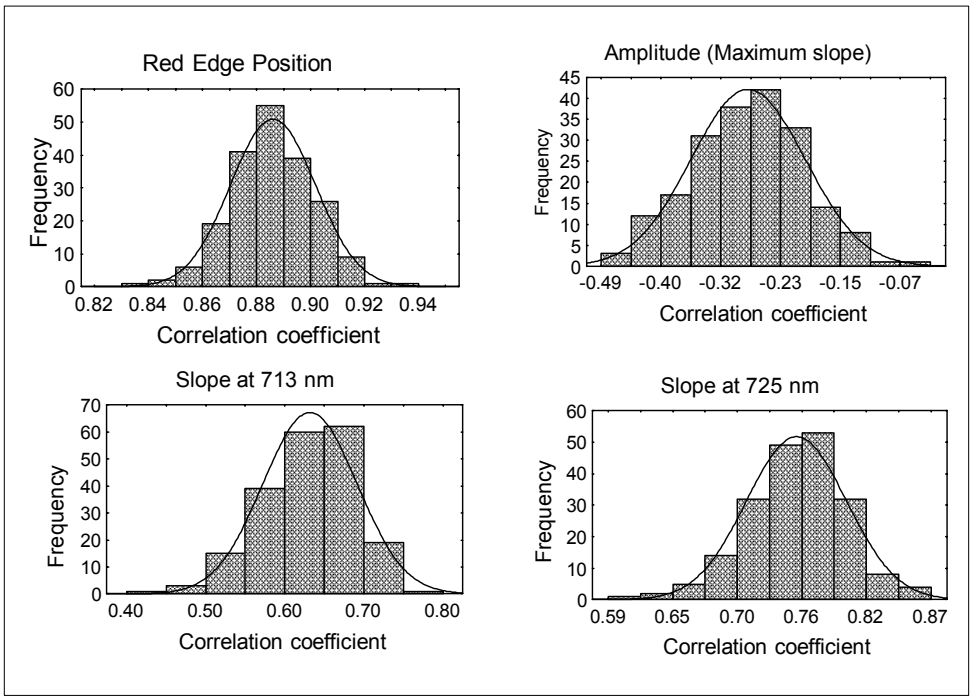

Figure 4.5. Bootstrapped correlation coefficients between nitrogen concentration and a) the red edge position, b) amplitude, c) slope at 713 nm and d) slope at 725 nm. A total of 200 simulations were run between the red edge position and nitrogen concentration ($n = 96$).

4.4. Discussion

Our results have shown that there is a difference in spectral reflectance with response to nitrogen supply. The red edge changed significantly with an increase in nitrogen supply to plants. There is a strong nitrogen-pigment relationship (Kokaly, 2001). Therefore an increase in nitrogen supply to plants results in an increase in chlorophyll (Penuelas *et al.*, 1994; Yoder & Pettigrew-Crosby, 1995), which ultimately widens the 680 nm absorption feature and thereby shifting the red edge to longer wavelengths.

The configuration of the curves in Figure 4.2 confirms the response of the red edge to nitrogen supply. The position of change from concave to convex is different for the three treatments. The control curve quickly changes around 703 nm whereas the high nitrogen treatment changes around 725 nm. This implies that there was not much widening of the absorption feature in the control treatment as compared to the high nitrogen treatment. This is clearly evident in Figure 4.3, which shows the red edge peaks as well as the box plots in Figure 4.4 that shows the position of the red edge. Statistical tests showed that the mean red edge positions of the three treatments were significantly different.

Of interest is the shape of the low nitrogen treatment (Figure 4.2). Visually, there is no sharp change of the curve from concave to convex. There is a straight line between the two slope forms, which implies a gradual transition from concave form to convex form. This explains the plateau observed in Figure 4.3. Horler et al., (1983) also identified two components in the first derivative spectrum with peaks around 700 and 725 nm. The plateau represents a gradual transition zone from concavity to convexity and confirms other studies that have also yielded two peaks in the first derivative analysis (Clevers & Jongschaap, 2001).

Many studies have shown that there is a relationship between the red edge position and chlorophyll concentration as well as LAI (Boochs *et al.*, 1990; Curran *et al.*, 1990; Fillella & Penuelas, 1994). They used this relationship to infer the nitrogen status of plants. We directly tested the relationship between several red edge parameters and the actual concentration of nitrogen at canopy level in this study. The design of this experiment resulted in a wide range of foliar biochemicals (Table 4.1) that resulted in different spectral signatures (Figure 4.1). The red edge position yielded the highest correlation coefficient with nitrogen ($r = 0.89$) as compared to the slope components tested. Analysis of variance and hoc-Scheffe´ test results indicate that the bootstrapped correlations obtained using the four methods are significantly different and therefore not comparable. The red edge position is therefore a better estimator of nitrogen concentration as compared to slope. The accuracy of the correlation was tested through the bootstrapping methodology, which resulted in very low confidence limits (Table 4.3), therefore a high precision of the estimate.

4.5. Conclusion

Results from this study show that the red edge shift is related to nitrogen supply in plants. The mean wavelengths (λ_{re}) of the red edge position were statistically different for all treatments. This implies a significant shift of the red edge position to longer wavelength as nitrogen supply increases. The red edge parameters were significantly correlated to nitrogen concentration even at canopy level - an interesting result for the remote sensing of foliar chemistry in rangelands. When the four methods used were compared, the red edge position yielded the highest correlation coefficient. The technique is important for strengthening models that have been developed to explain wildlife distribution and feeding patterns. However, the potential use of these laboratory methods developed from fine spectral resolution data (GER) can be made operational by investigating their capability to estimate grass quality using relatively coarser spectral resolution data such as the HYMAP spectra.

Acknowledgements

We would like to thank ITC for funding this project. We extend our gratitude to UNIFARM experimental station at Wageningen University in the Netherlands for providing optimum conditions for the success of the experiment. Our gratitude goes to Herman Masselink and Geurt Vesteeg for facilitating this task. We thank Sip van Wieren for his help in setting up the experiment and Jan van Walssem for his help in chemical analysis.

CHAPTER 5:
Discriminating tropical grass grown under different nitrogen treatments using spectra resampled to HYMAP

This chapter is based on

Onisimo Mutanga and Andrew K. Skidmore (**In Prep**) Discriminating tropical grass grown under different nitrogen treatments using hyperspectral data resampled to HYMAP**.**

Abstract

The development of techniques to estimate and map grass quality is important for a better understanding of wildlife feeding patterns. We tested whether canopy reflectance spectra, resampled to HYMAP resolution could discriminate between groups of tropical grass containing different levels of nitrogen concentration. Canopy spectral measurements were taken from *C. ciliaris* grass grown under three different nitrogen treatments using a GER 3700 spectrometer. Using the resampled spectra, the red edge position was calculated and continuum removal was applied on the red absorption feature between 550 nm and 757 nm. Canonical variate analysis was used to discriminate between the three nitrogen treatment groups using the spectra. Results show that canonical variates derived from continuum removed red absorption feature, in combination with the red edge position (resampled to HYMAP resolution) can discriminate between the three nitrogen treatment groups. The canonical structure matrix also revealed that the greatest discrimination power is contained in the red edge slope. The results show the importance of the visible portion of the electromagnetic spectrum (where foliar water effect is minimal) in predicting foliar nitrogen concentration. Overall, the study demonstrated the potential of airborne sensors such as HYMAP for mapping tropical grass quality.

Keywords
Canopy reflectance, canonical variate analysis, red edge position, red absorption feature, continuum removal, and nitrogen concentration

5.1 Introduction

The quality of tropical grass (as determined by the concentration of foliar nitrogen) is an important factor influencing the feeding patterns and distribution of wildlife and livestock in savanna rangelands (Drent & Prins, 1987; McNaughton, 1990; McNaughton & Banyikwa, 1995; Prins, 1989; Prins, 1996). Better quality patches in rangelands contain high percentages of total digestible nutrients and have high percentages of nitrogen concentration. Techniques for mapping grass quality are therefore important to better understand wildlife feeding patterns.

The advent of hyperspectral remote sensing has offered unprecedented opportunities to detect and map variations in grass quality due to its use of narrow spectral channels. These narrow spectral channels allow the detection of detailed features, which are otherwise masked by the broad bands of satellites such as Landsat TM (Kumar *et al.*, 2001; Landgrebe, 1999; Schmidt & Skidmore, 2001). In order to map grass quality, the underlying premise is that patches or sites with different nitrogen levels reflect differently in specific wavelengths.

The detection of foliar nitrogen concentration at canopy level has been largely achieved using very high-resolution spectrometers such as GER 3700 with a spectral sampling interval of less than 2 nm and a band width of less than 5 nm (Curran *et al.*, 1992; Mutanga & Skidmore, 2003; Mutanga *et al.*, In press). However, current operational airborne sensors do not reach such a fine spectral resolution. Instead, the current airborne sensors such as HYMAP MK 1 have wider bandwidths of 15 nm (Boegh *et al.*, 2002; Johnson *et al.*, 1994; Kokaly *et al.*, 2003; Kupiec & Curran, 1995). In view of the current availability of these relatively coarser spectral resolution airborne sensors, it is of interest whether specific spectral channels that are related to foliar nitrogen concentration from these sensors are investigated, for instance, through resampling fine spectral resolution data to coarser spectral resolutions. If positive, such results could make the mapping and monitoring of rangeland condition in space and time operational.

The aim of this study was to investigate whether canopy reflectance spectra, resampled to HYMAP spectral resolution could be used to discriminate between groups of tropical grass grown under different nitrogen treatments. We also sought to identify the spectral bands that are most important in discriminating the foliar groups.

In order to achieve this, we designed an experiment in which we varied the nitrogen concentration available to *C. ciliaris* grass and measured canopy reflectance spectra over four weeks. Subsequent analysis was done by applying canonical variate analysis (CVA) on the $R_{550\text{-}757}$ red absorption feature (Mutanga *et al.*, 2003) as well as the red edge position (Mutanga & Skidmore, In review), using spectra resampled to HYMAP MK 1 resolution. Canonical variate analysis (CVA) is a multivariate statistical tool that has been shown to be

effective in exhibiting optimal separation of groups and learning which variables are most related to the separation of groups (McGarigal *et al.*, 2000; Schmidt, 2003).

5.2. Materials and methods

Blue Buffalo grass (*C. ciliaris*), a sweet perennial grass (C4) that grows naturally in East and Southern Africa and is widely used as a pasture grass (Van Oudtshoorn, 1999, was grown in a greenhouse for this experiment. The grass forms swards that range between 10 cm and 150 cm in height and has proved to be a suitable species for growing in a greenhouse. The experimental set up, planting and monitoring of growth is detailed in Mutanga *et al.* (2003).

5.2.1 Canopy spectral measurements

Reflectance measurements were taken using a GER 3700 spectroradiometer. To manipulate a variation in chemical concentration, measurements were taken at the beginning of each week for four weeks from 3 September 2001. The measurement protocol is fully described in Mutanga *et al.* (2003). Figure 5.1 shows the mean and confidence limits of the measured spectra. A total of 96 samples were measured.

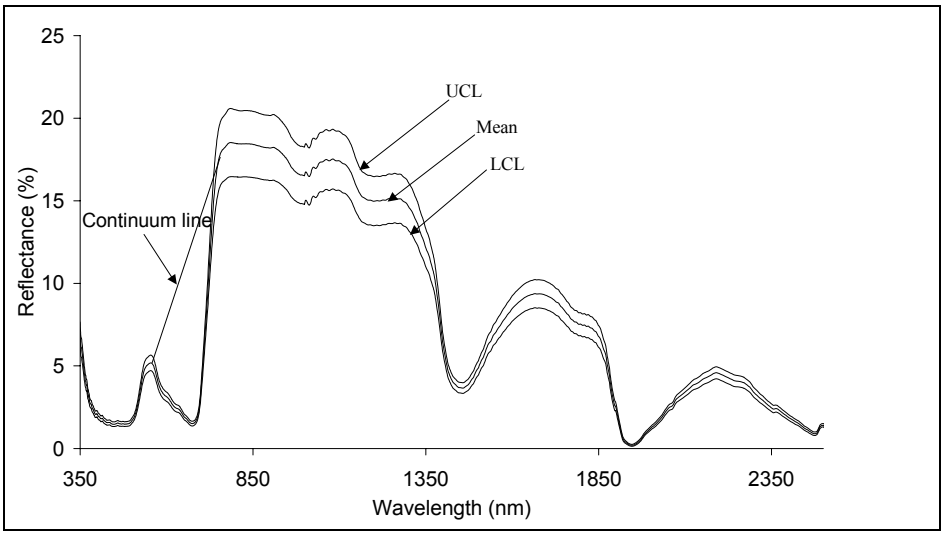

Figure 5.1. Canopy reflectance spectra of *C. ciliaris* grass (n = 96) measured over 4 weeks. The mean, upper 95 % confidence limit (UCL) and lower 95 % confidence limit (LCL) of the spectra are shown. The continuum line shows the start and end points of the absorption feature that was transformed for analysis in this study.

The high-resolution GER spectra were resampled to the HYMAP spectra using the ENVI (Environment for visualising images, Research Systems, Inc.)

software. The method uses a gaussian model with a full width at half maximum (FWHM) equal to the band spacings provided. The modelled HYMAP spectra were used for subsequent analysis.

5.2.2 Chemical analysis

Samples clipped from each pot were taken to the Department of Tropical Nature Conservation and Vertebrate Ecology, at Wageningen University in the Netherlands for chemical analysis. Samples were oven dried at 70º C for 24 hours and were ground through a 1 mm steel screen with a cyclone sample mill. Digestion of the samples was done before automated determinations. Salicylic acid was added to prevent loss of nitrate. After decomposition of the excess H_2O_2, the digestion was completed by concentrated sulphuric acid at elevated temperature under the influence of selenium powder as a catalyst. Nitrogen concentration was measured with a segmented flow analyzer at 660 nm wavelength and was expressed as milligrams per gram (mg/g).

5.3 Data analysis

5.3.1 Continuum removal

Continuum removal was applied on the resampled HYMAP spectra between 550 and 757 nm (Curran *et al.*, 2001; Mutanga *et al.*, 2003). The red absorption feature has been found to be related to foliar nitrogen concentration using fine spectral resolution data (Mutanga *et al*., 2003) and was therefore selected for this study. Furthermore, compared to other absorption features in the shortwave infrared, there is minimum foliar water effect on the red absorption feature therefore suitable for detecting nitrogen on fresh canopies. The waveband of 757 nm was selected as the endpoint on the absorption feature since it is the closest band to the formally used 750 nm band (Mutanga *et al.*, 2003), which is not available on the HYMAP sensor. Continuum removal is calculated by dividing reflectance at the continuum line by the absolute reflectance at the corresponding wavelength. This results in values between 0 and 1. Continuum removal normalizes reflectance spectra to allow comparison of individual absorption features from a common baseline (Kokaly, 2001). The technique also enhances the absorption features (Mutanga *et al.*, 2003; Schmidt & Skidmore, 2003). Figure 5.2 shows the $R_{550\text{-}757}$ continuum removed absorption feature for the HYMAP resampled spectra.

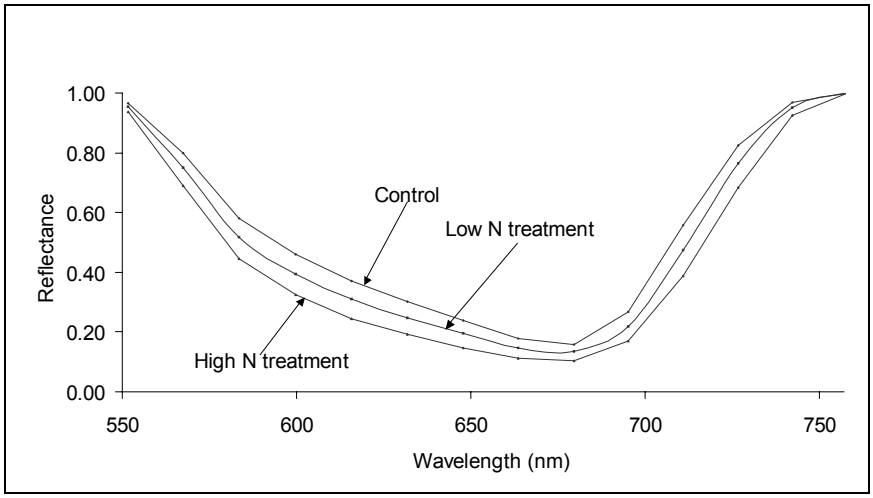

Figure 5.2. Continuum-removed absorption feature between 550 nm and 757 nm for the control, low nitrogen and high nitrogen treatments. Continuum removal was applied to the absorption feature after resampling the GER 3700 spectra to the HYMAP spectra.

Resampling resulted in 14 bands between 550 and 757nm. The first and last bands of the absorption feature were excluded since they had values of 1 after continuum removal. Therefore 12 bands were used for further analysis.

5.3.2 The red edge position (REP)

The red edge position (REP) was also calculated from the resampled spectra. The REP is the point of maximum slope (inflection point) in vegetation reflectance spectra (Fillella & Penuelas, 1994) that occurs in the 680 – 750 nm region. The REP has been found to be strongly correlated with nitrogen concentration (Mutanga & Skidmore, In review) and was therefore applied in this study.

The linear method was used to calculate the red edge position (Clevers & Jongschaap, 2001; Guyot & Baret, 1988). This interpolation method was used rather than the first derivative (Dawson & Curran, 1998) method because the degraded HYMAP spectrum has only five wavelengths in the red edge slope. The linear interpolation assumes that the reflectance at the red edge can be simplified to a straight line centred around a midpoint between the reflectance in the NIR at 780 nm (788 nm for the resampled spectra used in this study) and the reflectance minimum of the chlorophyll absorption feature at about 670 nm (663 nm for the resampled spectra used in this study). The procedure is as follows: First, the reflectance value at the inflection point is estimated (equation 1). Second, the linear interpolation procedure between the measurements at 695 nm and 742 nm is applied to estimate the wavelength corresponding to the estimated reflectance at the inflection point (equation 2). Formally stated:

Calculating the reflectance value at the inflection point (R_{re})

$$(R_{re}) = (R_{663} + R_{788})/2 \quad (1)$$

Calculating the red edge position

$$\lambda_{re} = 695 + 47\left[\frac{(R_{re} - R_{695})}{(R_{742} - R_{695})}\right] \quad (2)$$

where R_{663}, R_{695}, R_{742} and R_{788} are the reflectance values at 663, 695, 742 and 788 nm respectively. The value 695 refers to wavelength position belonging to R_{695}. The value 47 refers to the wavelength interval in nm between 695 nm and 742 nm. Figure 5.3 shows box plots of the red edge positions for the three treatments. The red edge position shifted to longer wavelengths with an increase in nitrogen concentration.

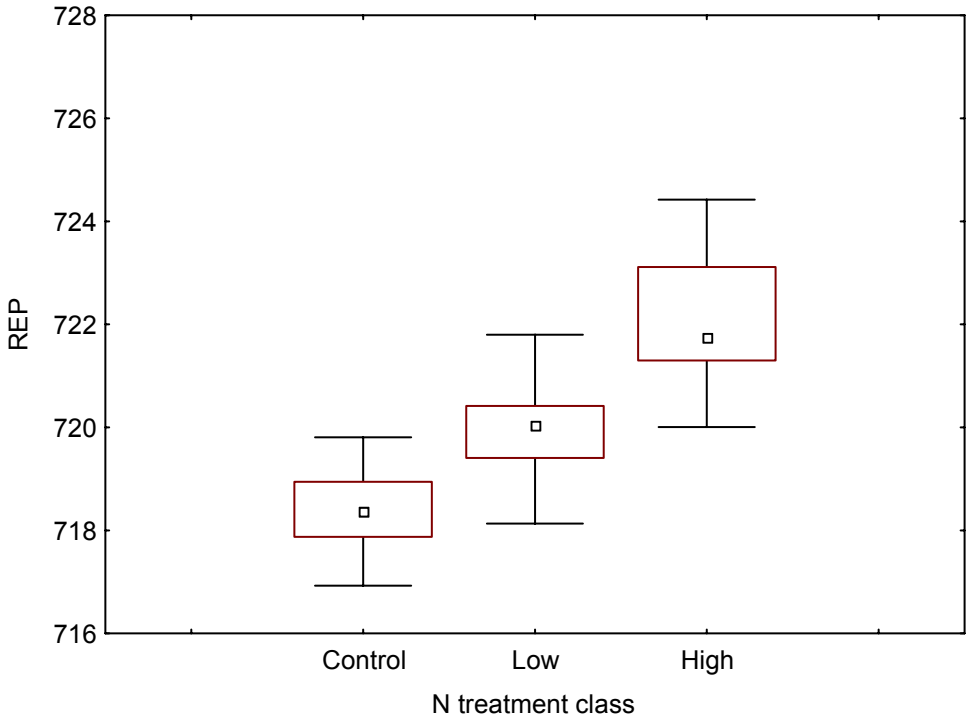

Figure 5.3. Box plots showing the mean and spread of the red edge position (REP) for the three nitrogen treatment groups (Control, Low and High). The REP was calculated using the resampled spectra (from GER 3700 spectra to HYMAP spectra). A linear interpolation technique (Guyot & Baret, 1988) was used to calculate the REP.

The REP was used with the variables from the continuum-removed absorption feature as input to canonical variate analysis (CVA).

5.3.3 Canonical variate analysis

Canonical variate analysis (CVA) is a multivariate analysis technique whose objective is to discriminate among prespecified groups of sampling entities based on a suite of characteristics (McGarigal *et al.*, 2000). The technique involves deriving linear combinations of two or more discriminating variables that will best discriminate among the *a priori* defined groups. The best linear combination of variables is achieved by the statistical decision rule of maximizing the among-group variance, relative to the within-group variance in canonical scores. Canonical variate analysis was applied in this study since it has been shown to significantly improve the mapping of saltmarsh vegetation as compared to other transformation techniques such as principal component analysis (Schmidt, 2003).

The CVA can only be solved for one less than the number of classes g (in this study two canonical functions were generated) and the result is a matrix of eigen vectors (A) with $(g-1)$ dimensions and $(g-1)$ single value decompositions or eigen values. In this regard, the canonical transformation matrix is used to transform the reflectance spectra into lower dimensional space y.

The first canonical function defines the specific linear combination of variables that maximizes the ratio of among-group to within-group variance in any single dimension. The second canonical function explains the remaining variance (also based on among-group to within-group variance) and so forth. Therefore a meaningful interpretation can be given to the gradient based on the relative importance of the original variables in the linear function and there is data reduction in the process.

From this background, we used CVA to achieve two main objectives:

(i) to exhibit optimal separation of the three treatment groups, based on linear transformations (canonical functions or canonical variates) of the HYMAP spectra and establish which wavelengths are most related to the separation of groups (called descriptive canonical variate analysis), and;

(ii) to predict the group membership for samples of undefined origin based on its measured values of the discriminating variables. In other words, to establish the potential of canonical variates derived from reflectance spectra in classifying samples to their respective treatment classes (called predictive canonical variate analysis or classification).

These two objectives were used to evaluate the potential of canopy reflectance spectra; resampled to HYMAP resolution (our main research question) in discriminating grass subjected to different nitrogen treatments.

Classification of the treatment groups was applied using spectra after a canonical variate transform. The classification method utilises a linear combination of discriminating variables that maximises group differences while minimising variation within groups. The linear combinations yield canonical functions for each group. Each function allows the computation of canonical scores for each case for each group. Each case is then classified into the group with the closest group mean canonical score.

We used the leave-one-out cross validation technique for estimating the error rate conditioned on the training data. Using this cross validation technique, each observation is systematically dropped, the canonical function re-estimated and the excluded observation classified. The confusion matrix was constructed to compare the true class with the class assigned by the classifier to the test samples. We also calculated a discrete multivariate technique called kappa analysis that uses the $\hat{K}$ statistic as a measure of agreement with the reference data (Cohen, 1960; Skidmore, 1999; Congalton, 1993). If kappa coefficient is one or close to one then there is perfect agreement between the training and test data.

5.4. Results

5.4.1 Variation in foliar nitrogen concentration

In order to evaluate whether the experiment yielded distinct groups with different foliar nitrogen concentration, we assessed the amount of nitrogen contained in the three foliar groups. Results showed that, the design of the experiment resulted in a variation in the foliar concentration of nitrogen between treatments (Table 5.1).

Table 5.1: Foliar nitrogen concentration

Treatment	Mean	Confidence level (95%)
Control	13.8	1.59
Low	19.3	2.36
High	34.2	2.23

We tested the research hypothesis that the mean nitrogen concentration (mg/g) for the control, low and high nitrogen treatments were different, *viz*. the null hypothesis Ho: $\mu1 = \mu2 = \mu3$ versus the alternate hypothesis Ha: $\mu1 < \mu2 < \mu3$, where: $\mu1$, $\mu2$ and $\mu3$ are the mean nitrogen concentrations for the control, low and high treatments respectively. We used a one-way ANOVA to test this

research hypothesis. The conclusion from this test is that the mean concentrations are significantly different ($p < 0.001$).

One - way ANOVA only shows that there is a significant difference in the mean nitrogen concentrations from the three treatments, but it does not show which pairs are different. We therefore executed a post-hoc Scheffe' test in order to establish differences between each treatment. Results indicated that the mean nitrogen concentration differed significantly for each treatment pair ($p < 0.001$), prompting an investigation of the potential of high-resolution reflectance data in discriminating between the treatment groups containing different mean foliar nitrogen concentrations.

5.4.2 Canonical variate analysis result

The overall discrimination between the three treatment groups was highly significant (Wilks' lambda = 0.14, F = 7.6, $p < 0.000$). Table 5.2 shows the eigen values as well as the factor structure matrix from the canonical variate analysis. The factor structure coefficients represent the correlations between the variables and the canonical functions and are used to interpret the meaning of the canonical functions.

The largest proportion of the explained variance (95%) is contained in the first canonical function. The highest factor structure coefficients are contained in the red edge slope (the coefficients are greater than 0.70 for the REP and the 726 nm, 710 nm, as well as 742 nm bands). The second canonical function also shows that the largest contribution is contained in the red edge slope (742 nm, 726 nm, REP) and to a lesser extent, the green portion of the electromagnetic spectrum (583 nm).

Table 5.2: Factor Structure Matrix representing the correlation between the variables and the canonical functions.

	Root 1	Root 2
Eigenvalues	4.6576 (95%)	0.2672 (100%)
REP	**-0.708376**	0.255207
567	0.670072	-0.095898
583	0.619955	-0.191510
599	0.594963	-0.053645
615	0.568852	-0.033682
631	0.537990	-0.016494
647	0.496565	-0.027894
663	0.417850	-0.054934
679	0.368828	-0.092437
695	0.558773	-0.037651
710	**0.723892**	-0.069436
726	**0.743228**	-0.220834
742	**0.706960**	-0.359094

Table 5.3 shows means of canonical variables, which indicate the nature of the discrimination for each canonical root or function. The results in Table 5.3 indicate that the first canonical function discriminates mostly between the control group and other treatments, followed by the high treatment group.

Table 5.3: Means of canonical variables to determine the nature of the discrimination for each canonical root

	Root 1	Root 2
Control	-2.61408	0.354514
Low	0.02523	-0.719493
High	2.58885	0.364979

The second canonical function discriminates mostly between the low treatment group and other treatments, however, based on the review of the eigenvalues (Table 5.2), the magnitude of the discrimination is much smaller for the second canonical function than that of the first canonical function. The scatter plot in Figure 5.4 shows the positions of samples in the canonical space.

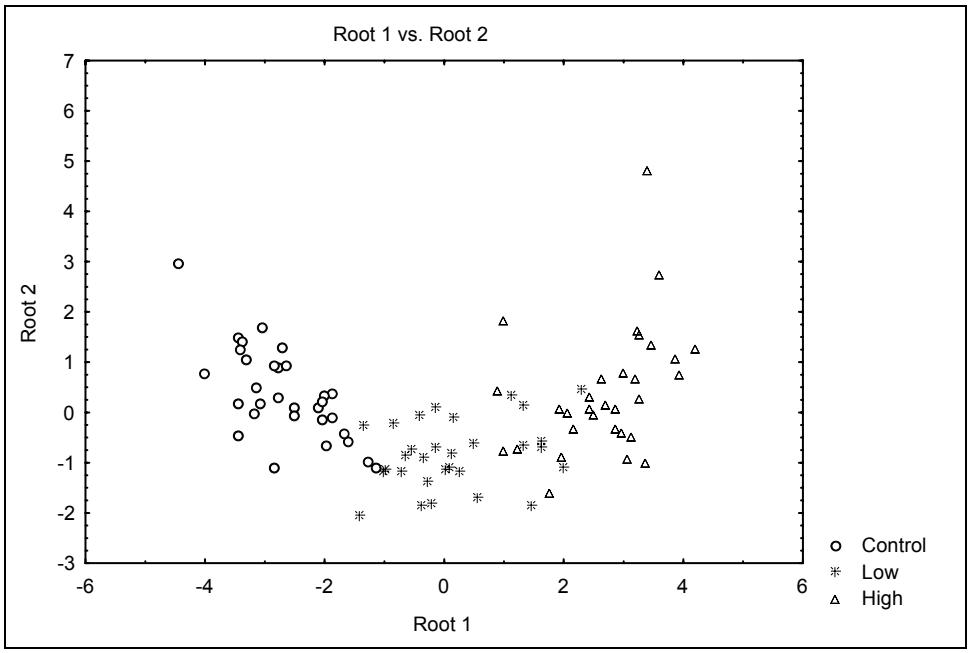

Figure 5.4. Scatterplot of two canonical scores produced by canonical variate analysis. The positioning of the treatment groups indicates the gradient of foliar nitrogen concentration contained by the groups.

The positioning of the canonical scores shows a gradient from the control, with very low nitrogen concentration, to the high treatment with high nitrogen concentration.

5.4.3 Classification

To further investigate the effectiveness of hyperspectral data to discriminate between treatment groups as well as explaining the observed patterns, we classified the samples using the Fisher's linear discriminant function with proportional to group size prior probabilities (McGarigal *et al.*, 2000; Richards, 1993). Following the leave one out cross validation, the confusion matrix in Table 5.4 shows that we could classify samples to their respective groups with an overall accuracy of 77.1%.

Table 5.4. Testing the predictive discriminatory power of the canonical functions. We used the leave-one-out technique for estimating the error rate conditioned on the training data. Consequently, each observation is systematically dropped, the canonical function re estimated and the excluded observation classified. The confusion matrix includes the kappa statistic, commission error (CE), user accuracy (UA), omission error (OE), and producer accuracy (PA).

	Control	Low	High	CE	UA
Control	27	5	0	16	84
Low	4	22	6	31.2	68.8
High	0	7	25	21.9	78.1
OE	12.9	35.3	19.4	% acc = 77.1	
PA	87.1	64.7	80.6	Kappa = 0.66	

This high classification rate indicates the degree of discrimination achieved by the canonical functions.

A posthoc analysis of the misclassified samples indicate that 56% of the misclassified samples have foliar nitrogen concentration values that falls within the lower and upper quartiles of the nitrogen concentration ranges of the treatment groups to which they were classified. These samples therefore represent the overlapping nitrogen concentration samples between the groups (Figure 5.4). This result confirms the effect of foliar nitrogen concentration on spectral reflectance.

5.5 Discussion

This study aimed at discriminating treatment groups of tropical grass containing different levels of nitrogen concentration using spectrometry. The motivation of the study was to investigate whether there is a possibility to map rangeland patches exhibiting different levels of nitrogen concentration using their reflectance spectra. To achieve this ultimate goal of mapping rangeland quality, an investigation of the utility of the operational airborne sensors with a coarser spectral resolution than the field spectrometers is critical.

We tested the utility of spectra, resampled to HYMAP resolution (15 nm band width in the visible domain) in discriminating between the treatment groups containing different foliar nitrogen concentrations. The study has shown that, canonical functions derived from continuum removed red absorption feature, in combination with the red edge position (resampled to HYMAP resolution) can discriminate between the treatment groups with different foliar nitrogen concentrations. This result permits the extension of laboratory experiments to airborne hyperspectral images for mapping the concentration of nutrients (quality) in tropical grasses. Furthermore, the successful use of the visible portion of the electromagnetic spectrum in accomplishing this task is of significance in remote sensing.

Relative to other parts of the electromagnetic spectrum such as the SWIR, the effect of water absorption in the visible portion of the electromagnetic spectrum is minimum. Therefore, the wavebands in this region can be used as additional information for mapping foliar biochemical concentration on fresh canopies. Experiments using the red edge slope have also shown that, this portion is insensitive to atmospheric and background effects (Broge & Leblanc, 2000; Clevers, 1999; Demetriades-Shah *et al.*, 1990; Guyot *et al.*, 1992), therefore useful for mapping grass quality under natural environmental conditions. These results are comparable to those of Mutanga *et al.*, (2003) who found out that the visible red absorption feature as well as the REP can discriminate between different nitrogen treatment groups using a high resolution field spectrometer (GER 3700). Such consistent results demonstrate the potential use of the visible region even at a coarser HYMAP spectral resolution, is of significance in mapping rangeland quality.

Canonical variate analysis (CVA) has helped to reduce dimensionality in the hyperspectral data set to two canonical functions as well as describing and exploring the relative importance of individual wavelengths in explaining foliar nitrogen differences. The technique also provided an insight in the relationships among the treatment groups, thereby unravelling the potential of hyperspectral remote sensing in discriminating between different levels of foliar nitrogen concentration.

The analysis using CVA has shown that the highest factor structure coefficients (canonical loadings) for the first canonical function are contained in the red edge slope (Table 5.2). As shown by the eigenvalues, the magnitude of

canonical discrimination in the first canonical function (the first function accounts for 95% of the explained variance) is higher than the other function, thereby indicating the importance of the significant red edge variables. The red edge is caused by strong chlorophyll absorption in the red region and canopy scattering in the near infrared (Dawson & Curran, 1998). As a result of a strong relationship between chlorophyll and foliar nitrogen concentration (Katz *et al.*, 1966; Penuelas *et al.*, 1994), a strong relationship between the red edge and nitrogen concentration is expected (Mutanga & Skidmore, In review)**.** Overall, this analysis shows the importance of the red edge slope in discriminating foliar treatment groups with different levels of nitrogen concentration.

The relative positioning of the groups along the canonical axes in Figure 5.4 provides an insight in the relationships among the treatment groups. Treatment groups in close proximity in canonical space are similar with respect to the gradients defined by the canonical functions. The control is positioned to the left, followed by the low treatment in the middle, and the high treatment is positioned to the right of the feature space. This positioning indicates the gradient of foliar nitrogen concentrations contained by the groups, thereby confirming the potential of hyperspectral remote sensing in separating groups with different levels of foliar nitrogen concentration.

Canonical variate analysis using hyperspectral data has also classified foliar nitrogen cases (entities) into their respective groups with an accuracy of 77%. Considering that the spectra was degraded to HYMAP resolution, this result shows potential to use airborne hyperspectral remote sensing to map foliar nitrogen concentration in rangelands.

In summary, the results presented in this study show the potential use of hyperspectral remote sensing to predict and map tropical grass quality.

5.6. Conclusions

This paper aimed at discriminating between the nitrogen treatment groups of tropical grass using a combination of continuum-removed spectra and the REP, resampled to HYMAP resolution. Our results have shown that:

(i) Canonical functions computed from spectral data can discriminate between the treatment groups containing different foliar nitrogen concentrations.

(ii) Even though the spectral resolution was degraded to HYMAP spectra it was still possible to classify test samples to their respective classes with an accuracy of 77.1 %.

(iii) The canonical structure matrix has revealed that greater discrimination power is contained in the red edge slope. The first canonical function (Root 1) is strongly related with the 726 nm, 710 nm, and 742 nm wavebands as well as the REP. This shows the importance of the red edge in predicting foliar nitrogen concentration, thereby confirming previous studies

that found strong correlations between foliar nitrogen and the red edge (Mutanga and Skidmore, 2003).

Overall, this study has demonstrated that, it is possible to discriminate grass containing different levels of nitrogen concentration at **canopy level,** thereby setting the basis to use hyperspectral data to predict grass quality under natural field conditions. In addition, the study demonstrated the possibility to discriminate grass with different levels of nitrogen concentration using **resampled** hyperspectral data. This permits the up scaling of the method to airborne sensors such as HYMAP for mapping tropical grass quality. Such studies will further enhance an understanding of wildlife feeding patterns and their spatial distribution.

Tropical grass quality at Field Level: Chapter 6-8

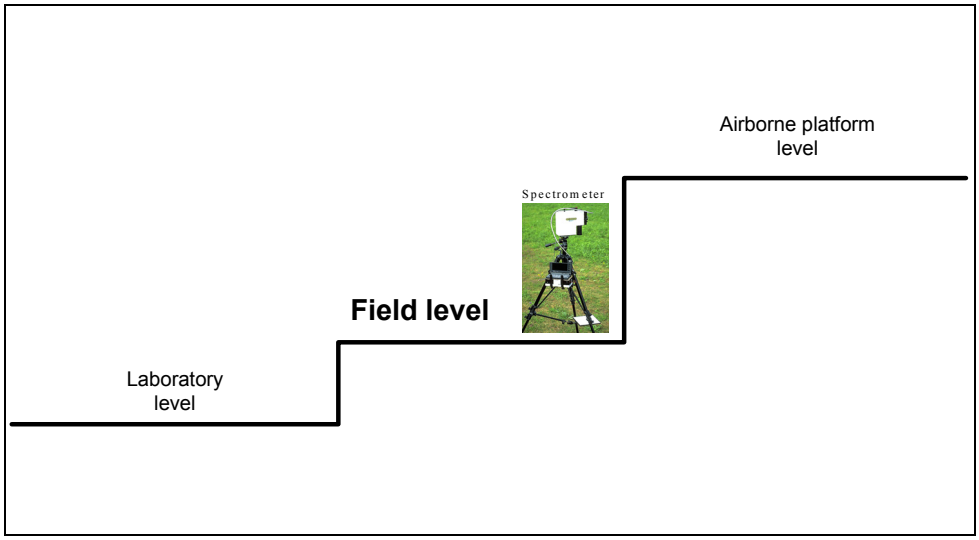

CHAPTER 6:
Predicting *in situ* grass quality in the Kruger National Park, South Africa, using continuum-removed absorption features

*This chapter is based on

1. Mutanga, O., Skidmore, A. K., and Prins, H.H.T, (2004), Predicting *in situ* pasture quality in the Kruger National Park, South Africa, using continuum-removed absorption features, *Remote Sensing of Environment,* **89** (3), 393-408.

The paper is a modified version of a conference paper entitled:

2. Mutanga, O., Skidmore, A. K, (2003), Continuum-removed absorption features estimate tropical savanna pasture quality *in situ, 3rd EARSeL Workshop on Imaging Spectroscopy*, 13-16 May 2003. EARSeL, Hersching , Germany

Best conference paper presentation award

Abstract

The remote sensing of grass quality as determined by nitrogen, phosphorous, potassium, calcium and magnesium concentration is critical for a better understanding of wildlife and livestock feeding patterns. Although remote sensing techniques have proved useful for assessing the concentration of foliar biochemicals under controlled laboratory conditions, more investigation is required to assess their capabilities in the field, where inconsistent results have been obtained so far. We investigated the possibility of determining the concentration of *in situ* biochemicals in a savanna rangeland, using the spectral reflectance of five grass species. Canopy spectral measurements were taken in the field using a GER 3700 spectroradiometer. We tested the utility of using four variables derived from continuum-removed absorption features for predicting canopy nitrogen, phosphorus, potassium, calcium and magnesium concentration: (i) continuum-removed derivative reflectance (CRDR), (ii) band depth (BD), (iii) band depth ratio (BDR) and (iv) normalised band depth index (NBDI). Stepwise linear regression was used to select wavelengths from the absorption-feature-based variables. Univariate correlation analysis was also done between the first derivative reflectance and biochemicals. Using a training data set, the variables derived from continuum-removed absorption features could predict biochemicals with R^2 values ranging from 0.43 to 0.80. Results were highest using CRDR data, which yielded R^2 values of 0.70, 0.80, 0.64, 0.50 and 0.68 with root mean square errors (RMSE) of 0.01, 0.004, 0.03, 0.01 and 0.004 for nitrogen, phosphorous, potassium, calcium and magnesium, respectively. Predicting biochemicals on a test data set, using regression models developed from a training data set, resulted in R^2 values ranging from 0.15 to 0.70. The error of prediction (RMSE) in the test data set was 0.08 (±10.25 % of mean), 0.05 (± 5.2 % of mean), 0.02 (± 11.11 % of mean), 0.05 (± 11.6 % of mean) and 0.03 (± 15 % of mean) for nitrogen, potassium, phosphorous, calcium and magnesium, respectively using CRDR. When data was partitioned into species groups, the R^2 increased significantly to > 0.80. With high-quality radiometric and geometric calibration of hyperspectral imagery, the techniques applied in this study (i.e. continuum removal on absorption features) may also be applied on data acquired by airborne and spaceborne imaging spectrometers to predict and ultimately to map the concentration of macronutrients in tropical rangelands.

Key words: Field spectra, absorption features, bootstrapping, continuum removal, and savanna rangelands

6.1. Introduction

Macronutrients (nitrogen, phosphorous, potassium, calcium and magnesium) are mainly responsible for plant development and health; therefore they determine nutritional quality of forage for herbivores (Salisbury & Ross, 1985). Nitrogen is commonly the most limiting nutrient for grazers (Grant *et al.*, 2000; Owen-Smith & Novellie, 1982; Prins, 1996; Scholes & Walker, 1993). Therefore, an understanding of nitrogen concentration in pastures is relevant to understanding the survival and productivity of wildlife and livestock populations. Studies of Southern African pastures have also shown that, besides nitrogen, phosphorous and to a lesser extent potassium are limiting factors (Du Toit & Malan, 1940). In the Serengeti ecosystem, McNaughton and Banyikwa (1995) discovered that phosphorous was an important element in discriminating between grazing hot spots and control swards. In the Tarangire ecosystem, nitrogen and phosphorous determine the migratory patterns of wildebeest (Voeten, 1999). Studies have also shown that potassium deficiency in wildlife results in muscle weakness, cardiac as well as respiratory failure (Groenewald & Boyazoglu, 1980; Robbins, 1983). Calcium and magnesium are largely responsible for bone and tooth formation. To prevent malnutrition and disease, wildlife exhibit preferences for certain sites and certain plant species or communities based on quality (Muya & Oguge, 2000). In this regard, the development of techniques to predict pasture quality is critical for explaining the distribution and feeding patterns of wildlife and livestock (Styles & Skinner, 1997; van Soest, 1994).

The traditional methods available for detecting pasture quality require detailed sampling and expensive laboratory analysis. This usually results in the collection and analysis of inadequate data that are not representative of the population if large areas are investigated (Foley *et al.*, 1998). Remote sensing offers potential to predict foliar biochemical concentrations in rangelands, thereby reducing the tedious process of intensive sampling and laboratory analysis.

The remote sensing of foliar biochemicals has developed rapidly since the late 1970s (Curran *et al.*, 1995; Peterson *et al.*, 1988; Wessman, 1994; Yoder & Pettigrew-Crosby, 1995), using mainly laboratory near-infrared spectroscopy (NIRS) methods (Marten *et al.*, 1989; Norris *et al.*, 1976). NIRS can provide accurate predictions of protein, amino acids, lignin and cellulose concentrations contained in dried ground forage (Norris *et al.*, 1976), and in many laboratories the technique has replaced wet chemistry as the standard analytical procedure for assessing plant biochemicals (Yoder & Pettigrew-Crosby, 1995).

Extending the use of empirical laboratory NIRS to predicting biochemicals at canopy level has not been very successful to date (Curran *et al.*, 2001; Kumar *et al.*, 2001). This is because the presence of water in fresh canopies masks the biochemical absorption features, particularly in the

shortwave infrared (Clevers, 1999; Kokaly & Clark, 1999). In addition, leaf orientation and soil background effects, as well as atmospheric absorption, further complicate the remote sensing of biochemicals in the field (Asner *et al.*, 2000). Studies that used NIRS methods such as multiple linear regression to predict canopy chemistry have yielded inconsistent results when applied across different vegetation types (Grossman *et al.*, 1996). NIRS-based techniques such as stepwise regression also suffer from problems of overfitting, especially when more wavebands than samples are used (Curran *et al.*, 2001).

In order to minimize the effect of spectral variability that is independent of the biochemical concentration, Kokaly and Clark (1999) applied a refined approach that enhances and standardises known chemical absorption features. In their study, continuum removal was applied to broad absorption features of dry leaf spectra in the shortwave infrared region (1730 nm, 2100 nm and 2300 nm) and absorption band depths relative to the continuum were calculated. Like NIRS, this approach uses stepwise regression. The risk of overfitting is minimised by concentrating on known absorption troughs that are enhanced by continuum removal (Clark & Roush, 1984). The method showed strong correlation (r^2 = 0.95) between nitrogen concentration and the continuum-removed and normalised band depths at five locations in the 2100 nm absorption feature. Recently, Curran *et al.* (2001) applied the Kokaly and Clark methodology to 12 biochemicals and achieved high accuracy. Mutanga *et al.* (In review) applied the method to predicting biochemicals in live standing canopies, using the major chlorophyll absorption feature in the visible domain. However, all the above studies were conducted under controlled laboratory conditions. The method has not been extended to the field to our knowledge. In addition, only a few studies (Gong, 2002; Milton *et al.*, 1991; Ponzoni & Goncalves, 1999) have attempted to determine the foliar nutrient status of potassium, phosphorous, magnesium and calcium.

A relationship between spectral reflectance, particularly visible absorption and macronutrients such as phosphorous, potassium, magnesium and calcium is expected due to their effect on the photosynthetic process in plants (Al-Abbas *et al.*, 1974; Thomas & Oerther, 1972). For example, phosphorous is fundamental to tissue composition as well as being one of the components of the nucleic acids and enzymes. Potassium is also important, both for activating enzymes responsible for the metabolism of carbohydrates and in the apical dominance (Ponzoni & Goncalves, 1999). These elements are therefore responsible for both the photosynthetic process and the tissue composition of plants, and hence related to the visible absorption bands (Salisbury & Ross, 1985). Nitrogen exhibits specific absorption features in the shortwave infrared (Curran, 1989) and is also responsible for the metabolic function of the chlorophyll. Since chlorophyll largely determines spectral reflectance in the visible, a strong relationship between visible absorption bands and nitrogen concentration is also expected.

In this study, we aimed at improving and extending the band depth analysis method in order to predict the concentrations of macronutrients in grasses (nitrogen, phosphorous, potassium, calcium and magnesium) measured in the Kruger National Park, South Africa. In addition to the shortwave infrared absorption features used by Kokaly and Clark, we considered the two major absorption features located in the visible region, where the effect of water is minimal. A modified first derivative reflectance approach and a new index were also developed and tested.

6.2. Materials and methods

6.2.1. The study area

The study area was located in the northern plains of the Kruger National Park (KNP) in South Africa. A strip of 2 km by 25 km was selected, stretching west (22º 49′ S and 31º 01′ E) to east (22º 44′ S and 31º 22′ E) and covering granitic and basaltic formations. The site is generally flat, particularly the eastern part, which is underlain by basalt. Grass production is higher in the basalts than in the granite area, and there is considerable variation in species as well as nutritional quality between the two geological formations (Grant *et al.*, 2000). The area is generally covered by open grassland in the east, mixed mopane (*Colophospermum mopane*) and grass in the basalt-granite transition, and woodland in the granite area.

Stratified random sampling with clustering was adopted in this study. The area was stratified (using the land cover map provided by the KNP GIS division) into open grassland in the basalt area, and mixed woodland and woodland in the granite area. Coordinates (x y) were randomly generated in each stratum to select plots. A total of 30 plots were initially generated. To increase the number of samples in a time and labour constrained situation, two extra plots were clustered at least 100 m from each of the initially generated plots. This resulted in a total of 90 plots that were sampled. Each plot covered 10 m by 10 m, largely homogenous in species cover. The plot size was decided in order to clearly identify the dominant grass species as well as for collecting other ancillary data (e.g slope, terrain position and species cover) that was used in a separate paper.

6.2.2. Canopy spectral measurements and collection of samples for laboratory analysis

Replicates of canopy spectral measurements were taken from a bunch of grass representing one dominant grass species in each plot using a GER (Geophysical and Environmental Research Corporation, Buffalo, New York) spectroradiometer and samples for laboratory analysis were collected from that particular bunch of grass. The GER 3700 is a three dispersion grating

spectroradiometer using Si and PbS detectors with a single field of view. The wavelength range is 350 nm to 2500 nm, with a spectral sampling of 1.5 nm in the 350 nm to 1050 nm range, 6.2 nm in the 1050 nm to 1900 nm range, and 9.5 nm in the 1900 nm to 2500 nm range. The bandpass is 3 nm, 11 nm and 16 nm in the 350 nm to 1050 nm range, 1050 nm to 1900 nm range, and 1900 nm to 2500 nm range, respectively.

The fibre optic sensor was pointed at the target (a bunch of grass species representing one dominant grass species) in nadir position from about 1 m height for each spectral measurement. The ground field of view was about 18 cm in diameter, which was large enough to cover a bunch of a grass species, without measuring possible surrounding bare areas. For each measurement, a single dominant species was represented in the field of view and a total of 25 replicate spectral measurements were taken from that dominant species in the plot. In other words, the replicates are repeated spectral measurements of the same field of view from a bunch of grass representing one dominant grass species. The resulting spectrum was determined as an average of the 25 spectral measurements. In few cases where two species dominated in a plot, replicates of spectral measurements were taken separately for each species. The calibrated GER spectrometer automatically converted the digital numbers to radiance units. These radiance units were in turn converted to reflectance using scans of a calibrated Spectralon reference panel (Labsphere, Inc, North Sutton, New Hampshire).

The fieldwork was conducted at the beginning of the dry season from mid April to mid May in 2002. Spectral measurements were taken on clear sunny days between 11:30 a.m. and 2:00 p.m. For the wooded western portion of the study area, spectral measurements were taken in sun lit areas between the trees. In the few cases where two species dominated in a plot, both spectra and samples were collected separately for each species and stored in separate paper bags. This means that both spectra and samples for laboratory analysis were collected according to species and subsequent analysis was done using subsets of individual species and then using a combined data set for all the samples. A total of 96 samples, comprising five grass species (*C. ciliaris, E. lehmanniana, U. mosambicensis, P. maximum and T. triandra*) were collected for analysis (Table 6.1).

Since the fieldwork was conducted at the beginning of the dry season, the grass was already starting to senesce. The senescing state of the grass is reflected in the mean spectral profile (Figure 6.1) of the data collected, which distinctively shows the $R_{2006\text{-}2196}$ biochemical absorption feature that could otherwise be masked by water in fresh plants (Kokaly & Clark, 1999).

Although it is known that foliar nutrient quality is important to herbivores at all times of the year (Prins, 1989), we carried our fieldwork during the beginning of the dry season because nutrient quality becomes more critical during the dry season as compared with the wet season (McNaughton, 1988; Prins & Olff, 1998). The wet season grass is green and highly nutritious,

whereas during the dry season nutrient concentration becomes low and patchy as the grass senesces causing herbivores to concentrate on patches with relatively high nutrient concentration (Owen-Smith & Novellie, 1982). In other words, we assert that nutrient concentration becomes an even more critical determinant of herbivore distribution during the dry season.

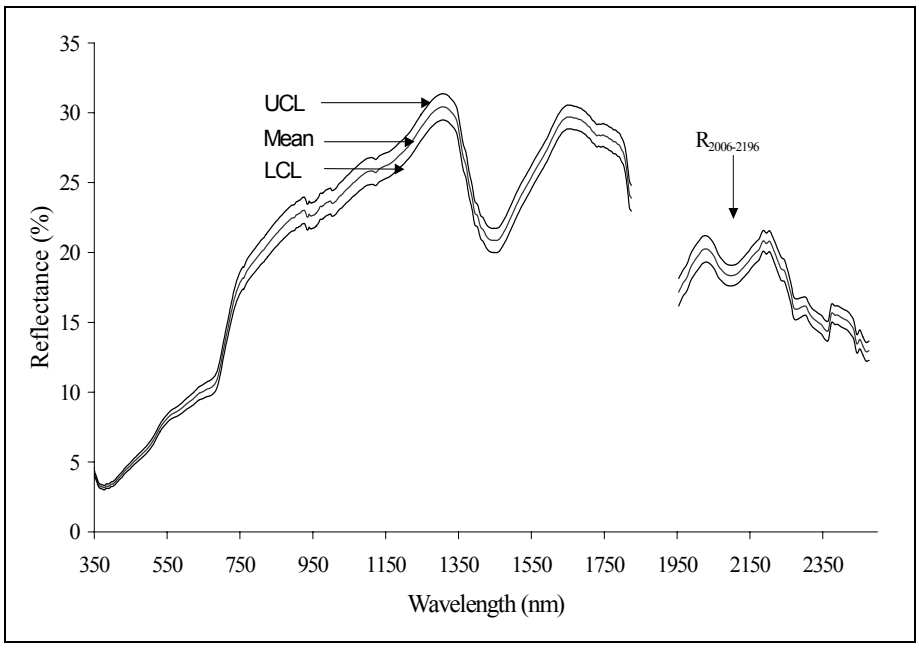

Figure 6.1: Mean reflectance spectrum (flanked by 95 % upper confidence limit (UCL) and 95 % lower confident limit (LCL)) of the data used in this study (n = 96). The $R_{2006\text{-}2196}$ biochemical absorption feature is shown indicating the senescing state of the grass during the period of measurement. The spectral region between 1824 nm and 1954 nm was removed due to excessive noise.

6.2.3. Biochemical analysis

The spectrally measured grass in the plots was clipped and oven-dried at 70º C for 24 hours. Plant tissue was analysed at the Institute of Tropical and Subtropical Crops under the Agricultural Research Council (ARC-ITSC) in Nelspruit, South Africa using the wet digestion techniques with 98% sulphuric acid and 30% hydrogen peroxide for N extraction and 55% nitric acid and 70% perchloric acid for P, K, Ca, Mg and Na extraction (Giron, 1973). Atomic absorption flame spectroscopy using air-acetylene was used for detecting potassium, calcium and magnesium (Poluektov, 1973). The colometric method was used to detect nitrogen (Technicon Industrial method 329 - 74W) and phosphorous (Technicon Industrial method 4 – 68W). For phosphorous detection the phosphomolybedenum complex was read at 660 nm and for

nitrogen detection the ammonia-salicylate complex was read at 640 nm (Grasshoff *et al.*, 1983).

6.3. Data analysis

Univariate as well as multivariate statistical techniques were applied in this study. Univariate correlations were calculated on standard first derivative reflectance (FDR). Multivariate analyses were carried out on variables calculated from continuum-removed absorption features, as proposed by Kokaly and Clark (1999), i.e. band depth (BD) and band depth ratio (BDR). We also proposed and tested two new variables: continuum-removed derivative reflectance (CRDR) and normalised band depth index (NBDI).

6.3.1. First derivative reflectance

A first difference transformation of the reflectance spectrum (FDR) calculates the slope values from the reflectance and can be derived from the following equation (Dawson & Curran, 1998):

$$FDR_{\lambda(i)} = (R_{\lambda(j+1)} - R_{\lambda(j)}) / \Delta\lambda \qquad (1)$$

where FDR is the first derivative reflectance at a wavelength *i* midpoint between wavebands j and j+1. $R_{\lambda(j)}$ is the reflectance at waveband j, $R_{\lambda(j+1)}$ is the reflectance at waveband j+1, and $\Delta\lambda$ is the difference in wavelengths between j and j+1. The GER spectrometer wavelength intervals (described earlier) were used to denote the intervals between channels j and j+1. Correlations between the FDR and foliar biochemicals were calculated at each wavelength, and correlograms were plotted.

6.3.2. Absorption features

Six known chemical absorption features were selected for this study: the chlorophyll absorption features in the visible domain ($R_{470-518}$ and $R_{550-750}$), which have been found to be related to nitrogen concentration and other biochemicals in both fresh standing canopies (Mutanga *et al.*, In review) and dried ground plant material (Curran *et al.*, 2001); and shortwave absorption features ($R_{1116-1284}$, $R_{1634-1786}$, $R_{2006-2196}$ and $R_{2222-2378}$) that have hitherto used in studies of dried plant material (Curran *et al.*, 2001; Kokaly & Clark, 1999).

Continuum removal was applied to the selected absorption features. Continuum removal normalises reflectance spectra in order to allow comparison of individual absorption features from a common baseline (Kokaly, 2001). The continuum is a convex hull fitted over the top of a spectrum to connect local spectral maxima. The convex hull can be considered as the shape that a rubber band would attain if it were stretched over the reflectance spectrum. This means

that the convex hull will be in contact with the reflectance spectrum at maximum reflectance points such as the red edge shoulder.

Since we were interested in isolating specific absorption features in this study, we defined local start and end points on a particular absorption feature. These endpoints were initially used by Kokaly and Clark (1999) as well as Curran *et al* (2001) and we adapted them in this study for comparison and consistency. Linear continua were fitted between the start and endpoints of the absorption features and then continuum removal was applied. The continuum-removed reflectance $R'_{(\lambda)}$ is obtained by dividing the reflectance value $R_{(\lambda)}$ for each waveband i in the absorption feature by the reflectance level of the continuum line (convex hull) $Rc_{(\lambda)}$ at the corresponding wavelength i:

$$R'_{(\lambda i)} = \frac{R_{(\lambda i)}}{R_{c(\lambda i)}} \quad (2)$$

The first and last spectral data values are on the hull and therefore the first and last values of the continuum-removed spectrum are equal to 1. The output curves have values between 0 and 1 in which the absorption troughs are enhanced (Schmidt & Skidmore, 2001). Continuum removal enhances bands by correcting for apparent shifts in the band minimum caused by wavelength-dependent scattering that imparts a slope to the spectrum. Removal of the continuum slope corrects the band minimum to that of the true band centre (Clark & Roush, 1984). Figure 6.2 shows continuum-removed absorption features (averaged over samples of each of the three species) in the visible region, with a variation in band depth for different species.

Continuum removal has proved useful in mapping the distribution of minerals by comparing remotely sensed absorption band shapes with those in a reference library (Clark & Roush, 1984). Efforts to apply the method in vegetation science have been made using dried plant material in the laboratory (Kokaly, 2001; Kokaly & Clark, 1999). At canopy scale, Kokaly *et al.*, (2003) applied spectral feature analysis of continuum removed plant absorption features to discriminate species composition of *in situ* forest stands. This method has not to our knowledge been extended to predict foliar biochemicals *in situ*.

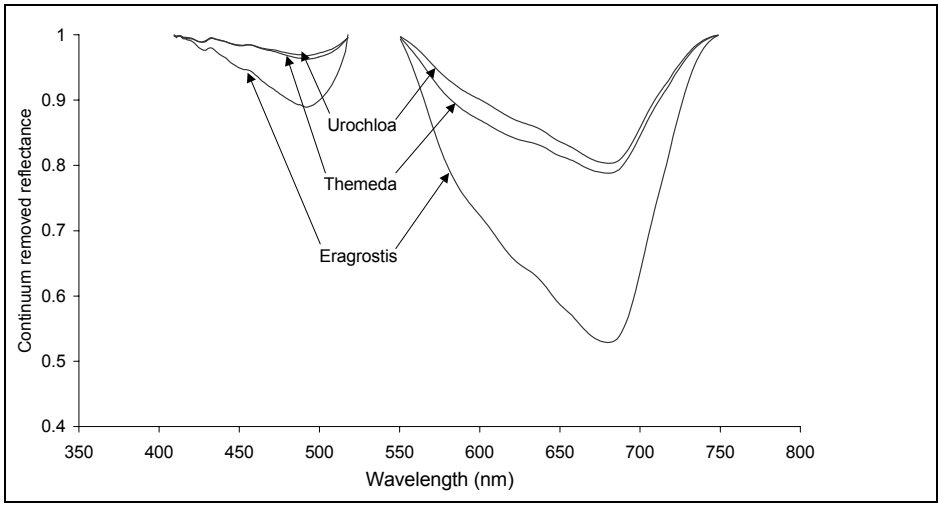

Figure 6.2: The absorption features ($R_{470-518}$ and $R_{550-750}$) enhanced by continuum removal for three species collected in this study (*U. mosambicensis, T. triandra, E. lehmanniana*). The absorption features shown are averaged spectrum of all the samples representing each of the three species respectively.

The four variables (CRDR, BD, BDR, NBDI) were calculated from the continuum-removed absorption features as follows:

(i) Continuum-removed derivative reflectance (CRDR) was calculated by applying the first difference transformation described in equation 1 to the continuum-removed reflectance spectrum R'. CRDR approximates the slope of reflectance, which is more closely related to absorption features enhanced by continuum removal (Schmidt & Skidmore, 2003) than the reflectance magnitude *per se* (Serrano *et al.*, 2002).

(ii) Band depth (BD) was calculated by subtracting the continuum-removed reflectance at wavelength *i* from 1:

$$BD_{(\lambda i)} = 1 - R'_{(\lambda i)} \quad (3)$$

(iii) Since remotely sensed measurements of vegetation canopies are affected by factors such as atmospheric absorptions, soil background and water, a normalisation procedure using band indices was also carried out to minimise these influences (Kokaly & Clark, 1999). The normalised band depth ratio (BDR) was calculated by dividing the band depth (BD) of each channel *i* by the band centre (D_c), which is the maximum band depth:

$$BDR_{(\lambda i)} = \frac{BD_{(\lambda i)}}{D_c} \quad (4)$$

(iv) The normalised band depth index (NBDI) was calculated by subtracting the maximum band depth (D_c) from the band depth (BD) and dividing it by their sum:

$$\text{NBDI}_{(\lambda i)} = \frac{BD_{(\lambda i)} - D_c}{BD_{(\lambda i)} + D_c} \quad (5)$$

Where *i* is the band depth at a particular wavelength.

6.3.3. Feature selection

Although the number of spectral bands used for analysis in this study had been reduced from 647 bands to 294 by concentrating on known chemical absorption features, we further reduced them by using stepwise linear regression. Stepwise regression has been widely used to relate remotely sensed data to vegetation variables (Curran *et al.*, 2001; Kokaly & Clark, 1999; Martin & Aber, 1997; Serrano *et al.*, 2002). To avoid overfitting problems, the maximum number of steps in the stepwise regression analysis for predicting individual species was set at three. This was extended to a maximum of six for the combined data set of all the species (n = 96). Most authors recommend 10 to 20 times as many observations as variables, otherwise the regression line predictions are very unstable and unlikely to replicate if the experiment is repeated (Serrano *et al.*, 2002; Skidmore *et al.*, 1997b).

Building regression models with field spectroradiometry is important for fast and efficient prediction of foliar biochemical concentrations in rangelands. In other words, the regression models can be applied on field reflectance spectra acquired at the same resolution and under similar ecological conditions. This in turn, saves time spend in field data collection, as well as reducing costs on laboratory biochemical analysis.

6.3.4. Testing the predictive capability of regression models

A modified bootstrap procedure was used to test the predictive capability of multiple linear regression models developed between selected absorption feature variables and biochemicals (Efron & Tibshirani, 1994; McGarigal *et al.*, 2000). The data was randomly divided into training and test samples (n = 72 and 24 respectively). A regression model was developed from the training data set. Next, the test data set was bootstrapped with replacement for n = 1000 times, and for each iteration a regression model from the training data set was used to predict biochemicals in the test subsample and the R^2 values as well as the root mean square errors were recorded. The mean and 95% confidence levels of R^2 values as well as RMSE values for the test data were calculated and recorded. A routine developed in IDL (Interactive Data Language) was used. Confidence levels of the bootstrapped R^2 as well as the

RMSE values were used in this study as the most conventional way to assess the degree of certainty in our results.

We adopted this bootstrap procedure in order to improve upon the approach followed in many similar studies on predicting foliar biochemicals. Several studies (Curran *et al.*, 2001; Kokaly & Clark, 1999) tested the predictive capability of a developed regression model on a single test data set. This resulted in only one RMSE between the predicted and the measured data. We therefore bootstrapped the test sample in order to obtain several RMSEs, thereby assessing the degree of certainty in our results (Efron, 1982; Efron & Tibshirani, 1994; McGarigal *et al.*, 2000), whilst maintaining the approach followed in similar studies. The method adopted in this study takes the form of the "split-sample" validation where data is divided into two sets (Burman, 1989; Goutte, 1997; Stone, 1977) and is deemed more objective than the standard bootstrap procedure because there is validation with a test data set (Stone, 1977).

To check the validity of the bootstrap approach that we used, we also applied a slightly different bootstrap procedure using the nitrogen data set as an example. This involves splitting the data into training and test samples several times (cross-validation), and for each iteration, the stepwise regression model from the training set is used to predict biochemicals on the test sample (Diaconis & Efron, 1983; Efron, 1982).

6.4. Results

6.4.1. Foliar biochemical concentration

The concentration of biochemicals varied among species. Table 6.1 details the descriptive statistics of the data set. Average nitrogen concentration ranged from 0.69 ± 0.12 % CL (95% confidence limit of the mean) in *T. triandra* to 0.94 ± 0.29 % CL in *E. lehmanniana*. The mean phosphorous concentration ranged from 0.14 ± 0.03 % CL in *T. triandra* to 0.2 ± 0.03 CL in *U. mosambicensis.* The lowest potassium concentration was found in *T. triandra* (mean concentration = 0.74 ± 0.15 % CL) and the highest in *E. lehmanniana* (mean concentration = 1.12 ± 0.54 % CL). The mean magnesium concentration ranged from 0.176 ± 0.035 % CL in *T. triandra* to 0.256 ± 0.035 % CL in *U. mosambicensis*. For foliar calcium concentration, the mean ranged from 0.35 ± 0.052 % CL in *T. triandra* to 0.57 ± 0.062 % CL in *U. mosambicensis.* The ranges of biochemical concentrations recorded in this study are relatively lower than the concentration levels usually recorded in green grass. Most of the foliar chemicals recorded are intercorrelated. Table 6.2 shows the intercorrelation between the measured biochemicals when all species were combined. Results indicate a significant positive correlation between all pairs of foliar biochemicals ($p < 0.05$), except between nitrogen and calcium. Most of the biochemicals measured constitute the productive function in plants and are

responsible for metabolic processes; hence there is a positive correlation among the biochemicals.

Table 6.1: Descriptive statistics of the biochemical variables measured (by species) in the laboratory

Biochemical by species	No. of samples	Mean (%)	Confidence CL of mean (95%)	Minimum (%)	Maximum (%)
Nitrogen					
P. maximum	17	0.76	0.068	0.5	1.06
T. triandra	20	0.69	0.117	0.38	1.38
U. mosambicensis	28	0.79	0.129	0.43	2
C. ciliaris	21	0.76	0.08	0.43	1.03
E. lehmanniana	10	0.94	0.299	0.44	1.81
All combined	96	0.78	0.055	0.38	2
Magnesium					
P. maximum	17	0.217	0.038	0.061	0.377
T. triandra	20	0.176	0.035	0.084	0.414
U. mosambicensis	28	0.256	0.035	0.07	0.409
C. ciliaris	21	0.189	0.034	0.08	0.336
E. lehmanniana	10	0.177	0.056	0.085	0.309
All combined	96	0.209	0.017	0.061	0.414
Calcium					
P. maximum	17	0.392	0.048	0.26	0.56
T. triandra	20	0.353	0.052	0.14	0.68
U. mosambicensis	28	0.57	0.062	0.24	1.03
C. ciliaris	21	0.41	0.055	0.18	0.6
E. lehmanniana	10	0.368	0.086	0.19	0.56
All combined	96	0.437	0.031	0.14	1.03
Potassium					
P. maximum	17	1.038	0.199	0.46	1.8
T. triandra	20	0.745	0.157	0.21	1.58
U. mosambicensis	28	0.97	0.198	0.33	2.43
C. ciliaris	21	1.01	0.211	0.22	1.85
E. lehmanniana	10	1.124	0.537	0.31	2.71
All combined	96	0.96	0.098	0.21	2.71
Phosphorous					
P. maximum	17	0.191	0.054	0.064	0.421
T. triandra	20	0.143	0.034	0.042	0.318
U. mosambicensis	28	0.202	0.032	0.108	0.423
C. ciliaris	21	0.19	0.053	0.046	0.479
E. lehmanniana	10	0.174	0.035	0.121	0.281
All combined	96	0.182	0.018	0.042	0.479

Table 6.2: Intercorrelation of biochemical concentrations measured in the laboratory

	P	K	Ca	Mg
P	1.00			
K	0.74**	1.00		
Ca	0.53**	0.39**	1.00	
Mg	0.75**	0.78**	0.60**	1.00
N	0.41**	0.72**	0.26	0.50**

** Significant: $p < 0.05$

6.4.2. Discriminating species using the continuum removal method

Prior to biochemical analysis of the species subsets, we tested whether the species could be discriminated with respect to their spectral signatures, thereby permitting their separation for analysis. The visible absorption ($R_{550\text{-}750}$) feature was used for this task, following its successful application in other studies (Kokaly *et al.*, 2003; Schmidt & Skidmore, 2003). We used one-way ANOVA to test the hypothesis that the mean reflectance (continuum-removed) values for *T. triandra, C. ciliaris, U. mosambicensis, P. maximum and E. lehmanniana* were significantly different at wavelength *i*, *viz*. the null hypothesis Ho: $\mu_1 = \mu_2 = \mu_3 \ldots \mu n$ versus the alternate hypothesis Ha: $\mu_1 \neq \mu_2 \neq \mu_3 \ldots \mu n$. Where, μ_1, μ_2, and $\mu_3 \ldots \mu n$ are the mean reflectance values of the *n* species at wavelength *i*. The conclusions obtained from these tests were that different species yielded different spectral responses (P values ranging between 0.000064 and 0.0049) for the wavelength region between 560 and 746 nm. Following this, subsequent analysis was done using species subsets as well as using a combined data set.

6.4.3. The first derivative reflectance (FDR)

The correlograms in Figure 6.3 show the correlations between the FDR and biochemicals for 647 bands.

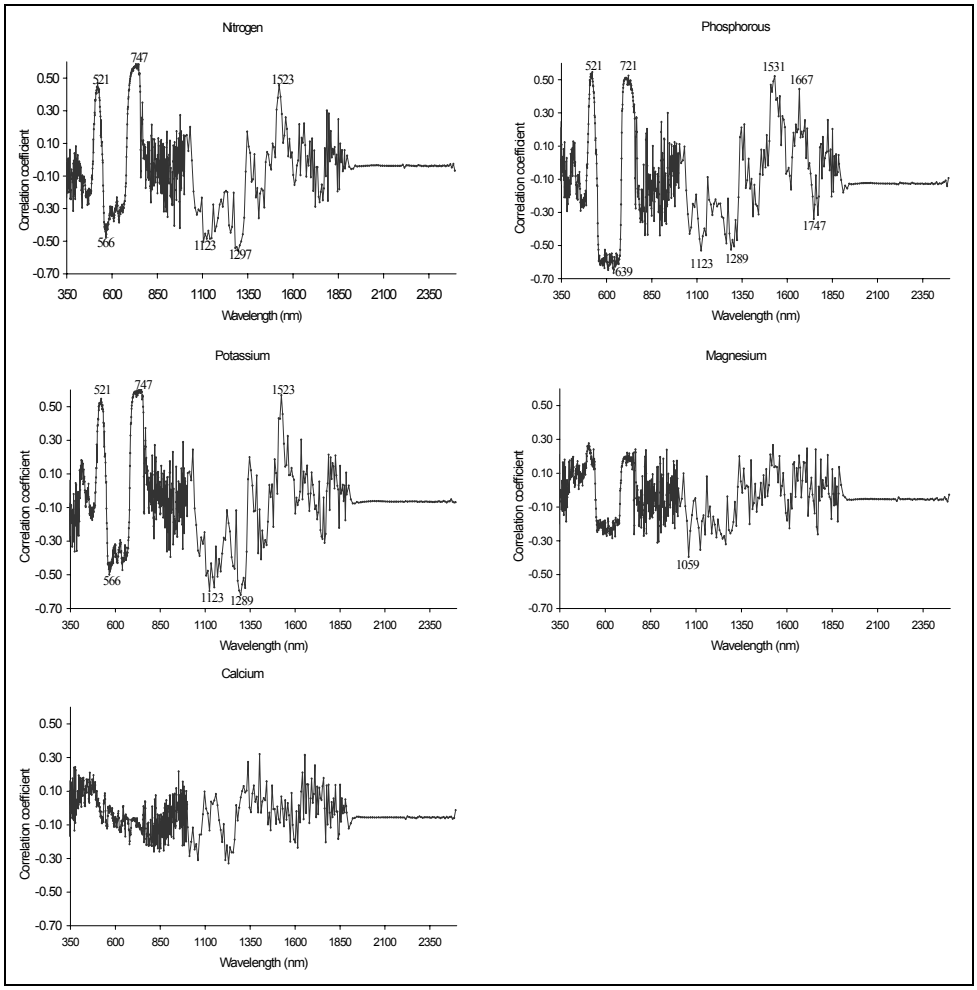

Figure 6.3:Relationship between the first derivative reflectance (FDR) and biochemicals using the whole data set (n = 96). Wavelengths of highly correlated picks are shown.

There are significant correlations between the FDR and biochemicals particularly in the red edge. Generally, the nitrogen, phosphorous and potassium correlograms show a strong correlation with the red edge. There are, however, poor correlations with calcium and magnesium in the whole region of the electromagnetic spectrum. All biochemicals also show weak correlations in the SWIR between 2000 nm and 2500 nm. For some intercorrelated biochemicals (Table 6.3), the correlograms of these chemicals are similar as shown in Figure 6.3 (nitrogen, phosphorous and potassium correlograms). This similarity largely depends on similarities in the absorption properties of the biochemicals themselves.

6.4.4. Species-based biochemical prediction using multiple linear regression on absorption features

Multiple linear regressions were used to predict biochemicals in different species studied in this research. All variables (CRDR, BD, BDR and NBDI) were applied. Table 6.3 shows regression terms and selected wavelengths by stepwise regression using the first derivative reflectance of the continuum-removed absorption features (CRDR) to predict biochemicals for *C. ciliaris*.

The majority of wavelengths selected for all chemicals are located in the visible domain of the electromagnetic spectrum. A detailed report of selected wavelengths is provided in section 6.4.5, using the pooled data set. Results in Table 6.4 show that all the variables tested in this study generally yielded high coefficients of determination for all species (R^2 ranged from 0.50 to 0.99). Low root mean square errors were also obtained. Compared with the other variables tested, CRDR yielded relatively higher coefficients of determination and lower RMSE for all biochemicals.

6.4.5. Using absorption features to predict biochemicals in the training data set

Stepwise linear regression was carried out between biochemicals and the four variables (CRDR, BD, BDR and NBDI), using the randomly selected training data set (n = 72) from the combined species data set. The maximum number of selected wavelengths was set at six for each regression equation in order to avoid overfitting. Detailed results of the frequency of wavelengths selected by stepwise regression using the four data sets (CRDR, BD, BDR, NBDI) are shown in Table 6.5.

The frequency of bands that occur within ± 12 nm of a known chemical absorption wavelength is shown. The ± 12 nm range was defined by Curran et al. (2001) to indicate causal chemical absorption. This was adapted in this study for consistency and comparison. The highest frequency of bands occurs in the $R_{1634 - 1786}$ absorption feature (frequency = 32), followed by the $R_{550 - 750}$ absorption feature (frequency = 29). A total of 64 % of the bands selected are attributed directly or indirectly to known causal wavelengths (Curran *et al.*, 2001) as well as to bands reported in other studies. Bands that are directly attributed means that they occur within ± 12 nm of the biochemical of interest and bands that are indirectly attributed means that they are within ± 12 nm of a biochemical with which the biochemical of interest was correlated.

Table 6.3: Regression terms and selected wavelengths by stepwise regression using first derivative reflectance of the continuum-removed absorption features (CRDR) to predict foliar chemicals for *C. ciliaris* (n = 21)

Index	Wavelength (nm)	Coefficient	R^2	P
Nitrogen				
Intercept		0.855		0.00
λ_1	438	-120.62	0.65	0.00
λ_2	2125	-164.06	0.82	0.00
λ_3	417	-63.82	0.88	0.01
Potassium				
Intercept		0.31		0.00
λ_1	599	-943.26	0.68	0.000
λ_2	738	-513.88	0.86	0.000
λ_3	444	-166.26	0.90	0.01
Phosphorous				
Intercept		0.089		0.000
λ_1	611	-105.83	0.84	0.000
λ_2	483	63.38	0.91	0.000
λ_3	429	-15.25	0.94	0.007
Calcium				
Intercept		0.304		0.000
λ_1	675	-193.10	0.60	0.000
λ_2	424	-62.90	0.73	0.000
λ_3	2310	44.29	0.88	0.000
Magnesium				
Intercept		0.14		0.000
λ_1	627	-129.56	0.63	0.000
λ_2	667	63.43	0.73	0.001
λ_3	422	-12.47	0.81	0.020

Table 6.4: Linear regression results by species (R^2 and the RMSE) between biochemicals and continuum-removed derivative reflectance (CRDR), band depth (BD), band depth ratio (BDR) and normalised band depth index (NBDI)

	Species	CRDR		BD		BDR		NBDI	
		R^2	RMSE	R^2	RMSE	R^2	RMSE	R^2	RMSE
N	P. maximum	0.94	0.04	0.83	0.05	0.93	0.03	0.97	0.02
	T. triandra	0.92	0.06	0.83	0.09	0.79	0.14	0.80	0.11
	U. mosambicensis	0.91	0.09	0.90	0.1	0.68	0.18	0.53	0.22
	C. ciliaris	0.88	0.01	0.67	0.02	0.58	0.03	0.52	0.02
	E. lehmanniana	0.99	0.008	0.97	0.02	0.97	0.02	0.87	0.04
	Average	0.93		0.84		0.79		0.74	
Mg	P. maximum	0.87	0.02	0.80	0.03	0.90	0.03	0.88	0.02
	T. triandra	0.93	0.02	0.93	0.02	0.70	0.03	0.77	0.03
	U. mosambicensis	0.72	0.04	0.62	0.05	0.54	0.06	0.52	0.06
	C. ciliaris	0.81	0.005	0.87	0.005	0.71	0.008	0.69	0.008
	E. lehmanniana	0.98	0.001	0.99	0.001	0.96	0.001	0.99	0.001
	Average	0.86		0.84		0.76		0.77	
Ca	P. maximum	0.89	0.03	0.84	0.03	0.87	0.04	0.88	0.03
	T. triandra	0.81	0.04	0.73	0.057	0.86	0.05	0.85	0.05
	U. mosambicensis	0.62	0.09	0.58	0.1	0.52	0.08	0.50	0.1
	C. ciliaris	0.88	0.01	0.82	0.01	0.78	0.01	0.79	0.01
	E. lehmanniana	0.98	0.001	0.98	0.005	0.98	0.003	0.99	0.002
	Average	0.84		0.79		0.80		0.80	
K	P. maximum	0.85	0.14	0.80	0.16	0.52	0.21	0.83	0.15
	T. triandra	0.86	0.11	0.75	0.17	0.80	0.14	0.85	0.12
	U. mosambicensis	0.92	0.14	0.89	0.16	0.78	0.24	0.65	0.24
	C. ciliaris	0.90	0.02	0.89	0.03	0.56	0.06	0.53	0.06
	E. lehmanniana	0.98	0.01	0.97	0.03	0.93	0.05	0.95	0.04
	Average	0.90		0.86		0.72		0.76	
P	P. maximum	0.92	0.02	0.93	0.02	0.77	0.04	0.75	0.05
	T. triandra	0.94	0.02	0.89	0.02	0.78	0.03	0.68	0.03
	U. mosambicensis	0.81	0.03	0.69	0.04	0.78	0.03	0.73	0.04
	C. ciliaris	0.94	0.004	0.94	0.005	0.71	0.01	0.68	0.01
	E. lehmanniana	0.98	0.001	0.99	0.000	0.97	0.001	0.96	0.002
	Average	0.92		0.88		0.80		0.76	

Table 6.5: Frequency of wavelengths selected for all dependent variables by stepwise regression applied to the four data sets (CRDR, BD, BDR, NBDI) and their relation with known absorption wavelengths. The unattributed are wavelengths that are not within ± 12 nm of known chemical absorption as well as those not reported in other studies. The total number of bands selected in each absorption feature is also expressed as a percentage of the total (in brackets).

Absorption feature	Wavelengths of known chemical influence (nm)	Known causal biochemical	Reference	Frequency of bands selected (± 12 nm of known wavelength)
$R_{408-518}$	430	Chlorophyll a	(Curran, 1989; Kumar *et al.*, 2001)	7
	460	Chlorophyll b	(Curran, 1989; Kumar *et al.*, 2001)	1
	Unattributed			4
	Total			12 (10)
$R_{550-750}$	570	Chlorophyll + nitrogen	(Penuelas *et al.*, 1994)	7
	640	Chlorophyll b	(Curran, 1989; Kumar *et al.*, 2001)	4
	660	Chlorophyll a	(Curran, 1989; Kumar *et al.*, 2001)	4
	Red edge (700 – 750)	Chlorophyll + nitrogen	(Clevers & Buker, 1991; Curran *et al.*, 1991; Fillella & Penuelas, 1994; Horler *et al.*, 1983)	8
	Unattributed			6
	Total			29 (25)
$R_{1116-1284}$	1120	Lignin	(Curran, 1989; Kumar *et al.*, 2001)	4
	Unattributed			10
	Total			14 (12)
$R_{1634-1786}$	1690	Nitrogen	(Curran, 1989; Kumar *et al.*, 2001)	8
	1730	Nitrogen	(Curran, 1989; Kumar *et al.*, 2001)	8
	Unattributed			16
	Total			32 (27)
$R_{2006-2196}$	2060	Nitrogen	(Curran, 1989; Kumar *et al.*, 2001)	2
	2130	Nitrogen	(Curran, 1989; Kumar *et al.*, 2001)	6
	2180	Nitrogen	(Curran, 1989; Kumar *et al.*, 2001)	8
	Unattributed			5
	Total			21 (18)
$R_{2222-2378}$	2240	Nitrogen	(Curran, 1989 (Kumar *et al.*, 2001)	5
	2300	Nitrogen	(Curran, 1989; Kumar *et al.*, 2001)	2
	2350	Nitrogen	(Curran, 1989; Kumar *et al.*, 2001)	2
	Unattributed			2
	Total			11 (9)

Table 6.6: Linear regression results between biochemicals and continuum-removed derivative reflectance (CRDR), band depth (BD), band depth ratio (BDR) and normalised band depth index (NBDI), using the training data set (n = 72)

Chemical	CRDR		BD		BDR		NBDI	
	R^2	RMSE	R^2	RMSE	R^2	RMSE	R^2	RMSE
N	0.70	0.01	0.62	0.02	0.53	0.02	0.60	0.02
K	0.64	0.03	0.72	0.02	0.56	0.04	0.60	0.04
P	0.80	0.004	0.69	0.005	0.51	0.006	0.64	0.007
Ca	0.50	0.01	0.47	0.01	0.46	0.01	0.56	0.02
Mg	0.68	0.004	0.58	0.006	0.43	0.007	0.55	0.01

Table 6.6 shows the results of linear regressions between foliar biochemicals and absorption feature variables when using the training data set (n = 72).

Generally, CRDR yielded the highest coefficient of determination for all biochemicals. The results are, however, lower than those obtained by Kokaly and Clark (1999) and Curran *et al*. (2001) using dried ground plant material.

6.4.6. Developing regression models from a randomly selected training data set to predict foliar biochemicals in a test data set

Regression models developed from the training data set were used to predict foliar biochemicals in an independent test data set. To install confidence in the predictive capability of the regression models, a modified bootstrap procedure was adopted (as already explained). Figure 6.4 shows an example of the predicted versus measured biochemicals for a test data set (n = 24) using a regression model developed from a randomly selected training set (n = 72). Histograms showing the sampling distribution of the R^2 values calculated from the predicted and measured biochemicals in the test data set (CRDR data) following bootstrapping are shown in Figure 6.5.

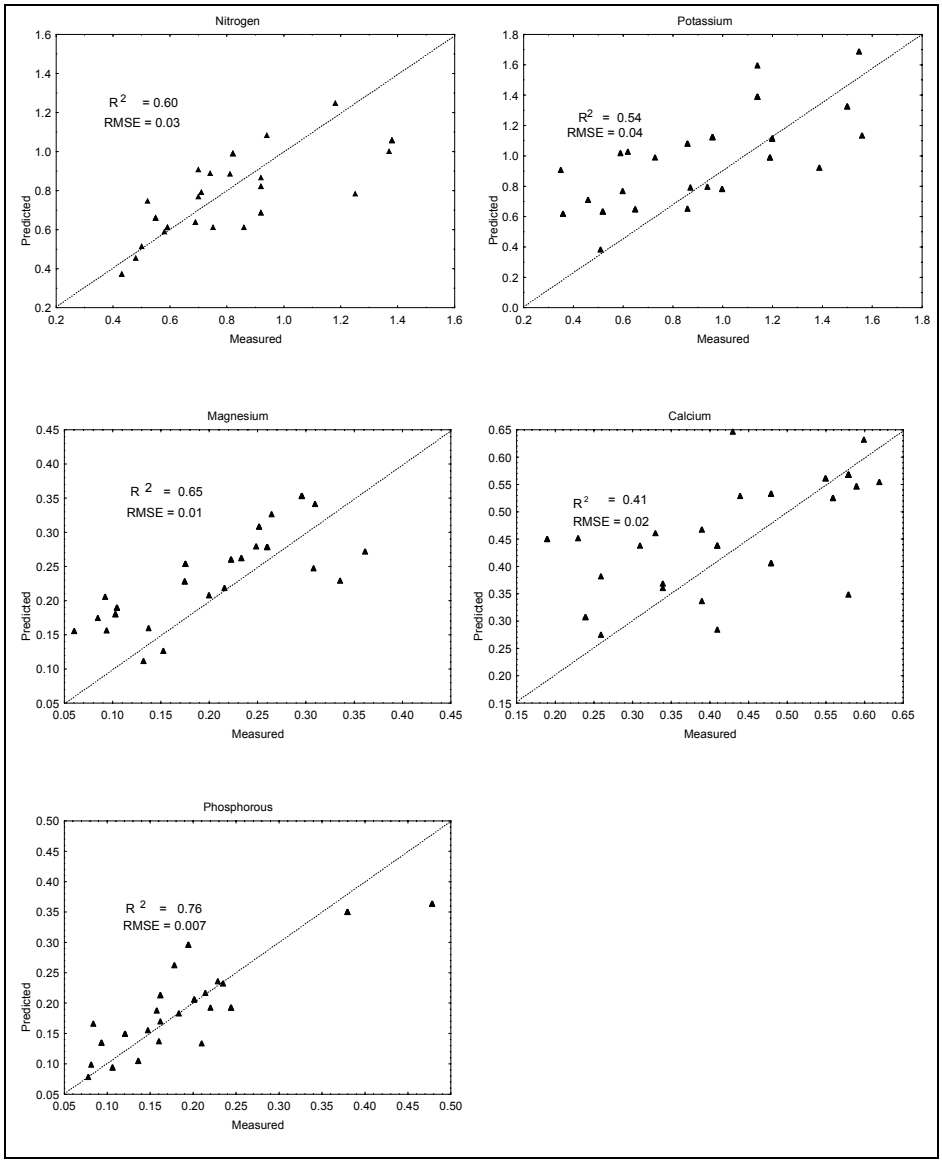

Figure 6.4: Measured versus predicted biochemicals for a randomly selected test data set (n = 24) using CRDR. Regression equations developed from the training data set (n = 72) were used to predict biochemicals on an independent test data set.

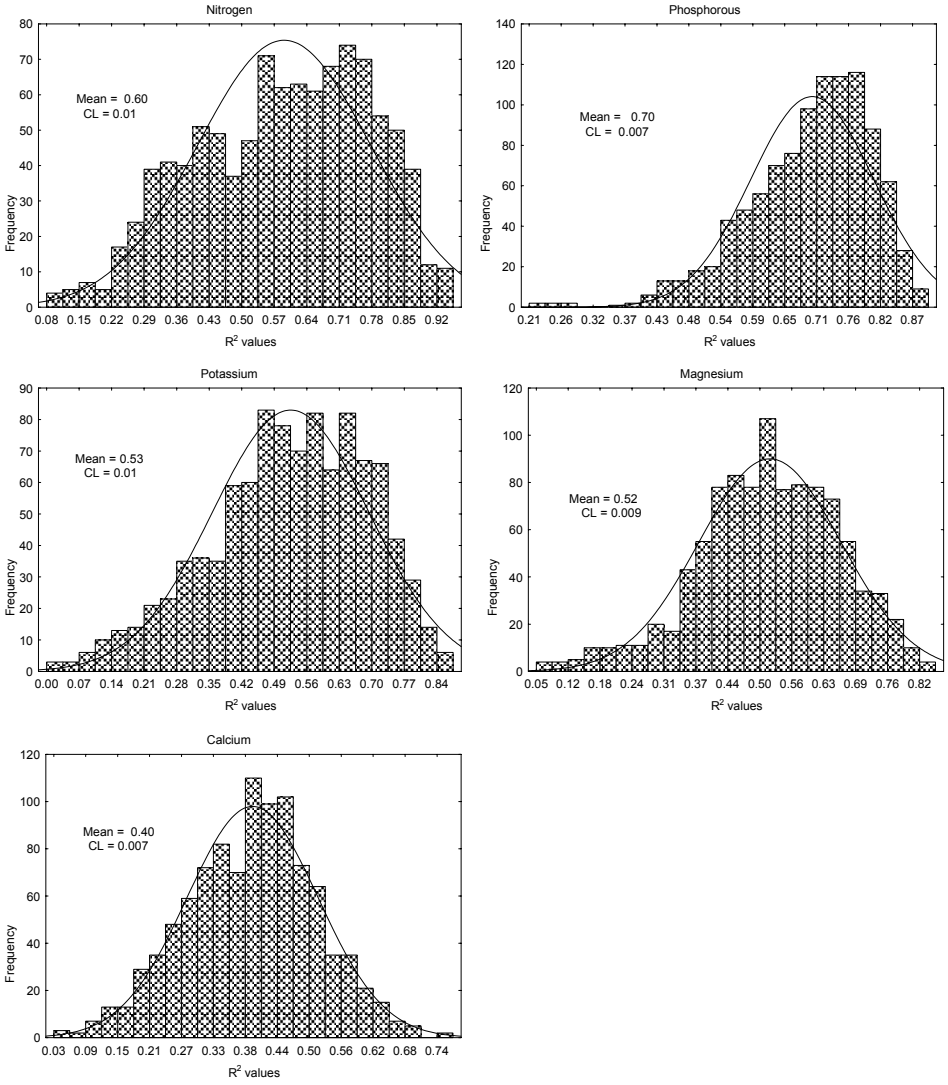

Figure 6.5: Histograms showing the frequency of R^2 values between the measured and predicted biochemicals in a test data set. Data was randomly divided into training and test data sets. Next, the test data set was bootstrapped with replacement for n = 1000 times, and for each iteration a regression model from the training data set was used to predict biochemicals in a test subsample and R^2 values were recorded.

The confidence intervals are narrower for all biochemicals, implying that the bootstrap method predicted with high precision. Table 6.7 details the mean bootstrapped regression results between the measured and predicted biochemicals for a test data set using the four variables (CRDR, BD, BDR and NBDI). The results are presented in form of the mean R^2 values as well as the

mean RMSE between the measured and predicted biochemicals. The confidence levels of the mean R^2 and the mean RMSE are also shown. The highest R^2 and the lowest RMSE were obtained using CRDR for phosphorous prediction. However, the coefficients of determination in Table 6.7 are lower than those presented in Table 6.4, where chemical concentrations were predicted according to species. Foliar biochemicals in the test data set could be predicted with mean R^2 values ranging between 0.15 and 0.70 and with the mean RMSE values ranging between 0.29 and 0.02 from the entire absorption feature based variables.

To check the validity of the bootstrapping procedure that we applied in this study, we also applied a slightly different procedure involving splitting data into training and test samples several times (cross-validation). Results for nitrogen concentration using CRDR data yielded a mean RMSE of 0.077 with a standard deviation of 0.011 on the test data set. The result is comparable to the modified bootstrap procedure, which yielded a mean RMSE of 0.08 (Table 6.7). We tested whether the mean RMSE values produced by the modified bootstrap procedure and the cross validation procedure were significantly different. Results of the t-test showed that there was no significant difference between the two RMSEs ($t = 1.949$, $p > 0.05$). However, a comparison of the standard deviations from the two approaches showed that, a much narrower distribution is observed using the cross validation (Diaconis & Efron, 1983) approach (Standard deviation = 0.011) than the modified bootstrap approach used in this study (Standard deviation = 0.023). Therefore, we conclude that the modified bootstrap approach gives better and more informative information output.

Table 6.7: Testing the predictive capability of the regression models developed from a training data set (n = 72) on an independent test data set (n = 24). The test data set was bootstrapped with replacement for n = 1000 times, and for each iteration a regression model from the training data set was used to predict biochemicals in a test subsample and R^2 values as well as the RMSE were recorded. The mean R^2 values and the mean RMSE are presented. The 95 % confidence levels (CL) for the mean R^2 as well as the mean RMSE are also presented.

		N	K	P	Ca	Mg
CRDR	Mean R^2	0.60	0.53	0.70	0.40	0.52
	CL	0.01	0.01	0.007	0.007	0.009
	Mean RMSE	0.08	0.05	0.02	0.05	0.03
	CL	0.001	0.0004	0.0003	0.0009	0.0004
BD	Mean R^2	0.50	0.60	0.54	0.29	0.42
	CL	0.013	0.009	0.009	0.008	0.009
	Mean RMSE	0.05	0.04	0.02	0.08	0.02
	CL	0.001	0.0009	0.0004	0.001	0.0004
BDR	Mean R^2	0.38	0.33	0.32	0.26	0.23
	CL	0.012	0.011	0.009	0.01	0.009
	Mean RMSE	0.06	0.07	0.04	0.3	0.13
	CL	0.002	0.002	0.0009	0.006	0.004
NBDI	Mean R^2	0.38	0.30	0.42	0.15	0.27
	CL	0.012	0.011	0.009	0.008	0.008
	Mean RMSE	1.58	0.54	0.09	0.29	1.58
	CL	0.049	0.008	0.001	0.01	0.049

6.5. Discussion

The results from this study are discussed in three main sections: (i) the utility of the methods applied for nutrient prediction, (ii) the effect of using the whole data set versus using data partitioned into species, and (iii) the selection of wavelengths from absorption features by stepwise linear regression.

6.5.1. Utility of the methods applied for quality prediction

Results from this study indicate that spectroscopic data contains information on the nutrient status of grass. Univariate correlation analyses have shown that substantial information on grass quality is contained in the red edge region, where significant correlations were obtained (Figure 6.3). This region has been shown to be insensitive to atmospheric and background effects (Clevers & Buker, 1991) and to be related to chlorophyll absorption. Since there is a strong pigment-nitrogen relationship, a relationship between the red edge and biochemicals with a productive function in plants is also expected (Katz *et al.*, 1966). This result confirms the laboratory analysis results presented in chapters 3, 4 and 5.

For multivariate analyses using continuum-removed absorption features, the methods presented in this study could explain between 43 % and 80 % of the variation in nutrient concentration of standing grass canopies measured in the field. The RMSE values ranged between 0.04 and 0.004. Considering that data was collected in the field under natural atmospheric and illumination conditions, this study has shown that there is potential to use reflectance spectra to predict *in situ* grass quality in rangelands. With high-quality radiometric and geometric calibration of hyperspectral imagery, the techniques applied in this study such as continuum removal on specific absorption features may also be applied on data acquired by airborne and spaceborne imaging spectrometers to predict and ultimately to map the concentration of macronutrients in tropical rangelands.

The methods benefited from continuum removal, which enhances differences in absorption strength (Clark & Roush, 1984; Schmidt & Skidmore, 2003). This assertion is confirmed by a separate study, which showed that continuum removal increases the separability of grass canopies grown under different nitrogen treatments as compared to absolute reflectance (Mutanga *et al.*, 2003). Furthermore, in a study on spectral discrimination of vegetation types in a salt marsh, Schmidt and Skidmore (2003) found that continuum removal in the visible domain increases the spectral separability of vegetation types on absorption features, as compared to absolute reflectance. Our results are therefore consistent with previous studies. It is also imperative to note that the standard first derivative approach (Figure 6.3) yielded little correlation between wavelengths in the SWIR (2000 nm – 2500 nm) and biochemical concentrations, however, stepwise linear regression selected bands in this region. This indicates the importance of continuum removal as well as using multiple bands to predict biochemical concentration.

There was a marked difference in the R^2 between predicted and observed biochemical concentration for the four variables derived from absorption features. The R^2 values for nitrogen prediction were 0.70, 0.62, 0.53 and 0.60 for CRDR, BD, BDR and NBDI, respectively, using the training data set. The same pattern occurred for the other biochemicals. Therefore, the new variable, CRDR, yielded higher correlations with biochemical concentrations than the other variables tested.

6.5.2. Partitioning data into species versus the combined data set

This study has shown that partitioning data into species increases the predictive capability of the regression models, as compared to using the combined data set. The average R^2 for nitrogen prediction from partitioned species data was 0.93 using CRDR (Table 6.4), compared with 0.70 for the pooled data set (Table 6.6) using the same method. Serrano *et al.* (2002) found that partitioning data into vegetation types yielded the highest R^2 value of 0.97 for nitrogen prediction, while pooling the data set yielded an R^2 value of 0.75. Our results are therefore

consistent with the existing literature. This result has profound implications for using airborne hyperspectral data to map biochemicals in savanna rangelands. To improve the mapping accuracy of grass quality, the plant type, morphology and structure should be taken into consideration for mapping grass quality in rangelands composed of mixed species in Southern Africa. Non- linear algorithms could be applied to capture this variation.

6.5.3. Wavelength selection

The selection of wavelengths by stepwise regression is an important step towards the development of general models for predicting chemicals in plants. The method presented in this study has partly solved the problem of inconsistencies found in wavelength selection from a full spectrum (Grossman *et al.*, 1996) by concentrating on a few known features of chemical absorption. However, there is still a need to understand particular absorption features, as well as wavelengths that are important for biochemical prediction.

Wavelengths selected for biochemical prediction in the visible region are linked to pigment absorption (Table 6.5). Several publications have shown a strong relationship between the concentration of nitrogen and the concentrations of chlorophyll *a* and *b* (Katz *et al.*, 1966; Penuelas *et al.*, 1994; Ponzoni & Goncalves, 1999). Nitrogen is related to the protein synthesis that promotes the photosynthetic process. Therefore, nitrogen deficiency disturbs the metabolic function of the chlorophyll, which is the photosynthetic element responsible for the absorption of electromagnetic energy at specific wavelengths in the visible region (Ponzoni & Goncalves, 1999). Since chlorophyll largely determines spectral reflectance in the visible, a strong relationship between visible absorption bands and nitrogen concentration is also expected. The same applies to other biochemicals such as phosphorous and potassium which are also responsible for both the photosynthetic process and tissue composition in plants.

Most wavelengths selected in the shortwave infrared (66 %) are within ± 12 nm of the known protein absorption bands, specifically bonds including nitrogen. The intercorrelation of chemicals (Table 6.2) explains the selection of most bands close to regions of nitrogen absorption. The selected wavelengths (Table 6.5) are linked to the absorption of electromagnetic radiation by biochemicals that originate from the energy transition of the molecular vibration (rotation, bending and stretching) of the C-H, N-H, O-H, C-N and C-C bonds in plant tissues (Elvidge, 1990). The chemical constituents of the plant tissue determine the nature and number of bonds present. Therefore, the wavelengths and the amount of energy reflected from the plant are partly a function of the chemical composition of that plant material (Foley *et al.*, 1998).

6.6. Conclusions

This study has applied an empirical method to predict grass quality in the field. Normalised band depths, as well as derivatives calculated from continuum-removed reflectance spectra, were used in stepwise regression using six major absorption bands in the visible and the shortwave infrared. The following conclusions can be drawn from this study:

1. Stepwise regression on normalised bands calculated from continuum-removed reflectance spectra could explain the variation of *in situ* grass quality, with R^2 values ranging between 0.43 and 0.80 and RMSE values ranging between 0.04 and 0.004.
2. The new variable, CRDR, performed better than any other variable tested in predicting grass quality, both when using the training data set and when data was partitioned into species. The NBDI variable did not perform any better than the other procedures.
3. The error of prediction (RMSE) in the test data set was 0.08 (±10.25 % of mean), 0.05 (± 5.2% of mean), 0.02 (± 11.11% of mean), 0.05 (± 11.6% of mean) and 0.03 (± 15% of mean) for nitrogen, potassium, phosphorous, calcium and magnesium, respectively using CRDR.
4. Prior partitioning of data into species classes increases the prediction capability of the method applied in this study.
5. The major absorption feature in the visible ($R_{550 - 750}$) and the nitrogen absorption features ($R_{1634 - 1786}$ and $R_{2006-2196}$) in the shortwave infrared account for 69 % of the wavelengths selected by stepwise regression. This serves as a guideline for the selection of important absorption features for mapping grass quality in tropical rangelands.

Overall, the successful use of absorption features for predicting grass quality at field level is an important step towards the remote sensing and mapping of rangelands. These results have important implications, not only for animal ecology but also for agriculture and for understanding biogeochemical cycles. The application of non-linear algorithms such as artificial neural networks to hyperspectral data may be useful in capturing the possible non-linear patterns due to species differences.

Acknowledgements

This study was carried out with the financial assistance of the International Institute for Geo-Information Science and Earth Observation (ITC) (formerly the International Institute for Aerospace Survey and Earth Observation). We would like to thank the Scientific Board of Kruger National Park for accepting our research proposal and for their subsequent assistance in field data collection. Many thanks to Mike Peel and Rina Grant for organising logistics in the field. Henk van Oosten helped in programming the bootstrap

procedure. Professor Alfred Stein helped in answering one reviewer's comment on the bootstrap procedure that we used.

CHAPTER 7:
Field spectrometry to discriminate foliar sodium concentration in mixed grass species

*This chapter is based on

Mutanga, O, Skidmore, A, K., Prins, H H.T, Grant, R, Peel, M. J. S. (**In review**), Discriminating sodium concentration in a mixed grass species environment of the Kruger National Park using field spectrometry, *International Journal of Remote Sensing*.

Abstract

Sodium has been found to be a scarce element needed and sought by mammals. To date, most geophagical studies have mainly concentrated on sodium in the soil with limited attention being given to the plant component. Mapping foliar sodium distribution is important to understand wildlife feeding patterns and distribution. In this study, we established whether remote sensing can be used to discriminate different levels of sodium concentration in grass. A GER 3700 spectrometer was used to measure spectral reflectance of grass in the field. Since savanna rangelands are characterised by mixed grass species, we first established the variation of foliar sodium concentration in different grass species and tested for possible effects of species - sodium interaction on spectral reflectance.

Our results showed statistically significant differences between the mean reflectance for the low and medium sodium classes. No significant differences were observed between reflectance in the high sodium class and the lower classes. However, there was a significant interaction between sodium classes and species in influencing reflectance. We concluded that, in combination with knowledge of grass species distribution, hyperspectral remote sensing maybe useful in mapping foliar sodium concentration in savanna rangelands. This may help to understand the distribution of mammals in some African savannas where mineral nutrient availability is limiting.

Keywords: Foliar sodium, sodic patches, visible reflectance, species – sodium interaction, Kruger Northern Plains

7.1 Introduction

Sodium (Na) is an essential element for mammals since it is responsible for regulating body fluid volume, acid-base balance and tissue pH, muscle contraction, and nerve impulse transmission (Brady *et al.*, 2002; Lammertsma & Bruinderink, 1998; Woolfenden & Millar, 1997). Mammals require sodium amounts ranging from 0.05 to 0.15% in the diet (Robbins, 1983). However, few terrestrial plants require sodium, therefore there is a potential for herbivores to incur sodium deficiencies in areas where plant species contain low amounts of sodium.

Research has revealed that herbivores are attracted to mineral licks or sodic sites, which are characterized by an increased concentration of cations, most frequently in the form of salts, relative to surrounding sites (Ruggiero & Fay, 1994; Scholes & Walker, 1993). In the northern plains of Kruger National Park (South Africa), roan antelope has been found to concentrate on sodic areas next to the drainage lines and vleis (Grant *et al.*, 2002). Grass species such as *S. ioclados, P. maximum* and *E. superba* have been intensely utilised in these patches (Grant *et al.*, 2002; Jourbert, 1976).

Whilst many studies demonstrated that natural lick soils ingested by ungulates had high concentrations of sodium (Ruggiero & Fay, 1994; Stark, 1986), few of them have analysed sodium concentration in different plant species, let alone its spatial variation in vegetation (Scholes & Walker, 1993). An understanding of the variation of sodium in plants may help to explain animal feeding patterns and productivity. Techniques for mapping sodium concentration in pastures are therefore critical.

Traditional techniques for vegetation analysis are time consuming resulting in the collection and analysis of inadequate data that is not representative of the population (Foley *et al.*, 1998). The use of hyperspectral remote sensing techniques with narrow channels of less than 10 nm may be useful in estimating foliar sodium. This is because of its potential to capture detailed spectral features, which could be masked by broadband satellite images such as Landsat TM or Aster (Kumar *et al.*, 2001). Attempts to estimate foliar biochemicals developed from the 1970s onwards mainly using methods from laboratory near infrared spectroscopy (Norris *et al.*, 1976). The methods paid attention to the estimation of amino acids, lignin, protein, and cellulose of dried ground forage. During the 1990s, emphasis was put on the use of airborne imaging spectrometers to estimate biochemical concentration of tree canopies (Curran, 1989; Curran *et al.*, 1992; Dungan *et al.*, 1996; Johnson *et al.*, 1994; Martin & Aber, 1997). Recently, Kokaly and Clark (1999) developed the band depth analysis methodology to estimate foliar concentrations of nitrogen, lignin and cellulose. This technique was successfully used by Curran *et al.*, (2001) to estimate 12 biochemicals using dried ground plant materials. To the best of our knowledge, no attempts have been made to estimate and map the foliar concentration of sodium in situ using remote sensing techniques.

The underlying principle behind mapping sodium concentration is that pastures with different sodium levels reflect differently in specific wavelengths. Sodium is important in regulating and stimulating the photosynthetic pathway in plants, especially the C4 plants (Johnston *et al.*, 1988; Matoh & Murata, 1990; Murata & Sekiya, 1992), and is therefore related to chlorophyll and nitrogen concentration (Salisbury & Ross, 1985). Since chlorophyll absorbs electromagnetic radiation in the visible domain, a relationship between sodium and reflectance is therefore expected. In addition, since tropical rangelands are characterized by mixed grass species, grass species type may also effect reflectance.

In this study we tested whether differences in foliar sodium concentration could be discriminated using reflectance signatures alone or whether differences in the type of species is also important. The study was conducted in two phases. First, we tested the differences in sodium concentration between grass species found in the northern plains of the Kruger National Park. Second, we tested for differences in reflectance between three different foliar sodium classes and for a possible interaction between sodium and species in influencing reflectance. Band depths of the two major absorption features (408 nm – 518 nm and 550 nm – 750 nm) in the visible region (Curran *et al.*, 2001; Mutanga & Skidmore, 2004; Mutanga *et al.*, 2003) were used to discriminate the foliar concentration of sodium.

7.2 Methods

7.2.1 The study area

The study area is located in the northern plains of the Kruger National Park in South Africa. A strip of 2 km by 25 km stretching from the west ($22^0 49'$ S and $31^0 01'$ E) to the east ($22^0 44'$ S and $31^0 22'$ E) covering granitic and basaltic formations was selected. The basalt formations are characterised by mafic rocks that are rich in iron, magnesium and rich clay minerals (Grant *et al.*, 2000). Sodium and other minerals occur at wetland edges in these basalt formations (Jourbert, 1976). Soil and geology play an important role in determining the vegetation structure and composition, with higher grass production in the basaltic areas than in the granitic area. The granitic area is characterised by uplands that support broadleaved savanna and a herbaceous layer dominated by moderate to low quality sandveld species. The midslopes (seepline areas) classically support few trees and a dense herbaceous layer. The base of the midslope and footslope are characterised by thorny microphyllous shrubs and a productive grass layer which is generally of high quality (Grant *et al.*, 2000). The area for this study was selected to cover a wide range of vegetation with different foliar sodium concentration.

Stratified random sampling with clustering in combination with purposive sampling was adopted to select field sites using a land cover map developed using aerial photographs and Landsat TM image. The area was stratified into open grassland in the basalt, mixed woodland and woodland in the granite area. Coordinates (x,y) were randomly generated in each stratum to determine plot locations. Each plot covered 10 m by 10 m. The dominant species (covering at least 30 per cent of the area) in each plot were recorded and foliar samples collected. Purposive sampling was done on known natural lick areas (sodic patches) where foliar samples were recorded. A total of 106 samples were collected. This was done in order to increase the range in the variation of foliar sodium of the samples.

7.2.2 Reflectance measurements and chemical analysis

In situ, canopy spectral measurements were taken for the dominant species in each plot using a GER (Geophysical and Environmental Research Corp.) spectroradiometer. The GER 3700 is capable of taking measurements in the wavelength range of 350 nm to 2500 nm. The spectrometer has a spectral sampling of 1.5 nm in the 350 nm to 1050 nm range, 6.2 nm in the 1050 nm to 1900 nm range, and 9.5 nm in the 1900 nm to 2500 nm range. The bandpass is 3 nm, 11 nm and 16 nm in the 350 nm to 1050 nm range, 1050 nm to 1900 nm range, and 1900 nm to 2500 nm range, respectively.

Background effects such as the rock and soil substrate usually attenuate in situ spectral measurements. To reduce these effects, replicates of canopy spectral measurements were taken from a bunch of grass representing one dominant grass species in each plot and a fiber optic sensor, with a field of view of 10 º was pointed on the target canopy at nadir position from about 1 m height. This resulted in a ground field of view of about 18 cm in diameter, which was large enough to cover a bunch of a grass species, with minimum measurement of possible surrounding bare areas. A total of 25 replicate spectral measurements were taken from the dominant species in the plot. The resulting spectrum was determined as an average of the 25 replicate spectral measurements per species in each plot, a technique used to control for variations in illumination (Mutanga *et al.*, 2004; Schmidt and Skidmore, 2001). The fieldwork was undertaken during the end early dry season (May 2002), a period of bright sunshine. Measurements were taken on clear sunny days at high sun angle between 11:30 A.M and 2:00 P.M. Six grass species were measured in the field *vis. C. ciliaris, P. maximum, T. triandra, U. mosambicensis, E. lehmanniana, and S.ioclados.*Figure 7.1 shows the average *in situ* reflectance of the species measured.

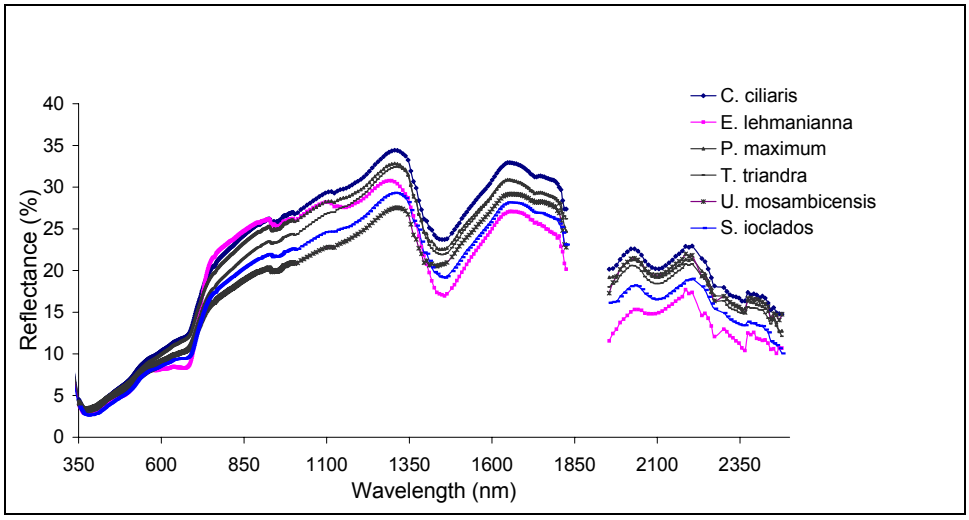

Figure 7.1: Mean reflectance values for the species measured

The spectrally measured grass species in the plots were clipped and oven dried at 70º C for 24 hours. The samples were taken to the Agricultural Research Council (ARC) laboratory in Nelspruit (South Africa) for chemical analysis. Sodium was extracted through wet digestion with 55 % nitric acid and 70 % perchloric acid (Giron, 1973). Atomic absorption flame spectroscopy using air – acetylene was used for the detection of sodium, which was expressed as percentage per 100 g of dry weight (Poluektov, 1973).

7.2.3 Data analysis

Using the reflectance spectra, continuum removal was applied to the known chemical absorption features (between 408 nm and 518 nm and between 550 nm and 750 nm) in the visible region (Curran *et al.*, 2001; Mutanga *et al.*, In review). These two regions are pigment absorption features. Since the amount of sodium influence the photosynthetic pathway in plants (Marschner, 1995), we hypothesised that the two absorption features are also related to sodium concentration. In addition, atomic absorption spectroscopy for sodium is done at 589 nm (Svanberg, 2001), which is within the $R_{550\ -\ 750\ nm}$ absorption feature. Continuum removal normalizes reflectance spectra in order to allow comparison of individual absorption features from a common baseline (Kokaly, 2001). The continuum is a convex hull fitted over the top of a spectrum to connect local spectrum maxima. The continuum-removed reflectance $R'_{(\lambda)}$ is obtained by dividing the reflectance value $R_{(\lambda)}$ for each waveband in the absorption trough by the reflectance level of the continuum line (convex hull) $Rc_{(\lambda)}$ at the corresponding wavelength (Mutanga *et al.*, 2004). Stated formally:

$$R'_{(\lambda i)} = \frac{R_{(\lambda i)}}{R_{c(\lambda i)}} \quad (1)$$

The first and last spectral data values are on the hull and therefore the first and last values of continuum-removed spectrum are always equal to 1. The output curves have values ranging between 0 and 1, in which the absorption troughs are enhanced (Schmidt & Skidmore, 2001).

The continuum-removed reflectance spectra were divided into three classes corresponding to pre-defined foliar sodium concentration classes. Foliar sodium was divided into three classes based on the amount of sodium required by most mammals. Sodium requirements for growth and reproduction of mammals range from 0.05 % to 0.15 % of the diet (Robbins, 1983). From this background knowledge, the lowest sodium class was taken to be any sample with less than 0.05 % sodium concentration, medium was taken to be any sample with between 0.05 % and 0.15 % sodium concentration (considered as the adequate range for herbivore consumption), and the high class was taken to be above 0.15 % sodium concentration. Analysis of variance as well as the t – test were used to ascertain whether differences in spectral reflectance between different classes of sodium concentration exist. Two-way factorial ANOVA was used to test whether the interaction between species and sodium concentration influences the reflectance spectra.

7.3 Results

7.3.1 Variation in foliar sodium concentration

The range of foliar sodium concentration was large as a result of sampling different species as well as sampling species growing at natural salt lick areas. Average amount of sodium ranged from 0.02 % in *T. triandra* to 0.2 % in *S. ioclados* (Table 7.1).

Table 7.1. Descriptive statistics of foliar sodium concentration by species

	No. of samples	Minimum (%)	Mean (%)	Maximum (%)	Std. Dev
P. maximum	17	0.00	0.10	0.27	0.08
T. triandra	20	0.00	0.02	0.08	0.02
U. mosambicensis	28	0.00	0.05	0.39	0.09
C. ciliaris	21	0.00	0.04	0.27	0.07
E. lehmanniana	10	0.00	0.08	0.31	0.10
S. ioclados	10	0.02	0.20	0.78	0.26

One-way ANOVA was used to test if differences in foliar sodium concentration between species were significant. We tested the research hypothesis that the mean percentage sodium concentration for the species measured in this study was different, *viz*. the null hypothesis Ho: $\mu_1 = \mu_2 = \mu_3 \ldots \mu n$ versus the alternate hypothesis Ha: $\mu_1 \neq \mu_2 \neq \mu_3 \ldots \mu n$ where: μ_1, μ_2 and

$\mu_3 \ldots \mu n$ are the mean percentage sodium concentrations of the *n* different species. The conclusions from these tests are that different species yielded different foliar sodium concentrations ($p < 0.001$). This is mainly explained by large disparities among species in uptake of sodium by roots and the translocation to the shoots as well as the varied availability of sodium in the soil (Marschner, 1995).

Foliar sodium concentration also varied between the known salt lick areas and non – salt lick areas. A large percentage (80 %) of *S. ioclados* recorded in this study was found on natural salt licks (sodic patches), followed by *U. mosambicensis* (34%). The average sodium concentration in these species is generally higher than the other species (the mean foliar sodium concentration was 1.6 % on salt licks and 0.05 in other areas). High foliar sodium concentration on these sites is strongly determined by the occurrence of nutrient – rich material exposed through weathering and erosion of dolerite and basalt intrusions (Klaus *et al.*, 1998). It should be emphasized that these variations in foliar sodium concentration relate specifically to the period when data was collected. Therefore there might be differences as a result of seasonal changes, which is beyond the scope of this study.

Sampling different species as well as different sites resulted in foliar sodium concentration ranging between 0 % and 0.78 %. Table 7.2 shows the descriptive statistics of foliar sodium concentration after partitioning into three different sodium concentration classes.

Table 7.2: Descriptive statistics of foliar sodium concentration by sodium classes. Low = < 0.05, Medium = 0.05 – 0.15 and High = > 0.15

Na concentration	No of samples	Minimum %	Mean %	Maximum %	Std. Dev
Low	61	0	0.02	0.047	0.014
Medium	21	0.053	0.091	0.146	0.032
High	24	0.149	0.296	0.78	0.176

A large amount of samples collected are in the low foliar sodium class indicating the scarcity of sodium in African savannas.

7.3.2 Reflectance differences between foliar sodium classes

We classified reflectance values according to three different levels of foliar sodium concentration and the continuum-removed reflectance is shown in Figure 7.2.

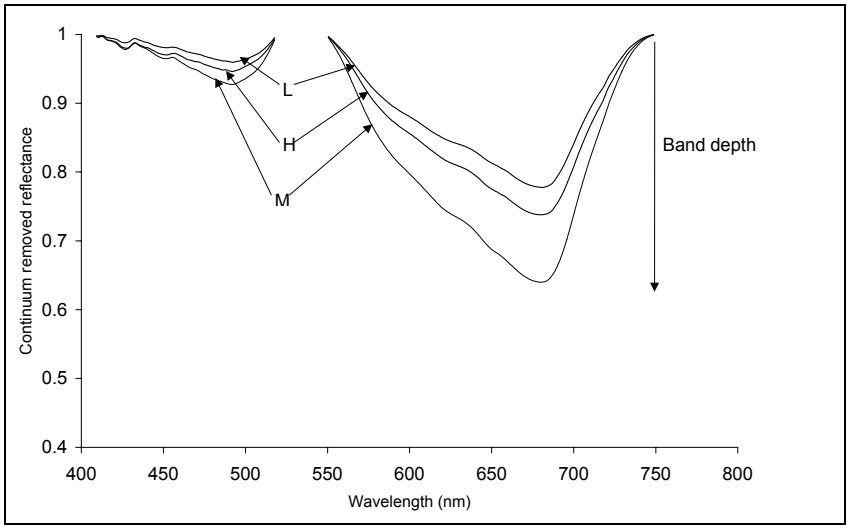

Figure 7.2: Continuum-removed band depth profiles for high (H), medium (M) and low (L) sodium classes.

A t-test was used to test the research hypothesis that there is a significant difference in mean spectral reflectance between different sodium classes, *viz*. the null hypothesis Ho: $\mu_{1i} = \mu_{2i}$ versus the alternate hypothesis Ha: $\mu_{1i} \neq \mu_{2i}$ where: $\mu_{1i,}$ and μ_{2i} are the mean reflectance values (at wavelength *i*) between each pair of low, medium or high sodium classes. Figure 7.3 shows probability values from the t-test executed at every wavelength.

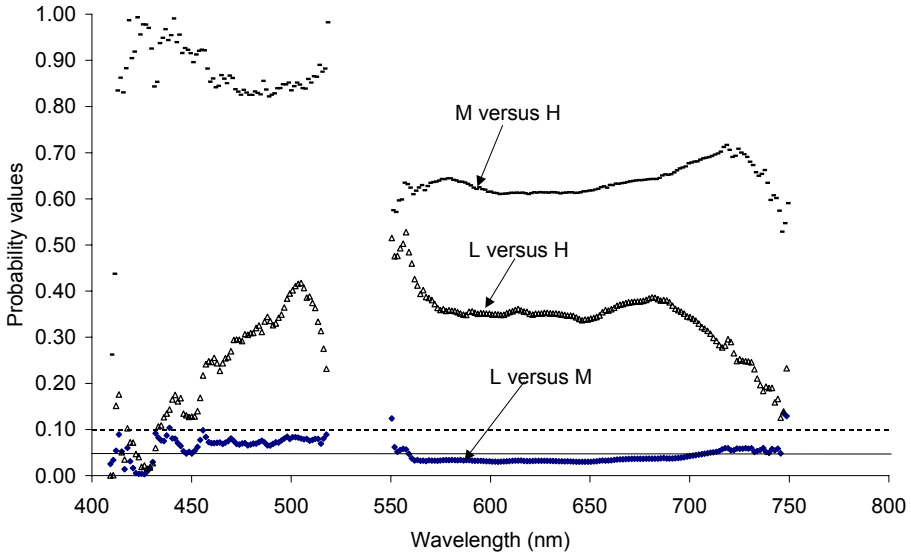

Figure 7.3: Results of T-test showing wavelengths where reflectance differences between different classes (L = low sodium, M = medium sodium, H = high sodium) of sodium concentration are significant. Horizontal dashed and solid lines show 90% and 95% confidence limits, respectively.

It can be seen that there were significant differences between low and medium sodium classes for most wavelengths ranging from 560 nm to 730 nm. Significant differences between low and high sodium classes were found in the blue wavelength region (410 nm to 430 nm). However there were no significant differences in mean reflectance between the medium and high sodium classes.

7.3.3 The interaction between sodium concentration and species in influencing reflectance

Research has revealed that there is difference in species tolerance to sodium supply in the soil (Flowers *et al.*, 1977; Johnston *et al.*, 1988; Qiu & Lin, 2002). Plant species such as *S. ioclados, P. coloratum,* and *E. superba* are salt tolerant whereas others are not (Matoh & Murata, 1990; Murata & Sekiya, 1992; Van Oudtshoorn, 1999). These plant species respond to sodium concentration by maintaining low cytosolic sodium concentrations and a high cytosolic potassium/sodium ratio (Flowers *et al.*, 1977; Murata & Sekiya, 1992), which implies that they can absorb high amount of sodium. For the plant species that do not have a salt tolerance mechanism, there is evidence of salt damage through chlorosis and rapid browning off when there is an oversupply of sodium. The variation in species response to sodium concentration causes a difference in spectral reflectance. We therefore hypothesize that both sodium concentration and species type influence spectral reflectance and there is an

interaction effect between the two factors. A Two – way factorial ANOVA was used to test the hypothesis that there is a significant interaction between species and foliar sodium concentration in influencing reflectance in the visible region. Table 7.3 shows results of the two-way ANOVA at the 589 nm wavelength.

Table 7.3: Two-way ANOVA results showing the effect of sodium and species on reflectance means at 589 nm wavelength. Absorption spectroscopy for sodium is done at 589 nm. ** Significant at $p < 0.01$.

	DF Effect	MS Effect	DF Error	MS Error	F	P
{1} Sodium	2	0.017	91	0.007	2.285	0.107
{2} Species	5	0.046	91	0.007	6.267	0.000**
1*2 Interaction	7	0.017	91	0.007	2.389	0.003**

Results indicate that, the interaction between species and sodium is significant ($p < 0.05$). Figure 7.4 details results of the two-way factorial ANOVA for the rest of the wavelengths between 410 nm and 750 nm.

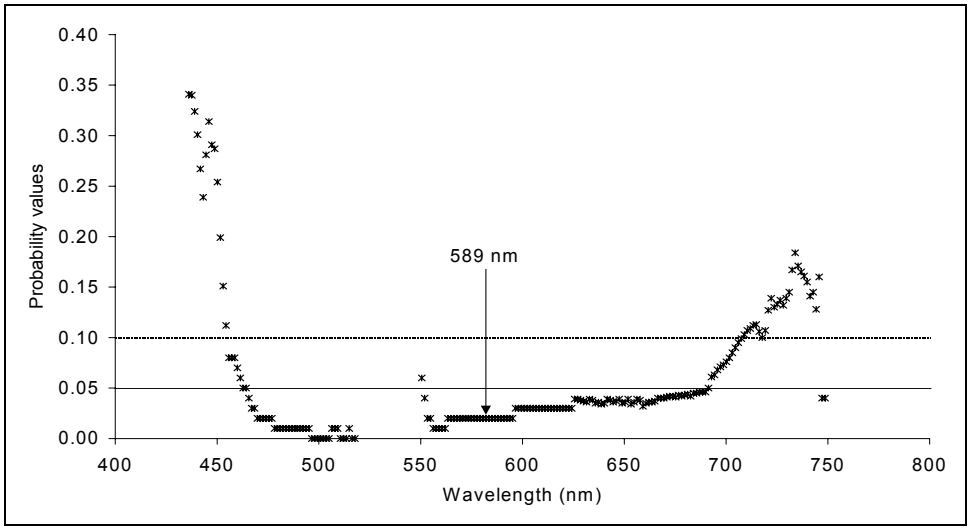

Figure 7.4: Results of two – way factorial ANOVA showing wavelengths where the interaction between sodium and species is significant in influencing reflectance in the visible domain. Horizontal dashed and solid lines show 90% and 95% confidence limits, respectively. Absorption spectroscopy for sodium is done at 589 nm.

There is a significant interaction effect between species and foliar sodium for most wavelength channels.

7.4 Discussion

Sodium is required by all terrestrial mammals, particularly ruminants that selectively utilize sodium rich vegetation (Stark, 1986; Wheelock, 1980). Therefore, the development of techniques that can estimate foliar sodium concentration helps to explain the distribution of mammals.

Results from this study have shown that for certain wavelengths in the visible, there is a significant difference in reflectance between grasses with different levels of sodium concentration. This is mainly explained by the relationship between foliar sodium and pigments, particularly chlorophyll which influences spectral reflectance in the visible domain. Sodium is important for regulating the photosynthetic pathway and functioning of the mesophyll chloroplasts in plants especially the C4 plants (Johnston *et al.*, 1988; Murata & Sekiya, 1992), and is therefore partly related to chlorophyll and nitrogen concentration (Salisbury & Ross, 1985).

From our study, statistically significant spectral differences were obtained between grasses in the low sodium concentration class and those in the medium sodium concentration class (Figure 7.3). The absorption trough in the medium sodium class is deeper than the absorption trough in the low sodium class (Figure 7.2). This confirms the hypothesis that an increase in foliar sodium concentration enhances the functioning of the mesophyll chloroplasts thereby stimulating growth and leaf expansion (Marschner, 1995; Ohta *et al.*, 1989), which in turn increases the absorption of electromagnetic radiation in the visible region.

However, no significant differences were obtained with the high sodium concentration class except for a few bands in the blue region. The high sodium class is in the middle (Figure 7.2). This implies that, after a certain concentration level of foliar sodium, band depth did not increase with a corresponding increase in foliar sodium. This may be because excess sodium concentration adversely affects certain grass species, which are not sodium tolerant by inhibiting metabolic functions and growth that in turn affect spectral reflectance (Pardo & Quintero, 2002; Ponzoni & Goncalves, 1999). This interpretation needs confirmation using data obtained from a controlled laboratory set up since the results reported in this study are based on situ measurements where there are possible effects of differences in soil background and senesced plant material.

This study has shown that not only sodium concentration but also the mixture of species in a savanna environment effects spectral reflectance. There is a significant interaction between species and foliar sodium concentration in effecting reflectance in the visible domain of the electromagnetic spectrum. An example of two – way factorial ANOVA in Table 7.3 shows that sodium classes alone could not significantly influence spectral reflectance at 589 nm channel ($p > 0.05$). However, with the addition of species type as a second factor, there was a significant interaction ($P < 0.05$). Including a second factor (species), that

influences spectral reflectance, has therefore reduced residual variation in the model.

The interaction effect between sodium and species type is based on the different response of different species to sodium supply. Some plant species such as *S. ioclados* are salt tolerant through maintenance of a high potassium/sodium ratio in the cytosol and the compartmentalization of sodium in the plant vacuole (Flowers *et al.*, 1977; Murata & Sekiya, 1992). Therefore, the rate of chlorosis and browning as a result of high sodium supply varies with different grass species. This grass species variation effects a variation in spectral reflectance. Therefore for mapping foliar sodium in savanna rangelands using GIS and remote sensing, additional information on species composition may be a useful input for obtaining a higher accuracy. Alternatively, the application of non-linear algorithms that are capable of capturing the response of different species to spectral reflectance may be useful in mapping quality in the tropical rangelands.

7.5 Conclusions

This study has shown that, there is potential to discriminate different levels of foliar sodium concentration using reflectance spectroscopy. Spectral reflectance could successfully discriminate between low and medium sodium classes. The result also emphasizes the importance of species types as a factor to estimate foliar sodium concentration using remotely sensed data. Species typing is possible in African rangelands given sufficiently detailed imagery (Schmidt & Skidmore, 2001). We anticipate that the results can be used as a precursor to mapping the concentration of grass quality in African rangelands using remotely sensed data derived from airborne (e.g. HYMAP) and space borne (e.g. ASTER, LANDSAT TM) sensors. This would facilitate a better understanding of the movement and behaviour of wildlife in relation to foliar sodium variation.

CHAPTER 8:
Explaining grass–nutrient patterns in a savanna rangeland of Southern Africa

This chapter is based on

Onisimo Mutanga, Herbert H.T Prins, Andrew, K. Skidmore, Herman Huizing, Sipke van Wieren, Rina grant, Mike Peel, and Harry Biggs **(In Press),** Explaining grass–nutrient patterns in a savanna rangeland of Southern Africa, *Journal of Biogeography*.

Abstract

The search for possible factors influencing the spatial variation of grass quality (N, P, K, Ca, Mg, Na) is an important step towards understanding the distribution of herbivores, as well as a step towards identifying crucial areas for conservation and restoration. A number of studies have shown that grass quality at a regional scale is influenced by climatic variables. At a local scale, site factors and their interaction are considered important. In this study, we aimed at examining environmental correlates of grass quality at a local scale. The study also sought to establish if biotic factors interact significantly with abiotic factors in influencing a variation in grass quality. Our results indicate that there is a significant relationship between grass quality parameters and site-specific factors such as slope, altitude, percentage grass cover, aspect and soil texture. Relatively, percentage grass cover and soil texture were more critical in explaining a variation in grass quality. Plant characteristics such as species type interact significantly with slope, altitude and geology in influencing nutrient distribution. The results of this study provide a better insight on foliar nutrient distribution patterns at a landscape scale in savanna rangelands.

Keywords: Landscape scale, biotic and abiotic factors, interaction, savanna rangelands, post rainy season, Kruger National Park

8.1 Introduction

Grass quality, as determined by the concentration of nitrogen, phosphorus, potassium, calcium, and sodium is an important factor influencing the distribution of grazing mammals (McNaughton, 1990, Olff *et al.*, 2002, Prins, 1987). Therefore, the search for factors determining the spatial variation of grass quality is an important step towards understanding the concentration of herbivores, as well as a step towards identifying crucial areas for conservation and restoration.

Explaining spatial patterns of grass quality is one of the most complex problems in biogeography. This is because these patterns are not influenced by a single factor, but by a complex array of interacting factors, both biotic and abiotic (McNaughton, 1990, Seagle & McNaughton, 1992), whose relative importance varies with spatial scale (Roberts, 1987). Research on factors influencing spatial variation of grass quality has been conducted mainly at a regional scale, demonstrating the importance of climatic variables such as temperature and rainfall (Robbins, 1983, Roberts, 1987, Seagle & McNaughton, 1992, Skarpe, 1992).

At landscape scale, topographic factors such as slope, aspect and altitude (McNaughton, 1983, Roberts, 1987), together with soil characteristics such as nutrients, structure and texture which largely depend on underlying geology (Anderson & Talbot, 1965; Bell, 1982) are critical. For example, Kumar *et al.*, (2002) found significant differences in the growth rates and quality of vegetation between clayey and sandy soils in Burkina Faso, an area where rainfall is a limiting factor. On sandy soils a large fraction of rainfall infiltrates and becomes available for plant growth, while on clayey soils low infiltration rates generate runoff, leading to slower herbage growth rates (Kumar *et al.*, 2002). Since the Kruger National Park is underlain by two major geological formations (granite and basalt), which support different soil characteristics, differences in quality are expected.

Other studies emphasize the importance of biotic factors such as species type or genotype, growth stage, above ground biomass and tree canopy cover, many of which vary between the grazed and ungrazed areas as important factors in influencing the spatial variation of grass quality (Bakker *et al.*, 1983; Ludwig, 2001; McNaughton, 1988; Olff & Ritchie, 1998; Orians *et al.*, 2003; Prins, 1987; Wilson, 1984). For example, Ludwig (2001) found out that grasses under trees are highly nutritious as compared to surrounding areas mainly due to the nutrient pump mechanism by tree roots.

It is also imperative to note that plant species exploit environments differentially (Duncan, 2000; Orians *et al.*, 2003; Via & Lande, 1985). Certain vegetation communities or plant species with different rates of nutrient accumulation can tolerate certain slope or catena positions whilst others may not (Bell, 1982; McNaughton, 1983). For example, Seagle & McNaughton, (1992) found out that a higher percentage of *T. triandra* is found on middle

catena position and *P. mezianum* (which accumulates nutrients such as sodium) is found on flat catena position. In addition, studies have shown that some species are tolerant to stress conditions such as high sodium supply whilst others quickly develop chlorosis (Duncan, 2000). We therefore hypothesise an interaction between both biotic and abiotic factors in influencing a spatial variation of grass quality.

Whilst studies have examined singly, the biotic (e.g. species type, biomass, vegetation type) or abiotic factors (e.g. slope, altitude, aspect, soil texture, and drainage lines) influencing nutrient distribution in savannas (Bell, 1982; Scholes & Walker, 1993, McNaughton, 1990), few of them have examined them simultaneously. In addition, an investigation of the interaction between environmental factors in influencing nutrient distribution patterns has been overlooked (Orians *et al.*, 2003; Via & Lande, 1985; Wilkinson, 2000).

The aims of this study were twofold: First, to identify environmental factors that correlate with grass quality at a landscape scale. The relationship between grass quality parameters and landscape variables (slope, altitude, aspect, soil texture, distance from drainage lines, vegetation type, geology, biomass, species type and percentage cover) were examined. Second, the study sought to establish if biotic factors interact significantly with abiotic factors in influencing a variation in grass quality. We used correlation analysis and ANOVA to relate environmental variables to grass quality. Multivariate analysis techniques were used to simultaneously analyse and explore the complex interactions between variables. Foliar nitrogen concentration was used in the interpretation of multivariate relationships since it is considered the most important limiting quality parameter for herbivores (Prins & Olff, 1998).

8.2 Methods

8.2.1 The study area

The study area is located in the Kruger National Park of South Africa. The study area stretches from west ($22^0 49'$ S and $31^0 01'$ E) to east, ($22^0 44'$ S and $31^0 22'$ E) covering an area of about 25 x 2 km in the far northern region of the Kruger National Park. This strip cuts across a basalt and granitic landscape mosaic. The granite areas are characterised by coarse sandy or gravelly soils with high infiltration rates and low clay forming potential. The uplands support broad–leaved savanna and a herbaceous layer dominated by moderate to low quality sandveld species. The midslopes (seepline areas) support few trees and a dense herbaceous layer. The base of the midslope and foot slope that are characterised by clay soils constitute thorny microphyllous shrubs and a productive grass layer (Grant *et al.*, 2000).

The basalt is a mafic rock that is rich in iron, magnesium and weathers to form rich clay minerals (Grant *et al.*, 2000). Sodium and other minerals occur

on wetland edges in these basalt formations (Jourbert, 1976). The vegetation of these soils consists mainly of mopane woodlands (*Colophospermum mopane*) in the north and knobthorn (*Acacia nigrescens*) and marula woodlands (*Sclerocarya birrea*) in the south (Grant *et al.*, 2002).

8.2.2 Field data collection

The data was collected in April and May 2002. Stratified random sampling with clustering was adopted in this study. The area was stratified into open grassland in the basalt, and into mixed woodland and woodland in the granite area. Coordinates (x y) were randomly generated in S - PLUS statistical software to select plots. Using a GPS, plots of 10 m by 10 m were located and demarcated in the field. The dominant grass species (covering at least 30 per cent of the area) in each plot were recorded. Purposive sampling was also done on known natural lick areas (sodic patches), which were located on wetland edges. Six grass species were recorded, viz. *C. ciliaris, E. lehmanniana, P. maximum, T. triandra, U. mosambicensis and S. ioclados*. Grass samples were taken from these species for chemical analysis.

Percentage grass cover was estimated as the total area occupied by grass canopy cover in a plot. This was calculated using the line intercept method, a technique that has been widely used in terresrial, wetland and aquatic systems (Bauer, 1943; Schmid, 1965). Two transect tapes were stretched along the diagonal lines of the 10 m by 10 m plots. The corner of the plot was the starting point of the transect (baseline), which stretched to join the opposite corner. The horizontal linear length of the grass canopy that intercepted the line was measured and recorded (Grieg-Smith, 1983; Titus, 1993). Percent grass cover was then calculated by totalling the intercept measurements for all plant species along the transect line and this total was expressed as percentage of the length of the transect line. The same was done on the other diagonal transect. The final percentage grass cover was calculated as the average percent grass cover from the two diagonal transect lines. To permit an analysis of the interaction between canopy cover and other categorical variables, the percentage canopy cover was categorized into four classes using the quartile ranges.

In situ grass biomass was measured in each plot using a weighing scale. A $1m^2$ wire was randomly thrown into the plot, and the standing grass that fell within the wire was clipped and measured (Kent & Coker, 1992). The process was repeated for 3 times in every plot and the resultant biomass was calculated as the average of the three-recorded biomass measurements in each plot. This was expressed as the fresh weight of grass per m^2.

Soil texture was measured in the field using the "feel" method (Thein, 1979). In each plot, a soil sample was collected and uniformly moistened. By squeezing the soil between fingers, the soil was classified into three classes. The first class was clay, which feels sticky and hard to squeeze (smooth). The

second class was silt, which feels soft (smooth). The third class was sand, which feels gritty and the grains are large to see individually (course). The data were verified and formatted before being stored in a GIS. Table 8.1 shows the explanatory variables that were used in this study.

8.2.3 GIS data layers

A raster GIS was developed coincident with the field plot centres. A digital elevation model (DEM) with a resolution of 5 m was used to derive elevation, slope and aspect using the map calculation functions in ILWIS GIS. Distance from river was derived by rasterising and resampling digitized topographic maps of a 1: 50 000 scale. The distance of sample locations from drainage lines was calculated using a distance function in ILWIS.

Table 8.1: Explanatory variables used in this study, together with their definitions

Variable	Definition
Altitude	Continuous variable derived from a DEM, measures height above sea level
Slope	Continuous variable derived from a DEM, expressed in degrees
Aspect	Continuous variable derived from a DEM, expressed in degrees
DLs	Continuous variable, measures distance from drainage lines
Cover	Area under grass canopy cover (%)
Biomass	Fresh weight of grass per m^2
Soil texture	Categorical variable, measures soil coarseness
Geology	Binary variable, 1 for Basalt areas and 0 for Granite areas
Vegtype	Categorical variable, vegetation types
Species type	Categorical variable, species types
Salt licks	Binary variable, 1 for lick sites and 0 for non lick sites

8.2.4 Laboratory analysis

For biochemical analysis, samples of grass species from each plot were clipped and oven-dried at 70º C for 24 hours. Plant tissue was analysed at the Institute of Tropical and Subtropical Crops under the Agricultural Research Council (ARC-ITSC) in Nelspruit, South Africa. A two-step analysis procedure was followed: (i) digestion and extraction, and subsequently (ii) automated detection. Sulphuric Acid and Hydrogen Peroxide microwave digestion was done for N extraction and Nitric Acid as well as Perchloric Acid digestion was done for P, K, Ca, Mg and Na extraction (Giron, 1973).

Atomic absorption flame spectroscopy using air-acetylene was used for detecting potassium, calcium, magnesium and sodium (Poluektov, 1973). The colometric method by auto analyzer was used to detect nitrogen (Technicon Industrial method 329 - 74W). Using this method for N detection, an emerald-green colour was formed by the reaction of ammonia, sodium salicylate, sodium nitroprusside and sodium hypochlorite. The ammonia-salicylate complex was then read at 640 nm (Grasshoff *et al.*, 1983). The determination of phosphorus was also based on the colorimetric method (Technicon Industrial method 4 –

68W) in which a blue colour was formed by the reaction of ortho phosphate and the molybdate ion. The phosphomolybdenum complex was then read at 660 nm.

8.2.5 Univariate data analysis

Correlation analysis was done to establish the relationship between continuous variables and foliar macronutrients. For categorical variables, one–way ANOVA and two-sided t–tests were used to test if there were any significant differences in foliar nutrient concentrations between different environmental classes.

8.2.6 Multivariate data analysis

Many patterns in a real world ecological system are driven by a number of interacting ecological processes that vary in space and time (McGarigal *et al.*, 2000). The multiplicity and interaction of many causal factors make it plausible to analyse relationships simultaneously. We applied two–way factorial ANOVA and Principal component analysis to assess the interaction of variables as well as identifying the most important factors explaining the variation in grass quality.

Two–way factorial ANOVA is a simultaneous analysis of the effect of more than one factor on population means. An interaction between factors means that the effect of one factor is not independent of the presence of a particular level of the other factor (McGarigal *et al.*, 2000). Biotic variables (species type, percentage cover and biomass) were tested if they significantly interact with the abiotic variables (soil texture, geology, altitude, slope and distance from drainage lines) to influence a variation in nitrogen concentration. Nitrogen was selected since it is generally considered the most critical limiting quality parameter for herbivores (Prins, 1987, Sinclair, 1977). Continuous variables were categorized using quartile ranges in order to compare them with the other categorical variables. Since interactions come in many shapes and forms (Moore & McCabe, 1998), plots of group means helped to properly interpret the data.

Principal component analysis (PCA) condenses information contained in a large number of original variables into smaller set of new composite dimensions, with a minimum loss of information (McGarigal *et al.*, 2000). The technique also reveals complex interrelationships among variables, which can be interpreted through the principal component structure (Griffith & Amrhein, 1997).

We used PCA to compose the original variables into linearly independent orthogonal principal components (PCs) thereby reducing dimensionality in the data. We used a correlation matrix *R* instead of a covariance matrix to summarize the variance structure of the original data

matrix since the scale or unit of measurement differed among variables (McGarigal *et al.*, 2000).

We used the principal component loadings to assess the relative importance of the independent variables in each principal component. The principal component loadings are defined as (McGarigal *et al.*, 2000):

$$S_{ij} = \nu_{i(j)}\sqrt{\lambda_i} \quad (1)$$

where S_{ij} is the correlation between the *i*th principal component and the *j*th variable, ν_{ij} is the principal component weight of the *j*th variable in the *i*th principal component and λ_i is the eigenvalues associated with the *i*th principal component.

8.3 Results

8.3.1 Variations in the data set

Table 8.2 shows the distribution of the macronutrients measured at the sample sites. There was a marked variation in the range of foliar macronutrients (dependent variables) between the granites and basalts as well as among species. Figure 8.1 shows histograms of the distributions. Data was tested for normality using the Kolmogrov-Sminov test. Magnesium, phosphorus and calcium follow a normal distribution ($p > 0.05$). A log 10 transformation was used to normalize nitrogen, potassium and sodium. This subsequently led to the use of parametric statistical tests, which assume a normal distribution of the data. Table 8.3 shows the distribution of the continuous environmental variables that were used in this study.

Table 8.2: Descriptive statistics of the measured biochemicals per species and per geology

Biochemical by species	Geology	No. of samples	Mean (%)	St dev
Nitrogen				
P. maximum	Granite	11	0.79	0.13
	Basalt	-	-	-
T. triandra	Granite	9	0.77	0.2
	Basalt	7	0.66	0.36
U. mosambicensis	Granite	16	0.84	0.49
	Basalt	9	0.66	0.26
C. ciliaris	Granite	1	1.01	-
	Basalt	12	0.79	0.15
E. lehmanniana	Granite	7	0.91	0.42
	Basalt	7	0.72	0.27
S. ioclados	Granite	-	-	-
	Basalt	12	1.21	0.94
All combined		91	0.86	0.46
Magnesium				
P. maximum	Granite	11	0.23	0.08
	Basalt	-	-	-
T. triandra	Granite	9	0.23	0.09
	Basalt	7	0.16	0.05
U. mosambicensis	Granite	16	0.26	0.1
	Basalt	9	0.23	0.08
C. ciliaris	Granite	1	0.31	-
	Basalt	12	0.24	0.04
E. lehmanniana	Granite	7	0.23	0.06
	Basalt	7	0.15	0.1
S. ioclados	Granite	-	-	-
	Basalt	12	0.27	0.1
All combined		91	0..23	0.09
Calcium				
P. maximum	Granite	11	0.38	0.09
	Basalt	-		-
T. triandra	Granite	9	0.42	0.13
	Basalt	7	0.33	0.06
U. mosambicensis	Granite	16	0.54	0.13
	Basalt	9	0.49	0.17
C. ciliaris	Granite	1	0.59	-
	Basalt	12	0.49	0.07
E. lehmanniana	Granite	7	0.39	0.05
	Basalt	7	0.40	0.17
S. ioclados	Granite	-	-	-
	Basalt	12	0.46	0.17
All combined		91	0.45	0.13
Potassium				
P. maximum	Granite	11	1.07	0.38
	Basalt	-	-	-
T. triandra	Granite	9	0.9	0.42
	Basalt	7	0.75	0.26
U. mosambicensis	Granite	16	1.01	0.66
	Basalt	9	0.60	0.195
C. ciliaris	Granite	1	1.39	-
	Basalt	12	1.33	0.42
E. lehmanniana	Granite	7	1.82	0.75
	Basalt	7	0.63	0.38
S. ioclados	Granite	-	-	-
	Basalt	12	0.59	0.39
All combined		91	0.97	0.57

Table 8.2: Descriptive statistics of the measured biochemicals per species and per geology (cont)

Phosphorous					
	P. maximum	Granite	11	0.23	0.11
		Basalt	-	-	-
	T. triandra	Granite	9	0.19	0.08
		Basalt	7	0.17	0.04
	U. mosambicensis	Granite	16	0.21	0.07
		Basalt	9	0.16	0.02
	C. ciliaris	Granite	1	0.16	-
		Basalt	12	0.28	0.09
	E. lehmanniana	Granite	7	0.21	0.07
		Basalt	7	0.16	0.04
	S. ioclados	Granite	-	-	-
		Basalt	12	0.21	0.05
	All combined		91	0.21	0.08
Sodium					
	P. maximum	Granite	11	0.1	0.09
		Basalt	-	-	-
	T. triandra	Granite	9	0.03	0.03
		Basalt	7	0.02	0.03
	U. mosambicensis	Granite	16	0.05	0.098
		Basalt	9	0.06	0.09
	C. ciliaris	Granite	1	0.1	-
		Basalt	12	0.02	0.05
	E. lehmanniana	Granite	7	0.14	0.06
		Basalt	7	0.03	0.05
	S. ioclados	Granite	-	-	-
		Basalt	12	0.21	0.25
	All combined		91	0.08	0.122

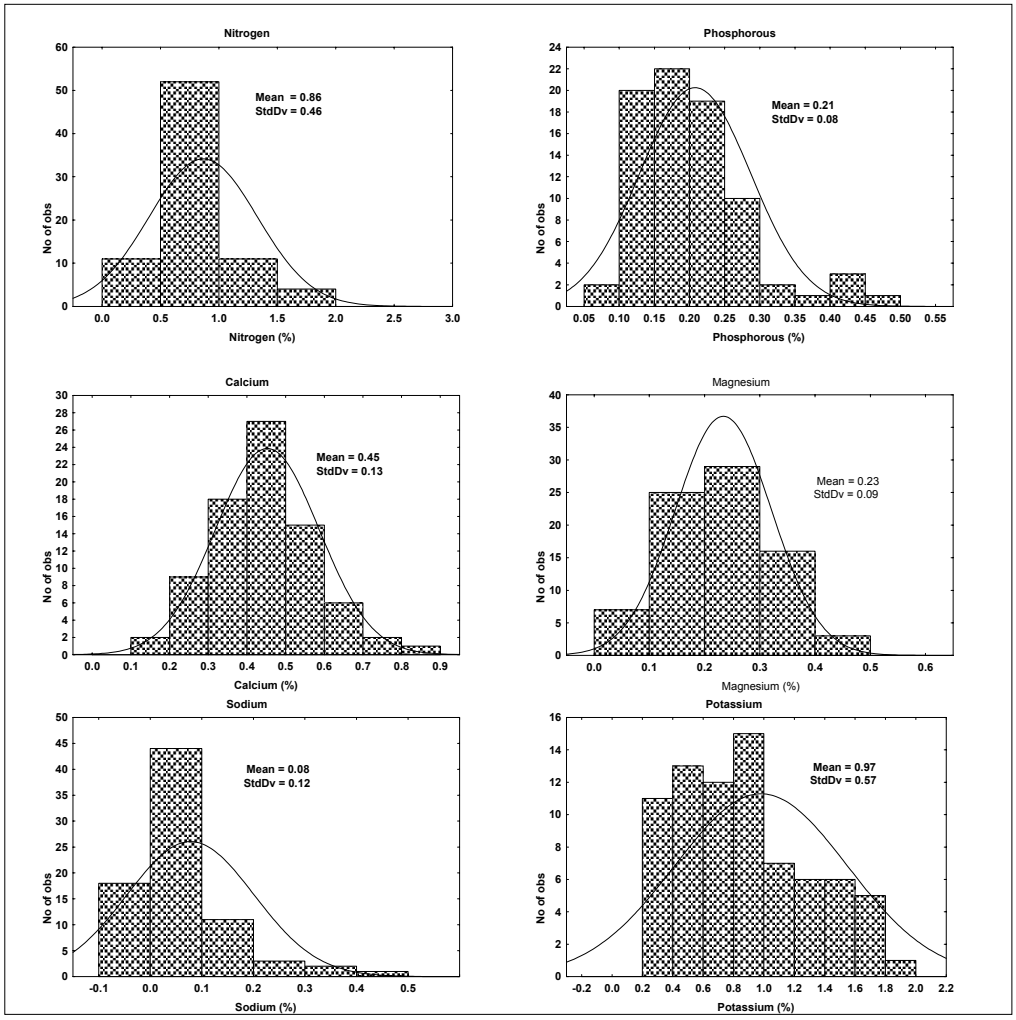

Figure 8.1. Distribution of the foliar macronutrients measured in the Kruger National Park.

Table 8.3: Mean and standard deviation of the continuous data collected (n = 91)

Variables	Mean	Standard deviation
Altitude (m)	401	18.87
Cover (%)	84.75	15.56
Biomass (kg/m^2)	0.48	0.33
Distance from DLs (m)	445	504
Slope (Degrees)	6.38	3.80
Aspect (Degrees)	187.6	95.16

* Significant level: $p < 0.05$

Table 8.4a: Correlation coefficients (r) between macronutrients and continuous environmental factors (n = 91). For the relationship between macronutrients versus slope as well as aspect, sample plots with slope and aspect values greater than 0 were used.

	N	Ca	K	P	Mg	Na
Altitude	-0.44*	0.26*	0.30*	0.31*	0.04	-0.21
Slope	-0.72*	-0.71*	-0.57*	-0.23	-0.26	-0.65*
Aspect	-0.62*	-0.14*	-0.79*	-0.53*	-0.65*	-0.60*
DLs	-0.09	0.23*	0.19	-0.05	-0.16	0.13
Cover	-0.29*	-0.04	-0.51*	-0.23	-0.23	-0.4*
Biomass	-0.24*	-0.20	0.14	0.08	0.06	-0.21

* Significant level: $p < 0.05$

Table 8.4b: Results of One-Way analysis of variance and t – tests between foliar chemical variables and categorical environmental factors. One-way ANOVA was used on factors with more than two groups of samples *viz.* Soil texture, vegetation type as well as species type and t–tests were used on binary factors *viz.* Geology, salt licks. S represents significant variables ($p < 0.05$) and NS represents variables that are not significant ($p \geq 0.05$)

	N	Ca	K	P	Mg	Na
Soil texture	s	ns	s	ns	ns	s
Geology	s	ns	s	ns	ns	ns
Vegtype	ns	ns	s	ns	ns	ns
Species type	s	s	s	s	ns	s
Salt licks	ns	ns	s	s	s	s

8.3.2 Univariate analysis

Results of Pearson's correlation analysis in Table 8.4a generally show that the independent variables are negatively correlated with the quality variables (N, Ca, K, P, Mg, Na), with a few exceptions. The strongest inverse correlation with all quality variables is observed with slope. Percentage grass cover and aspect also show significant inverse relationships with all quality variables. Relatively weak correlations were obtained between quality variables and distance from the drainage lines. There is also a negative relationship between nitrogen concentration and biomass. When data was partitioned into dry and wet biomass (observed in the field), the relationship was stronger between dry biomass and nitrogen concentration (correlation coefficient = -0.36, $p < 0.05$) as compared to the fresh biomass (correlation coefficient = -0.24, $p < 0.05$).

For categorical variables, significant differences were obtained between most quality variables and species type as well as the salt licks (Table 8.4b). Exploratory data analysis through box plots showed that the concentration of most quality variables was high on salt licks and in certain species such as *S.*

ioclados. Nitrogen and potassium also differed significantly between the two major geological types. Higher N and K were recorded in granitic areas as compared to the basalts.

8.3.4 Multivariate analysis

Two–way factorial ANOVA was used to test the interaction between the biotic and abiotic independent variables in influencing a variation in nitrogen concentration. Plots of means were used to identify the direction and form of interaction. Figure 8.2 shows the form and direction of the interaction between geology and grass cover. The interaction effect was tested using the two–way ANOVA.

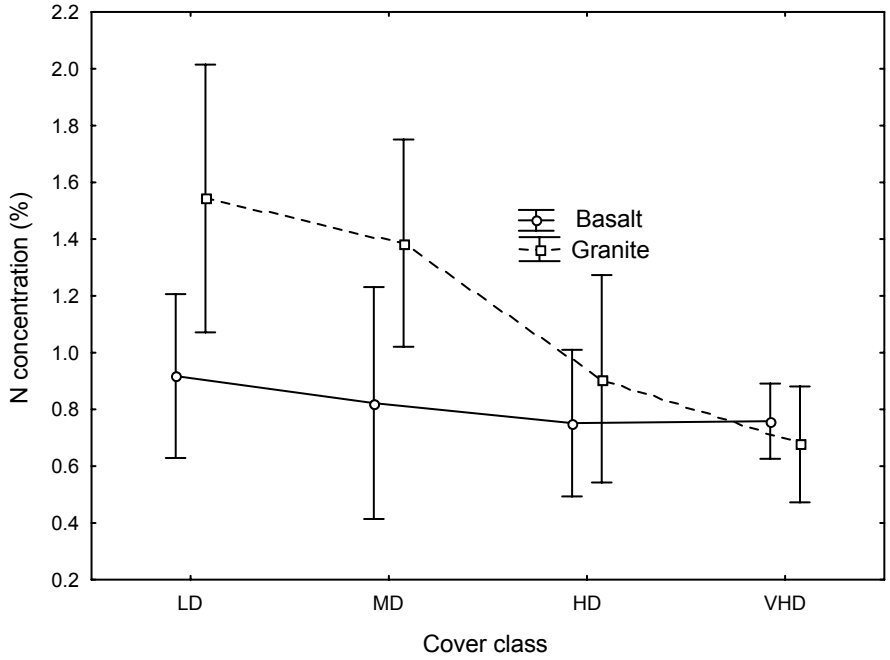

Figure 8.2: The form and direction of interaction between geology and grass cover (± 95% CL) in influencing a variation in nitrogen concentration. Grass cover was categorized into Low density (LD), Medium density (MD), High density (HD) and Very high density (VHD) using the quartile ranges.

In the low grass cover class, there are significant differences in nitrogen concentration between the granite and basalts ($P < 0.001$). However there are no significant differences in the high cover class ($P > 0.05$). Detailed pair wise results of the interaction between landscape variables in influencing a variation in nitrogen concentration are shown in Table 8.5.

There is also a significant interaction between cover and species type ($p < 0.001$). Although all species show a general decrease in nitrogen concentration with increasing grass cover, there is a marked difference in the rate of decrease between the species themselves. For example, species such as *S. ioclados* have very high nitrogen concentration in the low cover class, which decreases rapidly in the high cover classes, whereas there is a gradual decrease for *P. maximum*. Significant interaction between slope and species type, between salt licks and distance from the drainage lines as well as between geology and cover have also been uncovered.

Table 8.5: Two–way Factorial ANOVA testing for interaction between independent variables in influencing variation in foliar nitrogen concentration. S represents significant variables ($p < 0.05$) and NS represents variables that are not significant ($p \geq 0.05$)

	Soil texture	Geology	Salt licks	Altitude	Slope	DLs	Species type	Cover
Species type	-	S	S	S	S	NS	-	
Cover	NS	S	NS	S	NS	NS	S	-
Biomass	S	NS	S	NS	NS	S	NS	NS
Vegtype	NS	NS	S	NS	NS	S	NS	S

Principal component analysis was executed using 8 continuous variables described in Table 8.1. This list comprises all continuous variables as well as categorical variables that could be ranked according to a certain criteria i.e. soil texture and vegetation cover. Soil texture varied from fine to coarse texture, while vegetation type varied from open mopane to dense mopane. From the explanatory variables analysed, five PCs collectively yield 91 % of the total variance as shown by the eigen values in Figure 8.3.

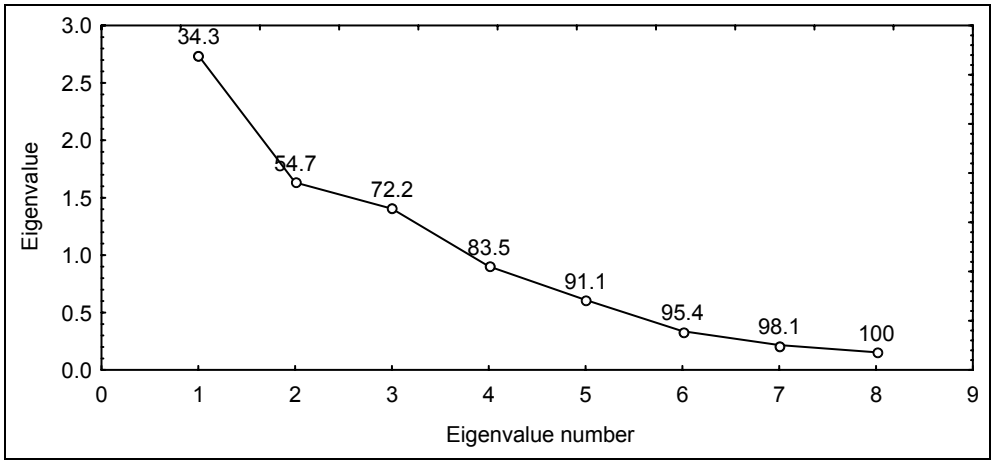

Figure 8.3: Scree plot for the eigenvalues associated with the 8 principal components. The eigenvalues were normalised as percentage of the total and the numbers on the scree plot indicate the cumulative percentage contribution.

Principal component loadings were used to explore and interpret the complex interrelationships represented in the principal component structure (Table 8.6).

Table 8.6: Principal components and their corresponding scores (loadings). ** shows the highest significant absolute loadings for each variable.

	PC_1	PC_2	PC_3	PC_4	PC_5
Eigen values	2.74	1.63	1.40	0.90	0.61
Altitude	-0.800924**	-0.073823	-0.445750	0.081822	-0.130805
Slope	-0.695063	0.241425	-0.698677**	0.026322	-0.108623
Aspect	-0.660718	0.153006	-0.668985**	-0.015838	-0.115422
Vegtype	-0.729681**	-0.032906	-0.300378	-0.340566	0.358929
Cover	-0.161445	-0.713498	0.339347	0.223477	0.515977**
Biomass	-0.027636	-0.815378**	0.010945	0.364344	-0.342848
Soil texture	0.061842	0.608907**	-0.072907	0.739646**	0.219295
Dls	-0.784820**	-0.013228	-0.435174	0.222641	-0.083641

The highest significant scores for each PC in Table 8.6 indicate the relative contribution of the independent variables to the principal component as follows:

PC_1 is related to altitude, distance from the drainage lines, and vegetation type with a negative sign, implying a positive relationship between these variables

PC_2 is related to biomass and percentage grass cover

PC_3 is inversely related to slope and aspect

PC_4 is related to soil texture, and,

PC_5 is related to percentage grass cover

Stepwise linear regression (both forward selection and backward elimination) between the principal components and nitrogen concentration resulted in the following model:

$$Y = 0.83-0.138PC_4-0.08PC_5-0.04PC_3+0.03PC_2$$

The model selected principal components dominated by percentage grass cover (PC_2 and PC_5) implying the relative importance of percentage grass cover in modelling nitrogen variation. The importance of edaphic factors is reflected in the selection of PC_4, whose major contribution comes from soil texture. It is surprising to note that, PC_1, which contains the largest variance, was not selected by the stepwise linear regression. The model could explain 58% of the variation in foliar N concentration, with a root mean square error (RMSE) of 0.035.

8.4 Discussion

The variation of grass quality in space is commonly invoked to explain the movement of grazers (McNaughton, 1990; Prins, 1996). We have demonstrated in this study that nutrient distribution in the Kruger National Park is significantly correlated with several environmental variables such as slope,

aspect, biomass and percentage grass cover. Whilst univariate statistical analyses have shown individual variables that are related to quality parameters, multivariate analyses have shown the interrelationships between the independent variables themselves as well as their relative importance in explaining a variation in quality, particularly nitrogen.

Contrary to the general notion that basalt areas that are rich in clay minerals support more nutritious grasses than granite areas, the results of this study indicated that there is higher nitrogen and potassium concentration in grasses over the granites as compared to grasses over the basalt. These findings are supported by similar results obtained by Grant *et al*., (2000) who found high foliar nitrogen concentration in granitic areas as compared to basaltic areas. There are two possible explanations for this, which are now discussed.

Firstly, data was collected during the post rainy season (in April and May), a period when most annual grasses in the basalt (open grasslands characterised with heavy clayey soils) had used their nutrients quickly (Prins *et al.*, 1996), and dried up as a result of higher soil moisture tension, a measure of energy a plant must apply to the soil in order to extract the available moisture (Murphy *et al.*, 2000). This is in contrast to perennial grasses on the granites such as *P. maximum*, which provided nutritious green leaves long into the dry season (Grant *et al.*, 2000). The granites are characterised by sandy and loamy soils (Ventor, 1990), which have low moisture tension, hence the plants could extract water for survival. This relationship is confirmed by PC_4 (whose major significant loading comes from soil texture) being significant in a stepwise modelling of nitrogen variation (Table 8.6). Secondly, the high tree density in granitic areas accumulates nutrients on the surface by pumping them from deeper soil layers (Scholes & Archer, 1997), thereby supporting many grasses. In a study on tree–grass interactions in an East African savanna, Ludwig (2001) found out that grasses under trees were highly nutritious compared to the surrounding grasses. Although this study did not focus at such a microscale of analysis, the explanation may still hold since the granites have higher woody cover as compared to the basalts.

In addition to the tree–grass interaction explanation, some grass species (e.g. *P. maximum and S. ioclados*) are also common along many drainage lines that traverse the granitic areas (Ventor, 1990). These drainage lines are rich in clay, minerals and soil moisture, and the grasses growing there have high foliar nitrogen concentration (Grant *et al.*, 2000). This probably explains the inverse relationship between drainage lines and quality parameters obtained in this study. The type of species and their location as reflected in the significant interaction between species and geology in Table 8.5 is therefore critical in explaining the variation in grass quality.

Generally, there is a strong inverse relationship between all quality parameters and micro variations in slope, altitude as well as aspect. The effect of slope and aspect were more pronounced in the granite areas where high slope and aspect values were obtained. The influence of slope, aspect and altitude act

through their effects on soil temperature and water runoff (Roberts, 1987). Steeper slopes result in higher runoff and are therefore characterised by thinner soils, which do not support high quality grass whereas there is deposition of nutrient soils on foot slopes resulting in high quality grasses. Higher radiation on slopes in the Kruger National Park generally results in drier soils that support xerophytic plant species with low nutrient content. Slope and aspect contribute significant negative loadings to PC_3 in the PCA and have been selected in the stepwise model indicating their relative importance in modelling nitrogen distribution. The effect of these site-specific factors is modified by the influence of other interacting variables such as plant characteristics as will be discussed.

Slope interacts significantly with species type in influencing nitrogen variation (Table 8.5). Grass species such as *E. lehmanniana* have high nitrogen concentration on steep slopes as compared to *S. ioclados*, which contains very high nitrogen concentration on flat to gentle slopes next to vleis (salt licks). *E. lehmanniana* can survive on thin soils whereas *S. ioclados* grows particularly in and around seasonal pans with deep soils (Van Oudtshoorn, 1999). Species type also interacts significantly with known salt lick areas and non-salt lick areas. Some plant species such as *S. ioclados* are salt tolerant through maintenance of a high potassium/sodium ratio in the cytosol and the compartmentalization of sodium in the plant vacuole (Flowers *et al.*, 1977). Therefore, even at high sodium concentration, the plants resist chlorosis and rapid browning off as compared to salt sensitive plant species. Therefore, species that are found on salt licks have higher mineral concentration, and these areas are selected for grazing (McNaughton, 1988; Wheelock, 1980).

This study has shown an inverse relationship between quantity (expressed as percentage cover and biomass) and most quality parameters (McNaughton, 1987; Prins *et al.*, 1996). From results of stepwise modelling using PCs, percentage grass cover and biomass turns out to be strong variables in explaining quality variation. This is reflected in the selection of PC_2 where biomass and then percentage cover contributes the largest loadings (Table 8.6). Percentage cover also contributes the largest loading in PC_5. This pattern can be partly explained by the dilution of nutrients in high biomass regions (van de Vijver, 1999, Wilson, 1984). A further analysis of the relationship between nitrogen concentration and dry biomass as well as fresh biomass that were observed in the field revealed a stronger negative relationship with dry biomass as compared to fresh biomass. This observation is expected due to the influence of water in the plants. Nevertheless, the relationship with nitrogen for both dry and fresh biomass indeed revealed a negative direction, confirming the results of other similar studies (Prins & Olff, 1998).

Principal component analysis has helped to reduce dimensionality in the data set as well as describing and exploring the relative importance of variables in explaining quality variation. Four PCs were retained to explain the variation in nitrogen concentration (the most limiting quality parameter for grazers). It is interesting to note that the stepwise regression model for nitrogen did not select

PC_1. Variables such as vegetation type and distance from drainage lines that contribute significantly to PC_1 are not related to nitrogen. These variables are relatively measured at a coarser scale than variables such as percentage cover (PC_2) and biomass that are measured at a finer scale. For example, within a vegetation type class, there is a variation in percentage grass cover, which is closely related to a variation in quality. Therefore, site-specific factors are considered more critical in explaining a variation in grass quality as compared to regional variables.

It should be emphasized that due to the large number of factors of the environment which may affect the vegetation nutrient patterns, it is usually impossible to measure more than a limited number of factors (Roberts, 1971). Therefore the factors considered in this study are undoubtedly not exhaustive in explaining nutrient distribution patterns. Nevertheless, the results presented in this study provide strong evidence that selected environmental factors and their interaction do influence foliar nutrient distribution patterns.

8.5 Conclusion

The pattern of grass quality at regional, continental or global scale is largely determined by major climatic factors such as rainfall, temperature and latitude (Robbins, 1983, Roberts, 1987). However, these factors are known to be largely constant at a local scale like the one considered in this study. The evidence presented in this study indicates that site-specific factors such as availability of herbage and species type, which interact significantly with abiotic factors such as slope and altitude, are critical in influencing nutrient distribution. In particular, we have shown that, under some circumstances nitrogen can be higher in a granitic landscape than a basaltic landscape. In this regard, we anticipate that the results of this study can be used to better understand factors influencing foliar nutrient patterns at a landscape scale in savanna rangelands. This can be further enhanced by developing techniques to map the variation in grass quality. However, we acknowledge that this study is based on one snapshot, therefore some slightly different findings maybe obtained during other times of the year. Nevertheless, the study has revealed that under the conditions experienced during the study period, nutrient distribution varies with varying biotic and abiotic factors.

Acknowledgements

This study was carried out with the financial assistance of the International Institute for Geo-Information Science and Earth Observation (ITC) (formerly the International Institute for Aerospace Survey and Earth Observation). We would like to thank the Scientific Board of Kruger National Park for accepting our research proposal and for their subsequent assistance in field data collection.

Tropical grass quality at airborne platform level: Chapter 9

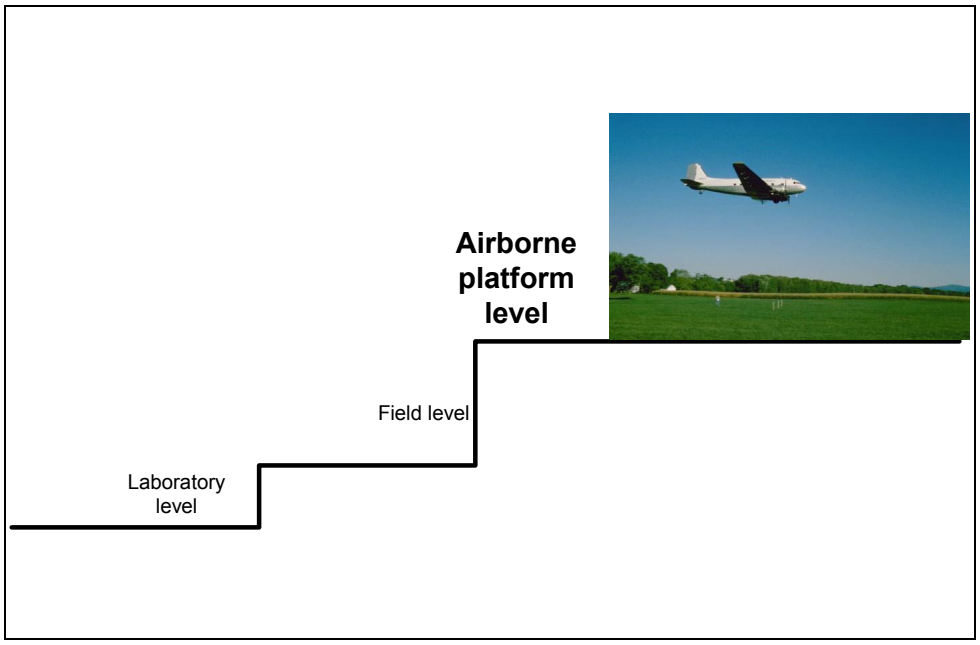

CHAPTER 9:
Integrating imaging spectrometry and neural networks to map grass quality in the Kruger National Park, South Africa

*This chapter is based on
O. Mutanga and A. K. Skidmore, 2004, Integrating imaging spectrometry and neural networks to map grass quality in the Kruger National Park, South Africa**,** *Remote Sensing of Environment,* 90 (1), 104-115.

Abstract

A new integrated approach, involving continuum-removed absorption features, the red edge position and neural networks is developed and applied to map grass nitrogen concentration in an African savanna rangeland. Nitrogen, which largely determines the nutritional quality of grasslands is commonly the most limiting nutrient for grazers. Therefore, the remote sensing of foliar nitrogen concentration in savanna rangelands is important for an improved understanding of the distribution and feeding patterns of wildlife. Continuum removal was applied on two absorption features located in the visible ($R_{550-757}$) and the SWIR ($R_{2015-2199}$) from an atmospherically corrected HYMAP MKI image. A feature selection algorithm was used to select wavelength variables from the absorption features. Selected band depths from the absorption features as well as the red edge position (REP) were input into a backpropagation neural network. The best-trained neural network was used to map nitrogen concentration over the whole study area. Results indicate that the new integrated approach could explain 60% of the variation in savanna grass nitrogen concentration on an independent test data set, with a root mean square error (rmse) of 0.13 (± 8.30% of the mean observed nitrogen concentration). This result is better compared to the result obtained using multiple linear regression, which yielded an R^2 of 38%, with a RMSE of 0.16 (±10.30% of the mean observed nitrogen concentration) on an independent test data set. The study demonstrates the potential of airborne hyperspectral data and neural networks to estimate and ultimately to map nitrogen concentration in the mixed species environments of Southern Africa.

Key words: Hymap image, absorption features, continuum removal, red edge position, foliar nitrogen concentration, savanna rangelands

9.1. Introduction

Research in Southern Africa has revealed that wildlife species such as roan antelope, wildebeest, zebra, tsessebe, warthog, reedbuck, hartebeest, topi, and buffalo favour open savanna or open grassland plains (Coetzee, 1983; Jourbert, 1976; Prins, 1989) and their spatial distribution is mainly influenced by a variation in grass quality, as determined by nitrogen concentration (Grant *et al.*, 2002; Heitkonig & Owen-Smith, 1998; McNaughton, 1988). In this regard, the determination and monitoring of spatial variations in nitrogen concentration in wildlife reserves is critical to facilitate an optimal management of wildlife resources. However, cost effective methods to accomplish the task of mapping grass quality remain largely underdeveloped.

The development of hyperspectral remote sensing has offered unprecedented opportunities to estimate and map foliar quality. This is mainly because hyperspectral images are acquired in many narrow, contiguous spectral bands that can detect local variations in absorption features (Kokaly *et al.*, 2003; Schmidt & Skidmore, 2003). Research has therefore focused on using remote sensing techniques such as those developed for laboratory near infrared spectrometry (NIRS) to estimate foliar biochemicals (Foley *et al.*, 1998; Marten *et al.*, 1989). NIRS can provide accurate estimates of protein, lignin, and cellulose contained in dried ground forage (Norris *et al.*, 1976), and in many laboratories the technique has replaced the standard analytical procedure for assessing plant biochemicals (Barton *et al.*, 1992).

The extension of empirical laboratory NIRS to estimating foliar biochemicals at canopy level has had increasing attention as hyperspectral remote sensor systems of high quality became readily available recently (Kumar *et al.*, 2001). However, the presence of water in fresh canopies masks the biochemical absorption features, particularly in the shortwave infrared (Clevers, 1999; Kokaly & Clark, 1999) and make the remote sensing of foliar biochemicals more difficult. In addition, leaf orientation and soil background effects, as well as atmospheric absorption, further complicate the remote sensing of biochemicals at field level (Asner *et al.*, 2000). NIRS-based techniques such as stepwise regression also suffer from problems of overfitting, especially when more wavebands than samples are used (Curran *et al.*, 2001).

To overcome these problems, some vegetation studies aimed at estimating foliar biochemical concentration have recently focused on the use of specific channels that correspond to the principal absorption features of vegetation at laboratory scale (Curran *et al.*, 2001; Kokaly & Clark, 1999; Mutanga & Skidmore, 2003; Mutanga *et al.*, In review) as well as field scale (Mutanga et al., 2004). The absorption feature analysis approach is based on isolation and normalisation of absorption features by continuum removal – a technique that was successfully applied in the geological sciences for mapping minerals (Clark & Roush, 1984). The advantages of using continuum-removed absorption features as compared to the standard NIRS approach are that; (i)

concentrating on specific absorption features reduces the problem of selecting wavebands that are non-causal (Curran *et al.*, 1992; Fourty *et al.*, 1996), and (ii), absorption features are enhanced and standardized to minimise the effect of spectral variability that is independent of the biochemical concentration (Curran *et al.*, 2001; Mutanga *et al.*, 2004).

Despite its advantages, the major drawback of the continuum-removed absorption feature analysis technique in combination with stepwise regression is that assumptions are made about the data characteristics such as assuming a linear relationship between the dependent and independent variables (Kokaly & Clark, 1999; Mutanga & Skidmore, 2003). Although the feature of linearity in a data set may be transformed mathematically, complex non-linearity in some data may never be approximated (Boyd, 2002; Zhang *et al.*, 2002). In such situations, the use of nonlinear regression requires *a priori* knowledge of the nature of the nonlinear behaviour, something that is not usually available and non-linear regression is cumbersome to implement (Keiner & Yan, 1998).

In view of the above, neural networks have been shown to be useful in modelling a variety of non-linear behaviour, including modelling a large range of transfer functions (Atkinson & Tatnall, 1997; Keiner & Yan, 1998). From this background, Mutanga *et al*., (2004) recommended the use of absorption features with a neural network algorithm, which does not assume linearity for mapping grass quality in the mixed species environments of Southern Africa.

The red edge position has also been found to be correlated with foliar nitrogen concentration (Mutanga *et al.*, In review; Penuelas *et al.*, 1994), because of a strong relationship between chlorophyll and nitrogen (Katz *et al.*, 1966; Penuelas *et al.*, 1994; Yoder & Pettigrew-Crosby, 1995; Mutanga *et al.*, In review). Therefore, the integration of neural networks with variables from continuum-removed absorption features as well as the red edge position might be applicable to mapping grass quality in mixed species environments such as those found in African rangelands.

The main objective of this study was to investigate whether a neural network, combined with continuum-removed absorption features as well as the red edge position could reliably map grass quality (nitrogen concentration) in a mixed species environment of the Kruger National Park, South Africa. We also compared the results obtained by the neural networks to those obtained by stepwise linear regression. This study is an extension of a field spectra study, which showed the potential of continuum-removed absorption features in predicting in situ grass quality (Mutanga *et al.*, 2004). The successful prediction of foliar quality using field spectroradiometry showed potential for the application of the approach using airborne sensors. The field spectra study also provided an insight on the most informative absorption features for predicting foliar biochemicals and these absorption features were used in this study. To the best of our knowledge, this study is the first to map nitrogen concentration at canopy level using high-resolution image in an African savanna rangeland.

9.2. Methods

9.2.1. Study area

The study area was located in the northern plains of the Kruger National Park in the Republic of South Africa. A strip of 2.5 km by 18 km was selected, stretching from west (22º 46′ S and 31º 11′ E) to east (22º 46′ S and 31º 21′ E) and covering basaltic formations. Grass production is high and there is considerable variation in species as well as nutritional quality (Grant *et al.*, 2000). This area is a subset of a larger study area that was used for estimating grass nutrient concentration using field spectrometry and the results are published in a separate paper (Mutanga & Skidmore, 2003; Mutanga *et al.*, 2004). For mapping grass nitrogen concentration using airborne hyperspectral imagery in this study, we concentrated on the eastern grassland plains, which had advantages of being generally flat with high grass cover and very few shrubs.

Initial sample sites were randomly selected within strata based on the land cover map of the area, which was provided by the GIS section of the Kruger National Park. To increase the number of samples in a time and labour-constrained situation, two extra samples were clustered at least 100 m from each of the initially generated plots. Samples to determine grass N concentration were collected in March 2003, the period of the Hymap MK1 overflight. The samples were collected from plots of 5 m by 5 m in area (largely homogenous in species cover), and x, y coordinates of the centre of each plot was recorded. Representative samples from each plot were collected by randomly clipping grass from several spots in the 5 m by 5 m plots. The samples from several spots in each plot were then mixed (about 300 g in total weight per plot) and collected in paper bags for laboratory analysis. A total of 44 samples falling within the subset window were used for this study.

The grass samples were oven-dried at 70º C for 24 hours. Plant tissue was analysed at the Institute of Tropical and Subtropical Crops under the Agricultural Research Council (ARC-ITSC) in Nelspruit, South Africa, using the wet digestion technique with 98% Sulphuric Acid and 30% Hydrogen Peroxide. The detection of nitrogen was based on the colorimetric method, (CHEMetrics, Inc) in which an emerald-green colour was formed by the reaction of ammonia, sodium salicylate, sodium nitroprusside and sodium hypochlorite (Grasshoff *et al.*, 1983). The ammonia-salicylate complex was read at 640 nm for nitrogen detection. The colorimetric method has been widely used for nutrient determination in terrestrial plants, agricultural and seawater analysis (Boltz, 1978; Giron, 1973; Grasshoff *et al.*, 1983; Koroleff, 1983; Norton *et al.*, 1987; Sapan *et al.*, 1999). Since the technique uses fewer samples and is less time-consuming than the standard Kjeldahl method, it is frequently used in many research laboratories (Sapan *et al.*, 1999). With the selection of a standard for the calibration that is representative of the population, the

colorimetric method provides accurate results, which are comparable to the Kjeldahl procedure (Sapan *et al.*, 1999).

9.2.2. Hyperspectral image acquisition and pre-processing

Hyperspectral imagery was acquired using the De Beers HYMAP MK1 scanner (originally called AMS scanner) on 18 March 2003. The De Beers diamond company (South Africa) commissioned the scanner from an Australian consortium consisting of Integrated Spectronics Ltd, CSIRO Division of Materials and Auspace. The system has three spectrometers covering the following wavelength regions:

500 nm-1100 nm visible to near infrared
1450 nm-1800 nm shortwave infrared 1
1950 nm-2450 nm shortwave infrared 2

Each spectrometer images 32 bands with approximately 15 nm bandwidths and is mounted on a zeiss stablised platform to minimise distortions due to pitch, yaw and roll of the aircraft during data collection. GPS and c-migits inertial navigation gyros were attached to the system to provide data for automated geometric correction. The De Beers Company processed the imagery and undertook the geometric and radiometric corrections. Atmospheric correction of the image was done using the ACORN (Atmospheric CORrection Now) model, a product of ImSpec LLC. The model uses the Modtran 4 radiative transfer model to calculate the effect of atmospheric gases as well as molecular and aerosol scattering on the spectra. These atmospheric characteristics are used to convert the calibrated sensor radiance measurements to apparent surface reflectance (Analytical and Imaging Geophysics, 2000). The term apparent surface reflectance is used to refer to the reflectance values derived mainly from the methods of radiative transfer calibration, which are not exact but show some residual atmospheric absorptions and scattering effects (Clark *et al.*, 1993). The acquired imagery had a pixel size of 4.2 x 4.2 meters.

9.3. Data analysis

9.3.1. Absorption features

Two known chemical absorption features were used for this study: the chlorophyll absorption features in the visible domain ($R_{550\ -\ 757}$), which have been found to be related to nitrogen concentration in both fresh standing canopies (Mutanga *et al.*, In review) and dried ground plant material (Curran *et al.*, 2001); and the shortwave absorption feature ($R_{2006–2196}$) which has been found to be strongly related to N concentration (Curran *et al.*, 2001; Kokaly & Clark, 1999). Compared to other absorption features used for estimating N concentration in *situ*, Mutanga & Skidmore, (2003) showed that the two absorption features selected for this study contained more information on foliar

quality. The other important absorption feature ($R_{1634\text{-}1786}$) was not used due to excessive instrument noise.

Continuum removal was applied to the selected absorption features. Continuum removal normalises reflectance spectra in order to allow comparison of individual absorption features from a common baseline. The continuum is a convex hull fitted over the top of a spectrum utilising straight-line segments that connect local spectral maxima. The convex hull can be considered as the shape that a rubber band would attain if it were stretched over the reflectance spectrum. This means that the convex hull will be in contact with the reflectance spectrum at maximum reflectance points such as the red edge shoulder (Mutanga *et al.*, 2004). Since we were interested in isolating specific absorption features in this study, we defined local start and endpoints on a particular absorption feature as defined above. Linear continua were fitted between the start and endpoints of the absorption features and then continuum removal was applied.

The continuum-removed reflectance $R'_{(\lambda)}$ is obtained by dividing the reflectance value $R_{(\lambda)}$ for each waveband in the absorption pit by the reflectance level of the continuum line (convex hull) $Rc_{(\lambda)}$ at the corresponding wavelength:

$$R'_{(\lambda i)} = \frac{R_{(\lambda i)}}{R_{c(\lambda i)}} \quad (1)$$

The first and last spectral data values are on the hull and therefore the first and last values of the continuum-removed spectrum are equal to 1. The output curves have values between 0 and 1, in which the absorption pits are enhanced (Schmidt & Skidmore, 2003). Continuum removal enhances bands by correcting for apparent shifts in the band minimum caused by wavelength-dependent scattering that imparts a slope to the spectrum. Removal of the continuum slope corrects the band minimum to that of the true band centre (Clark & Roush, 1984).

Continuum removal has proved useful in mapping the distribution of minerals by comparing remotely sensed absorption band shapes with those in a reference library (Clark & Roush, 1984). Efforts to apply the method in vegetation science have been made using dried plant material in the laboratory (Kokaly, 2001; Kokaly & Clark, 1999). This method has not to our knowledge been extended to canopies *in situ* for nitrogen concentration mapping.

Previous studies in both geological and vegetation science have calculated several parameters from the continuum-removed absorption features (Clark & Roush, 1984; Kokaly, 1999; Mutanga & Skidmore, 2003). In this study, we used the band depth, which is computationally efficient and therefore suitable for practical applications.

Band depth (BD) was calculated by subtracting the continuum-removed reflectance $R'_{(\lambda i)}$ from 1. Stated formally:

$$BD_{(\lambda i)} = 1 - R'_{(\lambda i)} \quad (2)$$

Where $R'_{(\lambda i)}$ is the continuum-removed reflectance at wavelength *i*.

Figure 9.1 shows band depths of the two absorption features following continuum removal. The band depths were calculated using extracted image spectra corresponding to the x,y centre coordinates of the field sample points (44 samples). Each image spectrum was extracted from a single pixel.

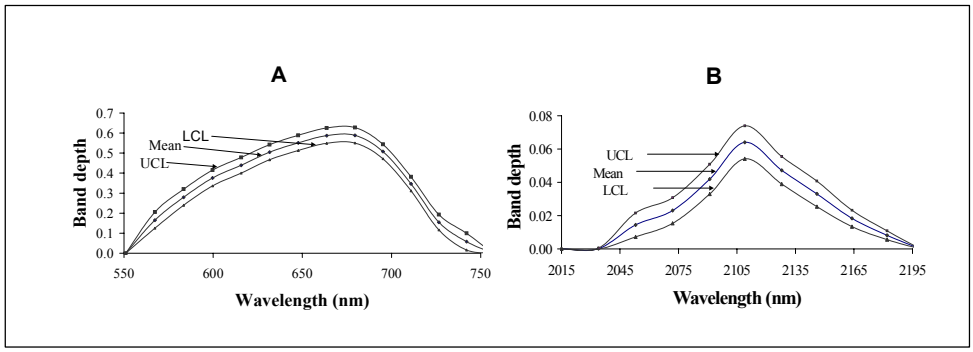

Figure 9.1. Continuum-removed absorption features located in the visible (A) and the SWIR (B), inverted to band depths. The means are flanked by the upper (UCL) and lower (LCL) 95 % confidence limits. The image spectra corresponding to the x,y centre coordinates of the field sample points (44 samples) were extracted and analysed.

The two absorption features used in this study had a total of 25 bands. The first and last wavebands of each absorption feature were removed since they all had values of 1 after continuum removal. Therefore 21 bands were used for further analysis. Figure 9.2 shows a band depth image at 679 nm.

9.3.2. The red edge position

The red edge position (REP) was also calculated as an input into the neural network. The REP is the point of maximum slope in vegetation reflectance spectra (Fillella & Penuelas, 1994) that occurs in the 680 – 750 nm region. This phenomenon is caused by strong chlorophyll absorption in the red and canopy scattering in the near infrared (Dawson & Curran, 1998). As a result of a strong relationship between chlorophyll and foliar nitrogen concentration (Penuelas *et al.*, 1994) the REP has been successfully related to nitrogen concentration in plants (Clevers & Buker, 1991;Mutanga *et al.*, In review). The REP was therefore used as an input variable to map nitrogen concentration in this study.

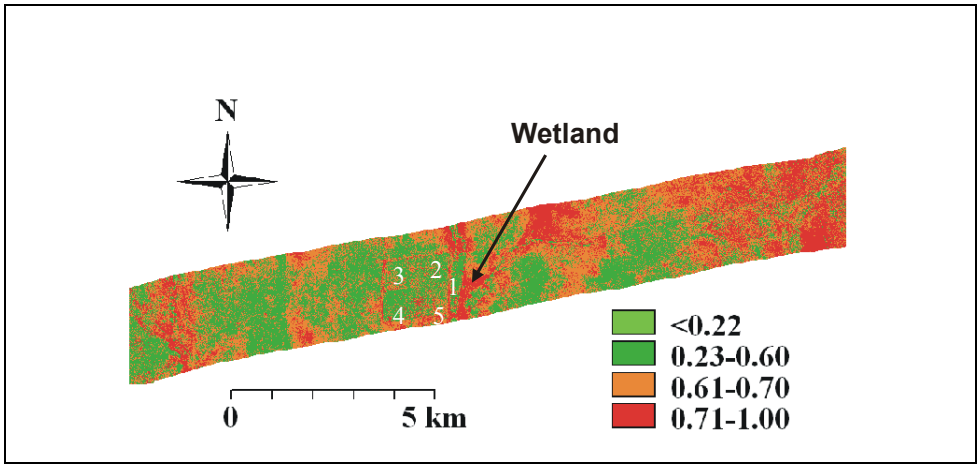

Figure 9.2. Band depth at 679 nm. The 679 nm waveband was selected for illustration since it was considered to be the centre of the $R_{550\text{-}557}$ absorption feature. Numbers 1-5 represent blocks in the roan antelope camp, a fenced area to conserve roan antelopes. The image was sliced for clarity.

The linear method was used to calculate the red edge position (Guyot & Baret, 1988). Clevers & Jongschaap (2001) successfully tested the technique against the other interpolation techniques. The linear interpolation assumes that the reflectance at the red edge can be simplified to a straight line centred around a midpoint between the reflectance in the NIR at 780 nm (788 nm for the censor used in this study) and the reflectance minimum of the chlorophyll absorption feature at about 670 nm (663 nm for the sensor used in this study). The procedure is as follows: First, the reflectance value at the inflection point is estimated (equation 3). Second, linear interpolation between the measurements at 695 nm and 742 nm is applied to estimate the wavelength corresponding to the estimated reflectance at the inflection point (equation 4). Formally stated:

Calculating the reflectance value at the inflection point (R_{re})

$$(R_{re}) = (R_{663} + R_{788})/2 \quad (3)$$

Calculating the red edge position

$$\lambda_{re} = 695 + 47\left[\frac{(R_{re} - R_{695})}{(R_{742} - R_{695})}\right] \quad (4)$$

Where R_{663}, R_{695}, R_{742} and R_{788} are the reflectance values at 663, 695, 742 and 788 nm respectively. The value 695 refers to wavelength position belonging to R_{695}. The value 47 refers to the wavelength interval between 695 nm and 742 nm. Figure 9.3 shows the calculated REP.

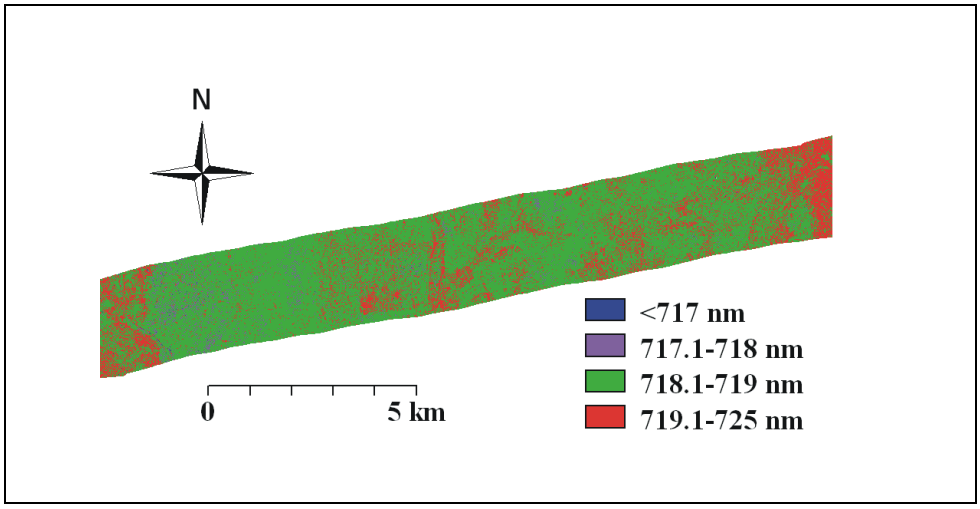

Figure 9.3. The red edge position as calculated using the linear method (Guyot and Baret, 1988). Wavelength positions were sliced into four classes for clarity

9.3.3. The neural network algorithm

An artificial neural network was used to map nitrogen concentration in grass using the band depth of absorption features as well as the REP. Neural networks are essentially learning systems consisting of interconnected networks of simple processing elements (Atkinson & Tatnall, 1997). They have powerful pattern recognition capabilities that enable them to learn to represent complex multivariate data patterns (Carling, 1992). Neural networks can perform more accurately than other statistical techniques, particularly when the feature space is complex and the source data has different statistical distributions (Atkinson & Tatnall, 1997).

In vegetation science, neural networks have been mainly used for land cover classifications (Bischof *et al.*, 1992; Civco, 1993; Hepner *et al.*, 1989; Zhang *et al.*, 1997), forest classifications (Ardo *et al.*, 1997; Skidmore *et al.*, 1997a) and wildlife habitat classifications (Liu *et al.*, 2002). Only a handful of studies have applied the technique to estimate continuous vegetation variables such as biomass or canopy density (Boyd, 2002; Smith, 1993), and none to our knowledge have applied it to map nitrogen concentration using hyperspectral data.

The back-propagation algorithm was used in a three-layer network consisting of an input, hidden and output layer. Figure 9.4 shows an example of the structure of a neural network.

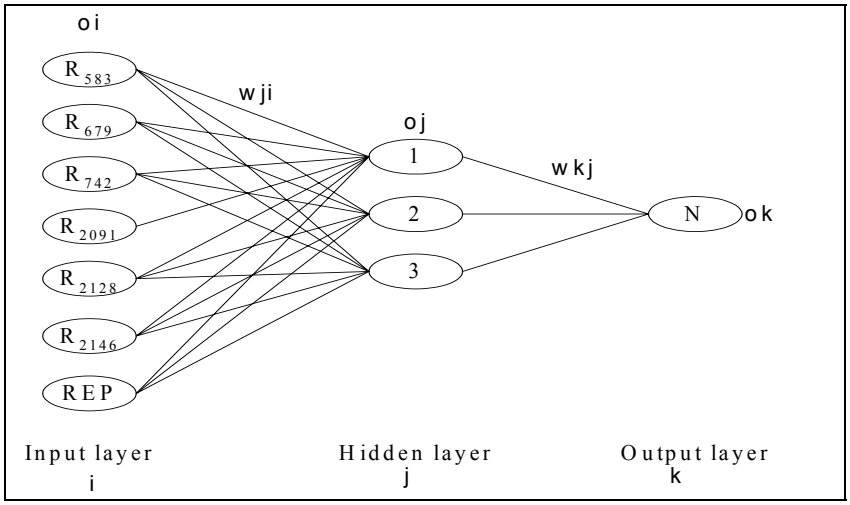

Figure 9.4. The neural network structure. The input layer (oi) consists of selected band depth variables as well as the red edge position (REP). The inputs are connected to hidden nodes (oj), which are in turn connected to the output layer (ok). Wji and wkj refer to the weights between the input layer and the hidden nodes and between the hidden nodes and the output layer respectively.

This algorithm was used because of its frequent use in many studies and it is generally applicable (Foody, 1995; Skidmore *et al.*, 1997a). The back-propagation algorithm is designed to minimise the root mean square error between the actual output of a multi-layered feed forward perception and the desired output (Skidmore *et al.*, 1997a). The following description of a network follows Skidmore *et al*., (1997a).

The algorithm can be divided into a feed forward phase and a back-propagation phase. The feed forward phase commences with input data values. In this case selected band depths (o_i) for a grid cell are being presented to a node of the neural network and multiplied by a weight factor (w_{ji}). The products are summed to produce a value z_j for the jth layer.

Stated formally:

$$z_j = \sum_j w_{ji} \times o_i \tag{5}$$

For a three-layer network lettered i, j, k and k being the output layer, z_k is similarly calculated as equation 5. To add non–linearity to the network, the value z_j for each hidden node is passed through a sigmoidal activation function. The output from this function is

$$o_j = \frac{1}{1 + e^{-(z_j + \theta)/\theta_o}} \tag{6}$$

where z_j is defined in equation 5, θ is a threshold or bias, and θ_o is a constant.

The feedforward phase stops after the output value (o_k) has been calculated. The second phase involves the comparison of the target values (measured nitrogen values during the training of the network) and the calculated output node values. The system error is calculated as the difference between the target value (t_{jk}) as defined by the training area pairs and the output value (o_{jk}). This process represents one epoch (iteration) of the backpropagation algorithm. Error is reduced by back-propagating it from the output nodes to the hidden nodes and from the hidden nodes to the input nodes. Back-propagation of the error is achieved by changing the weights of each node during training. The iteration process stops after the system error declines to a pre-specified level or after achieving a user-defined number of epochs.

9.3.4. Selecting and preparing the input data set

Although the neural network applied in this study (i.e multiplayer perceptron) can learn to weight the significant variables and ignore less important ones (implying that in principle all available wavebands may be input to the network) (Boyd, 2002), we reduced the input data using a feature selection algorithm. Data reduction has the advantage of improving the performance of the neural network by reducing the processing time (Kavzoglu & Mather, 2002). The input variables from continuum-removed absorption features were reduced (Figure 9.4) through a sequential forward selection algorithm, an efficient and fast procedure for hyperspectral data (Kavzoglu & Mather, 2002; Pudil *et al.*, 1994). The selected band depth variables as well as the REP were input into the neural network.

In order to speed convergence to a minimum error (Skidmore *et al.*, 1997a) the nitrogen concentration data were normalised to a range between 0 and 1 using the following equation:

$$\left(\frac{\left(X_i - X_{\min} \right)}{X_{\max} - X_{\min}} \right) \tag{7}$$

where, X in this case is nitrogen concentration, X_{min} is the minimum value and X_{max} is the maximum value in the data set.

9.3.5 Preparing the neural network parameters

Predictive modelling of foliar N concentration using artificial neural networks involved a search of system parameters (i.e. number of epochs and the number of nodes) that can increase the accuracy of the model. The possible combination of system parameters is large, and there is little literature to guide an analyst about the optimal values at which to set these parameters. Testing for suitable network parameters with the data set is also important to avoid overtraining of the neural networks (Atkinson & Tatnall, 1997).

The total data set was randomly divided into two groups, one subset for training (30 samples) and the other subset for testing (14 samples). A number of experiments were executed. In each experiment, one neural network system parameter was varied while holding the other system parameters constant. A combination of parameters that could predict foliar N concentration (as assessed by the R^2 and RMSE between the measured and predicted N concentration) was ultimately applied to model the spatial distribution of grass nitrogen concentration in the study area.

9.4. Results

9.4.1 Variation in N concentration (Standard statistical analyses)

Table 9.1 shows the variation in foliar nitrogen concentration in the study area.

Table 9.1: Descriptive statistics of foliar nitrogen concentration used in this study. The 95 % confidence limit (CL) is shown.

Nutrient	Minimum	Mean	Maximum	CL of mean (95 %)
N	0.83	1.55	3.42	0.151

The variation is mainly due to a large range of grass species as well as varying landscape variables such as soil type, slope and human induced fires (McNaughton, 1988). The N concentration data was tested for normality using the Kolmogorov-Smirnov test since normality is often a pre-requisite for certain statistical techniques. Parametric statistical tests are powerful but they are more efficient if the data follow a normal distribution. If the data are not normally distributed, then the less powerful but more robust non-parametric statistics should be used (Siegal & Castellan, 1988). We tested the null hypothesis that the data under test follow a normal distribution versus the alternate hypothesis that the data under test do not follow a normal distribution. Stated formally*:* Ho: $p>0.05$ versus the alternate hypothesis Ha: $p<0.05$, where p is the probability of normality from the Kolmogorov-Smirnov test. Results of this test showed that the data is normally distributed $p>0.05$. Therefore, in cases where statistical analysis was required in this study, we used parametric methods.

9.4.2 Selecting the neural network parameters

Figure 9.5 shows results of an experiment testing the effect of using an increasing number of epochs on system error, the training correlation coefficient as well as test correlation coefficient between the measured and predicted N concentration.

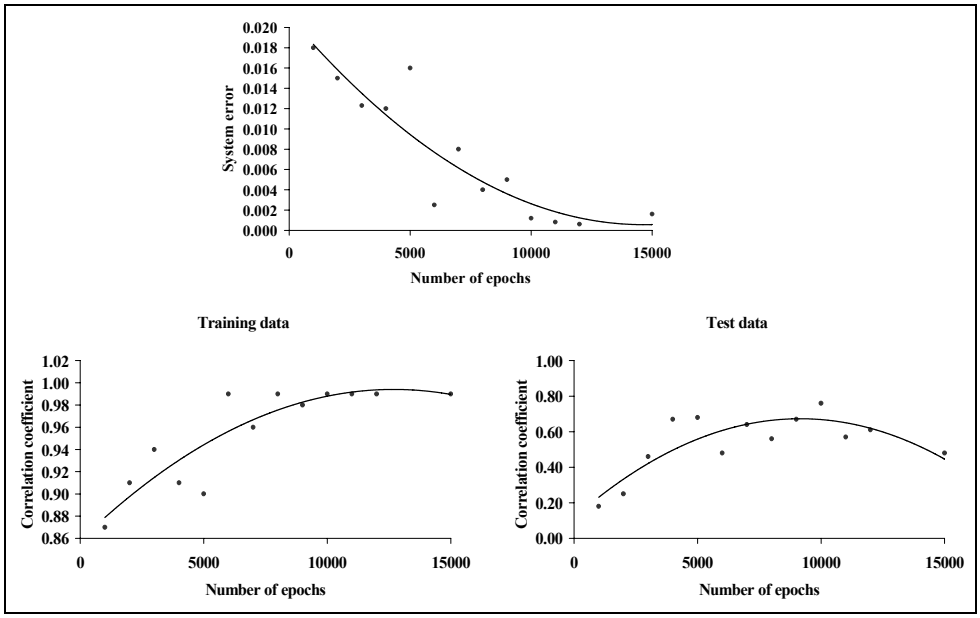

Figure 9.5. Number of epochs versus system error and number of epochs versus correlation coefficients for the training as well as the test data sets

The system error decreases as the number of epochs increases, while the correlation coefficient for the training data increases as the number of iterations increases. The system error as well as the correlation coefficient on the training data tends to become asymptotic around 10000 epochs. The correlation coefficient on the test data set increases with increasing number of epochs up to a threshold, beyond which it begins to decrease. The threshold indicates the point at which overtraining of the neural network commences. Overtraining occurs when the neural network memorizes specifics of the training data but is not able to generalize when applied to a different data set (Atkinson & Tatnall, 1997; Skidmore *et al.*, 1997a). In this experiment, the correlation coefficient for the training data continued to increase but the correlation coefficient for the test data began to decrease after 10000 epochs indicating the point at which the system was failing to generalize.

As shown in Figure 9.5, the system error is inversely correlated with the training accuracy (correlation coefficient of –0.97 at $p<0.0001$). The system error is also inversely correlated with the test accuracy, but the relationship is weak (correlation coefficient of –0.47 at $p< 0.09$). This result confirms that of Skidmore et al, (1997) who concluded that the system error is highly correlated with training accuracy because the training data are iteratively used to reduce system error. However the system error is not significantly correlated to the test

accuracy, therefore system error should not be used as the only criterion for assessing mapping capability of the neural network.

We also tested the effect of increasing the number of nodes on the performance of the neural network. In general, the larger the number of nodes in the hidden layer, the better the neural network is able to represent the training data, however at the expense of the ability to generalize (Atkinson & Tatnall, 1997). Figure 9.6 shows that the correlation coefficient for the training data is consistently high with an increase in the number of nodes. However the correlation coefficient for the test data increased up to 6 nodes, and then began to decline with some fluctuations.

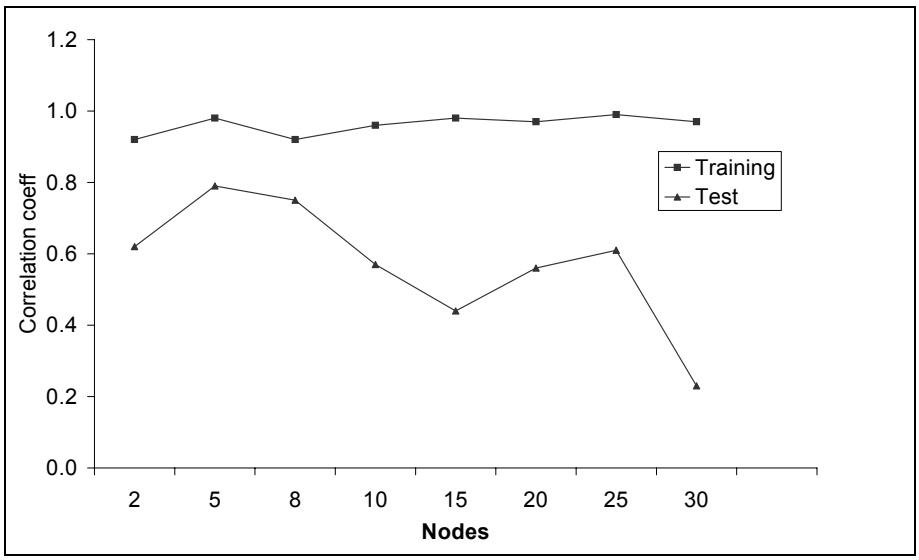

Figure 9.6. Number of nodes versus correlation coefficients for the training as well as test data sets

Table 9.2 shows the input parameters that were used for mapping nitrogen concentration.

Table 9.2. Parameters for the trained neural network used for mapping nitrogen

Parameter	Value
Number of inputs	7
Number of outputs	1
Number of layers	3
Number of nodes	6
Learning rate	0.7
Momentum	0.7
Number of epochs	10000

9.4.3. Training, testing and applying the network to map N distribution

The neural network parameters presented in Table 9.2 were used in training the neural network. The training process was run 5 times with random initial weights (Zhang *et al.*, 2002). The prediction capability of the neural network to map N concentration was assessed using the correlation coefficient as well as the RMSE. The network that yielded the highest correlation coefficient as well as the lowest RMSE between the measured and predicted nitrogen concentration on the independent test data set was retained for mapping nitrogen concentration. Figure 9.7 shows a scatter plot of the predicted and measured nitrogen concentration using the best-retained neural network.

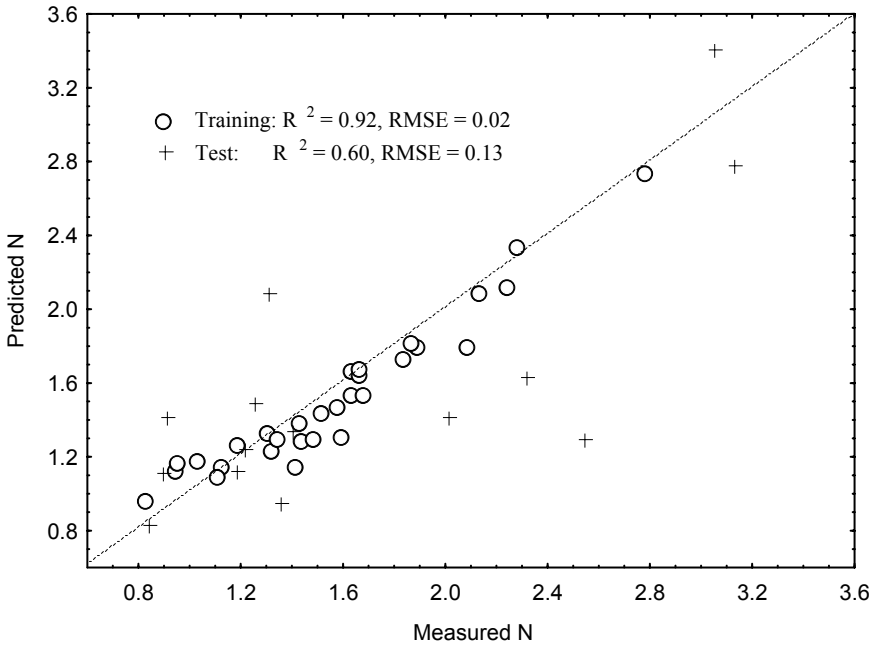

Figure 9.7. Scatterplot obtained from the best-trained neural network that was subsequently used for mapping

The retained neural network was applied on the study area to map nitrogen concentration using the selected image layers. Since the input data had been scaled to values between 0 and 1, the output nitrogen map from the neural network had a value range between 0 and 1. To transform the values to the actual nitrogen concentration (%), we used the inverse of equation 7. Figure 9.8 shows the continuous nitrogen map produced by the neural network.

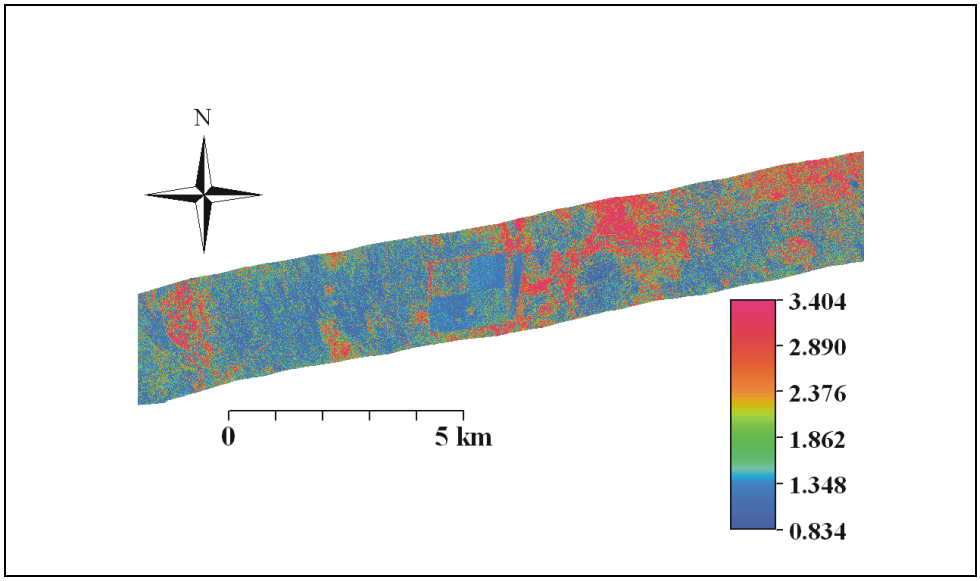

Figure 9.8. Spatial distribution of nitrogen concentration (%) using the integrated approach

The same map was sliced into 4 classes for better visualisation as shown in Figure 9.9.

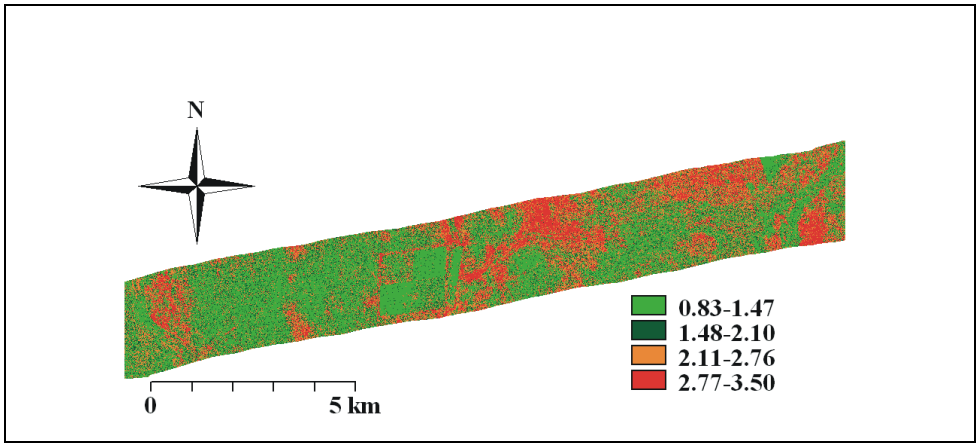

Figure 9.9. Spatial distribution of nitrogen concentration (%) using the integrated approach. The continuous map in Figure 9.8 was sliced for better visualisation

9.4.4. Comparison between neural networks and multiple linear regression

The performance of the neural network in mapping savanna grass quality was compared with that of stepwise linear regression using the two absorption features as well as the REP. A total of five variables were selected (REP, 583 nm, 2128 nm, 679 nm and 647 nm), largely similar to the bands used in neural networks. Table 9.3 shows results obtained from multiple linear regression as well as those yielded by the neural network.

Table 9.3. Comparison between multiple linear regression and Neural networks

	Multiple Linear regression		Neural networks	
	Training	Test	Training	Test
Nitrogen				
Correlation coefficient (r)	0.78	0.62	0.96	0.77
Coefficient of determination (r^2)	0.61	0.38	0.92	0.60
RMSE	0.05	0.16	0.02	0.13

Neural networks yielded a higher r^2 as compared to the linear regression results on the independent test data set. The prediction capabilities of the regression model and the neural network were also measured using the RMSE. The RMSE between the predicted and measured nitrogen concentration using neural networks on the independent test data is lower than that obtained using a regression.

9.5 Discussion

The distribution of tropical grass quality is pre-requisite to an understanding of the movement and feeding patterns of mammalian grazers. Traditionally, ecologists have estimated grass quality based on random field points scattered across the landscape. In this regard, estimates of grass quality have not been spatially explicit, thereby making spatially explicit rangeland management decisions imprecise. The results from this study are discussed in two main sections (i) the utility of the integrated approach to mapping nitrogen in savanna rangelands and (ii) an explanation of the foliar nitrogen patterns revealed on the map.

9.5.1 Utility of the integrated approach to mapping foliar nitrogen concentration

This study has demonstrated that hyperspectral data in combination with artificial neural networks has potential to map tropical grass quality. Using band depth variables as well as the REP in a neural network yielded an R^2 of 0.60 with a RMSE of 0.13 between the predicted and measured foliar N

concentration on an independent test data set. Considering that data were collected using an airborne sensor, this study has shown that there is potential to use imaging spectrometry to map nitrogen concentration in tropical rangelands. This can be attributed to the integration of continuum removal, the REP and neural networks. Continuum removal enhances differences in absorption strength thereby increasing the potential to discriminate between different levels of foliar nutrients. This confirms previous studies that have successfully applied the method in vegetation science. For example, Mutanga *et al*., (2003) demonstrated that the separability of grass grown under different nitrogen treatments was greater using continuum-removed spectra than absolute reflectance. In a study on spectral discrimination of vegetation types in the coastal wetland of the Netherlands, Schmidt & Skidmore (2003) could increase the number of pairs of vegetation types that were statistically different using continuum removal as compared to absolute reflectance. In addition, Kokaly *et al.* (2003) successfully applied spectral feature analysis of continuum-removed plant absorption features to discriminate the species composition of in situ forest stands.

The addition of the red edge position is also significant. The REP has been widely used to estimate chlorophyll concentration (Clevers, 1999; Curran *et al.*, 1990; Curran *et al.*, 1991; Jago *et al.*, 1999). A strong pigment-nitrogen relationship in plants (Katz *et al.*, 1966; Penuelas *et al.*, 1994) has been well established, therefore a relationship between nitrogen concentration and the red edge is expected (Clevers & Buker, 1991). A sensitivity analysis of the variables used in the neural networks showed that the REP was ranked the second most important variable in the neural networks (Table 9.4). This indicates the relative importance of the REP in modelling foliar nitrogen concentration.

Table 9.4. Sensitivity analysis of the variables used in the neural network. Values in the ratio column were calculated as follows. For each variable, the network is executed as if that variable is unavailable. Next, the error obtained when the variable is unavailable is divided by the error obtained when the variable is available. Important variables have a high ratio, indicating that the network performance deteriorates badly if they are not present.

Rank	Variable	Ratio
1	2128	1.33
2	REP	1.23
3	679	1.17
4	2146	1.16
5	710	1.10
6	2091	1.07
7	583	1.06

The neural network algorithm has a capability to model the non-linear transfer functions that may not be known or cannot be approximated (Boyd, 2002) for mixed species environments of Southern Africa. Compared with multiple linear regression, neural networks yielded a smaller RMSE between the predicted and measured nitrogen concentrations. Therefore, the combination of hyperspectral data and neural networks facilitated the mapping of foliar nitrogen concentration in a savanna rangeland.

9.5.2 An explanation of the foliar-nutrient patterns revealed

Although the area mapped is underlain by relatively homogeneous basalt formations, there are undoubtedly spatial variations in foliar nitrogen concentration as depicted in the final map. The nitrogen map (Figure 9.9) shows high nitrogen concentration in the wetland area (Figure 9.2) and the eastern part. Wetland areas are characterised by clay soils that are rich in nutrient concentration therefore support grasses of high quality. However, it should be noted that wetlands support high quality grass as long as the soil is moist (i.e during and soon after the rainy season) thereby facilitating extraction of nutrients from the soil. Since the image was taken soon after the rainy season in March 2003, and there was no dry spell during this period, the grass had high nitrogen concentration. In addition, nutrient-rich grass species such as *S. ioclados* are usually found in the wetland areas. The eastern part is also dominated by grass species such as *U. mosambicensis* that have high nutrient concentrations as compared to the western parts that are dominated by relatively nutrient poor species such as *C. ciliaris* and *S. papphoroides* (Mutanga & Skidmore, 2003). We therefore infer that the spatial variation of species characterised by different levels of nutrients do influence the variation of nitrogen in savanna rangelands.

The Roan Camp enclosure on the output map also shows some differences in nitrogen concentration between different blocks (divided by roads) shown in Figure 9.2. The Roan Camp is a fenced area in the Kruger National Park (2 km * 2 km) for protecting roan antelopes from predators. Blocks 3 and 5 were burned during the season prior to image acquisition and the other blocks were not burnt. From the field samples, the burnt blocks show high foliar nitrogen concentration. Figure 9.10 shows the spatial distribution of foliar nitrogen concentration in the burnt (block 3) and unburnt (Block 4) blocks as mapped by the integrated approach applied in this study, as well as box plots of the measured foliar N concentration in the blocks.

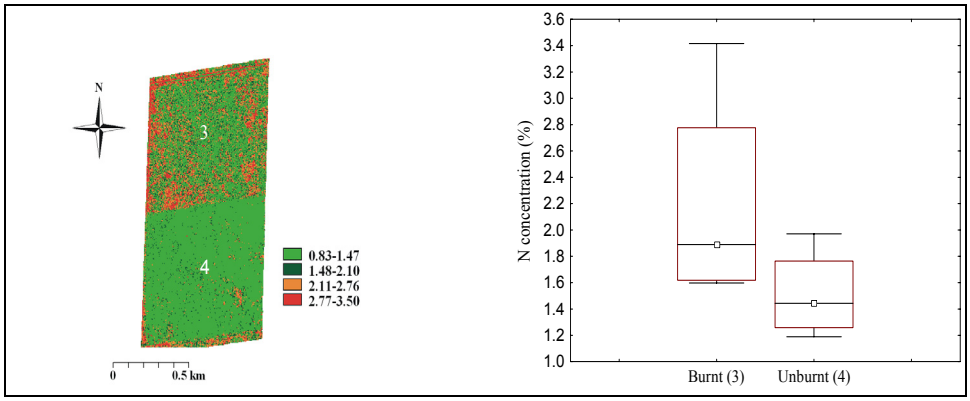

Figure 9.10. Percentage nitrogen distribution map and box plots showing the mean and spread of nitrogen concentration (%) in the burnt (Burnt (3)) and unburnt blocks (Unburnt (4)) of the Roan camp.

We tested whether the foliar nitrogen concentration in the burnt and unburnt blocks were significantly different. Results of T-test indicate that there is a statistically significant difference between the two blocks ($p < 0.05$). The phenomenon of high foliar nutrient concentration in post fire re-growth is well established in ecological literature (Christensen, 1977; Cook, 1994; Frost & Robertson, 1987). High nutrient concentration in burnt areas is primarily due to rejuvenation of plant material, distribution of similar amounts of nutrients over less above-ground biomass and change in plant tissue composition (i.e. higher leaf: stem ratios with leaves having higher nutrient concentration) (Boerner, 1982; Van de Vijver, 1999).

In summary, the technique applied in this study seemed to unveil spatial patterns of nitrogen concentration in the northern basalt plains of the Kruger National Park.

9.6 Conclusions

This study has applied an integrated approach to mapping foliar nitrogen concentration in an African savanna. Two continuum-removed absorption features located in the visible and the SWIR regions as well as the REP were used as input to the neural network algorithm. The following conclusions can be drawn from this study:

1. The new integrated approach (continuum-removed absorption features, the REP and a neural network) could explain 60 % of the variation in savanna grass nitrogen concentration on an independent test data set using airborne hyperspectral data,

2. The airborne sensor data could predict canopy nitrogen concentration with a rms error of 0.13 (± 8.30% of the mean observed nitrogen concentration) on an independent test data set,
3. Neural networks performed better than the traditional multiple linear regression analysis in predicting savanna grass quality; and,
4. Foliar nitrogen concentration in the re-growth of grass from fires of the previous season was successfully mapped in the roan antelope camp.

Overall, the utility of the new integrated approach to mapping foliar nutrient concentration in an African savanna has been demonstrated. This is an important step towards understanding the movement and distribution of wildlife. We recommend that future studies should focus on monitoring seasonal changes in foliar nutrient concentration using imaging spectrometry as well as extending the method to predict other macro nutrients (P, K, Na, Mg, Ca) in both grass and tree canopies. An improvement on the spectral resolution of the sensors and the development of algorithms that can remove the effect of water in the SWIR could further improve the prediction and mapping of foliar nutrients in African rangelands.

Acknowledgements

This study was carried out with the financial assistance of the International Institute for Geoinformation Science and Earth Observation (ITC). ITC funded the image acquisition from the De Beers company (South Africa). We would like to thank the scientific Board of the Kruger national Park for allowing us to carry out our study under excellent conditions. We extend our gratitude to Rina Grant, Mike Peel for organizing logistics in the field. We are also largely indebted to Henk van Oosten for his help in programming the neural network algorithm in IDL (Interactive data language).

CHAPTER 10:
Tropical grasses and hyperspectral remote sensing
A synthesis

10.1 Introduction

Why do we need to measure the quantity and quality of tropical grasses? Research in ecology has revealed that, both the quantity (biomass) and quality (the foliar concentration of nitrogen, phosphorous, calcium, magnesium, potassium and sodium) of grass are important factors influencing the feeding patterns and distribution of wildlife and livestock in savanna rangelands (Drent & Prins, 1987; McNaughton, 1990; McNaughton & Banyikwa, 1995; Prins, 1989; Prins, 1996). Therefore, mapping the quantity and quality of tropical grasses is critical for understanding wildlife distribution patterns. In this regard, remote sensing has offered possibilities to accomplish this task.

However, two critical problems have limited the application of remote sensing to map the quantity and quality of tropical grasses. Firstly, the use of remotely sensed indices such as NDVI has been bedevilled by the saturation problem at high canopy density. In other words, the widely used vegetation indices asymptotically approach a saturation level after a certain biomass density or LAI (Gao *et al.*, 2000; Sellers, 1985; Thenkabail *et al.*, 2000; Todd *et al.*, 1998; Tucker, 1977), thus yielding poor estimates of biomass during the peak of seasons. Secondly, the methods developed in the laboratory for the estimation of quality from remote sensing have had limited success when applied under outside or field conditions. This is mainly because; the presence of water in fresh canopies masks the biochemical absorption features, particularly in the shortwave infrared (Clevers, 1999; Kokaly & Clark, 1999) and make the remote sensing of foliar biochemicals more difficult. In addition, leaf orientation and soil background effects, as well as atmospheric absorption, further complicate the remote sensing of biochemicals at field level (Asner *et al.*, 2000). As a result, the extension of the laboratory-based spectrometry to canopy level has yielded inconsistent results so far. The challenge is therefore to develop techniques that can predict foliar quality at canopy level.

In this thesis, the objectives were: (1) to investigate the potential of hyperspectral remote sensing in solving the saturation problem when estimating biomass of tropical grasses at high canopy density, and, (2) to develop techniques to reliably estimate and map the quality of tropical grasses at canopy level using hyperspectral remote sensing, under both laboratory and field conditions (both ground and airborne spectrometry).

10.2 Overcoming the saturation problem in biomass estimation

The saturation problem (Figure 10.1) was addressed in this thesis (chapter 2) by evaluating the potential of narrow band vegetation indices in characterising the biomass of *C. ciliaris* grass measured at high canopy density.

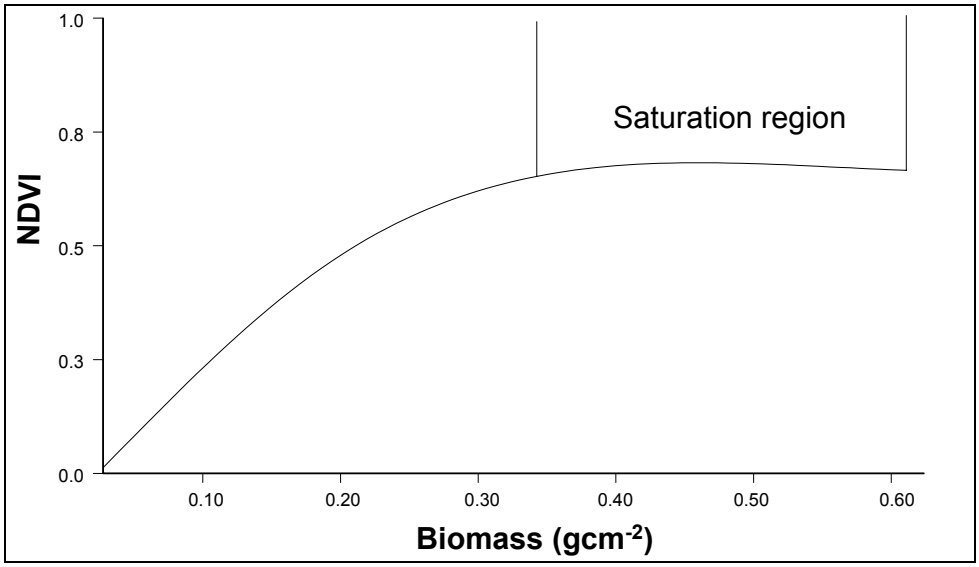

Figure 10.1 Relationship between NDVI and biomass. The saturation level is usually reached at about 0.3 g cm $^{-2}$

The utility of the widely used vegetation indices, particularly NDVIs involving all possible two band combinations between 350 nm and 2500 nm were tested. The narrow band hyperspectral data contained in 647 discrete channels allowed the computation of 418,609 narrow band NDVIs for biomass estimation. Results of this analysis are presented in form of R^2 for each λ_1 (350 nm to 2500 nm) and λ_2 (350 nm to 2500 nm) pair, in Figure 10.2.

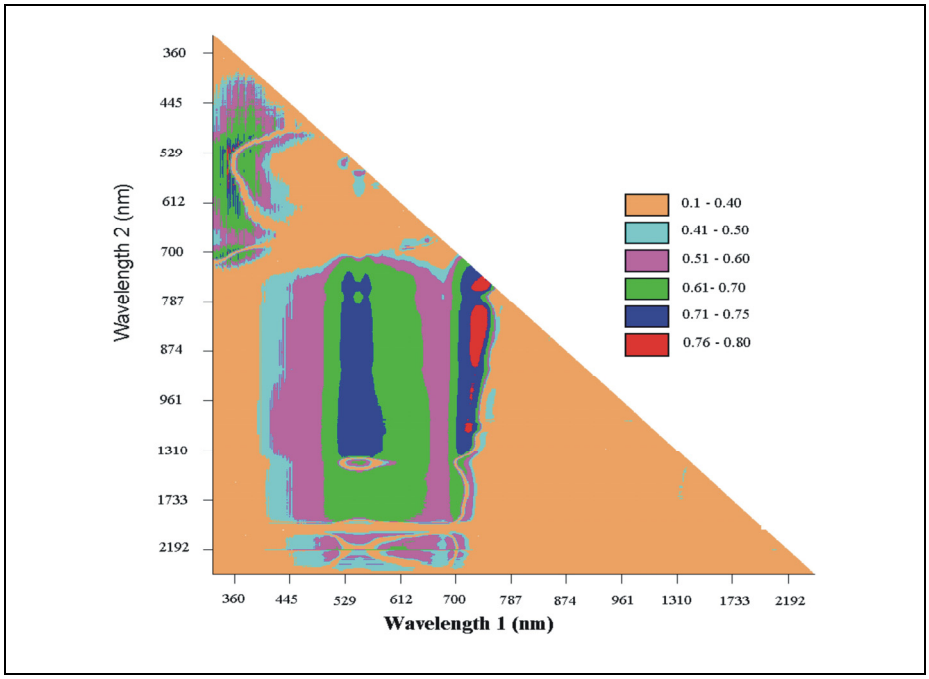

Figure 10.2. Map showing the correlation coefficients (R^2) between biomass and narrow band NDVI values calculated from all possible combinations spread across λ_1 (350 nm to 2500 nm) and λ_2 (350 nm to 2500 nm)

This study has shown that biomass information is not only contained in the red absorption trough and near infrared wavelengths. Most narrow bands selected by the indices (Normalized Difference Vegetation Index, Transformed Vegetation Index, Simple Ratio) that yielded the highest correlation with biomass are located in the red edge slope as shown in Figure 10.2. Figure 10.3 shows that the modified NDVI (R_{755}-R_{746}/$R_{755+}R_{746}$) involving narrow bands located in the red edge yielded a higher correlation coefficient with biomass as compared to the standard NDVI (R_{833}-R_{680}/$R_{833+}R_{680}$).

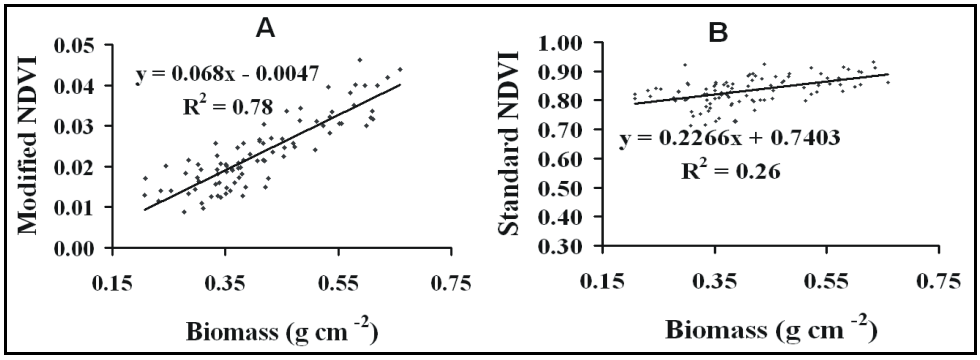

Figure 10.3. Relationship between biomass and the best-modified NDVI (A) calculated from 746 and 755 nm bands as well as the standard NDVI calculated from a near infrared (833 nm) and red band (680 nm) (B). Note the almost flat scatter plot in B (n = 96).

The red edge position also yielded a higher coefficient of determination with biomass as compared to the standard NDVI. In summary, the key finding in this chapter is that, at high canopy density, grass biomass may be more accurately estimated by vegetation indices based on narrow wavelengths located in the red edge slope than the standard NDVI involving bands located in the near infrared and the red absorption trough. The results in this study show that techniques for remotely estimating biomass have been steadily improved by using the full information content of hyperspectral data, calibration as well as improved field sampling techniques. In other words, the early results with red edge and vegetation indices have been refined to a point where biomass can be reliably estimated, including in areas of high grass canopy density.

10.3 Quality under controlled laboratory conditions

We assessed the potential to discriminate differences in nitrogen concentration using high-resolution reflectance by growing *C. ciliaris* grass with different fertilization treatments in a greenhouse. We measured canopy reflectance under controlled laboratory conditions. We found out that canopy reflectance can be used to discriminate differences in foliar nitrogen concentration in specific wavelength regions. Of particular importance is the widening and deepening of the red absorption feature ($R_{550\text{-}750}$) with an increase in nitrogen supply (chapter 3) - an important finding for using the visible absorption feature (where the influence of foliar water content on reflectance is minimal) to estimate grass quality.

We also revealed that transformation by continuum removal increased the separability of grass with different levels of nitrogen in the visible absorption feature (Figure 10.4). This result permitted the development of continuum-removed absorption feature variables, which were used to predict grass quality.

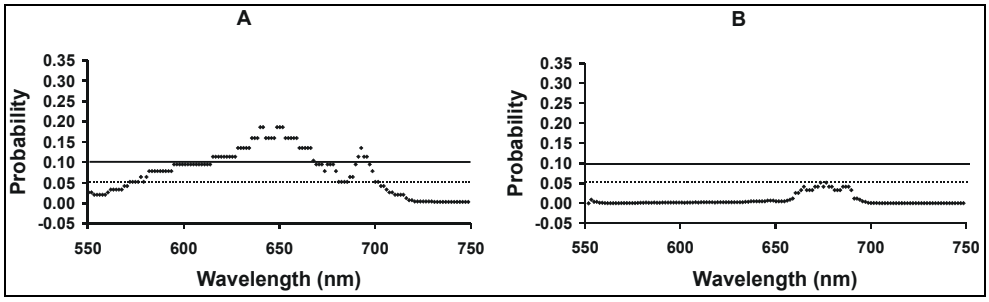

Figure 10.4. Results of One-way ANOVA showing wavelengths where reflectance differences between the treatments are significant for, (A) the original spectra and (B), continuum removed spectra in the $R_{550\text{-}750}$ absorption feature. Horizontal dashed and solid lines show 95% and 90% confidence limits, respectively. Note that the number of significant wavelengths in the $R_{550\text{-}750}$ absorption feature increased after continuum removal.

As shown in Figure 10.5, the experiment under controlled laboratory conditions also showed that there is a significant shift in the position of the red edge to longer wavelengths with an increase in nitrogen concentration at canopy level (chapter 4). The red edge position was significantly correlated to nitrogen concentration - an interesting result for the remote sensing of foliar chemistry in rangelands.

Observations made using a finer resolution GER 3700 data were also made using the degraded HYMAP data. Canonical functions (through canonical variate analysis) derived from continuum-removed red absorption feature, in combination with the red edge position (resampled to HYMAP resolution) could discriminate between the treatment groups containing different foliar nitrogen concentrations (chapter 5). This result permitted the extension of laboratory experiments to airborne hyperspectral images for mapping the concentration of nutrients (quality) in tropical grasses. The canonical structure matrix (Table 10.1) also revealed that greater discrimination power is contained in the red edge slope.

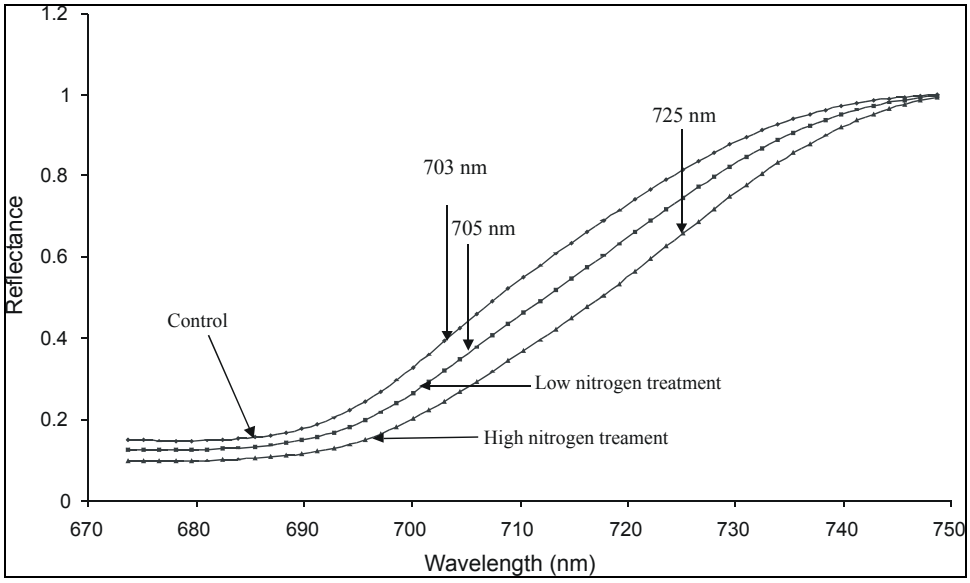

Figure 10.5. Continuum removed, mean canopy reflectance spectra of *C. ciliaris* grass by treatment. The red edge positions (703 nm, 705 nm and 725 nm) for each treatment are shown. There is red edge position shift to longer wavelengths with an increase in nitrogen concentration. The red edge positions for each treatment are shown. The low N treatment shows two peaks, at 705 nm and at 725 nm.

Table 10.1: Factor structure matrix representing the correlation between wavelengths and the canonical functions. The reflectance from GER 3700 was resampled to HYMAP spectra and continuum removal was applied on the $R_{550\text{-}757}$ absorption feature. The red edge position (REP) was calculated using the linear interpolation method. These variables were used in canonical variate analysis to discriminate groups of C. ciliaris grass containing different levels of nitrogen concentration.

	Root 1	Root 2
Eigenvalues	4.6576 (95%)	0.2672 (100%)
REP	**-0.708376**	0.255207
567	0.670072	-0.191510
583	0.619955	-0.095898
599	0.594963	-0.053645
615	0.568852	-0.033682
631	0.537990	-0.016494
647	0.496565	-0.027894
663	0.417850	-0.054934
679	0.368828	-0.092437
695	0.558773	-0.037651
710	**0.723892**	-0.069436
726	**0.743228**	-0.220834
742	**0.706960**	-0.359094

In summary, the experiments revealed that there is a strong relationship between spectral reflectance and foliar nitrogen concentration at canopy scale. Transformation of absorption features by continuum removal as well as an analysis of the red edge provides more information on foliar biochemical concentration. These observations were tested and further developed under natural environmental conditions using field data collected in the Kruger National Park, South Africa.

10.4 Quality at field level

Although remote sensing techniques have proved useful for assessing the concentration of foliar biochemicals under controlled laboratory conditions, more investigation is required to assess their capabilities at field level, where inconsistent results have been obtained so far. Building on the observations that we made under controlled laboratory conditions, we developed and improved on a new approach to quantify the biochemical concentration of tropical grasses in situ (chapter 6, and chapter 7). The new approach, analysis of continuum-removed absorption features, is superior to other techniques such as the conventional near infrared reflectance spectrometry (NIRS) in that:

1. there is concentration on known chemical absorption features, and therefore the problem of selecting non-causal bands in the prediction models is avoided (Curran *et al.*, 2001; Mutanga *et al.*, 2003);
2. the effect of over fitting, which usually occurs when more wavebands than samples are used is minimised by concentrating on fewer known absorption features (Curran *et al.*, 2001);
3. continuum removal enhances the absorption features (Mutanga *et al.*, 2003; Schmidt & Skidmore, 2003),and;
4. the normalisation procedure removes the overall albedo effects (Mutanga *et al.*, 2003; Schmidt & Skidmore, 2003).

We tested the utility of using four variables derived from continuum-removed absorption features for predicting canopy nitrogen, phosphorus, potassium, calcium and magnesium concentration: (i) continuum-removed derivative reflectance (CRDR), (ii) band depth (BD), (iii) band depth ratio (BDR) and (iv) normalised band depth index (NBDI). It was shown in this study (chapter 6) that stepwise regression on normalised bands calculated from continuum-removed reflectance spectra could explain the variation of *in situ* grass quality, with R^2 values ranging between 0.43 and 0.80 – an encouraging result under natural conditions. Low root mean square errors (RMSE) for an independent test data set were also obtained using the new variable, CRDR as compared to the other variables tested. Figure 10.6 shows an example of the predicted versus measured biochemicals, using randomly selected training and test data sets with CRDR data. Scatterplots between the measured and predicted biochemicals on the test data set are shown.

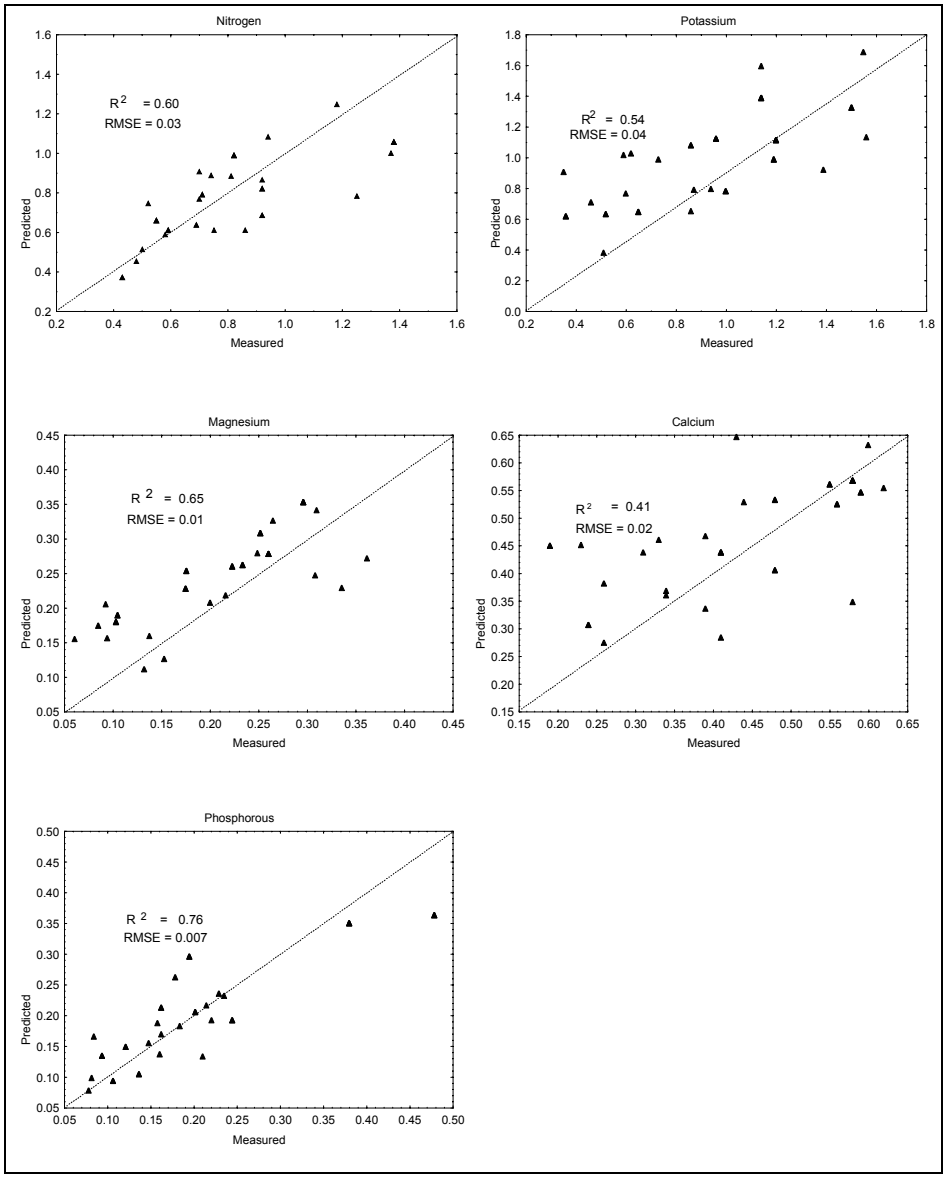

Figure 10.6: Measured versus predicted biochemicals for a randomly selected test data set (n = 24) using CRDR. Regression equations developed from the training data set (n = 72) were used to predict biochemicals on an independent test data set.

The message from this finding is that, we can reliably predict foliar quality using field spectrometry. The regression models built using field spectrometry are important for fast and efficient prediction of foliar biochemical concentrations in rangelands. In other words, the regression models can be applied on field reflectance spectra acquired at the same resolution and under

similar ecological conditions. This in turn, saves time spend in field data collection, as well as reducing costs on laboratory biochemical analysis. Rangeland management will therefore be done more efficiently by identifying grasses and patches with high quality nutrients or areas that require restoration.

To summarise, the successful prediction of quality using field spectrometry showed the potential application of the approach using airborne sensors. The experiment revealed the most informative absorption features (the major absorption feature in the visible ($R_{550 - 750}$) and the nitrogen absorption features ($R_{1634 - 1786}$ and $R_{2006-2196}$) in the shortwave infrared account for 69 % of the wavelengths selected by stepwise regression), which were later used for mapping quality using airborne sensors. Field spectrometry was therefore a step stone towards the mapping of grass quality as well as an important study to evaluate the potential of data collected using a field spectrometer in predicting tropical grass quality.

Another important finding in this study was that, prior partitioning of data into species classes increases the prediction capability of the method applied as compared to predicting biochemicals using data for all species combined. We attributed this to differences in the condition (biophysical and biochemical) of the various species thereby yielding different models. We also observed this in chapter 7, where there is a significant interaction between species and foliar sodium classes in influencing spectral reflectance (Figure 10.7).

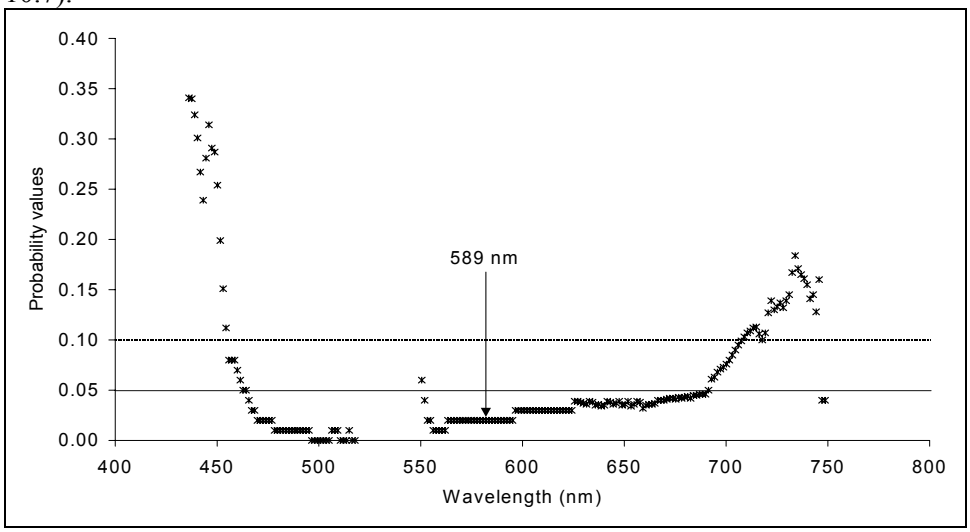

Figure 10.7 Results of two–way factorial ANOVA showing wavelengths where the interaction between sodium and species is significant in influencing reflectance in the visible domain. Horizontal dashed and solid lines show 95% and 90% confidence limits, respectively. Absorption spectrometry for sodium is done at 589 nm.

A solution for mapping biochemicals will therefore be to classify the area into species first and then predict biochemicals separately, or to apply a

non-linear model that caters for species differences. We adopted the latter for mapping quality since it is easier to implement than first developing methods for mapping species in a more complex savanna rangeland before any attempt at mapping quality.

In order to better understand the variation of the nutrients that were measured in the field, we established the possible factors influencing that variation at a local scale (chapter 8). Our results indicate that there is a significant relationship between grass quality parameters and site-specific factors such as slope, altitude, percentage grass cover, aspect and soil texture. Plant characteristics such as species type interact significantly with slope, altitude and geology in influencing nutrient distribution. The results of this study provide a better insight on foliar nutrient distribution patterns at a landscape scale in savanna rangelands.

10.5 Airborne hyperspectral remote sensing of grass quality

The last aspect in this thesis was to map quality using airborne hyperspectral imagery. This is, in my opinion the most challenging task since there are a lot of influences affecting reflectance signatures (leaf orientation, soil background effects, atmospheric absorption effects, water effects in fresh canopies as well as the occurrence of mixed species with different responses to electromagnetic radiation).

We developed a new technique, largely built upon the laboratory and field observations (chapter 3, 4, 5 6, and 7). The new integrated approach, involves continuum-removed absorption features, the red edge position (REP) and neural networks. The approach was applied to map grass nitrogen concentration in the Kruger National Park. Transformation by continuum removal has its advantages as shown by the evidence in chapter 3 and discussed in section 10.5. The red edge position was shown to be strongly related to quality (chapter 4) and has been found to be insensitive to atmospheric and background effects (Clevers & Jongschaap, 2001) and therefore suitable for measurements under natural conditions.

Finally, a neural network algorithm was applied so as to cater for the possible non-linear relationships in a mixed species environment. To permit a detailed study, only nitrogen (the most limiting nutrient for grazers) was selected for the development and application of the technique.

We showed that the new integrated approach (continuum-removed absorption features, the REP and a neural network) could explain 60 % of the variation in savanna grass nitrogen concentration on an independent test data set using airborne hyperspectral data, with a RMSE of 0.13 (± 8.30% of the mean observed nitrogen concentration). The resultant map is shown in Figure 10.8.

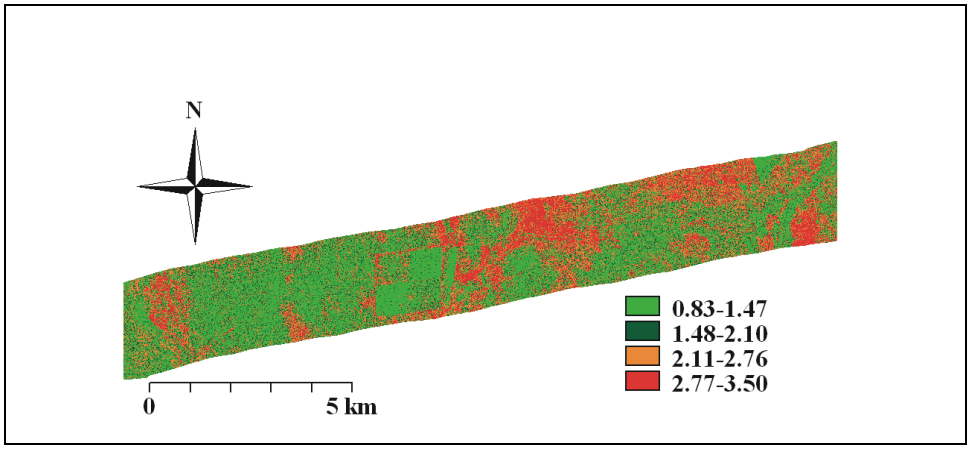

Figure 10.8. Spatial distribution of nitrogen concentration (%) in grass, mapped using the integrated approach involving continuum removed absorption features, the REP and a neural network.

This result was better compared to the conventional multiple linear regression analysis in predicting savanna grass quality. Figure 10.9 clearly shows the spatial patterns of nitrogen concentration (mapped by the new technique) in two blocks subjected to different fire regimes.

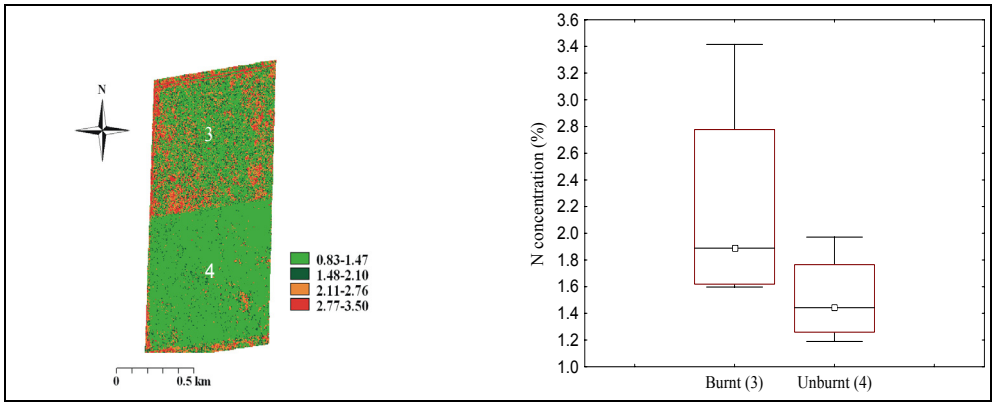

Figure 10.9. Percentage nitrogen distribution map and box plots showing the mean and spread of nitrogen concentration (%) in the burnt (Burnt (3)) and unburnt blocks (Unburnt (4)) of the Roan camp. The Roan camp is a 2 km by 2 km fenced area in the Kruger National Park, which was constructed for the protection of Roan antelopes from predators.

The result clearly shows that, a fenced area (Roan camp), which had been treated with a burnt and an unburnt area had noticeable difference in foliar nitrogen concentration. There is high nutrient concentration in the burnt areas, primarily due to rejuvenation of plant material, distribution of similar amounts of nutrients over less above ground biomass and change in plant tissue

composition (i.e. higher leaf: stem ratios with leaves having higher nutrient concentration) (Christensen, 1977; Cook, 1994; Frost & Robertson, 1987). This example shows the capability of the method developed in this thesis to unearth the spatial distribution of foliar nitrogen concentration in a mixed species environment of Southern Africa and to the best of our knowledge, this distribution is shown for the first time using remotely sensed data.

10.6 Conclusions

The main objective addressed in this thesis was to investigate the potential of hyperspectral remote sensing to predict and map tropical grass quality. The other objective was to investigate whether indices computed from hyperspectral data can estimate grass biomass at high canopy density. We have shown in this thesis that the information contained in hyperspectral data can accomplish these tasks. This main conclusion was reached from the following observations made in this thesis under three levels of investigation (Figure 10.10):

10.6.1 Laboratory level

1. We have shown that at high canopy density, pasture biomass may be more accurately estimated by vegetation indices based on wavelengths located in the red edge slope than the standard NDVI involving a strong chlorophyll absorption band in the red trough and a near infrared band
2. This thesis has shown that canopy reflectance can be used to discriminate differences in foliar nitrogen concentration in specific wavelength regions. Moreover, transformation of absorption features by continuum removal increased the separability of grass with different levels of quality thereby permitting the development of continuum-removed absorption feature variables, which were used to predict grass quality
3. We found a strong correlation between the red edge position and foliar nitrogen concentration - an interesting result for the further use of the red edge in combination with other hyperspectral techniques such as absorption features to map tropical grass quality.
4. Using the resampled (HYMAP) spectral data, canonical functions (through canonical variate analysis) derived from continuum-removed red absorption feature, in combination with the red edge position could also discriminate between the treatment groups containing different foliar nitrogen concentrations. This result permitted the extension of laboratory experiments to airborne hyperspectral images for mapping the concentration of nutrients (quality) in tropical grasses. The experiment with resampled data also showed the importance of the red edge slope in predicting nitrogen concentration.

10.6.2 Field level

The new approach, analysis of continuum-removed absorption features could predict the foliar concentration nitrogen, phosphorus, potassium, calcium and magnesium with R^2 values ranging between 0.43 and 0.80 – an encouraging result at canopy level and under natural conditions. The result confirmed observations made under controlled laboratory conditions. Knowledge of species type has also been shown to be significant in improving the modelling of quality in tropical rangelands.

10.6.3 Airborne platform level

The new integrated approach involving continuum-removed absorption features, the REP and a neural network could explain 60 % of the variation in savanna grass nitrogen concentration on an independent test data set using airborne hyperspectral data. This result was better as compared to the use of multiple linear regressions. Therefore for the mixed species environment of Southern Africa, the new approach with neural networks is preferred.

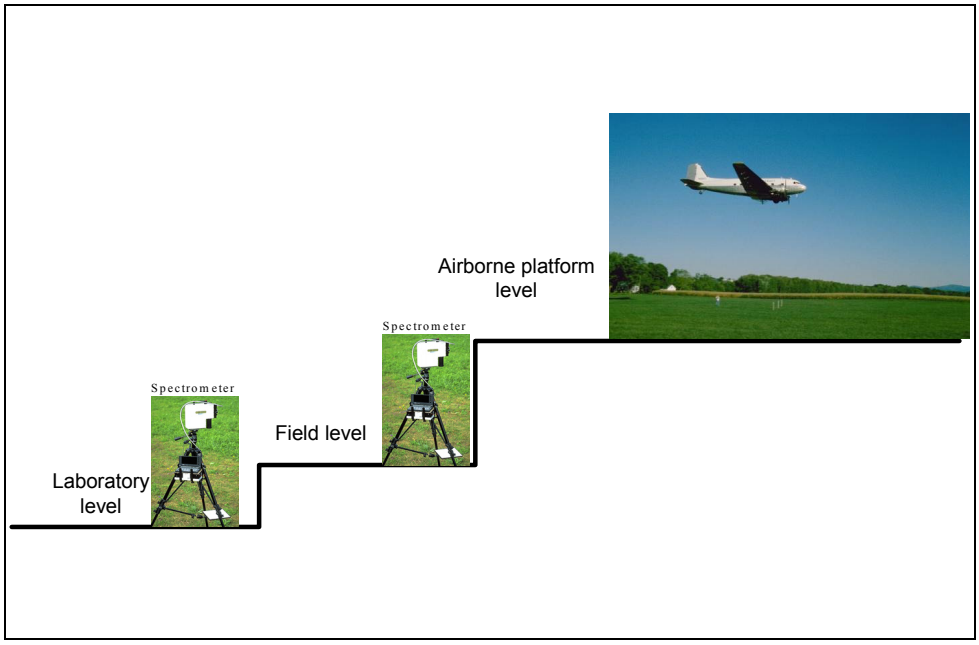

Figure 10:10. Conceptual diagram showing the levels of investigation carried out in this study

10.7 The future

The future lies in further understanding herbivory in a spatial context and as such, the improvement and application of techniques to model spatial phenomena is a pre-requisite. In line with the findings in this thesis, the prediction and mapping of other spatial variables that are important in the distribution and feeding patterns of wildlife is imperative. This includes the mapping of other macronutrients (P, K, Mg, Ca, Na) as well as deterrents such as polyphenols, lignin, cellulose and tannins in both trees and grass. An analysis of the interaction of these biochemicals in a spatial context helps in facilitating proper management decisions.

Research should also focus on mapping both species and quality. This facilitates an understanding of the species–quality interactions in a spatial context. The final focus will be to extend the methods developed in this study to space borne sensors such as MERIS, ASTER or Landsat TM for the prediction and mapping of vegetation quality on large areas. This can then be linked to spatial models explaining the distribution of herbivores. Therefore, the ultimate goal is to develop several GIS data layers of factors that derive the distributions of animals. These GIS layers will then be linked to animal population data and assess how the factors explain the distributions. In addition, habitat suitability models and maps can be generated from such GIS data layers and therefore used as a tool for managing the "hot spots" in African rangelands.

REFERENCES

Al-Abbas, A.H., Barr, R., Hall, J.D., Crane, F.L., & Baumgardner, M.F. (1974). Spectra of normal and nutrient deficient maize leaves. *Agronomy Journal*, 66 (16-20).

Anderson, G.D., & Talbot, L.M. (1965). Soil factors affecting the distribution of the grassland types and their utilisation by wild animals on the Serengeti Plains, Tanganyika. *Journal of Ecology*, 53, 33 - 56.

Ardo, J., Pilesjo, P., & Skidmore, A.K. (1997). Neural Networks, Multitemporal Landsat Thematic Mapper Data and Topographic Data to Classify Forest Damages in the Czech Republic. *Canadian Journal of Remote Sensing*, 23 (3), 217-229.

Asner, G.P., Wessman, C.A., Bateson, C.A., & Privette, J.L. (2000). Impact of tissue, canopy and landscape factors on the hyperspectral reflectance variability of arid zone ecosystems. *Remote Sensing of Environment*, 74 (69), 69- 84.

Atkinson, P.M., & Tatnall, A.R.L. (1997). Neural networks in remote sensing. *International Journal of Remote Sensing*, 18 (4), 699-709.

Bailey, D.W., Gross, J.E., Laca, E.A., Rittenhouse, L.R., Coughenour, M.B., Swift, D.M., & Sims, P.L. (1996). Mechanisms that result in large herbivore grazing distribution patterns. *Journal of Range Management*, 49 (5), 386-400.

Bakker, J.P., de Leeuw, J., & Van Wieren, S. (1983). Micro-patterns in grassland vegetation created and sustained by sheep grazing. *Vegetation*, 55, 153-161.

Baret, F., & Guyot, G. (1991). Potentials and limits of vegetation indices of LAI and APAR assessment, Proceedings, International Geoscience and Remote Sensing Symposium (IGARSS'89)/ 12th Canadian Symposium on Remote Sensing, July 10 - 14. IGARSS'89, Vancouver, BC, pp. 1355 - 1358.

Barton, F.E., Himmelsbach, D.S., Duckworth, J.H., & Smith, M.J. (1992). Two-dimensional bivariation spectroscopy: correlation of mid and near infrared regions. *Applied Spectroscopy*, 46, 420 - 429.

Bell, R.H.V. (1982). The effect of Soil nutrient availability on community structure in African ecosystems. In: B.J. Huntley & B.H. Bakker (Editors), *Ecology of Tropical Savannas*. Springer-Verlag, Berlin, pp. 193 - 216.

Bischof, H., Schneider, W., & Pinz, A.J. (1992). Multispectral classification of Landsat- images using neural networks. *IEEE Transactions on Geoscience and Remote sensing*, 30, 482-490.

Blackburn, G.A., & Pitman, J.I. (1999). Biophysical controls on the directional spectral reflectance properties of bracken (Pteridium aquilinum) canopies: results of a field experiment. *International Journal of Remote Sensing*, 20 (11), 2265-2282.

Blackburn, G.A., & Steele, C.M. (1999). Towards the Remote sensing of matorral vegetation physiology: relationships between spectral reflectance, pigment, and biophysical characteristics of semiarid bushland canopies. *Remote Sensing of Environment*, 70, 278 - 292.

Boegh, E., Broge, H.S.N., Hasager, C.B., Jensen, N.O., Schelde, K., & Thomsen, A. (2002). Airborne multispectral data for quantifying leaf area index, nitrogen concentration, and photosynthetic efficiency in agriculture. *Remote Sensing of Environment*, 81, 179 - 193.

Boerner, R.E.J. (1982). Fire and nutrient cycling in temperate ecosystems. *BioScience*, 32, 187-191.

Boltz, D.F. (1978). Colorimetric Determination of Nonmetals. Interscience Publishers, New York.

Boochs, F., Kupfer, G., Dockter, K., & Kubauch, W. (1990). Shape of the red as vitality indicator for plants. *International Journal of Remote Sensing*, 11, 1741 - 1753.

Bovey, R.W., Hein, J., H, & Meyer, R.E. (1984). Effect of Herbicides on the Production of Common Buffelgrass (Cenchrus ciliaris). *Weed Science*, 32, 8-12.

Boyd, D.S. (2002). Evaluation of approaches for forest cover estimation in the Pacific Northwest, USA, using remote sensing. *Applied Geography*, 22, 375 -392.

Brady, R.C., Trock, S.C., Jones, C.J., & Ross, P.F. (2002). Stunted growth and mortality associated with sodium deficiency. *Avian diseases*, 46 (3), 740-744.

Broge, N.H., & Leblanc, E. (2000). Comparing prediction power and stability of broadband and hyperspectral vegetation indices for estimation of green leaf area index and canopy chlorophyll density. *Remote Sensing of Environment*, 76, 156-172.

Burman, P. (1989). A comparative study of ordinary cross-validation, v-fold cross validation and the repeated learning-testing methods. *Biometrika*, 76, 503 -514.

Buschmann, C., & Nagel, E. (1993). In vivo spectroscopy and internal optics of leaves as basis for remote sensing of vegetation. *International Journal of Remote Sensing*, 14 (4), 711-722.

Carling, A. (1992). Introducing neural networks. Sigma Press, Wilmslow.

Carter, G.A. (1993). Responses of leaf spectral reflectance to plant stress. *American Journal of Botany*, 80, 239 - 243.

Christensen, N.L. (1977). Fire and soil-plant nutrient relations in a pine-wiregrass savanna on the coastal plain of North Carolina. *Oecologia*, 31, 27-44.

Civco, D.L. (1993). Artificial neural networks for land-cover classification and mapping. *International Journal of Geographic Information Systems*, 7 (2), 173-186.

Clark, A.F. (1999). Spectroscopy of rocks and minerals and principles of spectroscopy. In: A.N. Rencz (Editor), *Manual of Remote Sensing: Remote Sensing for the Earth Sciences*. John Wiley and Sons, New York, pp. 3-58.

Clark, R.N., & Roush, T.L. (1984). Reflectance spectroscopy: quantitative analysis techniques for remote sensing applications. *Journal of Geophysical Research*, 89 (B7), 6329-6340.

Clark, R.N., Swayze, G.A., Heidebrecht, K.B., & Goetz, A.F.H. (1993). Comparison of methods for calibrating AVIRIS data to ground reflectance. In: R.O. Green (Editor), *Summaries of the Fourth Annual JPL Airborne Geoscience Workshop*. Jet Propulsion Laboratory,, Pasadena, CA, pp. 35-36.

Clevers, J., & Buker, C. (1991). Feasibility of the red edge index for the detection of nitrogen deficiency, Proceedings of the 5th International Colloquium - Physical measurements and signatures in Remote sensing. ESA SP-319, Courchevel, France, pp. 165 - 168.

Clevers, J.G. (1988). The derivation of a simplified reflectance model for the estimation of leaf area index. *Remote Sensing of Environment*, 35, 53 - 70.

Clevers, J.G.P.W. (1999). The use of imaging spectrometry for agricultural applications. *ISPRS Journal of Photogrammetry and Remote Sensing*, 54, 299-304.

Clevers, J.G.P.W., De Jong, S.M., Epema, G.F., Addink, E.A., van der Meer, F., & Skidmore, A.K. (2000). Meris and the Red- edge index. In: F. van der Meer, A.K. Skidmore & W. Bakker (Editors), Second EARSeL workshop on Imaging spectroscopy. EARSeL, Enschede, pp. 1 - 16.

Clevers, J.G.P.W., & Jongschaap, R. (2001). Imaging spectrometry for agricultural applications. In: F.D. van der Meer & S.M. De Jong (Editors), *Imaging spectrometry : basic principles and prospective applications*. Kluwer Academic, Dordrecht, The Netherlands, pp. 157-199.

Cochrane, M.A. (2000). Using vegetation reflectance variability for species level classification of hyperspectral data. *International Journal of Remote Sensing*, 21 (10), 2075-2087.

Coetzee, B.J. (1983). Phytosociology, Vegetation structure and Landscapes of the central district, Kruger National Park, South Africa. Srauss & Cramer GmbH, Hirschberg 2.

Cohen, J. (1960). A coeffficient of agreement for nominal scales. *Educational and Psychological Measurement*, 20 (1), 37 - 46.

Collins, W. (1978). Remote sensing of crop type and maturity. *Photogrammetric Engineering and Remote Sensing*, 44, 43 - 55.

Cook, G.D. (1994). The fate of nutrients during fires in a tropical savanna. *Australian Journal of Ecology*, 19, 359-365.

Curran, P.J. (1989). Remote sensing of foliar chemistry. *Remote Sensing of Environment*, 30 (3), 271-278.

Curran, P.J., Dungan, J.L., & Gholtz, H.L. (1990). Exploring the relationship between reflectance red edge and chlorophyll content of slash pine. *Tree Physiology*, 7, 33 - 48.

Curran, P.J., Dungan, J.L., Macler, B.A., & Plummer, S.E. (1991). The effect of a Red leaf pigment on the relationship between red edge and chlorophyll concentration. *Remote Sensing of Environment*, 35, 69-76.

Curran, P.J., Dungan, J.L., Macler, B.A., Plummer, S.E., & Peterson, D.L. (1992). Reflectance spectroscopy of fresh whole leaves for the estimation of chemical concentration. *Remote Sensing of Environment*, 39, 153-166.

Curran, P.J., Dungan, J.L., & Peterson, D.L. (2001). Estimating the foliar biochemical concentration of leaves with reflectance spectrometry: testing the Kokaly and Clark methodologies. *Remote Sensing of Environment*, 76, 349-359.

Curran, P.J., Windham, W.R., & Gholz, H.L. (1995). Exploring the relationship between reflectance red edge and chlorophyll concentration in slash pine leaves. *Tree Physiology*, 15, 203-206.

Danson, F.M., & Plummer, S.E. (1995). Red edge response to forest leaf area index. *International Journal of Remote sensing*, 16 (1), 183-188.

Dawson, T.P., & Curran, P.J. (1998). A new technique for interpolating the reflectance red edge position. *International Journal of Remote sensing*, 19 (11), 2133-2139.

Demetriades-Shah, T.H., Steven, M.D., & Clark, J.A. (1990). High resolution derivative spectra in remote sensing. *Remote Sensing of Environment*, 33, 55-64.

Diaconis, P., & Efron, B. (1983). Computer-intensive methods in statistics. *Scientific American*, 248, 96-108.

Drent, R.H., & Prins, H.H.T. (1987). The herbivore as prisoner of its food supply. In: J.v. Andel, J. Bakker & R.W. Snaydon (Editors), *Disturbance in grasslands; species and population responses.* Dr. W. Junk Publishing Company, Dordrecht, pp. 133 - 149.

Du Toit, P.J., & Malan, A.I. (1940). A study of the mineral content and feeding value of natural pastures in the Union of South Africa. *Onderstepoort Journal of Veterinary Science*, 14, 123 - 176.

Duncan, R.R. (2000). Plant Tolerance to Acid Soil Constraints: Genetic resources, Breeding Methodology, and Plant Improvement. In: R.E. Wilkinson (Editor), *Plant - Environment Interactions*. Marcel Dekker, Inc., New York, pp. 1 - 38.

Dungan, J.L., Johnson, L., Billow, C., Matson, P., Mazzurco, J., Moen, J., & Vanderbilt, V. (1996). High spectral resolution reflectance of Douglas Fir grown under different fertilisation treatments: Experimental design and treatment effects. *Remote Sensing of Environment*, 55, 217 - 228.

Efron, B. (1982). The jacknife, the bootstrap, and other resampling plans. Society of industrial and applied mathematics, Philadelphia.

Efron, B., & Tibshirani, R.J. (1994). An introduction to the bootstrap. Monographs on statistics and applied probability, 57. Chapman and Hall, Boca Raton, 436 pp.

Elvidge, C.D. (1990). Visible and near infrared reflectance characteristics of dry plant materials. *International Journal of Remote Sensing*, 11 (10), 1775-1795.

Elvidge, C.D., & Chen, Z. (1995). Comparison of broad-band and narrow band red and near infrared vegetation indices. *Remote Sensing of Environment*, 54, 38 - 48.

Filella, I., & Penuelas, J. (1994). The red edge position and shape as indicators of plant chlorophyll content, biomass and hydric status. *International Journal of Remote Sensing*, 15 (7), 1459- 1470.

Fillella, I., & Penuelas, J. (1994). The red edge position and shape as indicators of plant chlorophyll content, biomass and hydric status. *International Journal of Remote sensing*, 15, 1459 - 1470.

Flowers, T., Troke, P.F., & Yeo, A.R. (1977). The mechanisms of salt tolerance in halophytes. *Annual Review of Plant Physiology*, 28, 89 - 121.

Foley, B., Mcllwee, A., Lawler, I., Agragones, L., Woolnough, A.P., & Berding, N. (1998). Ecological applications of near infrared spectroscopy - a tool for rapid, cost effective prediction of the composition of plant and animal tissues and aspects of animal performance. *Oecologia*, 116, 293 - 305.

Foody, G.M. (1995). Landcover classification by an artificial neural network with ancillary information. *International Journal of Geographical Information Systems*, 9, 527-542.

Fourty, T.H., Baret, F., Jacquemoud, S., Schmuck, G., & Verdebout, J. (1996). Leaf optical properties with explicit description of its biochemical composition: direct and inverse problems. *Remote sensing of Environment*, 56, 104-117.

Franklin, J., Prince, S.D., Strahler, A.H., Hanan, N.P., & Simonett, D.S. (1991). Reflectance and transmission properties of west African savanna trees from ground radiometer measurements. *International Journal of Remote Sensing*, 12 (6), 1369-1385.

Frost, P.G.H., & Robertson, F. (1987). The ecological effects of fire in savannas. In: B.H. Walker (Editor), *Determinants of tropical savannas*. IRL Press, Oxford, pp. 93-140.

Gao, X., Huete, A.R., Ni, W., & Miura, T. (2000). Optical - Biophysical relationships of vegetation spectra without background contamination. *Remote Sensing of Environment*, 74, 609- 620.

Gastellu-Etchegorry, J.P., & Bruniquel-Pinel, V. (2001). A modelling approach to assess the robustness of spectrometric

predictive equations for canopy chemistry. *Remote Sensing of Environment*, 76, 1-15.

Gates, D.M., Keegan, H.J., Schleter, J.C., & Weidner, V.R. (1965). Spectral properties of plants. *Applied Optics*, 4, 11-20.

Giron, H.C. (1973). Atomic Absorption Newsletter, pp. 28.

Gitelson, A.A., Buschmann, C., & Lichtenthaler, H.K. (1999). The Chlorophyll Fluorescence Ratio F735/F700 as an Accurate Measure of the Chlorophyll Content in Plants. *Remote Sensing of Environment*, 69 (3), 296-302.

Gong, P. (2002). Analysis of in situ hyperspectral data for nutrient estimation of giant sequoia. *International Journal of Remote sensing*, 23 (9), 1827 - 1850.

Goutte, C. (1997). Note on free lunches and cross-validation. *Neural Computation*, 9, 1211-1215.

Grant, C.C., Davidson, T., Funston, P.J., & Pienaar, D.J. (2002). Challenges faced in the conservation of rare antelope: A case study on the Northern basalt plains of the Kruger National Park. *Koedoe*, 45 (2), 1 - 22.

Grant, C.C., Peel, M.J.S., Zambatis, N., & van Ryssen, J.B.J. (2000). Nitrogen and phosphorous concentration in faeces: An indicator of range quality as a practical adjunct to existing range evaluation methods. *African Journal of Range and Forage Science*, 17 (1), 81 - 92.

Grasshoff, K., Erhardt, M., & Kremling, K. (Editors). (1983). Methods of seawater analysis. Verlag Chemie, Weinheim, Germany, 600 pp.

Griffith, D.A., & Amrhein, C.G. (1997). Multivariate statistical analysis for Geographers. Prentice Hall, New Jersey.

Groenewald, J.W., & Boyazoglu, P.A. (1980). Animal nutrition: concepts and application. J.L van Schaik (Pvt) Ltd, Pretoria.

Grossman, Y.L., Ustin, S.L., Jacquemoud, S., Sanderson, E.W., Schmuck, G., & Verdebout, J. (1996). Critique of Stepwise Multiple Linear Regression for the Extraction of Leaf Biochemistry Information from Leaf Reflectance Data. *Remote Sensing of Environment*, 56, 182-193.

Guyot, G., & Baret, F. (1988). Utilisation de la haute resolution spectral pour suivre l'etat des couverts vegetaux, Proceedings of the Fourth International colloquium on Physical Measurements and Signatures in Remote Sensing. European Space Agency, Noordwijk, pp. 279-286.

Guyot, G., Baret, F., & Jacquemoud, S. (1992). Imaging spectroscopy for vegetation studies. In: F. Toselli & J. Bodechtel (Editors), *Imaging spectroscopy: Fundamentals and prospective Applications*. Kluwer Academic Publishers, Dordrecht, pp. 145 - 165.

Heitkonig, I.M.A., & Owen-Smith, N. (1998). Seasonal selection of soil types and grass swards by roan antelope in a South African savanna. *African Journal of Ecology*, 36, 57 - 70.

Hepner, G.F., Logan, T., Ritter, N., & Bryant, N. (1989). Artificial neural network classification using a minimal training set: Comparison to

conventional supervised classification. *Photogrammetric Engineering and Remote Sensing*, 56 (4), 469-473.

Himmelsbach, D.S., Boer, J.D., Akin, D.E., & Barton, E.E. (1988). Solid state carbon-13 NMR, FTIR and NIR spectroscopic studies of ruminant silage digestion. In: C.S. Creaser & A.M.C. Davis (Editors), *Analytical Applications of spectroscopy*. Royal Society of Chemistry, London, pp. 410-413.

Hoffer, R.M. (1978). Biological and physical considerations in applying computer-aided analysis techniques to remote sensor data. In: P.H. Swain & S.M. Davis (Editors), *Remote sensing: the quantitative approach*. McGraw-Hill International Book Company, New York, pp. 227-289.

Horler, D.N.H., Dockray, M., & Barber, J. (1983). The red edge of plant leaf reflectance. *International Journal of Remote Sensing*, 4 (2), 273-288.

Huete, A.R. (1988). A soil adjusted vegetation index (SAVI). *International Journal of Remote Sensing*, 9, 295 - 309.

Hurcom, S.J., & Harrison, A.R. (1998). The NDVI and spectral decomposition for semi - arid vegetation abundance estimation. *International Journal of Remote Sensing*, 19 (16), 3109 - 3125.

Jago, R.A., Cutler, M.E.J., & Curran, P.J. (1999). Estimating Canopy Chlorophyll Concentration from Field and Airborne Spectra. *Remote Sensing of Environment*, 68 (3), 217-224.

Johnson, L.F., Hlavka, C.A., & Peterson, D.L. (1994). Multivariate Analysis of AVIRIS data for canopy biochemical estimation along the Oregon transect. *Remote Sensing of Environment*, 47, 216-230.

Johnston, M., Grof, C.P.L., & Brownell, P.F. (1988). The effect of sodium nutrition on the pool sizes of intermedites of the C-4 photosynthetic pathway. *Australian Journal of Plant Physiology*, 15 (6), 749-760.

Jordan, C.F. (1969). Derivation of leaf area index from quality of light on the forest floor. *Ecology*, 50, 663 - 666.

Jourbert, S.C.J. (1976). *The population ecology of the roan antelope (Hippotrugus equinus) in the Kruger National Park*. DSc Thesis, University of Pretoria, Pretoria.

Katz, J.J., Dougherty, R.C., & Boucher, L.J. (1966). Infrared and nuclear magnetic resonance spectroscopy of chlorophyll. In: I.P. Vernon & G.R. Seely (Editors), *The Chlorophylls*. Academic Press, New York, pp. 186-249.

Kavzoglu, T., & Mather, P.M. (2002). The role of feature selection in artificial neural network applications. *International Journal of Remote Sensing*, 23 (15), 2919-2937.

Keiner, L.E., & Yan, X.H. (1998). A neural network model for estimating sea surface chlorophyll and sediments from thematic mapper imagery. *Remote Sensing of Environment*, 66, 153 - 165.

Klaus, G., Klaus - Hugi, C., & Schmid, B. (1998). Geophagy by large mammals at natural licks in the rain forest of the Dzanga national park, Central African Republic. *Journal of Tropical Ecology*, 14, 829 - 839.

Kokaly, R.F. (2001). Investigating a physical basis for spectroscopic estimates of leaf nitrogen concentration. *Remote Sensing of Environment*, 75, 153-161.

Kokaly, R.F., & Clark, R.N. (1999). Spectroscopic determination of leaf biochemistry using band-depth analysis of absorption features and stepwise multiple linear regression. *Remote Sensing of Environment*, 67, 267-287.

Kokaly, R.F., Despain, D.G., Clark, R.N., & Livo, K.E. (2003). Mapping vegetation in Yellowstone National Park using spectral feature analysis of AVIRIS data. *Remote Sensing of Environment*, 84, 437 - 456.

Koroleff, F. (1983). Determination of nutrients. In: K. Grasshoff, M. Erhardt & K. Kremling (Editors), *Methods of seawater analysis*. Verlag Chemie, Weinheim., pp. 125-187.

Kumar, L., Rietkerk, M., van Langevelde, F., van de Koppel, J., van Andel, J., Hearne, J., de Ridder, N., Stroosnijder, L., Skidmore, A.K., & Prins, H.H.T. (2002). Relationship between vegetation growth rates at the onset of the wet season and soil type in the Sahelof Burkina Faso: implications for resource utilisation at large scales. *Ecological Modelling*, 149, 143 - 152.

Kumar, L., Schmidt, K.S., Dury, S., & Skidmore, A.K. (2001). Imaging spectrometry and vegetation science. In: F. van der Meer & S.M. de Jong (Editors), *Imaging spectrometry*. Kluwer Academic publishers, Dordrecht, The Netherlands, pp. 111-155.

Kupiec, J.A., & Curran, P.J. (1995). Decoupling effects of the canopy and foliar biochemicals in AVIRIS spectra. *International Journal of Remote Sensing*, 16 (9), 1731-1739.

Lammertsma, D., & Bruinderink, G.G. (1998). Selsustainability of ungulates on the Veluwe. *Levende-Natuur*, 99 (7), 268-271.

Landgrebe, D. (1999). Information Extraction Principles and Methods for Multispectral and Hyperspectral Image Data. In: C.H. Chen (Editor), *Information Processing for Remote Sensing*. World Scientific Publishing Co., Inc., 1060 Main Street, River Edge, NJ 07661, USA, pp. Chapter 1.

Lichtenthaler, H.K., Gitelson, A., & Lang, M. (1996). Non-destructive determination of chlorophyll content of leaves of a green and an aurea mutant tobacco by reflectance measurements. *Journal of Plant Physiology*, 148, 483-493.

Lillesand, T.M., & Kiefer, R.W. (1994). Remote sensing and image interpretation. John Wiley and sons, New York.

Liu, X.-H., Skidmore, A.K., & Oosten, V. (2002). Integration of classification methods for improvement. *ISPRS Journal of Photogrammetry and Remote Sensing*, 56, 257-268.

Lucas, N.S., Curran, P.J., Plummer, S.E., & Danson, F.M. (2000). Estimating the stem production of a coniferous forest using an ecosystem simulation model driven by the remotely sensed red edge. *International Journal of Remote Sensing*, 20 (4), 619 - 631.

Ludwig, F. (2001). *Tree - grass interactions on an East African Savanna*. PhD Thesis, Wageningen Agricultural University, Wageningen, 141 pp.

Luther, J.E., & Carroll, A.L. (1999). Development of an Index of Balsam Fir Vigor by Foliar Spectral Reflectance. *Remote Sensing of Environment*, 69 (3), 241-252.

Marschner, H. (1995). Mineral nutrition of higher plants. Academic Press, London.

Marten, G.C., Shenk, J.S., & Barton, F.E. (1989). Near Infrared Reflectance Spectroscopy (NIRS): Analysis of Forage quality. USDA Handbook 643, US Department of Agriculture, Washington, D.C, 1 - 96 pp.

Martin, M.E., & Aber, J.D. (1997). High resolution remote sensing of forest canopy lignin, nitrogen and ecosystem process. *Ecological applications*, 7, 431- 443.

Matoh, T., & Murata, S. (1990). Sodium stimulates growth of Panicum coloratum through enhanced photosynthesis. *Plant physiology*, 92 (4), 1169-1173.

Maxwell, E.L. (1976). Multivariate Systems Analysis of Multi spectral Imagery. *Photogrammetric Engineering and Remote Sensing*, 42 (9), 1173 -1186.

Mayeux, J., HS, & Hamilton, W.T. (1983). Response of Common Goldenweed (Isocoma coronopifolia) and Buffelgrass (Cenchrus ciliaris) to Fire and Soil - Applied Herbicides. *Weed Science*, 31 (3), 355-360.

McGarigal, K., Cushman, S., & Stafford, S. (2000). Multivariate statistics for wildlife and ecology research. Springer, New York.

McNaughton, S.J. (1983). Serengeti grassland ecology: the role of composite environmental factors and contingency in community structure. *Ecological monographs*, 53, 291 - 320.

McNaughton, S.J. (1987). Adaptation of Herbivores to seasonal changes in nutrient supply. In: J.B. Hacker & J.H. Ternouth (Editors), *The nutrition of Herbivores*. Academic Press, Sydney, pp. 391 - 408.

McNaughton, S.J. (1988). Mineral nutrition and spatial concentrations of African ungulates. *Nature*, 334, 343 - 345.

McNaughton, S.J. (1990). Mineral nutrition and seasonal movements of African migratory ungulates. *Nature*, 345, 613 - 615.

McNaughton, S.J., & Banyikwa, F.F. (1995). Plant communities and herbivory. In: A.R.E. Sinclair & P. Arcese (Editors), *Serengeti II - dynamics, management, and conservation of an ecosystem*. Chicago Press, Chicago, pp. 49 - 70.

Milton, N.M., Eiswerth, B.A., & Ager, C.M. (1991). Effect of phosphorous deficiency on spectral reflectance and morphology of soybean plants. *Remote Sensing of Environment*, 36, 121 - 127.

Moore, D.S., & McCabe, G.P. (1998). Introduction to the practice of statistics. W.H. Freeman and Company, New York.

Murata, S., & Sekiya, J. (1992). Effects of sodium on photosynthesis in Panicum coloratum. *Plant and cell physiology*, 33 (8), 1239 - 1242.

Murphy, J.A., Murphy, S.L., & Samaranayake, H. (2000). Soil Physical Constraints and Plant Growth Interactions. In: R.E. Wilkinson (Editor), *Plant - Environment Interactions*. Marcel Dekker, New York, pp. 387 - 406.

Mutanga, O., & Skidmore, A.K. (2003). Continuum - removed absorption features estimate tropical savanna grass quality in situ, 3rd EARSeL Workshop on Imaging spectroscopy, 13 - 16 May 2003. EARSeL, Hersching, Germany.

Mutanga, O., & Skidmore, A.K. (In review). Red edge shift and the quality of pasture canopies. *ISPRS Journal of Photogrammetry and Remote Sensing*, In review.

Mutanga, O., Skidmore, A.K., & Prins, H.H.T. (2004). Predicting in situ pasture quality in the Kruger National Park, South Africa using continuum removed absorption features. *Remote Sensing of Environment*, 89(3), 393-408.

Mutanga, O., Skidmore, A.K., & Van Wieren, S. (2003). Discriminating tropical grass canopies (Cenchrus ciliaris) grown under different nitrogen treatments using spectroradiometry. *ISPRS Journal of Photogrammetry and Remote Sensing*, 57, 263 - 272.

Mutanga, O., Skidmore, A.K., Van Wieren, S., & Kumar, L. Ferwerda, J. (In review). Estimating pasture quality at canopy level using band depth analysis with continuum removal in the visible domain. *International Journal of Remote Sensing*.

Muya, S.M., & Oguge, N.O. (2000). Effects of browse availability and quality on black rhino diet in Nairobi national park, Kenya. *African Journal of Ecology*, 38, 62 - 71.

Norris, K.H., Barnes, R.F., Moore, J.E., & Shenk, J.S. (1976). Predicting forage quality by infrared reflectance spectroscopy. *Journal of Animal Science*, 43 (4), 889-897.

Norton, G.A., Adams, N.S., Markuszewski, R., & Brayton, S.V. (1987). Rapid dissolution technique for colorimetric determination of nitrogen in coals. *Fuel*, 66 (7), 996-1001.

Ohta, D., Yasuoka, S., T, M., & Takahashi, E. (1989). Sodium stimulates growth of *Amaranthus tricolor* L. plants through enhanced nitrate assimilation. *Plant physiology*, 89, 1102 - 1105.

Olff, H., & Ritchie, M.E. (1998). Effects Of Herbivores on Grassland Plant Diversity. *Trends In Ecology And Evolution*, 13 (7), 261-265.

Olff, H., Ritchie, M.E., & Prins, H.H.T. (2002). Global environmental controls of diversity in large herbivores. *Nature*, 415, 901 - 905.

Orians, C.M., Lower, S., Fritz, R.S., & Roche, B.M. (2003). The effects of plant genetic variation and soil nutrients on secondary chemistry and growth in a shrubby willow, *Salix sericea*: Patterns and constraints on the evolution of resistance traits. *Biochemical Systematics and Ecology*, 31, 233 - 247.

Osborne, B.G., Fearn, T., & Hindle, P.H. (1993). Practical NIR spectroscopy with applications in food and beverage analysis. Longman, Singapore.

Owen-Smith, N., & Novellie, P. (1982). What should a clever angulate eat? *The American naturalist*, 119, 151 - 178.

Pardo, M., & Quintero, F.J. (2002). Plants and sodium ions: Keeping company with the enemy. *Genome Biology*, 3, 1017.1-1017.4.

Penuelas, J., Gamon, J.A., Freeden, A.L., Merino, J., & Field, C. (1994). Reflectance indices associated with physiological changes in nitrogen and water-limited sunflower leaves. *Remote Sensing of Environment*, 48, 135-146.

Peterson, D.L., Aber, J.D., Matson, P.A., Card, D.H., Swanberg, N., Wessman, C.A., & Spanner, M. (1988). Remote sensing of forest canopy and leaf biochemical contents. *Remote Sensing of Environment*, 24, 85-108.

Poluektov, N.S. (1973). Analytical methods of Flame photometry. Tehnicka Knjiga, Belgrade.

Ponzoni, F.J., & Goncalves, J.L. (1999). Spectral features associated with nitrogen, phosphorous, and potassium deficiencies in Eucalyptus saligna seedling leaves. *International Journal of Remote sensing*, 20 (11), 2249-2264.

Pooley, E. (1998). Southern African Green Guide: Flowers, Grasses and Fungi. Southern African Book Publishers, Cape Town.

Prins, H.H.T. (1987). *The Buffalo of Manyara, the individual in the context of herd life in a seasonal environment of East Africa*. PhD Thesis, Groningen, Groningen.

Prins, H.H.T. (1989). A balanced diet as a goal of grazing: the food of the Manyara buffalo. *African Journal of Ecology*, 27, 241 - 259.

Prins, H.H.T. (1996). Ecology and behaviour of the African buffalo : social inequality and decision making. Wildlife Ecology and Behaviour Series. Chapman Hall, London, 293 pp.

Prins, H.H.T., & Olff, H. (1998). Species Richness of African Grazer Assemblages: Towards a Functional Explanation. In: D. Newbery, H.H.T. Prins & N.D. Brown (Editors), *Dynamics Of Tropical Communities*. Blackwell Scientific, Oxford, pp. 449-490.

Prins, H.H.T., Olff, H., Newbery, D.M., & Brown, N.D. (1996). Species-richness of African grazer assemblages: towards a functional explanation. *Dynamics of tropical communities : the 37th symposium of the British Ecological Society*, 449-490.

Pudil, P., Novovicova, J., & Kittler, J. (1994). Floating search methods in feature selection. *Pattern Recognition Letters*, 15, 1119 - 1125.

Qiu, D.L., & Lin, P. (2002). Advances in molecular mechanisms of salt tolerance in plants. *Journal of Tropical and Subtropical Botany*, 10 (3), 281-292.

Richards, J.A. (1993). Remote Sensing Digital Image Analysis: An Introduction. Springer-Verlag, Berlin.

Richardson, A.J., & Wiegand, C.L. (1977). Distinguishing Vegetation from Soil Background Information. *Photogrammetric Engineering and Remote Sensing*, 43 (12), 1541 - 1552.

Robbins, C.T. (1983). Wildlife feeding and nutrition. Academic Press, London.

Roberts, B.R. (1971). Habitat preferences of twenty - seven grasses. *Proceedings of the Grassland Society of Southern Africa*, 6, 44 - 49.

Roberts, B.R. (1987). The availability of Herbage. In: J.B. Hacker & J.H. Ternouth (Editors), *The nutrition of Herbivores*. Academic Press, London, pp. 47 - 63.

Rouse, J.W., Haas, R.H., Schell, J.A., & Deering, D.W. (1973). Monitoring vegetation systems in the great plains with ERTS, Third ERTS Symposium. NASA, Washington, DC, pp. 309 - 317.

Ruggiero, R.G., & Fay, J.M. (1994). Utilization of termitarium soils by elephants and its ecological implications. *African Journal of Ecology*, 32, 222 - 232.

Salisbury, F.B., & Ross, C.W. (1985). Plant Physiology. Wadsworth Publishing Co, Belmont, California.

Sandmeier, S., & Deering, D.W. (1999). Structure Analysis and Classification of Boreal Forests Using Airborne Hyperspectral BRDF Data from ASAS. *Remote Sensing of Environment*, 69 (3), 281-295.

Sandmeier, S., Müller, C., Hosgood, B., & Andreoli, G. (1998). Physical mechanisms in hyperspectral BRDF data of grass and watercress. *Remote Sensing of Environment*, 66, 222-233.

Sapan, C.V., Lundblad, R.L., & Price, N.C. (1999). Colorimetric protein assay techniques. *Biotechnology and applied Biochemistry*, 29, 99-108.

Schmidt, K.S. (2003). *Hyperspectral remote sensing of vegetation species distribution in a saltmarsh*. PhD Thesis, ITC, Enschede, 249 pp.

Schmidt, K.S., & Skidmore, A.K. (2001). Exploring spectral discrimination of grass species in African rangelands. *International Journal of Remote Sensing*, 22 (17), 3421 - 3434.

Schmidt, K.S., & Skidmore, A.K. (2003). Spectral discrimination of vegetation types in a coastal wetland. *Remote Sensing of Environment*, 85, 92 - 108.

Scholes, R.J., & Archer, S.R. (1997). Tree - grass interactions in savannas. *Annual Review of Ecology and Systematics*, 28, 517 - 544.

Scholes, R.J., & Walker, B.H. (Editors). (1993). Nutrients. An African savanna: synthesis of the Nylsvlei study. Cambridge University Press, Cambridge, 81 - 110 pp.

Schowengerdt, R.A. (1983). Techniques for Image Processing and Classification in Remote Sensing. Academic Press, Inc, New York.

Seagle, S.W., & McNaughton, S.J. (1992). Spatial variation in forage nutrient concentrations and the distribution of Serengeti ungulates. *Landscape ecology*, 7 (4), 229 - 241.

Sellers, P.J. (1985). Canopy reflectance, photosynthesis and transpiration. *International Journal of Remote sensing*, 6 (8), 1335 - 1372.

Serrano, L., Penuelas, J., & Ustin, S. (2002). Remote sensing of nitrogen and lignin in Mediterranean vegetation from AVIRIS data: Decomposing biochemical from structural signals. *Remote Sensing of Environment*, 81, 355 - 364.

Siegal, S., & Castellan, N.J. (1988). Non parametric statistics for the behavioural sciences. McGraw Hill, Singapore.

Sinclair, A.R.E. (1977). The African Buffalo, a study in resource limitations of populations. University of Chicago press, Chicago.

Skarpe, C. (1992). Dynamics of savanna ecosystems. *Journal of Vegetation Science*, 3, 293 - 300.

Skidmore, A.K. (1999). Accuracy assessment of spatial information. In: A. Stein, F. van der Meer & B. Gorte (Editors), *Spatial statistics for remote sensing*. Kluwer Academic Publishers, Netherlands, pp. 197-209.

Skidmore, A.K., Turner, B.J., Brinkhof, W., & Knowles, E. (1997a). Performance of a Neural Network: Mapping forests using GIS and Remotely sensed data. *Photogrammetric Engineering and Remote Sensing*, 63 (5), 501-514.

Skidmore, A.K., Varekamp, C., Wilson, I., Knowles, E., & Delaney, J. (1997b). Remote sensing of soils in a eucalypt forest environment. *International Journal of Remote sensing*, 18 (1), 39-56.

Smith, J.A. (1993). LAI inversion using backpropagation neural network trained with a multiple scattering model. *IEEE Transactions on Geoscience and Remote Sensing*, 31, 1102-1106.

Stark, M.A. (1986). Analysis of five natural soil licks, Benoue National park, Cameroon, West Africa. *African Journal of Ecology*, 24, 181 - 187.

Stone, M. (1977). Asymptotics for and against cross-validation. *Biometrika*, 64, 29-35.

Styles, C.V., & Skinner, J.D. (1997). Seasonal variations in the quality of mopane leaves as a source of browse for mammalian herbivores. *African Journal of Ecology*, 35, 254-265.

Svanberg, S. (2001). Atomic and molecular spectroscopy. Springer - Verlag, Berlin.

Thenkabail, P.S., Smith, R.B., & De Pauw, E. (2000). Hyperspectral vegetation indices and their relationships with agricultural crop characteristics. *Remote Sensing of Environment*, 71, 158 - 182.

Thomas, J.R., & Gaussman, H.W. (1987). Leaf reflectance vs leaf chlorophyll and carotenoid concentration for eight crops. *Journal of Agronomy*, 69, 799-802.

Thomas, J.R., & Oerther, G.F. (1972). Generic combustion method for determination of crude protein in feeds: Collaborative study. *Journal of the Association of Official Analytical Chemists*, 72, 770-774.

Todd, S.W., Hoffer, R.M., & Milchunas, D.G. (1998). Biomass estimation on grazed and ungrazed rangelands using spectral indices. *International Journal of Remote sensing*, 19 (3), 427- 438.

Treitz, P.M., & Howarth, P.J. (1999). Hyperspectral remote sensing for estimating biophysical parameters of forest ecosystems. *Progress in Physical Geography*, 23 (3), 359-390.

Tucker, C.J. (1977). Asymptotic nature of grass canopy spectral reflectance. *Applied Optics*, 16 (5), 1151 - 1156.

Tucker, C.J. (1979). Red and photographic infrared linear combinations for monitoring vegetation. *Remote Sensing of Environment*, 8, 127 - 150.

Van de Vijver, C. (1999). *Fire and Life in Tarangire: Effects of Burning and Herbivory on an East African Savanna System*. Phd Thesis, Wageningen Agricultural University, Wageningen.

Van Oudtshoorn, F. (1999). Guide to grasses of Southern Africa. Briza, Pretoria.

van Soest, P.J. (1994). Nutritional Ecology of the Ruminant. Comstock publishing associates, New York.

Ventor. (1990). *A classification of land for management planning in the Kruger National Park*. Phd Thesis, University of South Africa, Pretoria.

Via, S., & Lande, R. (1985). Genotype -environment interaction andthe evolution of phenotypic plasticity. *Evolution*, 39, 505 - 522.

Voeten, M.M. (1999). *Living with wildlife - coexistence of wildlife and livestock in an east African savanna system*. PhD Thesis, Wageningen, Wageningen.

Wessman, C.A. (1994). Estimating canopy biochemistry through imaging spectroscopy. In: J. Hill & J. Mégier (Editors), *Imaging Spectroscopy - a tool for environmental observation*. ECSC, EEC, EAEC, Brussels and Luxembourg, pp. 57-69.

Wessman, C.A., Aber, J.D., & Peterson, D.L. (1989). An evaluation of imaging spectroscopy for estimating forest canopy chemistry. *International Journal of Remote Sensing*, 10 (8), 1293-1316.

Wheelock, N.D. (1980). Environmental sodium as a factor in the behaviour and distribution of African Elephants. *Elephant*, 1 (4), 169 -177.

Wiegand, C.L., Richardson, A.J., Escobar, A.J., & Gerbermann, A.H. (1991). Vegetation indices in crop assessments. *Remote Sensing of Environment*, 35, 105 - 119.

Wilkinson, R.E. (Editor), (2000). Plant - Environment Interactions. Marcel Dekker, Inc, New York, 456 pp.

Wilson, J.R. (1984). Environmental and nutritional factors affecting herbage quality. In: J.B. Hacker (Editor), *Nutritional limits to animal production from pastures*. Commonwealth Agricultural Bureaux, Slough, pp. 111 - 131.

Woolfenden, B.E., & Millar, J.S. (1997). Effects of salt on the growth and timing of reproduction of the deer mouse (Peromyscus maniculatus borealis). *Canadian Journal of Zoology*, 75 (1), 110 - 115.

Yoder, B.J., & Pettigrew-Crosby, R.E. (1995). Predicting nitrogen and chlorophyll content and concentrations from reflectance spectra (400-2500 nm) at leaf and canopy scales. *Remote Sensing of Environment*, 53, 199-211.

Zagolski, F., Pinel, V., Romier, J., Alcayde, D., Fontanari, J., Gastellu-Etchegorry, J.P., Giordano, G., Marty, G., Mougin, E., & Joffre, R. (1996). Forest canopy chemistry with high spectral resolution remote sensing. *International Journal of Remote Sensing*, 17 (6), 1107-1128.

Zhang, X., Li, C., & Yuan, Y. (1997). Application of Neural Networks to identify vegetation types from satellite images. *AI Applications*, 11, 99-106.

Zhang, Y., Pulliainen, J., Koponen, S., & Hallikainen, M. (2002). Application of an empirical neural network to surface water quality estimation in the gulf of Finland using combined optical data and microwave data. *Remote Sensing of Environment*, 81, 327-336.

Curriculum vitae

Onisimo Mutanga was born on the 6th of January 1974 in Gutu district, Zimbabwe. He completed his Ordinary level and Advanced level education at Dewure Secondary school (1987-1990) and Mashoko High school, respectively (1991-1992). He proceeded to the University of Zimbabwe to study his bachelor's degree in 1993. He joined the Ministry of education in 1996, where he taught Geography at a secondary school in Masvingo province. He enrolled for special honours in Geography at the University of Zimbabwe in 1997 and graduated with a first class.

He joined the University of Zimbabwe (Department of Geography and Environmental Science) in January 1998 as a research fellow. In August 1998, Onisimo was appointed as a staff development fellow in the Department of Geography and Environmental Science under a scholarship to do an MSc in Rural Land Ecology at ITC in The Netherlands. He completed his MSc with a distinction in March 2000.

He went back to the University of Zimbabwe and was appointed as a full time lecturer in the Department of Geography and Environmental Science in April 2000. He taught Remote sensing, GIS and Natural Resource Evaluation/Management. In October 2000, he won an ITC scholarship to read for a PhD with ITC and Wageningen University, which resulted in this thesis. He is currently working for the University of Zimbabwe as a Lecturer on Environmental modelling (GIS and RS) with special emphasis on vegetation pattern analysis.

Author's Bibliography

Mutanga, O., Skidmore, A.K., & Van Wieren, S. **(2003**). Discriminating tropical grass canopies (Cenchrus ciliaris) grown under different nitrogen treatments using spectroradiometry. *ISPRS Journal of Photogrammetry and Remote Sensing*, 57, 263 - 272.

Mutanga, O., Skidmore, A.K., & Prins, H.H.T. (**2004**). Predicting in situ pasture quality in the Kruger National Park, South Africa using continuum removed absorption features. *Remote Sensing of Environment,* 89 (3), 393-408.

Mutanga, O. **(2000**). Natural woodland distribution in parts of Mashonaland West province in Zimbabwe using GIS based spatial statistics. *Geographical Journal of Zimbabwe*, 30, 1-9.

Tevera, D.S., Mutanga, O., & Kundishora, P. **(1999**). Land Tenure, Population change and Environmental stress in Mupfure Catchment. *Geographical Journal of Zimbabwe*, 30, 31- 44.

Mutanga, O., Prins, H.H.T., Skidmore, A.K., Huizing, H., Grant, R., Peel, M.J.S., Biggs, H., & Van Wieren, S. (**In Press**). Explaining pasture - nutrient patterns in the Kruger National Park, South Africa. *Journal of Biogeography*.

Mutanga, O., & Skidmore, A.K.,2004. Integrating Imaging spectrometry and Neural Networks to map tropical grass quality. *Remote Sensing of Environment*, 90 (1), 104-115.

Mutanga, O., & Skidmore, A.K. (2004). Narrow band vegetation indices solve the saturation problem in biomass estimation. *International Journal of Remote Sensing*, 25, pp. 1-16

Mutanga, O., Skidmore, A.K., & Prins, H.H.T. **(In review**). Discriminating sodium concentration in a mixed grass species environment using spectroradiometry. *International Journal of Remote Sensing*.

Mutanga, O., Skidmore, A.K., Van Wieren, S., & Kumar, L. Ferwerda, J. (**In Press**). Estimating pasture quality at canopy level using band depth analysis with continuum removal in the visible domain. *International Journal of Remote Sensing*

Mutanga, O., & Skidmore, A.K. (**In Press**). Hyperspectral band depth analysis for a better estimation of grass biomass (*Cenchrus ciliaris*) measured under controlled laboratory conditions, *International Journal of Applied Earth Observation and Geoinformation Science*

Mutanga, O., & Skidmore, A.K. (**In review-b**). Red edge shift and the quality of pasture canopies. *ISPRS Journal of Photogrammetry and Remote Sensing*.

Mutanga, O., & Skidmore, A.K. **(In review**) Merging double sampling with remote sensing for a rapid estimation of fuelwood, *Geocarto International*.

Mutanga, O., & Skidmore, A.K. **(In review)** Fuelwood distribution pattern in North-western Zimbabwe is modelled using a Neural Network, *Asian Journal of Geoinformatics*.

Mutanga, O., & Skidmore, A.K **(In Prep**) Discriminating tropical grass grown under different nitrogen treatments using hyperspectral data resampled to HYMAP**.**

Mutanga, O., & Skidmore, A.K. **(2003a**). Continuum - removed absorption features estimate tropical savanna grass quality in situ, 3rd EARSeL Workshop on Imaging spectroscopy, 13 - 16 May 2003. EARSeL, Hersching, Germany

Ferwerda, J.G. Skidmore, A.K. van Wieren, S.E. Mutanga, O. **(2002**), Field Spectrometry of leaves for nutrient assessment, ISPRS proceedings Vol. XXXIV, part 7, 3-6 December 2002, Hyderabad, India.

Key

1. **In Press –** papers accepted for publication in refereed journals and are in the publication process.
2. **In review-** papers submitted to refereed journals and are either with the reviewers or with the editor.
3. **In prep-** papers written by the authors and ready to be submitted to journals.

Thesis cover by J. G. Ferwerda
Photographs by J. G. Ferwerda